PHD

Air injection into light oil reservoirs: oil oxidation studies

Elmurabet, Mohamed Ali

Award date:
2002

Awarding institution:
University of Bath

Air Injection into Light Oil Reservoirs: Oil Oxidation Studies

Submitted by: Mohamed Ali Elmurabet

For the degree of Doctor of Philosophy

of the University of Bath

Department of Chemical Engineering

University of Bath

England

Dedication

I would like to dedicate this work to my father, mother, my wife and my children's for their great support.

Acknowledgements

I would like to express my deepest gratitude to my supervisor Prof. Malcolm Greaves, who being most generous with his time provided useful ideas, and encouragement throughout the course of this project.

Gratitude is also extended to Dr. R. Rathbone for his help and useful discussion. Thanks also due to department's technicians for their help especially S. Duggan, R. Bull, F. Accosta. And former department's technician A. Tuddenham

I would also like to express my gratitude to my family for their encouragement and moral support throughout the time of this project.

Finally, I would like to thank Veba Oil Operation Company for their financial support.

Abstract

Air injection is a promising Improved Oil Recovery technique that shows promise for increasing the world's oil reserves to meet the growing oil demand over the entire world. The feasibility of air injection into light oil reservoirs relies on the ability to achieve complete consumption of oxygen from the injected air by reaction with the crude oil in the reservoir. This generates a flue gas to displace residual oil. Some light crude oils may not have sufficient exothermicity to propagate full In-Situ Combustion (ISC), and will only sustain low temperature oxidation (LTO) reactions. The reaction kinetics of light crude oils was investigated, and also a number of physical and chemical changes that accompanied the oxidation process.

A high-pressure small batch reactor (SBR) was used for the LTO studies. It was designed to simulate a light oil reservoir condition, at temperatures of 110-160 °C and pressures of 150-200 bar. Four light crude oils, including 3 North Sea and an Australian oil, and also seven pure hydrocarbon compounds: pentane, hexane, toluene, xylene, iso-butylbenzene, n-hexylbenzene, and dodecane were also investigated.

The SBR experiments results show that light crude oils have a high capacity to consume oxygen at reservoir conditions. The activation energy for the LTO reactions depend on the type of oil, as well as the properties of oil and reservoir matrix. The values of the activation energy were determined to be in the range 55 - 150 kJ/mole. The order of reaction with respect to oxygen partial pressure was found to be close to one.

Analysis of oxidised oil samples from the SBR indicated that the density and viscosity of the oxidised dead oil were increased by 2-9% and 20-85% respectively. The increases in density and viscosity depended on the API gravity of the crude oil and its composition.

During LTO, the asphaltene and coke content of the oxidised oil increased by 6 and 10 percent, respectively. Asphaltene content was higher for oils which had a high initial

asphaltene content. Simulation distillation showed that the LTO has an effect on the carbon number distribution of the oil. Pure saturates components showed a higher reactivity compared to aromatics components, the oxidised products were ketones, and aldehydes, formed respectively from saturates and aromatics.

Table of contents

List of Figures — Page

Chapter 1

Chapter 2

Chapter 3

Chapter 4

Chapter 5

List of Tables Page

Chapter 4

Chapter 5

CHAPTER ONE

INTRODUCTION

Introduction

Crude oil will for some coming decades remain one of the most important sources of energy for mankind. In recent years, oil demand has continued to increase worldwide. This, combined with the increasing difficulty of finding new large oil reservoirs, the maturity of many oil fields and fields that have experienced steep production decline, imposes more constraint on energy supply. All this has put pressure on the producing companies to develop new advanced recovery techniques to recover more of the remaining oil from these fields. Therefore, the goal of any advanced recovery process is to recover a major part of the remaining oil in place after conventional pressure depletion and water displacement techniques. Worldwide, their remains approximately 50-60% of the original oil in place.

There are three major reasons why over half of the original oil in place in many reservoirs is unrecoverable by conventional production methods.

(1) The displacing fluid can contact only a portion of any reservoir due to the geophysical and hydrodynamic complexity of the reservoir formation.
(2) Not all of the oil can be displaced from the reservoir rock that is contacted by the displacing fluid because of the physicochemical trapping forces.
(3) Low gravity oils are frequently too viscous to move to the production well at rates sufficient to support an economic operation.

To overcome one or more of these limitation, or at least partially, new Enhanced Oil Recovery (EOR) techniques are needed.

Air injection has been widely applied in the past for the recovery of viscous heavy oils. Due to its availability, it does not suffer from any constrains on supply and the heat generated by in situ combustion (ISC) is a valuable part of the recovery process.

Over the past few years, the focus has changed somewhat to the potential of using air injection for light oil recovery from deep high-pressure reservoirs. The air injection process for displacement of light oil is fundamentally different from the heavy oil combustion process. For heavier crude oils, heat and steam generation and subsequent viscosity reduction is the primary oil displacement mechanism. For light oils, the heat generated is of secondary value and the aim is to consume all the oxygen in the injected air via low temperature oxidation reactions. The principal objective of generates of a flue gas (85% N_2 & 15% CO_2) to be used as displacement front to move the oil and water. The feasibility of an air injection process relies on the complete consumption of oxygen from the injected air and so generate flue gas. Its considered that the flue gas recovers the oil by two competing mechanisms: a gas displacement mechanism provided by N_2, and a partial or fully miscible mechanism provided by CO_2.

Air injection in to deep light oil reservoirs is a potential technique for large scale improved oil recovery (IOR), allowing efficient oil recovery because only a small amount of the oil in place is consumed to maintain a propagating in situ combustion front or low temperature oxidation process.

The air injection process can be offer unique economic and technical opportunities for improved oil recovery in many candidate reservoirs. Some of these advantages are[1]:

- Reservoir pressurization.
- Mobilization of combustion oil.
- Flue gas stripping of the reservoir oil.
- Oil swelling.
- Injection gas substitution.
- Spontaneous oil ignition and complete oxygen utilization.
- Operation above the critical point of water with possible super extraction benefits, and near miscibility of the generated flue gas and the oil.

In the last five to six years a number of commercial projects involving air injection into light oil reservoirs have proved successfull[1-4]. In the United States, considerable interest has developed concerning the application of air injection for recovery of residual light oil as a secondary recovery method for pressure maintenance operation in cases where water injection is not effective (West Heidelberg field, Mississippi)[1], or as a tertiary recovery method to improve oil production after water flooding process, and also as an immiscible gravity drainage process in some cases (West Hackberry Field, Louisiana)[3].

Interest has also been shown in the North Sea UKCS and the Norwegian sector, where most of the reservoirs have low residual oil saturation and high water-cut post Waterflooded. Other countries, including Indonesia, China, and Argentina are also investigating the use of air injection.

Light oil air injection falls into two distinct IOR categories

- Air injection, low temperature oxidation (LTO) mode.
- Air injection, full in-situ combustion (ISC) mode.

In figure 1.1, Yannimaras et al.[4] illustrates that there are two regions of crude oil oxidation. The LTO technique uses the low temperature oxidation (LTO) region, whereas the full ISC technique uses the high temperature oxidation region (HTO). The movement, or transition from LTO to HTO in the reservoir is determined by the rate of temperature increase, which is influenced by many factors, such as the reaction rate, exothermicity and heat losses.

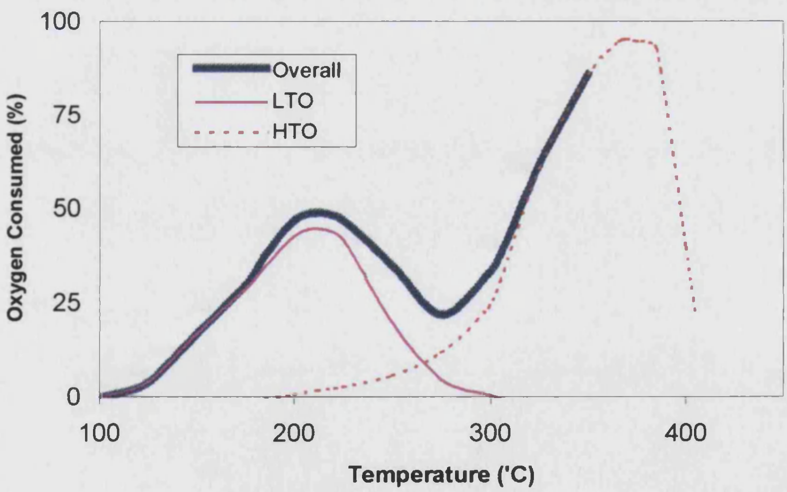

Figure 1.1: LTO and HTO domains (Yannimaras et al.[4])

In reactive light oil reservoirs, the heat generated by low temperature oxidation reactions (80 to 160 °C) can lead to spontaneous ignition of the oil in the formation and also initiate full in situ combustion. Christopher[5] mentioned that only 20% of light crude oils exhibited a continuous exotherm and would be considered candidates for propagating full ISC. This suggests that perhaps majority of light oils will sustain only LTO, although Christopher's estimated is based on a limited number of light oils. If the primary objective is only to generate nitrogen and carbon dioxide in situ, then a less intensive oxidation process, without combustion, is sufficient. For many oils and reservoir conditions, especially where the residual oil saturation post waterflood is low, the reactions may be limited to LTO.

Although it is not possible in the research domain to perform an extensive set of measurements on every reservoir of interest, a model which would relate certain key criteria as to whether a potential reservoir is a primary candidate for LTO or HTO, and would be of considerable practical value, especially if supported by the relevant kinetic parameters for each. Such information would unable oil companies to quickly screen and assess the air injection potential of their oil fields.

The kinetics of crude oil combustion in porous media have been studied for a long time, a specially for heavy crude oils. The techniques used have involved thermogravimeteric analysis (TGA), the evolved gas analysis technique (EGA), and differential scanning calorimetry (DSC).

The reaction kinetics of crude oil oxidation and the composition changes occurring during air injection are less well understood, especially when applied to light oils in the temperature range 100 – 160 °C. Most previous researchers have studied viscous or medium viscosity oils to investigate LTO kinetics and composition changes. Therefore, it is important to study the reactivity and composition changes in the low temperature oxidation region.

In this study, a high-pressure small batch reactor (SBR) was used to investigate air injection LTO in light oil reservoirs at reservoir conditions. Three North Sea light oils designated C, D, Esso. Mix1, and an Australian oil were investigated. A single type of reservoir core (Core D) was also used in conjunction with these oils, to investigate the effect of the reservoir matrix.

The main objective of this study was to investigate the kinetic of low temperature oxidation reactions to elucidate further the possible pathways for LTO reactions. The investigation has concentrated on the key parameters that effect the kinetic of oil oxidation and consumption of oxygen. The kinetic parameters: activation energy, pre-exponential factor and order of reaction were determined and this data is useful for including in reservoir simulation models, which can be used to predict the performance of an air injection LTO process in light oil reservoirs. The changes in the composition of the oxidised light crude oils and the contribution of the saturates and aromatics fraction in the crude were also studied. A small batch reactor was designed and constructed specially for the investigation.

The results obtained from this research project provide new insight into the light oil air injection technique.

The structure of the thesis is organised in the following manner:

Chapter Two:	Review of EOR Methods
Chapter Three:	Literature Review of Air Injection
Chapter Four:	Experimental Apparatus and Procedures
Chapter Five:	Experimental Results and Discussion
Chapter Six:	Conclusions and Recommendation for Future work
Chapter Seven:	References and Nomenclature

CHAPTER TWO

REVIEW OF OIL RECOVERY METHODS

2.1 General Introduction to Oil Recovery Methods

Oil recovery methods are classified into three type based on the internal energy of the reservoir (pressure potential); namely, primary recovery, secondary recovery, and enhanced oil recovery.

2.1.1 Primary Recovery:

This method is used to produce any reservoir containing oil and gas dissolved under pressure or a reservoir that has a strong water drive. There are two phases of primary recovery. In the first phase, the reservoir pressure causes natural flow of fluid through the porous media to the well bore by either expansion of the dissolved gas, gas-cap, water aquifer or combined two of the three. During this phase reservoir are allowed to produce naturally until a certain stage of depletion has been reached, generally when the production rates become uneconomic. The lack of sufficient natural drive or the sharp decline of the pressure in most reservoirs has led operators to introduce some form of artificial drive known as second phase of primary recovery. The most basic methods are the injection of natural gas or water. In many reservoirs, the main purpose of second phase is to maintain the reservoir pressure so that a high differential pressure can exist between the well bore and the formation. This is the case, for example, in the Parentis field in France and the Zelten field in Libya[6], in which water injection was not intended to improve the recovery but to increase the production rates. It was shown that the presence of a gas-cap or an active aquifer generally results in a high recovery factor, by providing a strong natural drive.

2.1.2 Secondary Recovery:

Over time, the primary recovery (natural energy drive) declines, and energy must be added to the reservoir to produce significant amounts of additional oil. Conventional secondary recovery methods introduce additional energy through the injection of water or gas, under pressure into the formation. This method of recovery is now introduced much earlier in the life of a field, often before the end of the primary production phase (second phase of primary recovery). This method is used to recover more oil from the reservoir; water flood has become the principle technique associated with secondary recovery.

The main limitations of using this method are:

- The injected gas or water does not displace all the oil, and 25 to 50% of the oil is left behind in form of small droplets or ganglia held, and is trapped in the pores.
- Low sweep efficiency in case of high oil viscosity.

2.1.3 Enhanced Oil Recovery (Tertiary recovery):

Enhanced oil recovery is defined as the incremental ultimate oil recovery that can be economically produced from a petroleum reservoir, in addition to that which can be recovered by conventional primary and secondary methods. A substantial amount of oil (an average 50-60% of the OOIP) remains in the reservoir after water or gas injection. This oil is trapped due to capillary forces and interfacial tension. Therefore, an EOR method should, ideally, improve the sweep efficiency by reducing the mobility ratio between injected and in-place fluids, eliminate, or reduce, the capillary and interfacial forces, and thus improve displacement efficiency. The effectiveness of an EOR method is its ability to provide greater hydrocarbon recovery than by natural depletion, at an economically attractive production rate.

Oil production from EOR, including heavy oil recovery has increased from 1.44 million barrels of oil per day, which represents 2.7% of the world oil production in 1990 to 2.3 million barrel oil per day or 3.5% of the world production in the first quarter of 1998. Both 1998 and 1999 were marked by an oil price collapse that lasted until mid-1999. As of April 2002, according to Oil & Gas Journal[7], the EOR production was 2.9 million barrel oil per day. The percentage of oil production by thermal, miscible and chemical methods are 46.9, 51.9 and 1.2% respectively. The highest EOR activity process to occurs in the USA. The other countries with significant EOR production at the beginning of year 2002 are Venezuela, Canada, Indonesia and China. The main drawback of EOR process is the high investment involved, so economic is still inhibiting more wide implementation.

2.2 *Review of EOR Methods*

The Various EOR methods can be broadly classified into thermal and non-thermal methods. These methods are shown in Figure 2.1. Application of any enhanced oil recovery technique requires a detailed reservoir description, incorporating both engineering and geological considerations. Field production data must be analyzed to determine the oil remaining as the target for enhanced oil recovery application. The various enhanced oil recovery techniques should be screened for possible field application. Appropriate laboratory programs should be designed to focus on the most profitable processes. A field pilot project should be designed to provide results that can be extrapolated to a field-wide application. Some of these methods will be discussed in this section.

2.2.1 Chemical Methods (Non Thermal):

Chemical flooding is any isothermal EOR process whose primary goals are to recover oil by reducing the mobility of the displacing agent and lowering the oil/water interfacial tension to a very low value to enabling the trapped oil to flow by using surface active agents and detergents. This method is the most expensive process of EOR methods and can be classified into three sub-classes namely:

2.2.1.1 Polymer Flooding:

The polymer flooding technique involves the addition of thickening agent (polymer) to the injected water. It is used in EOR methods as water-soluble polymer, to increase the viscosity of injected water and also to reduce the permeability of the rock to water, in other words, to reduce the water-oil mobility ratio close to unity or less. This technique has proved to be very successful in the case of high water cut oil-producing wells.

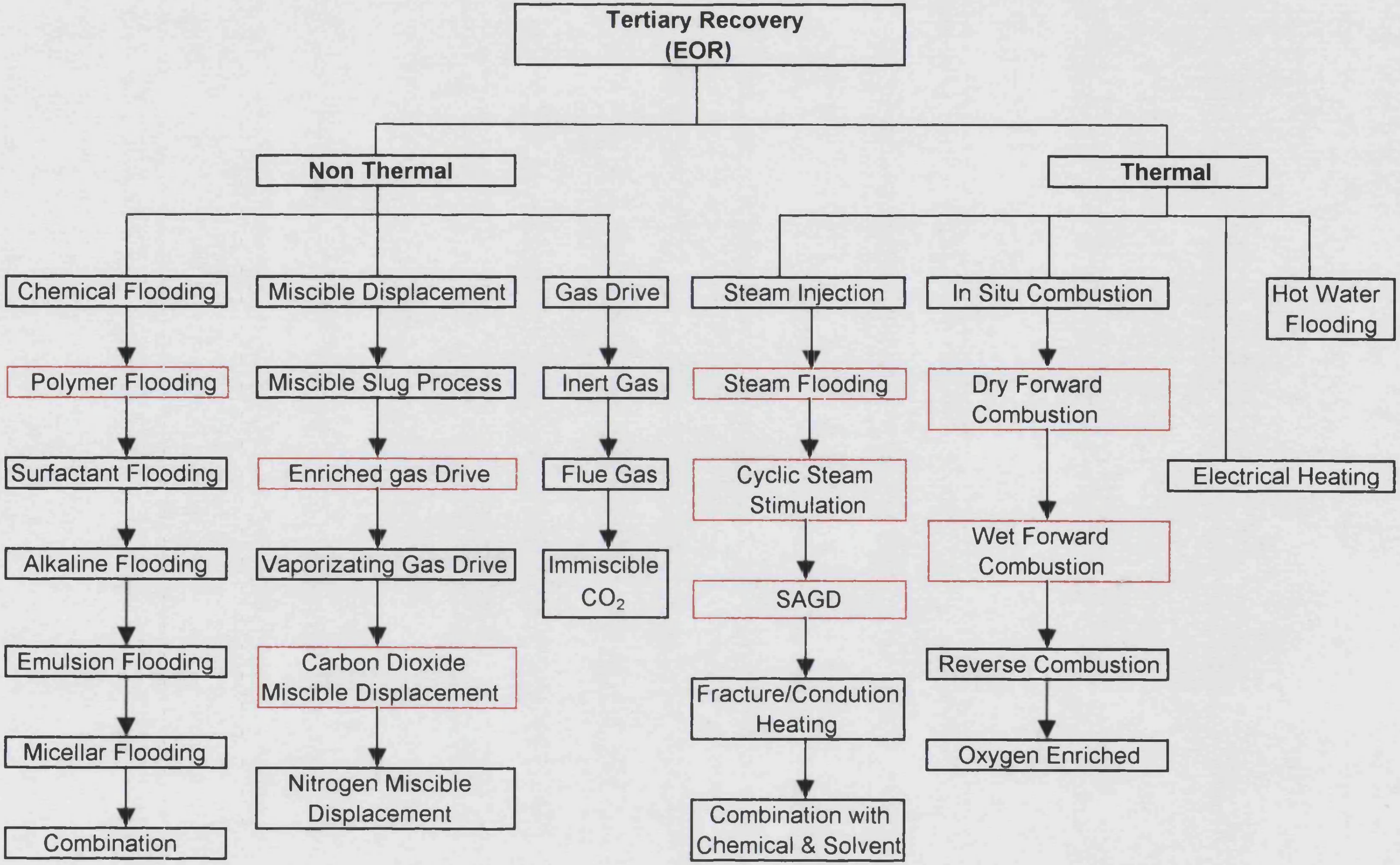

Figure 2.1: Classification of EOR Methods. Commercial processes are in red blocks.

2.2.1.2 Surfactant Flooding:

Surfactants are surface-active agents, which are used to reduce the interfacial tension between water and oil to a low value and to maintain this value for the duration of the displacement. The trapped oil become mobilized and forms a flowing oil bank. Surfactants that are used to date are petroleum sulphonates derived from crude oil, they are easily obtainable in large quantities and have high interfacial activity. Various mineral additives are used with the surfactant slug to protect it against mineral salts in the formation water by the precipitation or sequestration of the divalent captains. Surfactant flooding sometimes is considered to be uneconomic method of EOR, because it is very expensive method compared with the other methods.

2.2.1.3 Alkaline Flooding:

Alkaline or caustic flooding is another method by which oil displacement efficiency can be improved. Alkaline flooding involves the injection of cheaper chemical agent as compared to expensive surfactant. The principle mechanism considered in alkaline flooding is the reduction of the oil water interfacial tension, spontaneous emulsification, and formation wettability. This alters the relative permeability and thus leads to improved fractional flow and reduces oil saturation under favorable conditions. The principle goal in designing an alkaline system is to achieve a minimum IFT in the reservoir. Practically, this method is recommended for reservoir crudes containing organic acids such as naphthenic acids.

2.2.2 Miscible Hydrocarbon Displacement Methods:

Miscibility is defined as the ability of two or more substance to form a single homogeneous phases when mixed in all proportions. Miscible displacement methods account for the biggest share of the world's enhanced oil recovery, it is contributing about 66% of the total oil produced by EOR methods in USA and Venezuela[7].

For petroleum reservoirs, miscibility is defined as that physical condition between two or more fluids that will permit them to mix in all proportions without the existence of an interface.

The miscible displacement process involves the introduction of a fluid that will completely dissolve or become miscible with the trapped reservoir oil without the presence of an interface and all mixtures remain as a single phase. This eliminates the inter-facial force between oil and solvent that causes oil preservation in the rock matrix. When miscibility occurs the forces of capillary pressure, which formerly held the oil immobile, disappear and the oil is then free to be carried forward to the producing well and the displacement efficiency approaches 100% in the sweep zone. This method has greatest potential for enhanced recovery of low-viscosity oils. The miscibility between the reservoir oil, solvent and gas is function of the composition of these fluids and the pressure and temperature in the reservoir during the displacement process.
Two types of miscible displacement are usually employed namely first contact and multiple contact processes.

2.2.2.1 First Contact or Direct Miscibility Process (FCM)

This process is the simplest method of achieving miscibility, the term first contact means that any amount of the injected solvent will be completely soluble in the oil at all proportions and the mixture remains as a single-phase in the reservoir. First contact miscibility is achieved at the pressure when the interface between the fluids disappears. This is usually the case for solvents that consist of low molecular weight hydrocarbons such as propane, butane, or a mixture of LPG. In practice, solvent for first-contact miscibility are usually too expensive for continuous injection. Therefore, this process is the most expensive process of miscible floods.

2.2.2.2 Multiple-contact or dynamic miscible process (MCM)

This process is less expensive than the FCM process. In this process, the light to intermediate components are exchanged between oil and injected fluid, the injected gas is not miscible on first contact with the reservoir oil. In practice, for a fixed gas composition, the minimum pressure required to achieve the multiple contact miscibility between injected fluid and oil is called minimum miscibility pressure (MMP). The MMP is determined in the laboratory by carrying out a series of oil displacement tests using injected gas at different pressures in a slim tube test apparatus. Due to the long and tedious work of experimental determination, correlations were used to establish if miscibility could be achieved between target reservoir oil and solvents. Some of the published correlations have met with great success, both for their predictive qualities and their ease of use. The multiple contact or dynamic miscibility can be sub-divided into two processes:

- Condensing; in the condensation gas drive process, an enriched hydrocarbon gas (containing hydrocarbon heavier than methane) is injected, and as it travel through the reservoir, it gives up heavier components to the oil. When the oil become sufficiently enriched, it become miscible with freshly injected enriched gas.

- Vaporizing gas drive process is a particular case of multiple contact miscibility. It is based on the vaporization of the intermediate components from the reservoir oil to the injected gas creating a miscible transition zone. This mainly occurs at high pressure, by injecting natural gas, carbon dioxide, flue gas or nitrogen.

A) Carbon Dioxide Miscible Displacement

The use of carbon dioxide for improving the recovery of crude oil, following primary production, has received considerable attention because of the promising results from the current projects. Both laboratory and field studies have established the capability of carbon dioxide to displace oil from the reservoir formations with reported recovery efficiencies which approach 100 percent, when operating at optimum displacement pressures. Carbon dioxide is injected into the reservoir to dissolve in the crude oil under high pressure to form a single liquid phase, which is much lighter than the original oil.
The beneficial effects from the use of carbon dioxide that is responsible for improved recovery efficiencies pertaining to crude oil are promotes swelling, reduce viscosity, increase density, and vaporizes the oil into the CO_2 phase which resulting in high displacement efficiency of the contacted oil.

Some of the carbon dioxide properties such as high solubility in water, and acidic effect on the rock formation can be used to enhance this mode of recovery. The mode of CO_2 application ranges from complete miscibility to partial or multi-contact miscibility condition.

Carbon dioxide is preferred over hydrocarbon gases (e.g., ethane, propane) because it is cheaper, has higher density, and offers environmental benefits by providing storage for CO_2 in the reservoir. The economic feasibility of the CO_2 process depends highly on CO_2 availability, identifying CO_2 sources, and their distances to prospective reservoirs, CO_2 price, and oil price.

In the immiscible displacement of oil by carbon dioxide gas, the solubility and diffusivity of carbon dioxide are important factors that determine the efficiency of the process, because an increase in the carbon dioxide solubility and diffusivity into oil lead to an increase in oil recovery.

CO_2 Solubility in Crude Oil

The solubility of CO_2 in oil depends on the pressure, temperature and characteristic of the oil. The solubility of carbon dioxide in crude oils could be result to the following:

(a) Reducing the viscosity of the oil, the viscosity reduction becomes greater when the original oil viscosity is higher.

(b) Promotes the swelling of the oil (lower the water oil mobility ratio), this phenomenon becomes greater for light oils and leads to lowering the residual oil saturation. The amount of swelling depends on the pressure, temperature, crude oil and the mole fraction of CO_2 in the oil. For light oil, the swelling factor increases rapidly with pressure at first before flatting up and then decreasing due to extraction of lighter hydrocarbons. In the case of heavy oil, the absence of lighter hydrocarbon suppresses the shrinkage induced by vaporization and thus the swelling factor response almost linearly to the solubilization of CO_2.

(c) Increase in the injectivity and act as internal solution gas drive.

The solubility of pure carbon dioxide in oil was higher than that of a carbon dioxide-nitrogen mixture.

CO_2 Solubility in Water

CO_2 flooding also recovers oil through a CO_2-water solubility mechanism, because CO_2 dissolves in formation brine and diffuses into oil. The solubility of carbon dioxide in water is directly proportional to the pressure and inversely to a temperature below 80 °C where, for a temperature greater than 90 °C, the solubility is almost constant. Also, the solubility of CO_2 in water increases with decrease in water salinity[8]. As carbon dioxide goes into solution, there results some expansion that accounts for reduction in density of water and shifts the densities of oil and water closer to each other, which will reduce the effect of gravity segregation. The solubility of CO_2 in formation water become important in design when CO_2 is injected after waterflood, or when CO_2 is being injected alternative with water (WAG process).

Effect of CO_2 on Rock Matrix

CO_2 is an acid gas and it can react with water to form carbonic acid according to the below reversible reaction. This reaction creates a number of challenges when CO_2 is processed in EOR projects.

$$CO_2 + H_2O \leftrightharpoons H_2CO_3$$

In a clay-laden rock matrix, it stablises the clays by lowering the pH, thus preventing swelling.

In carbonate reservoirs, it can improve the injectivity by partial dissolution of the rock, mainly in the vicinity of the injection well according to the following reactions:

$$H_2CO_3 + CaCO_3 \leftrightharpoons Ca(HCO_3)_2$$

$$H_2CO_3 + MgCO_2 \leftrightharpoons Mg(HCO_3)_2$$

B) ***Nitrogen Miscible Displacement***

Nitrogen is usually cheaper than carbon dioxide or hydrocarbon gas displacement in EOR application and is not corrosive. Nitrogen has been used successfully as the injection fluid for EOR and widely used in oil field operation for gas cycling, reservoir pressure maintenance and gas lift. Reservoir conditions that favor miscibility of crude oils with N_2 include relatively high reservoir pressure and light or volatile oils rich in light and intermediate hydrocarbon components. Reservoirs that fit these conditions must be deep enough for the producing formation to withstand the high pressure required to achieve miscibility. Therefore, the numbers of reservoirs that are good candidates for this method are very limited.

C) ***Flue Gases***

Flue gas is a mixture of approximately 15 % carbon dioxide and 85 % nitrogen. The flue gas recovers oil by two competing mechanisms, the first mechanism is that carbon dioxide component dissolves in the oil to reduce oil viscosity, while the second is that nitrogen component provided the energy for driving the mobilized oil and displaced to the producing well. The carbon dioxide solubility decreases as the percent of carbon dioxide decreases in the mixture. It was noted that increasing the concentration of nitrogen in the carbon dioxide stream decreased the solubility and diffusivity of carbon dioxide in oil, consequently leading to a reduction in the swelling of the oil by carbon dioxide[9]. The producing GOR increased with increasing nitrogen concentration in the mixture. A possible explanation is that nitrogen, being non-condensable, remained as free gas phase, consequently increasing the relative permeability to the gas phase and increasing the resistance to the diffusion of carbon dioxide into oil[8].

Flue gas sometimes can be used as gravity drainage, N_2 is a light gas and will stay in the gas cap, while CO_2 at high pressure maybe heavier than the gas cap fluid and thus have a tendency to migrate down-dip.

2.2.3 Thermal Methods

Thermal methods account for the second highest share of the world's enhanced oil recovery, it is contributing about 85%, 34%, and 33% of the total oil produced by EOR methods in Canada, Venezuela, and USA, respectively[7]. Generally, it refers to processes for recovering oil from underground formations as result of improving both sweep efficiency and displacement efficiency by the use of heat. The difference between thermal recovery methods and the other EOR methods lies in the fact that the injection fluid supplies thermal energy (heat) to the reservoir to reduce oil viscosity and/or to vaporize the oil. In both instances, the oil is made more mobile so that it can be more effectively driven to producing wells. There are two categories of thermal methods hot fluid injection (steam or hot water) and in-situ combustion. In the first case, the injected fluid carries the heat, which is produced at the surface, Where in the second case the injected fluid is one of the reactants involved in an exothermic reaction, which takes place in the reservoir. There is a very basic difference between the two methods; the heat lost will be much greater in the first case than the second. The common factor in all thermal methods is the increase in temperature in part of the reservoir. During thermal oil recovery, the elevated reservoir temperature and pressure in combination with the possible catalytic effect of rock matrix could lead to significant changes in the composition of the phases and their physical and chemical properties. This can modify the capillary forces in the oil/rock matrix and the oil displacement. The main problems facing oil recovery by thermal techniques are economic; i.e. these methods must compete with alternative recovery processes. The most commonly used thermal recovery processes are steam injection process and in situ combustion.

2.2.3.1 Steam Injection:

Steam injection is a thermal process, which supplies the heat needed to increase the reservoir temperature and the energy to displace oil. In steam injection processes a suitable well pattern is chosen and steam is injected into a number of wells while the oil is produced from adjacent wells. Ideally, the steam forms a steam zone around the injection well at some distance from the injected well; the steam condenses and forms a hot water bank. In the steam zone, oil is displaced by steam distillation and gas (steam) drive. In the hot water zone, physical changes in the characteristics of the oil and reservoir rock take place and result in oil recovery. These changes included thermal expansion of the oil, reduction of viscosity and residual saturation and change in relative permeability.

There are two methods of steam injection. First method is continuous steam injection also known as steam drive. In this method, the steam is injected into a number of injected wells and the displaced fluid is driven to the production wells. Second method, is cyclic steam injection and also known as steam sock, in this method a single well operation is used; one well used alternatively as injector and producer.

The development of steam injection, as cyclic steam injection and as steam drive, has had a substantial effect on EOR oil production. Most steam injection operation have been applied to heavy crude oil reservoirs with densities between 12 and 18° API and viscosities between 600 to 6000 cp.

2.2.3.2 In Situ Combustion:

In situ is a Latin word for "in place" and can be simply defined as the burning of fuel where it exists in a reservoir, also known as fire flooding. In situ combustion is an enhanced recovery technique offering many advantages over other enhanced recovery processes especially in heavy oil reservoirs. Among these are, the availability of air at any location, more efficient overall drive mechanism, less energy consumption and less total environment impact. The term is applied to recovery processes in which an oxygen containing gas (air or oxygen enriched air) is injected into a hydrocarbon-bearing reservoir, where it reacts with organic fuel to burn part of the oil in place in order to generate heat. The burning zone is propagated through the formation toward the production well. Combustion is generally set off by spontaneous ignition or an artificial ignition, which raises the zone surrounding well to a sufficiently high temperature. In some fields, the reservoir temperature is so high that spontaneous ignition would occur only a few days after starting air injection. In some other fields, reactive crude or other fuels will be added to help ignition. Many other fields need artificial ignition devices, which include electrical heater, gas burner, and catalytic ignition system. The heat generated from burned oil is used to:

- Reduce the viscosity of the oil and increase its mobility.
- Increases sweep efficiency and reduce oil saturation.
- Vaporize some of the liquid in the formation generating steam and hot gases.
- Produce miscible fluid by condensation of the light components of the vaporized oil.

- Improve the flow of the unburned crude and displace it towards the production wells.

In-situ combustion is ideal for heavy oils because it burns about ten percent of the desirable fraction of the oil, at the same time upgrading the rest. In the case of light oils it can be very useful in tertiary production from reservoirs which have been depleted by primary and secondary techniques.

This technique is known to be the most complicated oil recovery method, because it includes some aspects of nearly every oil recovery process.

The application of this method in oil reservoirs depends on many factors such as:

- Depth of the oil reservoir.
- Thickness of the oil-bearing bed.
- Amount of oil in place within the reservoir.
- Degree of water saturation of the petroliferous formation.
- Specific gravity of the crude and its fractional composition.
- Reservoir pressure.
- Geological type of the oil trap.
- Physical characteristics of reservoir rocks.
- The initial oil recovery factor prior to ISC.

All these factors must be thoroughly studied before it is decided to apply the ISC method.

Failure to stimulate production using ISC can be attributed to the following reasons:

- Inability of the oil to deposit enough fuel to sustain and support combustion front.
- Low air injectivity and saturation.
- Gross channeling and leaking of the injected air from the formation.
- Excessive air requirements.
- Plugging of porous rock leading to restriction of air supply.

CHAPTER THREE

LITERATURE REVIEW: AIR INJECTION INTO LIGHT OIL RESERVOIRS

3.1 In-situ Combustion (ISC) Technique

3.1.1 History of In-Situ Combustion

In situ combustion is a recovery process in which an oxygen containing gas is injected into an oil-bearing formation and where it reacts with organic components from the oil. ISC is an enhanced recovery technique, which offers many advantages over other processes, such as a more efficient overall drive mechanism, less energy consumption and less total environmental impact. Air is most frequently used for sustaining the process, but enriched air and even oxygen can be considered.

The first test attempts to ignite oil in a reservoir were conducted in the Soviet Union in 1933. Laboratory work was initiated in 1947, while the true testing of an ISC process occurred in USA in 1950. The major field test of the process was performed in 1958 in West Newport field, USA.

The in-situ combustion process can be used to recover oil from reservoirs that contain oil from tar to very high gravity crude oil. It has been used successfully in reservoirs found at depths from 30 to 3353 m (100 to 11,000 ft). As of April 1992, according to OGJ oil report, the incremental daily oil production due to in-situ combustion was about 32,000 BOPD. 4,700 BOPD (from 8 processes) for USA, 8,000 BOPD from 10 projects for former Soviet Union, 7300 BOPD from 5 projects for Canada and 12,000 BOPD from 5 projects for Romania. As of 1994, more than 160 ISC field pilot projects have been in operation and at least 40-field projects[10]. The world's largest operations are found at Suplacu de Barcau in Rumania, Battrum in Saskatchewan (Canada) and the West Heidelberg field in Mississippi (USA). Forest Hill field is the most complete testing of the enriched air ISC process was conducted; feasibility was demonstrated. Karajanbas (Kazakhstan) was the fastest development from a pilot to a very large commercial ISC operation[10].

3.1.2 Methods of In-Situ Combustion

There are two methods of in situ combustion processes. First method is forward combustion, in this method the combustion is ignited in the injection well, so that the front propagates in the same direction as the fluid flow (direction of the production well). Forward combustion can be used as dry or wet mode. Second method is reverse combustion, in this method the combustion front travels towards the injection well (in the opposite direction to the fluid flow).

3.1.2.1 Dry forward combustion

In the earlier days, this was the most commonly used form of the combustion processes. In forward combustion, the crude in the reservoir is ignited in the vicinity of an air injection well either spontaneously or by use of an igniter, and part of the crude is burned in the formation to generate heat while the unburned oil is swept towards the production well. The combustion front is then propagated by continuous air injection within the reservoir rock away from the injected well towards the production wells. The combustion front pushes the unburned crude fractions from the swept zones a head of it, where the heavier fractions are transformed into a carbonaceous deposit with low hydrogen content. This deposit is used as fuel to sustain combustion and burned with the oxygen from the injected gas. The region swept by the combustion front no longer contains any organic compounds. Continued injection of air or oxygen enriched air maintains the combustion and drives the combustion front through the reservoir in the general direction of airflow. The main advantage of burning the undesirable fraction of the oil (the heavier components) is one of the forward combustion processes advantages over the reverse combustion processes. The process is called dry combustion because no water is injected with air or oxygen enriched air. In this process any heat generated in the matrix, which is not used to preheat the injected gas is lost by conduction to the overburden and under-burden. Under steady state conditions, the reservoir can be divided into four main zones in the direction of upstream to downstream, as shown in figure 3-1 These zones are described as following[11]:

Zone1 Combustion has already taken place and the formation in this zone is completely clean. The injected air heats up as it contacts with the matrix as a result a small amount of heat is released by combustion. This zone constitutes a sort of heat exchange with the temperature decreasing towards the inlet end.

Zone 2 The combustion zone. Oxygen is consumed by combustion reactions involving the hydrocarbons and the coke remaining in the rock surface.

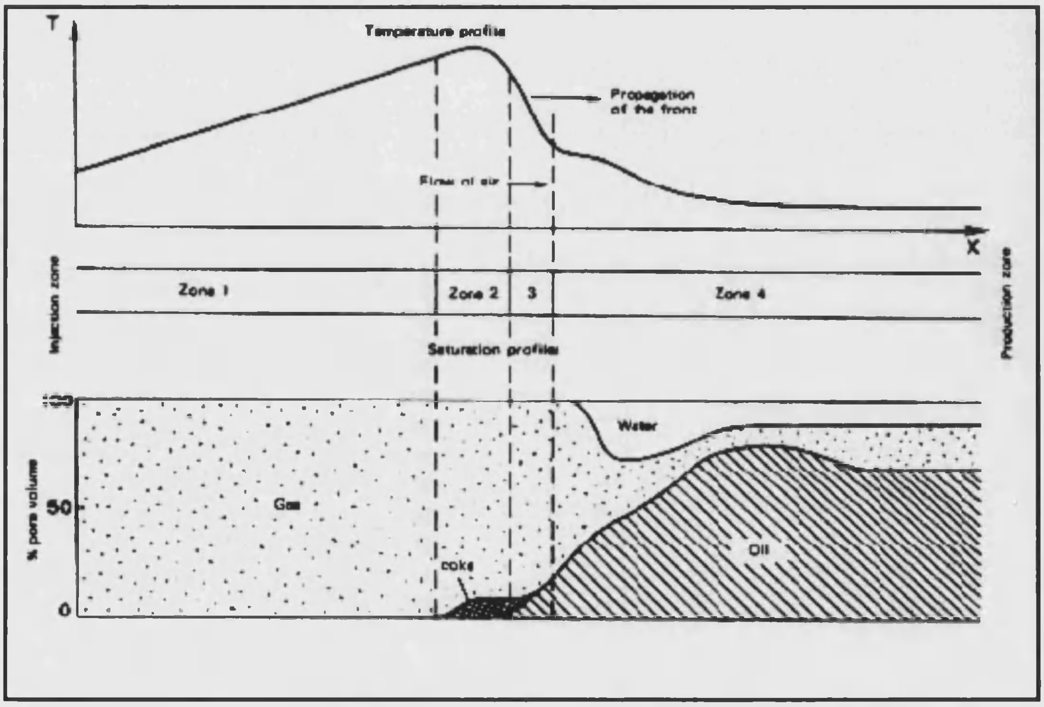

Figure 3-1: Dry forward combustion, temperature and saturated profile (Burger et al.[11])

Zone 3 The coke formation zone. The heavy fractions, which have been neither displaced nor vaporized, undergo pyrolysis. Volatile light hydrocarbons are formed.

Zone 4 There is no further significant chemical change happens in this zone. This zone is swept by the combustion gases and the displaced fluids, The following phenomena take place:

- In the downstream region nearest the reaction zone, successive vaporization and condensation of the light oil fractions and the interstitial water take place, as condensation of combustion, water also occurs.
- In the region where the temperature is lower than that of water condensation, a zone with water saturation higher than the initial water saturation exists (water bank) which pushes a zone with an oil saturation higher than original (oil bank).

3.1.2.2 Wet forward combustion

The term wet-combustion is used to describe any process that involves the injection of air and water either alternately or simultaneously. Wet combustion, optimal wet combustion, super wet combustion, and quenched combustion have all been used to describe the various WAR's used in a combustion drive. The important two are optimal wet and quenched combustion (COFCAW). In optimal wet combustion process the HTO front is maintained at all times. In the COFCAW process the WAR is sufficiently high to quench the high temperature zone and low temperature zone as steam temperature moves through the reservoir.

In low-permeability reservoir, it may be difficult to inject both air and water simultaneously at the desired rates. In this case the water and air can be injected on an alternate base. The duration of air and water injection period is controlled to achieve the desired average water air ratio. If the water air ratios are low therefore, all water that has reached the combustion front already has been converted to steam. On the other hand, if the water air ratios are kept sufficiently high, most of the water reaching the combustion front will still be in the liquid phase. The choice of water air ratio depends on water availability, quality of the water available, well injectivity, on the oxidation characteristics of the oil, and economic consideration. Greaves et al.[12] found that by increasing WAR for a three fold, the fuel consumption decreased by over 40% given a figure which is only 31% of that required in dry combustion. Also, they indicated that the water air ratio depends on number of factors including reservoir pressure, porosity, oil characteristics and the extent of heat losses.

The region effected by wet forward combustion can be divided into five zones as shown in figure 3-2

Zone 1: This zone has already been swept by the combustion front and contains little or no hydrocarbons. However, since the temperature is lower than the boiling point of water, the pores contain liquid water saturation, and the remainder of the space being occupied by the injected air.

Zone 2: Water is in the vapor phase in this zone, and the pores are saturated with a mixture of injection air and steam.

Zone 3: The combustion zone. Oxygen is consumed in the combustion of the hydrocarbons and of the deposited coke formed in the down stream part of the zone.

Zone 4: The vaporization-condensation zone. The temperature in this zone is close to that of vaporization of water. Progressive condensation of steam and combustion water takes place in this zone. In addition some light and intermediate oil fractions are vaporized and carried down stream.

Zone 5: Just down stream, the vaporization-condensation zone is a zone of high back-pressure, due to the formation of a water bank preceded by an oil bank. Further downstream the formation gradually approaches its initial conditions.

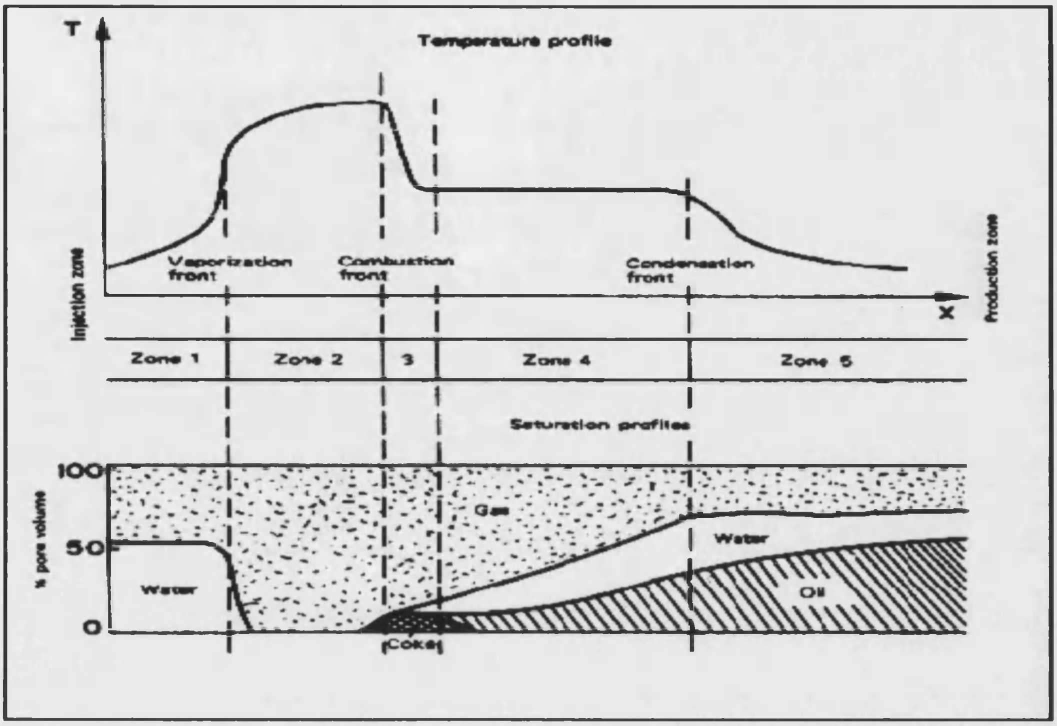

Figure 3.2: Wet forward combustion, temperature and saturated profile (Burger et al.[11])

The addition of water during the combustion process has several interesting consequences.

- The heat is transferred more effectively, so that greater heat utilization is achieved.
- Large area of oil saturated sand is affected by higher temperature.
- The amount of residual oil (or coke) left to be burned as fuel by the burning front is substantially decreased.
- The steam zone a head of the combustion front is larger, consequently the reservoir is swept more efficiently.
- Less air is required to sweep the reservoir, therefore more economical.

- It has been observed that water injection can reduce fuel and air requirement by as much as 30 to 50 percent.

3.1.2.3 Reverse combustion

The reverse combustion process is first started as a forward combustion process by injection air through wells that will finally become oil-producing wells. After burning a short distance from the ignited wells, air injection is switched to adjacent wells. Continued injection of air in the adjacent wells drives the oil towards the previously ignited wells, the reverse combustion front propagates from the ignition well (i.e. production well) and travels in the opposite direction of the air flow (towards the adjacent wells) upstream to the oil saturation regions. If the oil around the adjacent wells ignites spontaneously, the oxygen supply for reverse combustion is cut off and process essentially reverts to a forward combustion process. This may explain why many pilot reverse combustion field test have failed, in spit of the fact that laboratory studies have led to satisfactory results.

Reverse combustion is drastically different in concept from forward combustion. It's processes are not as efficient as the dry forward combustion because an attractive fraction of the oil (lighter components) is burned and an unattractive fraction of the oil (the heavier component) remains in the region behind the combustion front. This makes the ratio of injected air to oil recovered extremely high. Also damage to the production well completion can occur on ignition. Four zones can be defined in reverse combustion, starting from the injection well, as shown in Figure 3-3

Zone 1: The formation is at original condition. However it is being swept by air. If the formation temperature and oxidability of the oil are high certain oxidation reactions may occur.

Zone 2: The temperature increases conduction from the hot zone downstream. The start of oxidation also contributes to the temperature increase. The following phenomena occur: vaporization of the formation water, distillation of the light fraction of the oil and cracking of certain hydrocarbons in the presence of oxygen. The liquid and vapour fractions are displaced downstream while certain components from the carbon deposit or "coke".

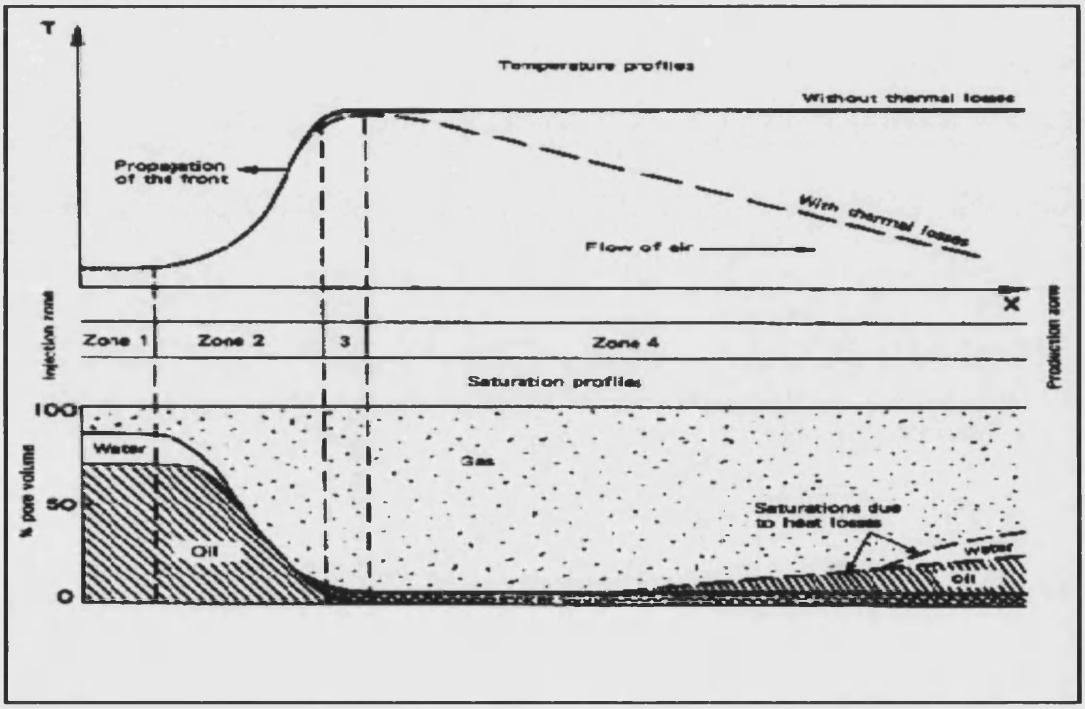

Figure 3.3: Reverse combustion, temperature and saturated profile (Burger et al.[11])

Zone 3: The combustion zone. The temperature reaches its maximum value. The oxidation and combustion reactions involving the most reactive hydrocarbon molecules consume all the oxygen not used by the reaction in the proceeding zones.

Zone 4: The unburned coke remains deposited on the matrix while the vapour and liquid phase's flow down stream. If there were no heat loses, the down stream temperature would remain equal to that of the combustion front.

In reality, the temperature decreases with distance from the combustion zone. Thus condensation of the distilled oil fraction occurs, and possibly of the steam.

3.1.2.4 In situ combustion with oxygen enriched air

This is one of the advance techniques that have been made in the field of in-situ combustion. In this technique the injected air was modified to either oxygen enriched air or pure oxygen injection. Use of high purity oxygen as the oxidizing agent for oil recovery in the in situ combustion process has received considerable attention since 1980. The potential advantages of oxygen enrichment or pure oxygen have been recognized since 1983 from the result obtained from the Forest Hill field in Taxas[13]. These advantages include:

- The time for spontaneous ignition would be reduced significantly and ignition should occur closer to the injection well.
- Increase production of carbon dioxide by five times, since there is little nitrogen diluent in the flowing gas. The high solubility of CO_2 in crude oil, promote swelling of the oil and reduce oil viscosity[14-17].
- The use of oxygen in place of air can dramatically reduce the GOR[15].
- Faster oil production[16-18].
- Lowering the total required gas injection, which reduce compression costs per unit of injected oxygen[14-18].
- Large increase in front velocity, the ability to sustain combustion under reservoir condition where air was unsatisfactory[16-18].
- The high content of CO_2 in the exhaust gas makes it an excellent source for CO_2 for other EOR projects.

Hansel et al.[14] presented the design of combustion tube system and the results of the first runs over a range of 21-95% oxygen. They concluded that most of the combustion characteristics; fuel availability, H/C ratio, peak temperature, CO/CO_2 ratio and oxygen utilization between 40 and 95% oxygen were similar to those obtained with air injection. The oxygen utilization efficiency was ranged between 89 and 97% for the oxygen percents that have been studied. Hughes et al.[19] found that the increases of oxygen partial pressure cause a reduction in the activation energy of the coke oxidation reaction, the peak temperature for both LTO and HTO shifted to a lower temperature. Shahaniet al.[15] studied five light, medium, and heavy crude oils in a combustion tube at 51 and 136 bar (750 and 2000 psig). They used oxygen concentration between 21 (air) and 95%. They found for light and medium oils (21 – 32 °API), combustion was strong at an oxygen concentration of 40% or more with almost no change in the calculated coke parameters (coke loading and hydrogen carbon ratio) and the oxygen use efficiency. At pressure of 136 bar with an increase in the oxygen concentration, the rate of oil production increased by 2.5 times and also the peak front temperature decreased from 427 to 399 °C (800 to 750 °F). Combustion characteristics were excellent for the heavy crude oil examined, in addition they have found that at high oxygen concentration, the apparent coke loading was reduced and the rate of oil production increased. These effects if they occur in actual reservoir combustion, could improve the overall economics of ISC of heavy oil.

Oxygen fireflood projects require more attention in the design of pipeline and injector system than air flood projects due to the high percent of oxygen and CO_2 will be presented in the produced gas stream.

One pilot test with oxygen enrichment has been completed[13]. The decision to develop a given reservoir with air or oxygen will depend primarily on economic, safety and materials compatibility.

3.1.2.5 In situ combustion using horizontal wells

Several authors[20,21] have reported many applications of horizontal well operations in hydrocarbon reservoirs. These applications are in low-permeability reservoirs, formation damaged, sand control to lengthen producing period prior to the accumulation of fine particles carried by formation fluids, reservoirs having gas or water coning to delay gas or water breakthrough, natural fracture reservoirs to enhance well productivity by intersecting natural fractures. The application of horizontal wells in EOR process includes miscible flooding to produce thin oil zone sandwiched between the top solvent zone and the bottom water zone, steam injection, and ISC methods.

A promising method for the recovery of heavy oils that utilizes the improved reservoir contact achievable with horizontal wells is steam-assisted gravity drainage. The main advantages of the use of horizontal wells in thermal recovery are as following:

- Improved sweep efficiency.
- Enhancement of the oil production rates from two to five times greater than vertical wells due to large reservoir contact area.
- Enhancement of the ultimate reserves and the injectivity rate.
- A decrease in the number of wells required for field development.

On the other hand, the main disadvantage of horizontal wells is their initial cost.

In heavy and light oil reservoirs, a combination of ISC and horizontal wells will result into the following; the combustion heat reduced oil viscosity, thermal cracking reduces the molecular weight and horizontal wells provide a large contact area. This phenomenon could be used to increase oil production rates, total recovery and also upgrade the quality of the produced oil. For the time being, there is some laboratory research data in the area of horizontal well-assisted in-situ combustion, but in the field testing, there is a scarcity of data. Greaves et al.[22] used "direct line drive", a vertical air injector well, and a horizontal producer well. They found significant improvement to that of vertical producer. These included a higher rate of oil production and recovery of OOIP. Greaves et al.[23] found that using 3D physical model experiments can provide valuable information on sweep efficiency and oil recovery, which is more meaningful than that achievable from 1D combustion tube experiment. 3D cell tests are more indicative of field performance. Greaves et al.[24] concluded that the use of continuous 'sleeve-back' operation to control the level of de-saturation in the downstream section of a sand pack containing light oil was successful. This confirmed by the very high oil recovery achieved equivalent to 93.5% OOIP. The use of sleeve-back of the horizontal producer well made the light oil in ISC more efficient compared to that of a full open well.

The application of horizontal wells in the ISC process has been tested in the field as producers and/or injectors. In 1993, Mobil Oil Canada drilled and completed two horizontal wells in Battrum field, Saskatchewan, Canada to improve the sweep efficiency in a mature combustion project. During the first year of production, the oil production from one of the horizontal wells was four times as compared to the oil production from nearby vertical well that completed in the same year and zone[25]. Recent field application of horizontal wells in conjunction with two existing Canadian ISC projects showed promising results both in the thermal oil production area and as a mean to substantially reduce the operational difficulties. The only problem which still remains when using the horizontal well as a producer is that the combustion front can intersect the horizontal leg close to the heel and can prematurely damage the whole horizontal portion of the well[26].

Amoco Canada Petroleum Co. Ltd. and Alberta Department of Energy tested a novel combustion related heavy oil (14° API) recovery scheme utilizing horizontal wells in thin pay in the Wabasca area[26]. The cyclic combustion pilot utilizes a central horizontal air injection well with two outside producing horizontal wells. This is a unique system in that it is the first time a horizontal well has been used as an air injector. The central horizontal injection well was preheated to above 120 °C with steam and then subsequently igniting it by air injection. After a certain volume of air was injected, the air injection was terminated and the two outside horizontal producers were placed on production. The production response after the first injection cycle was favourable[27].

3.1.3 Chemical Reactions of In-Situ Combustion

Success of oil recovery by air injection greatly depends on good knowledge of the chemical reaction mechanism between oxygen and oil in porous media. Oil oxidation during in-situ combustion is simply a chemical reaction in which the addition of oxygen or elimination of hydrogen from a compound takes place. It involves numerous competing reactions occurring through different temperature ranges. Many investigators[28-31] identified that, the over all chemical reaction of crude oil in porous media might be represented by grouping the reaction into three major oxidation reactions occuring at different temperature levels in an ISC process. These oxidation reactions are known as:

- Low Temperature Oxidation reactions (LTO), which are heterogeneous (gas - Liquid) and takes place below 300 °C.
- Medium Temperature Oxidation reactions (MTO) or Fuel deposition reactions, which are homogeneous (gas phase) and may occur between 300 °C to 370 °C.
- High Temperature Oxidation reactions (HTO) or oxidation of coke, which are heterogeneous (gas –solid) and takes place at or above 400 °C.

Some researchers[32,33] have observed that the oxidation of crude oil consists of only two oxidation reactions; low temperature oxidation and high temperature oxidation, with reaction peaks at about 250 °C and 400 °C respectively. This observation more predominate in light crude oil rather than heavy crude oil.

3.1.3.1 Low Temperature Oxidation

The oxidation reaction in the low temperature regime is important and plays a significant role in the overall combustion process. The reactions are carried out between oxygen and petroleum hydrocarbons at temperature less than 300 °C and take place upon air injection either before or after ignition. LTO involve about 5-10% of the reservoir oil, consuming oxygen in the injected air. In the low temperature regime, the oxidation of hydrocarbons is a very complex process, involving different type of propagation to full ISC, and chain branching reactions. LTO reactions are evidenced by a rapid increase in the oxygen uptake rate as well as generation of carbon oxides. Several published studies have investigated the chemical and physical changes accompanying LTO of many different grades of oil. They have used the heat released during LTO to estimate the spontaneous ignition time for an in situ combustion projects.

Dabbous and Fulton[28] concluded that in the temperature range (50 - 370 °C), the diffusion of oxygen towards the hydrocarbon molecules is very fast compared with the rate of oxidation, so that oxygen is dissolved throughout the oil phase during LTO. It was found that most of the oxygen consumed by the LTO reactions is used in reactions involving hydrogen and hydrocarbon oxidation to produce oxygenated hydrocarbons such as carboxylic acids, aldehydes, ketones, alcohols and hydro peroxides. Additionally, oxidation of carbon occurs to produce low levels of carbon oxides. Kisler and Kisler and Shallcross[34], also used the EGA technique, at low pressure to investigate the oxidation kinetics of a light Australian crude oil, they found that more oxygen was consumed and more CO_2 was produced, compared to LTO of heavy oil as shown in Figures 3.4a and 3.4b. The oxygen consumed is greater than the carbon oxides produced. Carbon oxides are the only gaseous products of the LTO reaction; carbon oxides production becomes significant at temperature higher than 100 °C and rises rapidly as the temperature increases.

The LTO reactions may take place in forward in situ combustion when oxygen is available down stream from the combustion front [28,29,35]. This may result from:

- Incomplete oxygen consumption in the high temperature combustion zone.
- Air channeling around the front.
- A tilted combustion front.

The order of the overall LTO reaction of crude oil appear to be between one-half and first-order, depending on the type of crude oil, but not on the properties of porous media. For high API gravity crudes the assumption of a first order reaction with respect to oxygen partial pressure is accepted[28]. Babu et al.[36] observed that LTO of Athabasca bitumen proceeded by three distend kinetic regimes.

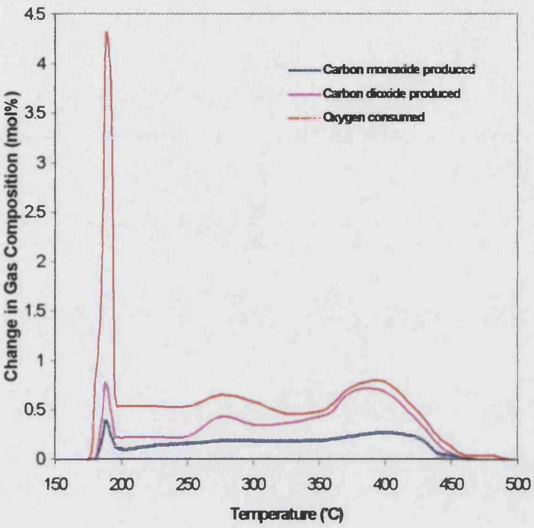

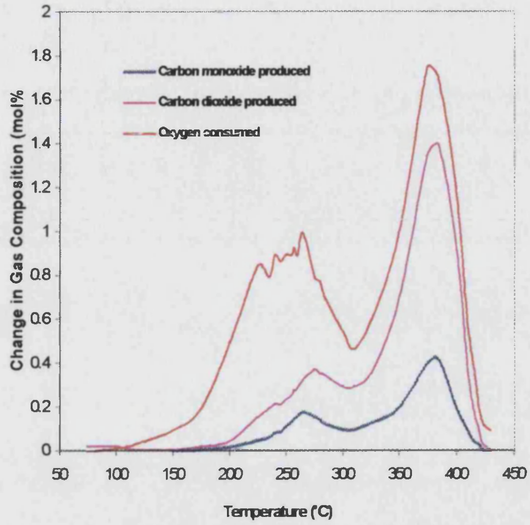

Figure 3.4a. Typical light oil EGA data (Kisler and Shallcross[34])

Figure 3.4b. Typical heavy oil EGA data (Kisler and Shallcross[34])

Two regimes were first order in oxygen concentration; depending on oxygen concentration. The rate of oxidation differed; one below 1.7×10^{-3} and the other greater than 1.7×10^{-3} mole O_2/g of bitumen. The third regime was second order; reflecting a lower extent of oxidation at temperature greater than 150 °C. They noted that the transition from first-order to a second-order was dependent on the temperature of oxidation (> 150 °C). Millour et al.[37] found that LTO of Athabasca bitumen could classified into three reaction regions, based on the oxygen uptake temperature, and coke concentration percent. These regions are:

- Region I : corresponding to total oxygen uptake of less than 0.04 g O_2/g oil, in the temperature range 22 to 150 °C and coke concentration of less than 3 percent.
- Region II : corresponding approximately to a total oxygen uptake between 0.04 and 0.2 g O_2/g oil, coke concentration between 3 and 55 percent and at temperatures ranging from 125 to 200 °C.

- Region III: coke concentration greater than 55 percent in the temperature range 150 to 275 °C.

Certain minerals and metallic derivatives in reservoir rock have catalytic effects on the oxidation reactions. Therefore, the mineralogy of the reservoir rock may have a great influence on the economic success of recovery of heavy and also lighter oils by thermal methods.

The LTO reaction rate was found to be proportional to the matrix specific area raised to a power between 0 and 1[28,38]. Greaves et al.[39] studied the influence of reservoir rock on the oxidation kinetic of light crude oils using accelerated rate Calorimetry (ARC), and found that the LTO reaction could be broadly defined as comprising three main reactions, instead of just one. The three reactions are initiation, propagation, and termination. They found that clays had little or no effect on the LTO stage. Also, they noticed from ARC plots that an autocatalytic reaction appears to take place during the LTO.

Vossoughi et al.[40] observed from TGA & DSC experiments that an increase in the surface area of the porous medium increased LTO reactions, resulting in the formation of more fuel, and better sustainability of the combustion front. This was confirmed by Hughes et al.[19] they found that the extent of LTO reactions increased with increase in surface area of the matrix, and that carbon oxides were also produced at lower temperature.

Certain metallic additives (nickel, zinc, vanadium, and copper), and solids have a catalytic effect on LTO reactions[30,38,41,42]. The catalytic effect of the reservoir minerals on LTO is evidenced by more than 50 °C lower peak temperatures for the core sample compared to the oil alone (no matrix)[43]. Alexander et al.[44] investigated the effect of LTO on fuel formation, they found that a coke-like residue was formed as a result of low temperature oxidation. For a 21.8 °API crude oil, the amount of residue increased linearly from zero near 150 °C to a maximum at about 345 °C. The apparent atomic hydrogen-carbon ratio decreased from about 50 at 121 °C to about 1 at 345 °C. The large apparent atomic hydrogen-carbon ratio is a result of oxygen being consumed in LTO reaction which do not produce carbon dioxide. Also they concluded that LTO reactions had a pronounced effect on fuel deposition and composition. Mamora et al.[32] found that the fuel during LTO run was determined to be an oxygenated hydrocarbon with an atomic oxygen-carbon ratio of 0.3. Moore et al.[45] observed that the coke formation occurred rapidly over the temperature range 200 °C to 300 °C, which is the range of LTO. They also conclude that, at 40% oxygen the heat generated by LTO is much higher than that from HTO at all pressures.

The chemical pathway for fuel laydown during LTO can be described as the conversion of asphaltenes and resins into coke[46]. The dominant trend in the LTO region is the formation of higher molecular weight, more complex reactions.

The behavior of SARA fraction of Garzan and B.Raman crude oils, which have API gravity of 26.12 and 14.95, respectively, were studied by Kok et al.[47]. They found that the LTO of asphaltenes was very weak with very little weight loss, while LTO of saturates was very active and with a large weight loss. LTO studies of Athabasca bitumen carried out by Babu and Cormack[48] showed a decline in the aromatic content, increase in the asphaltenes content, and a stable saturates content. Adegbesan et al.[46] used a Magna drive stirrer type semiflow batch reactor for the study of LTO reaction kinetics; He extracted bitumen from Athabasca tar sand and conducted experiments by varying the total and partial pressure of the oxidant gas in an isothermal mode. Within a range of 60 °C to 150 °C and pressure of (9-40 bar), they note that there was no significant effect of total pressure on the reaction rate, but that the partial pressure of oxygen had a relatively strong influence on the overall rate of oxygen consumption. These results have been observed by Wichert et al.[49] during their study of the effect of LTO on heavy oils in the presence of caustic additives. With an increase in the caustic concentration they observed higher oxygen uptake, decrease in CO and CO_2 production, increase in oil viscosity and density and asphalten production. Finally, they concluded that the total pressure did not affect the reaction significantly, at total pressures of 9 to 18 bar. Al-Saffar et al.[50] used high-pressure flow reactor to study the kinetic of selected North Sea light crude oils, using consolidated reservoirs core impregnated with oil. They identified the onset of LTO reactions from isothermal experiments, and found that LTO reactions were still occuring to some extent together with HTO, so that there was a degree of interaction between the LTO and HTO reaction regimes.

The low temperature oxidation of light oil is quite different from low temperature oxidation of heavy oil reservoirs. Fassihi et al.[51] found during their study of LTO of heavy and light crude oils that, LTO was evidenced by a drop in the reactor pressure and a change in the oil's physical properties (viscosity and density) and composition. For heavy oil, the viscosity of the oxidised oil increases exponentially with extent of oxidation. Density was not affected as dramatically as the viscosity. For the light oils, LTO produced only a minor effect on the viscosity and did not significantly affect its density and mobility. In fact the increase in viscosity was attributed to an increase in the content of the asphaltenes and resins, depending on the extent of reaction. Furthermore, analysis of the oxygen content of the oxidised oils indicated that approximately fifty percent of the oxygen was consumed during LTO was converted to water.

3.1.3.2 Medium temperature oxidation (MTO)

Medium temperature oxidation (MTO) is a low reaction rate region existing between the LTO and HTO regions. It is associated with fuel deposition reactions or thermal cracking. MTO is homogeneous (gas phase). It is involves by distillation and cracking of the crude oil, which leads to upgrading of the oil as well and deposition of heavy ends residue on the reservoir matrix as fuel, commonly called coke. Thermal cracking produces fuel or coke and also lighter components, which are transported ahead with the flue gases. The fuel deposition processes play an important role in the overall in-situ combustion process. The reaction may be represented by:

$$\text{Heavy Hydrocarbons} \rightarrow \text{Light Hydrocarbons} + \text{Heavy Residue} \quad \ldots\ldots\ldots\ldots (3.1)$$

The formation of heavy residue, "coke" is an important parameter to be considered in the design of ISC projects. If there is only a low level of fuel deposition, the heat of combustion will not be sufficient to raise the temperature of the rock and fluids to a level to sustain combustion. This leads to an unstable burning front and combustion failure. On the other hand, excessive fuel deposition causes a slow rate of advance of the burning front and high air compression costs[32]. When the combustion temperature is lower than the thermal cracking temperature, the fuel for the process is mainly supplied by LTO reaction.

The maximum oil recovery is also affected by fuel deposition and can be represented by the difference between the OOIP and the oil consumed as fuel. The amount of oil consumed is a function of the reservoir characteristics and the volumetric sweep efficiency of the process.

Alexander et al.[44] studied the factors affecting the fuel availability for combustion. They concluded that (a) high oil saturation, high oil viscosity and low combustion front temperatures can cause more fuel deposition, (b) the fuel deposition is inversely dependent on the API gravity and H/C ratio of the crude and (c) low temperature oxidation prior to high temperature oxidation has a greater effect on fuel composition and fuel availability than any other process variables investigated. Many investigators have looked at the effect of the porous rock matrix on fuel deposition. Vossoughi et al.[42] focused on the effect of the specific area of the reservoir rock. They concluded that a large specific area results in an increased fuel deposition, especially when clays were added to the matrix. Clay and sand fines reduced the permeability of sand pack in combustion tube experiments and also provide a large reaction surface area. Consequently, residual oil saturation and hence fuel concentration increased, resulting in HTO. In contrast, LTO arose from low fuel concentration. Burger and Sahuquet[38] and Ranjbar[52] found that heavy metal derivatives such as copper, nickel and iron catalyze the oxidation of the crude and also increase fuel deposition. Mamora et al.[33] concluded that pyrolysis of crude oil in a porous media goes through three over-lapping stages: distillation, visbreaking, and coking. During distillation, the oil loses most of its light ends and part of its medium gravity components. During visbreaking, the oil mildly cracks into a slightly different product. At high temperature, the oil remaining in the porous media cracks into a semisolid residue. They also observed that, distillation stage plays an important role in shaping the nature and extent of cracking reactions, and could be the main mechanism for fuel deposition. A low rate of coke deposition has been observed for light oil. This can be attributed to the low amounts of heavy components in the light oil and also to lighter end components C_{15+} fraction, which vaporizes, to a large extent at the head front[24]. Greaves et al.[53] found that, an induction period is required before the reaction mechanism changes from LTO to HTO. In the temperature range 250 to 300 °C, the process was characterized by decreasing oxygen uptake rates with increasing temperature, and it was therefore analogous to the negative temperature region (NTR). Failure of the process transcend this negative temperature region will lead to the reaction being inhibited to LTO.

Both light and heavy oils can exhibit a negative temperature gradient region over the approximate temperature range of 280 – 350 °C. Heavy oil ISC must operate at temperatures in excess of 350 °C in order to achieve efficient pore-scale displacement efficiencies; hence the reaction temperature must pass through the NTR.

3.1.3.3 High Temperature Oxidation (HTO)

HTO synonymous with fuel combustion reactions, they are heterogeneous gas-solid reactions. HTO reactions take place in combustion zone between oxygen in the gas phase and the heavy residue of oil (fuel) that has deposited on the rock matrix during the medium temperature reaction. HTO is the main source of energy for the ISC process, which extends up to 500 °C for light oils, and up to 700°C or more for heavy oils and bitumen. The rate of heat generation by the combustion process depends on reaction rate, which depends on coke (fuel) concentration, oxygen partial pressure and air injection rate. All investigators agree that the principal products of HTO are water, carbon monoxide and carbon dioxide.

The use of catalyst can speed up the HTO reaction[29]. Mamora[32] studied the oxidation of crude oil in the reactor tube experiments. He found that the fuel during HTO is an oxygenated hydrocarbon instead of carbon, which has been found by other investigators[28-29,31]. He also concluded that the overall stochiometric equation for HTO could be written as:

$$CH_xO_y + \left(1 - \frac{m}{2} + \frac{x}{4} - \frac{y}{2}\right)O_2 \rightarrow (1-m)CO_2 + mCO + \frac{x}{2}H_2O \quad \ldots\ldots..(3.2)$$

Instead of stochiometric equation which, was previously described by other researchers

$$CH_xO_y + \left(1 - \frac{m}{2} + \frac{x}{4}\right)O_2 \rightarrow (1-m)CO_2 + mCO + \frac{x}{2}H_2O \quad \ldots\ldots\ldots\ldots(3.3)$$

During high temperature oxidation, oxygen consumption is stoichiometrically equivalent to the carbon oxides produced (CO_2+0.5CO), i.e. essentially all of the consumed oxygen is utilized to produce carbon dioxides. Results obtained by Al-Saffar et al.[50] indicated a slower oxygen consumption rate at high temperature compared to lower temperature. The low level of oxygen utilization by light crude oil was attributed to the low fuel deposition. Another feature of HTO is that the concentration of CO_2 is much greater than that of CO. This is attributed to the oxidation of CO to CO_2 in the gas phase, or to the water gas shift reaction, which normally occurs at high temperatures 427-500 °C. The apparent hydrogen/carbon ratio for the fuel used in the HTO has a value between 0 and 1. This low hydrogen content fuel is formed from heavy fraction of the oil.

University of Salford[54] found that the burned fuel for light oil was mainly composed of carbon, having a low H/C ratio of about 0.5, compared to 1.7 for the original oil.

The ratio of oxygen consumed to carbon oxides produced was an identifier for the boundary between the LTO and HTO reaction regions.

3.1.4 Kinetics of In-Situ Combustion

In situ combustion kinetics deals with the dynamics of the reactions occuring during the combustion processes.

The study of the chemical kinetics of in-situ combustion is undertaken for the following reasons:

- To assess the in-situ combustion potential of major crude oil reservoirs.
- To determine if spontaneous ignition will take place in the reservoir with air injection, for light crude oils.
- To obtain values for the Arrhenius kinetics parameters such as the activation energy, order of reaction and pre-exponential factor. These values are needed for numerical modeling studies. They can also be used to calculate ignition energy requirements or the ignition induction period.

The main parameters which influence the kinetic and rate of oxidation reaction are:

- temperature is reported to have the greatest influence due to the exponential rate of increase as described by an Arrhenius rate expression (-E/RT)
- previous history of oxidation or thermal cracking
- oxygen partial pressure: the reaction order are vary from zero order to first order, depending on mass transfer effects.
- oxygen influx: mass transfer effects become more important as the reaction rate increases.
- total pressure: the influence is generally believed to be small compared to the other parameters.
- reservoir rock and fluid, and surface area clay fractions in the rock matrix may have a significant catalytic effect.

The most critical zone of air injection is the oxidation zone where the following four transport processes occur[29]:

- oxygen diffuses from the bulk gas stream to the fuel interface
- oxygen adsorbs and reacts with the fuel
- The combustion products desorb.
- The products finally transfer into the bulk gas stream

If any of these steps is inherently much slower than the remaining ones, then the overall rate will be controlled by that step, i.e. rate limiting.

In general, the combustion rate (R_c), of the crude oil "Fuel" in a porous medium can be described by[29,35,41]:

$$Rc = -dC/dt = K\ P_{o2}^{n}\ C_{o}^{m} \quad \ldots\ldots\ldots\ldots\ldots\ldots\ldots(3.4)$$

Where C_o is the instantaneous concentration of the fuel, K is the specific reaction rate constant, P_{o2} is the partial pressure of oxygen and m,n are the reaction orders. The reaction rate constant K, is often a function of temperature using the equation:

$$K = A\exp(-E/RT) \ldots\ldots\ldots\ldots\ldots\ldots\ldots(3.5)$$

where E is the activation energy, A is the Arrhenius constant and R is the universal gas constant.

Bousaid and Ramey[41] found that the oxidation reaction rate of crude oil in a porous medium depends on the carbon concentration, combustion temperature and oxygen partial pressure. In their experiments, they showed first order reaction rates in both fuel concentration and oxygen partial pressure during their investigation of the combustion reaction by using combustion cell. Finally, they noted that the water saturation is one of the parameters affecting oxidation kinetics. Greaves et al.[12] have indicated that the combustion of coke in porous media is first order in oxygen and carbon concentration. They have also reported that the activation energy varied from 58.9 kJ/mole up to 157.3 kJ/mole. Greaves et al.[18] concluded that the combustion kinetics are dependent on fuel concentration, oxygen partial pressure and combustion front temperature. The reaction order in both carbon concentration and oxygen partial pressure was unity for dry combustion run. Where in the wet combustion run, the reaction order in carbon concentration and oxygen partial pressure was unity and < 0.5 respectively. Dabbous and Fulton[28] postulated a reaction of nearly first order with respect to oxygen concentration. Burger and Sahequet[38] also substantiated these results as they observed that when the oil saturation and the specific area were low, the activation energy increased. Fassihi et al.[55] studied the reaction kinetics of in-situ combustion of three different kinds of crude oil having API gravity of 9.5, 11.2 and 18 °API. They observed that the activation energy for LTO and fuel deposition reactions were almost similar and almost twice as high as for the fuel combustion. The activation energy decreased as clay and metallic additives were added to sand mixture. The activation for combustion reaction in the original core was found much lower than in the sand mixture and almost independent on the API gravity of the crude oil. At LTO reaction, a higher Arrhenius constant was obtained without a significant change in the activation energy when copper was added to the sand mixture and it was different for different oils. They also found that the reaction order with respect to fuel concentration did not change, whereas the reaction order with respect to oxygen partial pressure varied and was always less than one. Finally, they concluded that the three chemical reactions (LTO, MTO, and HTO) were kinetically controlled, and diffusion effects were minimal.

Vossoughi et al.[42] found that there was a significant reduction in activation energy of crude oil combustion resulting from the addition of clay to the mixture. When sand was used with bitumen, a lower activation energy and higher values of the Arrhenius pre-exponential factors were obtained for both reactions (LTO and cracking)[56]. These results were in support of a catalytic effect by sand in both the oxidation and cracking of bitumen. The decrease in the activation energy in the presence of sand appears to be a catalytic effect rather than a thermal effect. The use of crushed cores may distort the results as original permeability, porosity and the porous network are dramatically altered.

Phillips and Hsieh[57] studied the effect of oxygen partial pressure at 175-300 °C (LTO region) using Athabasca tar sands. They found the reaction to be first order with respect to oxygen partial pressure when oxygen was in the range of 5.25-22.0 volume percent. Hughes et al.[19] investigated the effect of oxygen partial pressure and sand surface area on the overall activation energy of the process as well as on the peak burning temperature. They found that an increase in oxygen partial pressure and specific surface area of the sand caused a decrease in both the activation energy and the peak temperature.

3.1.5 Laboratory Experimental Investigation of In Situ Combustion

Five main types of experimental apparatus have been used to study the reaction and behavior of air injection process to improve oil recovery.

3.1.5.1 Differential Thermal Technique (DTA, TGA, DSC, and PDSC)

This technique has been used to identify the physical and chemical changes that crude oil undergoes during an in-situ combustion process as function of temperature or time. Milligram samples of oil and sand are used. In this technique, air is passed through the cell chamber or through the sample at constant heat flux and also to a reference. Differential Thermal Analysis (DTA) involves the measurement of the difference in temperature between the sample and the reference. Thermogravimetric Analysis (TGA) entails the continuos recording of the weight changes produced when heating a sample at constant rate, this technique is complementary to DTA technique since the weight variation data are related to the DTA peaks. Differential Scanning Calorimetry (DSC) measures the deviation in heat flow for the crude oil sample compared with a reference. DSC is operating at low pressure (< 10 bar), where PDSC operates at medium pressure (up to 100 bar). The effluent gas is analysed by a gas chromatograph (GC). The DSC usually calibrated with two recommended standard reference materials (Indium and Zinc), both of that have known heats and temperatures of diffusion. Several combustion parameters can be obtained directly from TGA/DSC data. These include minimum front temperature, heating value of the crude oil, amount of fuel deposited, the average hydrogen carbon (H/C) ratio, $CO/CO+CO_2$ ratio, and the kinetic parameters such as activation energy during combustion process.

3.1.5.2 Effluent Gas Analysis (EGA)

This method involves charging a reactor cell with a mixture of sand, oil, and water. The cell is then heated at constant rate of temperature increase, whilst air is passed through the sample at controlled flow rate and pressure. The effluent gas is then analysed continuously for oxygen and carbon oxides content.

3.1.5.3 Combustion cell

A combustion cell uses tens of grams of oil and sand it can be run at constant temperature or variable temperature (increasing at constant rate). The air flows through the cell at constant flow rate during each run. This means that this system takes into account the effects of flow. The variable temperature run is very similar to the behavior of a reservoir element a head of the combustion front, the temperature in the core sample is increased linearly with time by thermocouples, and the effluent gases are analysed and measured. The reactivity of different oils can be obtained from the combustion cell/Oxidation cell. However, the effect of residence time is not taken into account.

3.1.5.4 Adiabatic Rate Calorimeter

It is designed to assess the oil ability to self sustain the heat generation process in adiabatic conditions in the presence of oxygen at reservoir conditions. It is also used to measure the rate of heat released by any reactions to study and characterize the exothermic and oxidative kinetics of crude oils under air injection. It adiabatically follows reactions without disturbing it in any way and is capable of obtaining reaction kinetic parameters based on Arrhenius kinetic theory. Small amount of oil and core are only required, adiabatic conditions are maintained by using electrical heaters to match the temperature of the surroundings to that of the sample. A separate electrical heater is used to raise the temperature of the sample to the selected initial temperature and then adiabatic conditions are maintained as the temperature and pressure increase due to exothermic reaction of the sample. If there is no increase in temperature due to exothermic reaction, the instrument operates in "heat-wait search" mode by using the sample heater to produce a series of temperature steps until exothermic reaction is detected. Temperature is controlled with thermocouples placed on the bomb and on the outer walls of calorimeters that contain heaters.

The instrument is sensitive enough to detect self-heat reaction rates down to 0.02 °C/min and at the same time fast enough to track reaction rates over 200 °C/min. It is capable of operating at pressure up to 400 bar and at a maximum temperature of 500 °C, these operating conditions can cover any possible reservoir conditions.

There are many types of Adiabatic Rate Calorimetry such as Accelerating Rate Calorimetry (ARC), DIERS vent-size package (VSP), and PHI-TEC II. The Calorimeters have been used by many researchers as quick and relatively inexpensive tool aiming at developing a screening tool for the application of air injection as an Improved Oil Recovery process in light oil reservoirs. The crude oil & rock sample is usually subjected to "closed" system testing i.e., fixed amount of air initially at reservoir pressure over the sample. Amoco and University of Bath have upgraded ARC under "flowing" condition i.e. the oil & rock sample is under a continuously replenished stream of air at reservoir pressure. Yannimaras et al.[4] found that some oils are more equal than others in their suitability for air injection are. They also concluded that ARC data could provide insight in explaining the occurrence of the LTO and HTO reactions in ISC. They postulated that the basis for using ARC to select oils for air injection depends on whether there is a continuity or discontinuity of the oxidation exotherm during their screening of oils for air injection using ARC. If the oxidation exotherm shows a continuous curve (Figure 3.5, Oil B), then the oil is considered a good candidate for ISC. On the other hand, if the oxidation exotherm shows a discontinuity (Figure 3.5 Oil A), ISC will be difficult as the natural temperature rise is limited and the reaction remains in the LTO region.

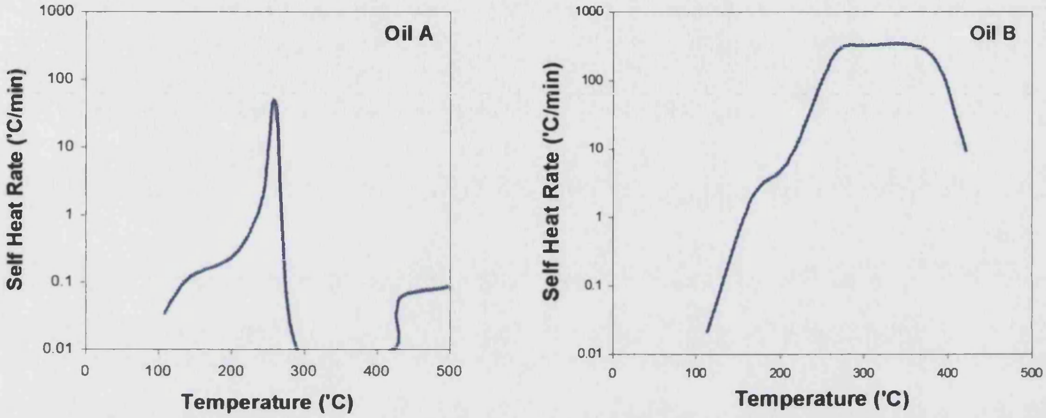

Figure 3.5: ARC Exotherm Profile (Yannimaras et al.[4])

Gillham et al.[58] used ARC to study the chemical kinetics of W. Hackberry oil. They observed autoignition and significant temperature rise within 5 days period. Indeed, field results confirmed this conclusion.

Reactivity tests performed by Zelenko et al.[59] with a closed ARC apparatus on different mixture of oil and oxygen proved that, in a certain range of temperature and oxygen partial pressure, LTO and HTO zones are separated by the NTC zone where oxidation reaction is almost stopped. If oxygen partial pressure is high enough to pass through this NTC zone, oxidation reaction proceeds to reach the HTO zone. The NTC zone was also observed by Greaves et al.[53] during their study of exothermicity and kinetics of crude oil oxidation using PHI-TEC II. They concluded that the temperature drop in the NTC zone is due to a change in the reaction mechanism or a shortage of oxygen at the start of the second reaction mode. Therefore, the closed ARC system can hardly be used to select reservoir oil for air injection in a heavy oil reservoir since oxygen partial pressure drops and reactions do not reach the HTO zone. For effective reservoir screening and real IOR simulators, it is essential that the kinetic measurements be made at real reservoir conditions; porosity, permeability, rock properties, pressure, temperature and flow condition. To meet these conditions a flowing ARC system or combustion tube experiments with consolidated core samples are recommended to study oil reactivity at reservoir conditions to avoid erroneous conclusions on field selection for air injection technique.

3.1.5.5 Combustion Tube

The combustion tube test is a dynamic experiment. The main purpose of the combustion tube facility is to enable physical simulation of the air injection, or oxygen enriched injection processes (HTO or LTO) at reservoir conditions of temperature and pressure. It provides an ideal platform with which to investigate dry or wet combustion and air injection (LTO) for either immiscible or miscible displacement. It provides a wealth of information such as combustion front velocity, oxygen consumption, air requirement, fuel requirement, and fluid displacement. A number of other in situ combustion process parameters are also determined from combustion tube such as peak temperatures, fuel laydown, and overall combustion stoichiometry. The combustion tube experiments have been the most commonly used approach for studying in-situ combustion in the laboratory. However, despite the comprehensive information obtained by combustion tube tests, these are expensive and time consuming.

The design of the combustion tube mainly consists of a high-pressure shell (up to 400 bar), a thin stainless steel tube of 80 to 210 cm long and 7 - 20 cm in diameter, gas injection system, sampling and analysis system. The combustion tube is packed with a mixture of reservoir sand, oil and water to simulate a section in the reservoir. To allow high pressure, the tube is placed in a large pressure shell and surrounded with heating collars or bands, which are used to compensate for heat losses so as to maintain adiabatic conditions. The annulus between the combustion tube and the outer shell is filled with highly efficient insulating material so that even at maximum pressures the effect of natural convection in the annulus is negligible. The annulus is pressurized with nitrogen or argon at a pressure that approximately (0.5-1 bar) higher than the injection pressure of the air into the tube to avoid any damage to the cell. The orientation of the tube can be horizontal or vertical, with air flowing from one end. As the sand pack is ignited the produced fluids are collected and analysed from the other end. Most of the combustion tube runs are performed vertically with air flowing from the top and the produced fluids are collected from the bottom to avoid gravitational segregation effects. In order to avoid gravitational segregation effects in the horizontal combustion tube system the pressure shell can be supported on steel rollers that enable the cell to rotate. An adiabatic condition in tube runs can be achieved either by insulative the tube with high levels of insully material or by reducing the temperature gradient between the sand pack and the environment surrounding the tube. Band heaters along the length of and surrounding the combustion tube have been used by many researchers to reduce the temperature difference[14,42]. Thermocouples placed along the axis and at the wall of the combustion tube allow the propagation of the combustion front to be monitored. In order to start combustion, the ignition temperature should be achieved either by spontaneous or artificial ignition. The effluent gases are analysed continuously, gases may be sampled in situ for subsequent chromatograph analysis. The amount of oil and water produced are measured and their main physical properties are determined (density and viscosity).

3.2 Air Injection into Light Oil

High-pressure air injection into light oil reservoir is basically different from the heavy oil in situ combustion process. It is important, therefore, to distinguish between these two processes. In both processes, a number of oxidation reactions take place.

For heavier crude oils, heat, and steam generation occur so that the subsequent viscosity reduction is the primary oil displacement mechanism. For light oil recovery, the heat generates is of secondary importance and the aim is to consume all of the oxygen in the injected air via low oxidation reactions with the principal objective of generating a flue gas (85% N_2 and 15% CO_2) for displacement of residual oil. The highest oxidation temperatures that can be reached are ± 800 °C and ± 400 °C, respectively, for heavy and for light oils. This difference in temperature is largely due to amount and nature of the fuel formed in the process.

3.2.1 Composition of Light Crude Oil

3.2.1.1 Hydrocarbon Compounds

Light crude oil contains a large number of complex and chemically diverse components. A typical crude oil can possess thousands of different components, and consequently the classification and grouping of oils is a very difficult task. However, a crude oil may also be characterised by physical properties as well as its chemical structure.

SARA analysis provides a usefull method of describing crude oils as these fractions have been shown to possess characteristic common properties. It divides the oil up into its saturates, aromatic, resins, and asphaltene fractions. These fractions are lumped chemical spieces having the same functional groups displaying similar chemical behavior. During oxidation, however, they do not react in similar manner, so it is expected that the individual SARA fractions will show distinct oxidation behavior. Some 80 to 85 percent of a light crude oil is composed of saturates and aromatics, with the rest resins and asphaltene.

Saturates and Aromatics

The saturate and aromatic hydrocarbon compounds can be divided into three classes: paraffin, naphthenes, and the aromatic groups. The proportion in which they occur in crude oil various from one crude to another. These differences in hydrocarbon composition will also effect the oil density and viscosity.

Paraffins: Saturated hydrocarbon with straight or branched chain. These comprise the alkane, alkene and alkyne series, of respective general formula C_nH_{2n+2}, C_nH_{2n}, and C_nH_{2n-2}. At low conversion and pressure of a few atmospheres, higher paraffin's is selectively cracked to form olefins, methane, and ethane. Small amount of hydrogen and propane are also formed[60].

Naphthenes: Saturated hydrocarbons containing one or more rings, each of which may have one or more paraffin side chain. With the general formula C_nH_{2n} for the ring structure. Naphthenes tend to produce tars and coke more readily than paraffin's, presumably because they can readily dehydrogenate to aromatics.

Aromatics: Aromatics hydrocarbons are cyclic in nature and are derivatives of benzene, which has the formula C_6H_6. Aromatics hydrocarbons has general formula C_nH_{2n-6R} where R is the number of rings. Aromatics found in the crude oil include benzene, toluene and xylene. Aromatics cause health and environmental problems, for instance, benzene is a documented carcinogen and a priority pollutant. Aromatics also have low smoke points (i.e. burn with a smoky flame). Alkyl aromatics tend to make coke and tars because of tendency of benzyl radicals to combine or added to other aromatics to make heavier species, which ultimately condense to polynuclear aromatic.

Asphaltenes and Resins

Asphaltenes: Asphaltenes are recognized as brown to dark-brown powder materials at room temperature and are normally precipitated in pentane or heptane and soluble in toluene or benzene. It consists of high-molecular-weight polyaromatic, aliphatic chain, and naphthenic rings with linkage of heteroatoms such as N, O, and S. Due to its polar nature, asphaltene tends to agglomerate into larger aggregates. Asphaltenes have high particle mass, are larger in size (10-35 μm), and tends to contain oxygen and sulfur compounds, organic and inorganic salts, porphyries, (and thus the metals).

Resins: Resins are deep red to brown in color and semisolid material. It is also contain polycyclic ring compounds that are insoluble in the bulk of the crude oil but are soluble in n-paraffins. They are less aromatic than asphaltene, but also contain hetroatoms (S, N, O, and metals).

3.2.1.2 Non-hydrocarbon compounds

There are some non-hydrocarbon compounds associated with light crude oils as impurities. These compound include sulphur, oxygen, and nitrogen, as well as compounds containing metalic constituents, such as vandium, nickel, iron, and copper.

3.2.2 Air injection into light oil reservoirs using (LTO) Technique

Recently air injection in low temperature oxidation (LTO) mode has been developing as a production process for extraction of light crudes. This has been investigated since 1994, by Total[2], Amoco[3] and University of Bath[53, 61]. The aim in air injection using LTO mode is not to burn the oil as in the thermal method, simply remove the oxygen by LTO reaction, so generating a flue gas for displacement of the residual oil. Air injection (LTO technique) offers some advantages over the full ISC technique: it consumes less oil, operates at lower temperatures (reservoir temperature), and may be easier to control.

The main restriction on the air injection in LTO mode is to ensure a sufficiently long residence time in the reservoir for complete oxygen removal. Also, the reservoir should have sufficiently high temperature, and the oil is reactive to consume oxygen at the lower temperature. This should not present too many problems in deep light oil reservoirs which has a fairly long well spacing and have relatively high temperatures (100-140 °C).

Light oils contain lighter paraffinic components that are highly reactive to oxygen, and light crude oils are more susceptible to partial oxidation at low temperature than heavy oils because of their relatively high hydrogen content[28, 62]. In light oil reservoirs, the oxygen is consumed by spontaneous LTO reactions, producing a flue gas comprising 10-14% CO_2 and N_2. For many light oil reservoirs where the residual oil saturation, post-waterflood, is low, the reactions may be limited to LTO. The reaction zone in the LTO process is characterized by a steadily decreasing oxygen-concentration profile in the reservoir, which may extend (Figure 3.6).

Three main zones can be distinguished in the reservoir as shown in Figure 3.6

- A zone around the injector swept by the injected air in which the residual oil saturation is low. The reservoir oil in this region is partially oxidised.
- An oxidation zone where oxygen is consumed by the residual oil left after flue gas sweeping. In this case, the oxygen concentration in the gas phase progressively decreases from 21% to 0%.
- A wide zone downstream of the oxidation zone, swept by the flue gas at reservoir temperature. Carbon oxides are generated by the oxidation's reaction, but flue gas contains mainly nitrogen (85%).

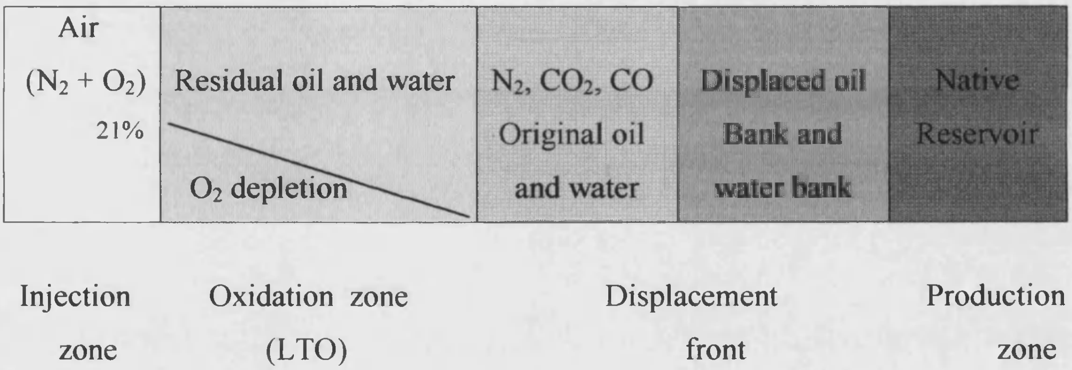

Figure 3-6: Schematic diagram of Air Injection LTO Process

Oxygen in the injected air is totally consumed, or reduced to a sufficiently low level by oxidation reactions with the oil. If oxygen is not totally consumed problems can occur at the production well, such as corrosion, bacterial growth, and the creation of emulsions due to accumulation of oxygen in the reservoir. There is also the risk of explosion.

The light oil air injection LTO process could be applied to many reservoirs, either for secondary (pressure maintenance), tertiary (DDP of water flooded reservoir) and in others where nitrogen, or flue gas injection is suitable. If spontaneous ignition is expected due to the high reactivity of the light oil, then it may be possible to control the process by lowering the air injection flux.

The displacement efficiency from region swept by air injection LTO process will be lower than when operating in the full in situ combustion mode. In theory, the light oil air injection (LTO) process can be operated until the injected air/produced oil ratio reaches the economic limit, or the contact between the flowing air stream and the oil is no longer sufficient to remove the oxygen before the flue gases reaches the production well.

During studies of the feasibility of air injection technique (LTO) process in light oil reservoirs, Sakthikumar et al.[2] and Greaves et al.[61] showed that the oxygen was depleted to very low levels and a considerable amount of CO_2 was produced (5 - 12%). The production of carbon oxides is most probably due to decomposition of oxygenated species produced at low temperature oxidation. This suggests the following overall reaction for the air injection LTO technique:

$$\text{Oil} + O_2 \longrightarrow \text{Oxidised Hydrocarbon} \longrightarrow CO_2 \quad \ldots\ldots\ldots\ldots(3.6)$$

During an air injection test, Sakthikumar et al.[2] observed that the production of oil continued after flue gas breakthrough. This can be contributed the effect of gas drive due to generation of CO and CO_2 by LTO. Kisler and Shallcross[34] used the EGA technique, at low pressure to investigate the oxidation kinetics of a light Australian oil, they found that more LTO occurring for the light oil compared with the heavy oil. Clara et al.[63] carried out a laboratory evaluation, to investigate the potential application of an air injection in light oil reservoir (Handil Field). Isothermal Disc Reactor experiments were performed on a large temperature range (92 to 210 °C) to assess the stoichiometry, the reactivity of oil with air, and to characterize the kinetic parameters of the oxidation reactions. Also, they run isothermal air-flood experiments to simulate the air sweeping at reservoir temperature (92 °C) when the thermal effects are not dominant. From the first sets of experiments they conclude that at least two reactions were required to describe the fact that oxygen is not only used to form carbon oxides and water, but also stable oxygenated components, a two step reaction scheme was proposed.

$$CH_x + \frac{y}{2} O_2 \rightarrow CH_xO_y \quad \ldots\ldots\ldots\ldots\ldots\ldots\ldots\ldots\ldots(3.7)$$

$$CH_xO_y + \left[\frac{2+\beta}{2(1+\beta)} + \frac{x}{4} + \frac{y}{2}\right] O2 \rightarrow \frac{1}{1+\beta} CO_2 + \frac{\beta}{1+\beta} CO + \frac{x}{2} H_2O \quad \ldots\ldots(3.8)$$

CH_x and CH_xO_y are respectively called fuel and polar compounds. They called the first reaction "oxidation reaction" and second reaction "combustion reaction". In first reaction oxygen is consumed to form polar compounds, where in the second reaction the oxygen react with the polar compounds to form the combustion gases CO_2 and CO.

Two activation energy were calculated, one for oxidation reaction (90 to 175 °C), and the other one for combustion reaction (170 to 210 °C). The two activation energy were 70 kJ/mole and 103 kJ/mole respectively. From the second set (isothermal air-flood experiments), they observed low CO_2 and CO production. The flue gas produced flux had the following molar composition: N_2 : 98%, CO_2 : 2%, and CO <<1%.

A high-pressure oxidation tube was used by Greaves et al.[64] to investigate oxygen consumption and the improved oil recovery from light oil reservoir using air injection technique (LTO process). The oxidation tube (1.25 m in length and 10 cm ID) was originally designed for in situ combustion. Three major modifications were made on the tube to facilitate very low rate air injection for LTO mode. Their modifications are:

- A low rate mass flow controller was used to control the air injection flux at rates equivalent to 10-100% HCPV/day.
- A gas sampling tube (1/16") was inserted into the production line (just below the sandpack) in order to take fluid samples for gas analysis.

- A liquid/gas separator equipped with a level detector was combined with a high-pressure liquid accumulator having a large volume. This system was used to measure the oil and water production rates.

Several oxidation tube experiments using low air injection rates with 100% in situ fluid saturation of the sandpack with North Sea light oils were conducted at 200 bar and a reservoir temperature of 110-120 °C. Complete oxygen consumption and high levels of produced CO_2 (12%), and CO (1.4%) were obtained.

Salford University[54] found that LTO reaction of light crude oils is normally associated with a high level of carbon oxide production. Carbon oxide production accounted for around 30% of oxygen consumption at low temperature oxidation. Also they found that the oxidation reaction appear to be limited to the low temperature region in wet formation with depleted oil saturation. Tiffin and Yannamaras[65] used a combustion tube of 1.8 m long and 7.6 cm in diameter to investigate the effect of pressure on the air injection process for light oils. Twenty-two heaters of 7.6 cm wide each were used to heat the tube wall, to maintain adiabatic conditions in the tube. Eight runs were performed using two light oils of about 35° API and a natural reservoir rock. Reservoir temperatures were at 120 °C for California runs and 90 °C for Hackberry runs with different operating pressures ranging from 68 to 370 bar. The main characteristics of these tests were very high air flux 35-165 scm/m^2-hr resulting in very high displacement front velocity and heat wave velocity. The combustion tube was operated vertically with a downward flow of fluids. Before ignition nitrogen was injected in order to simulate the flue gas displacement during the air injection process. The main conclusions obtained from these tests were: the oxygen utilization was 80 to 95%, higher air injection rates found to be required at higher pressures to sustain the combustion front, air injection can be a viable oil recovery process for light oil reservoirs and additional water from waterfloding had little effects on combustion tube results based on a comparison with similar testing without waterfloding. Flue gas generation and oil displacement characteristics were good at all runs.

Low Temperature Oxidation process has been observed during the normal air injection into a pilot project in water flooded reservoir in the Kinsella field[66], which has API gravity of 20°. Initially it was designed as an in-situ combustion pilot project, but the pilot performance was characterized by low temperature oxidation as the maximum recorded temperatures in the observation well was 189 °C. The incremental oil recovery as result of air injection using LTO process was estimated to be 1.2% of the original oil in place with 10-11 mole percent of carbon dioxide. A similar LTO process was observed in Borislav field, former Soviet Union[10]. The reservoir temperature is about 50 °C and the project is operated at low air injection rates (10,000 sm3/d), the LTO process was not recognized until it was reported that the viscosity of produced oil increased by 2-2.5 times (from 30 to 60-70 mPa.s).

3.2.3 Spontaneous Ignition phenomenon

In light oil reservoirs due to LTO, a slow and mildly exothermic reaction is promoted whenever air contacts crude oil within the reservoir at reservoir temperatures. In situation where heat losses by convection and conduction are relatively small, the LTO generated heat could accumulate within the rock causing the oil temperature to rise to ignition levels. Spontaneous ignition in light oil reservoirs is usually signaled by two indicators: a sharp rise in sand-face temperature, typically by 150 – 300 °C, and a drop in the oxygen concentration in the produced gas[67].

The ignition delay, (t_i) is defined as the time required for the temperature at a point of porous medium to rise from its initial value up to (±200 °C). This temperature was chosen as one where the heat given out by oxidation reaction is greater than or equal to that lost by convection and conduction, in other word the oxidation rate is high enough to sustain the oxidation rate. It was found to be dependent on the reservoir temperature, porosity, permeability, oil and water saturation, and other parameters such as oil viscosity, activation energy, and oxygen supply. During spontaneous ignition process, the value of peak temperature increases and the location of the peak temperature moves backwards the injection well before taking off in the direction of the airflow[10].

Two methods of calculating the ignition delay time are reported in the literature (analytical approach[68] and numerical model[69]). The delay time could take between a few days to several months to occur in the field, it's estimate will assist operates in deciding the maximum lifecycle of the project. An ignition delay of 10-20 days is seen in oil reservoirs whose reservoir temperature are 50-60 °C. On the other hand, where the reservoir temperature is higher than 70-80 °C, the ignition take place very quickly[10]. Delay time is expected to be only few hours in the presence of a plentiful oxygen supply[1]. The distance at which the spontaneous ignition found to occur increased with an increase in the flow rate. The spontaneous ignition potential of super light crude oil has API gravity of 51.1 was investigated by Abu-Khamsin et al.[67] using adiabatic packed bed reactor. Different parameters such as initial reactor temperature, oxidation gas flux, oxygen concentration in the oxidant gas, initial oil and water saturation and reactor pressure were varied to determine the set of conditions that would cause the sand oil mixture to ignite spontaneously. All attempts to ignite the oil failed even when they made the tests at very favorable ignition condition (174 °C initial temperature and 70 bar reactor pressure). They reflect the failure of super light crude oil to self ignite to its low content of unsaturated, the weight percent of SARA fractions in the super light oil are 80%, 19.5%, 0.3, and 0.2 respectively. Samara et al.[70] performed a series of ARC and TG/PDSC tests on oil rock system from three light oil reservoirs to screen and evaluate the potential of the air injection process in these reservoirs. They observed from isoaged tests that two oils are likely to autoignite at the reservoir condition and they need low activation energy in the range of 25-32 kcal/g mole in order to favor autoignition. The third oil showed no positive impact of the rock material on the start of exothermicity; it did not respond at all during isoaged test.

The absence of autoignition in a laboratory test does not necessary predict the field performance because the reservoir is usually more adiabatic.

3.2.4 Air injection into light oil reservoirs using full-in situ combustion Technique

The application of air injection full in-situ combustion in light oil reservoirs is initiated, if the reservoir contains a sufficient reactive crude oil, which can spontaneously ignite and create the required exothermicity to increase the reservoir temperature to the combustion temperature of that crude. The application of full in-situ combustion technique depends mainly on reservoir temperature and pressure, and on the oil and rock properties. The other critical factor for the success of full in situ combustion process is the need for the oxidation kinetic to operate in the bond scission mode[71]. Also, the air injection capacity must be sufficient to deliver the required flow rate of oxygen to the oxidation reaction region to sustain the combustion front. If the air flux is not sufficient to sustain full in situ combustion process in light oil reservoirs, then the air injection process will continue as LTO process (gas flood). The parameters influencing the air/oil ratio are reservoir porosity, initial oil saturation, and air and fuel requirements. In light oil reservoirs, typical oxidation front temperature of 200 °C to 400 °C can be reached[63]. When a high temperature front is ignited, four main zones can be distinguished in the reservoir and they areas following:

- The zone swept by the combustion front, where the residual oil saturation is low and the temperature higher than the initial reservoir temperature.
- The oxidation front area, where oxygen is consumed. Temperature is high (250 - 400 °C), a part of the original oil is burned (about 5 to 10% OOIP) and CO_2 and CO are produced. The gas formed by remaining nitrogen from the air and the combustion gases is called flue gas (typically 85% of N_2, 13% of CO_2, and 2% of CO) and sweeps the reservoir downstream.
- A short zone downstream of the combustion front where thermal effects participate to the formation of oil bank, this oil bank is partially displaced by the flue gas and by the hot water or steam front.
- A wide zone downstream of the combustion front, where no thermal effect occurs. This zone contains original oil and is swept by the flue gas.

An adiabatic air flood experiment was carried out by Clara et al.[63] on light crude oil (Handil field) to investigate the feasibility of air injection full in situ combustion process in the field. Their results show the ability of air injection to displace a stable high temperature oxidation front in Handil field. An average oxidation front temperature of 271 °C was achieved. The generated flue gas by oxidation process at high temperature was very efficient in term of CO_2 production, with an average molar gas composition of 12% of CO_2, 1% of CO, and 87% of N_2. The produced fluid was strong oil-water emulsion, therefore not possible for them to get on line distinct oil and water productions. Combustion tube tests were carried out at high initial water saturation by Greaves et al.[72] to investigate the feasibility of air injection into a light oil reservoir, using an oil with API gravity of 38.8°. The initial oil and water saturations were 45 and 50% respectively; the operating pressure was 70 bar. The peak temperature during these runs was in the range of 220 to 340 °C. The high levels of oxygen in the produced gas are an indication that the process was low temperature combustion rather combustion, limited by fuel availability and the high water saturation. Greaves et al.[24] found that in light oil if the oil rock reactivity were high, full in situ combustion reaction would take place that with a sufficient high air injection rate and combustion front can propagate through the reservoir.

Kisler and Shallcross[73] studied the effect of metallic salt on the oxidation kinetic of a light Australian crude oil using Effluent gas analysis (EGA). They found that an addition of metals such as sodium, copper, and iron to the Australian oil and quartz sand mixture enhances the fuel combustion reactions and sustained the combustion front. The addition of 1.0 mol% iron nitrate solution to the light oil and quartz sand mixture led to the formation of stable combustion front. Greaves et al.[12] used combustion tube to investigate the EOR by forward ISC of North Sea Forties light crude oil (36.6° API gravity). They conclude that it was not possible to sustain a stable combustion front using a clean silica sand media without first incorporating a clay additive, or other combustion surface promoter. Also they observed that changing the mode of combustion from dry to wet greatly reduced the air requirement and the fuel consumption were found; 31% of that required for dry combustion. During wet combustion, the highest oil recovery achieved was 79% of the initial oil in place oil. Gillham et al.[58] used high pressure, automated adiabatic combustion tube to test Hackberry oil and core mixture, in order to determine if a stable combustion front can be propagated in-situ at a pressure of 3,500 psi. The oil recovery was 88% of original oil in place, fuel deposition was 1.85 Ibm fuel/ft^3 and the air requirement was 193 scf/Ibm fuel. These experiments showed a rare behavior sign in the peak temperatures. They interpreted this behavior either as oscillation between the LTO and HTO combustion mode, or as a very efficient displacement of light oil by flue gas and steam. As the combustion front passes this low fuel region, in-situ combustion temperature decreases resulting in increased oil and fuel deposition ahead of the combustion front and thus combustion front heats up again to high temperatures.

3.3 Influence of Reservoir Properties on performance of Air Injection Process

The success of any air injection process depends on the reservoir characteristic and the combustion process. Therefore, the knowledge of the geological characteristics is important for a complete evaluation of the oil recovery prospects.

3.3.1 Reservoir Heterogeneities

Permeability Barriers

Permeability barriers can have both positive and negative effect upon the air injection process. As a positive effect, vertical permeability barrier can divide a thick reservoir into smaller units, which may be more compatible with air injection process. Vertical barrier can also act as seal to upward migration of injection air and may result in a more uniform burning in relatively thick reservoirs. As negative effect horizontal permeability barrier can reduce the reservoir continuity and recovery. The actual value of permeability has very little effect on the mechanics of air injection process.

Natural Fractures

Fracture and joints are one of the reservoir properties that may create preferential flow channels and influence the recovery. A thin zone of high permeability at the top of the reservoir extending from one well to another constitutes a hazard to air injection process by thieving air and starving the combustion front of needed oxygen.

Presence of Gas Cap

Presence of a gas cap or a thin layer of high gas saturation at the top of the sand is not a desirable geological feature for the air injection process because they can act as thief zones for the injected air and promote non-uniform burning. The presence of a water aquifer should not be an impediment to the success of air injection project.

Many successful air injection projects were implemented in reservoirs with active aquifer[74]. The aquifer in these projects not only provided pressure support to the reservoir but also acted as a medium to transfer the heat ahead of the combustion front.

From the above discussion, we can note that the reservoir heterogeneity can have adverse effect on any air injection project.

3.3.2 Other Important Reservoir Characteristics

Reservoir depth

The reservoir depth is particularly important since it has a pronounced effect on the fraction of the introduced heat that remains in the reservoir "heat efficiency". The upper limit for depth is related to the heat losses between the surface and the reservoir and to the constraints of high-pressure injection. On the other hand, the shallower depth would severely limit the pressure at which the air could be injected to obtain good injectivity without exceeding the fracture pressure. Economically successful combustion projects have been implemented in reservoirs ranging in depth from 100 to 3450 m[74]. Depth however, is a factor in term of temperature, pressure, and well cost, deeper reservoirs are usually hot enough, that spontaneous ignition if in situ hydrocarbon is likely upon air injection. On the other hand deeper reservoirs required high injection pressure consequently large compressor are needed to meet the injection pressure requirements, larger compressor are more expensive to purchase, operate and maintain. Depth also effects the fluid lifting cost. Thus economic and operation considerations will impose the upper and lower depth limit.

Reservoir thickness

Sand thickness is one of the more important parameters for the air injection process. The large difference in density between air and the reservoir fluids gives the air a tendency to override the oil column and consequently by pass much of the oil if the reservoir exceed a critical thickness. A thin oil sand tends to counter this override tendency and favor a more uniform displacement. If the sand, however, is too thin high overburden heat losses may drop the temperature below that necessary to sustain a combustion front and can lead to low temperature oxidation. Preferably pay thickness should at least be four feet and should not exceed 50 feet[74].

Structure Inclination and Dip

Structure attitude and dip are important consideration in the location of wells for a combustion project. Injected air and combustion front movement will be more rapid toward up dip wells than toward wells low in structure. In a dipping reservoir, it is advisable to locate the air injector's down-dip and production wells up the structure to compensate for expected flow of air up dip. Turta[25] recommended locating the ISC pilot at the upper most part of the structure. The reason behind this recommendation is that the burning volume of the pilot located at the upper part of the reservoir can be more accurately be determined and both air oil ratio and the incremental oil recovery due to combustion can be estimated more reliably.

Porosity

High porosity is attractive, since it directly reflects the volume of hydrocarbon that the rock can hold. Therefor the economic success of air injection project is dependent more on the actual value of the oil saturation-porosity product (ϕSo) than on porosity. As porosity decreases, the amount of heat stored in the rock increases. Turta and Singhal[10] pointed out that the air injection is not feasible in low porosity matrix reservoirs due to heat losses within the matrix. In the U.S., economically successful air injection projects have been implemented in reservoirs whose average porosity range from a low of 0.16 to high of 0.38[74].

Oil Saturation

As oil content is function of porosity and initial oil saturation, then the higher the porosity and the residual oil saturation after primary and secondary phases, the more attractive an air injection project. Although there is no limit to oil content of a reservoir for air injection, but a minimum oil content is required to consume the injected oxygen in the injected air and to offset the consumption of oil as fuel during the air injection process. Also, a certain amount of oil content is required to make the air injection operation profitable.

Composition of reservoir matrix

The economic and applicability of air injection process in any reservoir is dictate to a large extend by the natural and amount of fuel formed in the reservoir. Considerable laboratory and some field evidence exists in the open literature indicated that the mineralogical composition of the reservoir rock can effect the amount of fuel available to sustain combustion front. The clay and metallic content of the rock as well as its surface area has a profound influence on fuel deposition rate and its oxidation rate as mentioned earlier.

Effect of well spacing

Problem may arise in two ways when determining well spacing. If the well spacing too close, the combustion front may experienced early gas breakthrough, in the other hand if well spacing is too large, the oil production rate will be slow, consequently prolonging the life of the project and making the economic unattractive.

3.4 Commercial Field Projects Using Air Injection

A review of some of these projects is carried out in order to emphasise the important factors, which contributed to the success of the Air injection process in light oil reservoirs.

Until 1979, ISC process was commercially applied mainly in heavy oil. The extension of the ISC to light oil reservoirs was very slow due to the misconception about non-sufficiency of fuel deposited which would not sustain the ISC front. The widespread acceptance of high-pressure air injection into light oil reservoirs as an IOR process started in 1994, when the results of commercial high-pressure air injection processes in the Williston Basin were published. These results were reported after 15 years of commercial operation[10]. Air injection into light oil reservoirs can be divided in two principal modes[77]:

- The conventional drive process, in which a combustion front displaces the oil horizontally such as in Medicine Pole Hills Unit field.
- Drainage process, in which the injection of air into a dipping reservoir causes gravity drainage such as, West Hackberry field.

The designing of air injection project for light oil with knowledge of the critical technical and economical parameters of air injection can lead to attractive rates of return.

West Heidelberg Project

The air/flue gas injection project in West Heidelberg field began by Gulf in 1971, currently the field is operated by Chevron. The field was completed in sandstone formation at an average depth of 11,400 ft (3475 m), with a maximum dip of 15 degrees and a net pay thickness of 30 ft (9 m) in Cotton Valley Unit, Mississippi, USA. The original oil in place (OOIP) from the eight producing layers was estimated at 12 million barrels of oil of 27 °API gravity (15° downdip near the tar deposit) and a viscosity of 6 cp at a reservoir temperature of 220 °F (104 °C). The low primary recovery of 6.1 % was produced by liquid and rock expansion. The sharp decline of primary production was observed with a pressure decline from the initial value of 5100 psi to 1500 psi (347 to 102 bar). Three wells were used as injectors, two of them were used to inject air while the third was used to reinject flue gas for pressure maintenance. The combined air/flue gas injection has increased the ultimate recovery to 30% of OOIP[1]. As of 1994, the daily oil production was 400 BOPD (63.6 m^3) with an air/oil ratio of 10 Mscf/bbl (1,78 Msm^3/m^3)[25]. This project is classified as one of the deepest in situ combustion-assisted pressure maintenance operations [1,8,75,76].

Medicine Pole Hills Unit Project

It is the deepest air injection/in-situ combustion project in the Williston basin[77-79]. The field was discovered in April 1967, It is located near the southwestern flank of the Williston Basin and produces from the Red River carbonate formation which present at an average depth of 9,500 ft (2896 m), it contain 40 MMSTB as original oil in place of 39 °API gravity. The recovery mechanism under primary recovery was by liquid expansion with partial water drive, the primary recovery was estimated to be 15% of OOIP (6 MMSTB). In March 1986 Koch Exploration Company began post-primary air injection into the field after one year of comprehensive laboratory studies. There studies were conducted to design and to evaluate the feasibility of air injection in the field. They include reservoir fluid study, combustion tube tests and packed-column displacement study. The air injection was suspended after 2 months of injection due to the decline in oil price. In Oct. 1987, high pressure air injection operations were resumed and have continued to the present. The air is being injected into ten injectors at a rate of 12 MMscf/D (340 Msm^3/m^3) and a pressure of 4,300 psi (292.5 bar). The oil production was increased to 950 BOPD (151 m^3) with air oil ratio of 7.3 Mscf/bbl (1.3 Msm^3/m^3). As of 1998, the oil production was 600 BOPD (95.5 m^3) with air/oil ration of 12 Mscf/bbl (2.1 Msm^3/m^3)[10]. The air injection incremental recovery has been estimated as and additional 14.2%.

West Hackberry Project

During 1994 Amoco production company in partnership with the United State Department of Energy began the use of air injection for tertiary light oil recovery at West Hackberry field (salt dome oil field) in Southwestern Louisiana, after the reservoir had been watered out in 1993. The field was completed in Camerina sands at an average depth between 7500 and 9000 ft and permeability of 300 to 1000 md. The oil was of 33 °API gravity with a viscosity of 0.9 cp at a reservoir temperature of 200 °F (93.5 °C). The project represents a new EOR process which combines the double displacement process with air injection.[3,58,77] The goals of the project were to displace the oil by gravity drainage and to push the encroached aquifer toward its original water oil contact. Four million standard cubic feet per day (113 Msm^3/d) of injected air was split between the high pressure reservoir 2500 to 3300 psi (170 to 224.5 bar) on the west flank of the field and low pressure reservoirs 300 to 600 psi (20.5 to 40.8 bar) on the north flank. By May 1997, air injection had increased oil production in reservoir A (low reservoir pressure) and B (high reservoir pressure) by 60% above the normal decline.

The Horse Creek Project

This field is located in the south-center portion of the Williston Basin, Bowman County, North Dakota. The field was discovered in 1972 and completed in the Red River Formation (zone D) at depth of 9200 ft (2804 m) [80]. The reservoir porosity and average permeability within the Red River "D" zone were 12-20% and 10-20 md respectively. The reservoir fluid properties of the Horse Creek crude oil were 32.2 °API gravity, oil viscosity of 1.4 at a reservoir temperature and bubble point pressure of 198 °F (92 °C) and 625 psi (42.5 bar) respectively. The total cumulative primary production from the field prior to use air injection as secondary recovery was 3.3 MMBBLS (525M m^3) under liquid and rock expansion mechanism with an initial and final pressure of 4000 and 600-700 psi (272 and 40.8-47.6 bar) respectively. In May 1996, Total Minatome Corporation (U.S subsidiary of Total) started air injection into the field at rate of 8.9 MMscf/d (252 Msm^3/d). Six months after air

CHAPTER FOUR

EXPERIMENTAL APPARATUS AND PROCEDURES

4.1 Introduction

This chapter describes the experimental apparatus, which were used in this research. The SBR (Small Batch Reactor apparatus was designed to investigate the reactivity and kinetics of light crude oil oxidation at reservoir condition during air injection. The size of SBR was sufficient to allow samples of the oxidised light crude oil to be taken for analysis. In addition to the SBR, a Soxhlet apparatus, two gas chromatograph (Perkin Elmer Model 8500 GC and Perkin Elmer Auto System Gas Chromatograph), and CE-440 Elemental Analyser were used.

Detailed descriptions of the above mentioned apparatus, the preparation of samples and operating procedures are given below.

4.2 Small Batch Reactor Facility

4.2.1 Experimental Methodology

Small Batch Reactor (SBR) experiments were performed for the purpose of studying low temperature oxidation kinetics of light crude oil at reservoir condition. Three North Sea oils and an Australian oil were used in the research. The properties of these light crude oils are given below.

Table 4.1: Properties of dead light crude oils

	Australian oil	Oil C	Oil D	Esso Mix1 Oil
API Gravity	39	40	37	32.5
Density (cc @ 24 °C)	0.828	0.824	0.838	0.864
Viscosity (cp @ 20 °C)	30	36	75	79
Saturates *	65	74	71	N/A
Aromatic *	18	11	13	N/A
Resin *	17	15	15.45	N/A
Asphaltene	0	0	0.55	1.18
Carbon Percent	83.86	86.43	85.1	85.36
Hydrogen Percent	11.9	12.82	12.34	11.74
Atomic H/C ratio	1.7	1.78	1.74	1.65

* Osindero[81]

Five different sets of experiments were conducted using the SBR. They are as follows:

(1) Light crude oils alone: To study the alteration in physical properties of the oxidised crude oils accompanying the LTO process. The physical properties investigated were density, viscosity, asphaltene, and coke precipitation, simulated carbon number distribution and carbon and hydrogen fractions in the oxidised oils.

(2) Oxygen Consumption: The oxygen consumed during the oxidation of light crude oil producing water and carbon oxides was measured. The effect of oxidation temperature, crushed reservoir sand, initial oil saturation, water, initial water saturation, volume of air charged to the SBR, and the total pressure on the rate of oxygen consumption, reacted oxygen, and the production of carbon oxides were also investigated in this set of experiments.

(3) Effect of Oxygen Concentration: Oil D and crushed core D at an initial oil saturation of 15 % was used. The initial oxygen concentration in the reactor was varied from 5 to 21%. The other operating pressure and temperature were kept constant.

(4) Oxidation temperature (160 to 200 °C): This set of experiments was investigate the autoignition temperature which could occur during oxidation of light crude oils during LTO process.

(5) Oxidation Reactivity of Pure Hydrocarbon Compound: The oxidation of pure saturates and aromatics component was investigated using single organic component of particular interest was the composition changes occurring during LTO process. The single organic components used were n-pentane, n-hexane, toluene, xylene, iso-butylbenzene, n-hexylbenze, and n-dodecane,

4.2.2 Small Batch Reactor System

The SBR system used for the oxidation experiments is shown in Figure 4.1. In addition to the reactor, the system comprises gas injection, a computer for data acquisition and gas analyser.

SBR: The reactor is constructed from high-grade stainless steel (SS 304) and designed for operation to a maximum pressure of 400 bar and temperature of 200 °C. The reactor dimensions are shown in Figure 4.2. It was designed for the purpose of investigating the oxidation reactivity and composition changes of light crude oils at reservoir conditions, which are mainly the same as the reactor design specifications. The design calculations for the reactor are given in Appendix A-1.

The reactor consists of the main body and a reactor sealing-head. The main body consists of a thick-walled (15 mm) stainless steel cylinder measuring 150 mm long with an I.D. of 30 mm. One end of the cylinder is blanked and has a base 30 mm in thickness. The inner volume of the reactor is 85 cc. A glass sleeve insert (94 mm long, OD of 27 mm) was used inside the reactor to minimize the corrosion effect due to low temperature oxidation products. The head of the reactor has seven ports: Attached to the inlet/outlet port is a 15 μ filter and a high pressure ball valve, which allows charging and discharging of the reactor. A pressure transducer for continuous pressure measurement is connected to the port on the other side of the head. As a safety precaution, a third port was located on the top of the head to which a high-pressure relief valve (400 bar) was connected. Two of the other four remaining ports are equipped with 40 cm long K type thermocouples. There were used to monitor the temperature of the gas phase and liquid sand mixture inside the reactor. The other two ports were used as 1.6 mm sampling lines to obtain gas and oxidised oil sample for GC analysis.

Gas Injection System: The Gas system is consist of a set of high pressure (200 – 230 bar) air and depleted oxygen cylinders. The high-pressure air/depleted oxygen cylinder was used to pressurize/purge the reactor to the required charging pressure through a pressure regulator.

Heating System: Heat was supplied by an electric furnace. The furnace was controlled by a controller and power regulator. The electric furnace and furnace controller were supplied by Seven Science Limited (SSL) England, model TF105.4.5.1_z.F.

Computer System: data acquisition was achieved using a PC via Genie software [Bede Technology Ltd.].

Gas Analysis: The produced gases (CO_2, CO, and O_2) were analysed by two analysers. These were a Servomex Oxygen analyser 570A for oxygen analysis and Servomex 1440 Gas analyser for carbon monoxide and carbon dioxide analysis. A high inlet and low outlet pressure regulator was used to discharge the produced gas from the SBR, the produced gas is dried in a silica gel drier and passed to the oxygen, carbon dioxide, and carbon monoxide analysers. Some of the produced gases are also collected in a PTFE sample bag for analysis using a Varian Chrompack Gas Chromatograph to measure the concentrations of light hydrocarbon fractions (Methane, Ethane, Butane, and Pentane) in the produced gases due to LTO (low temperature oxidation) process.

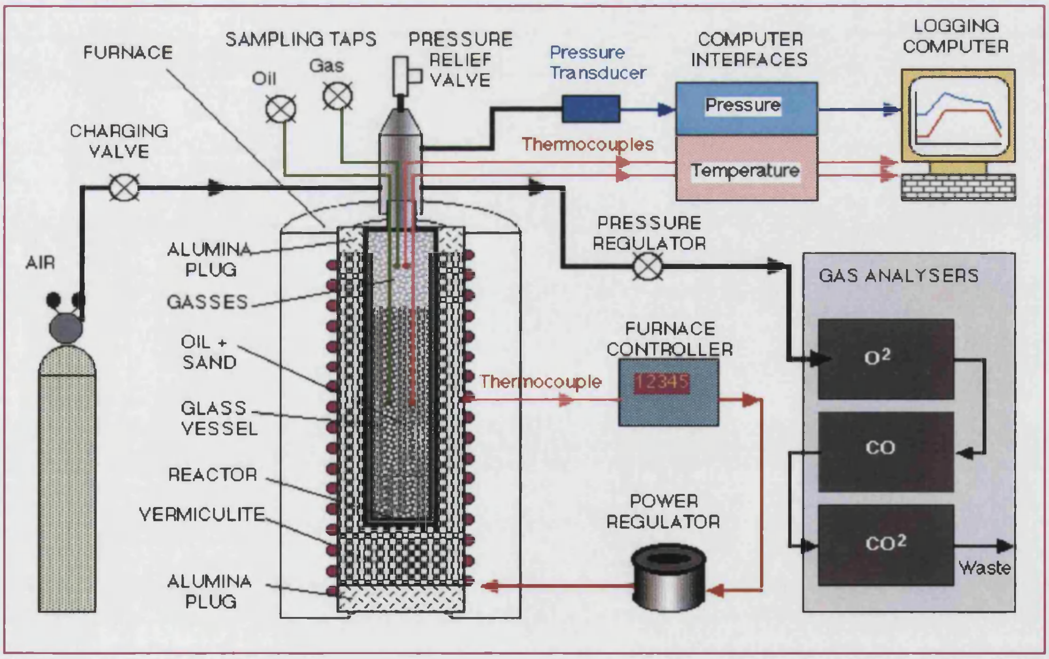

Figure 4.1: Small Batch Reactor System

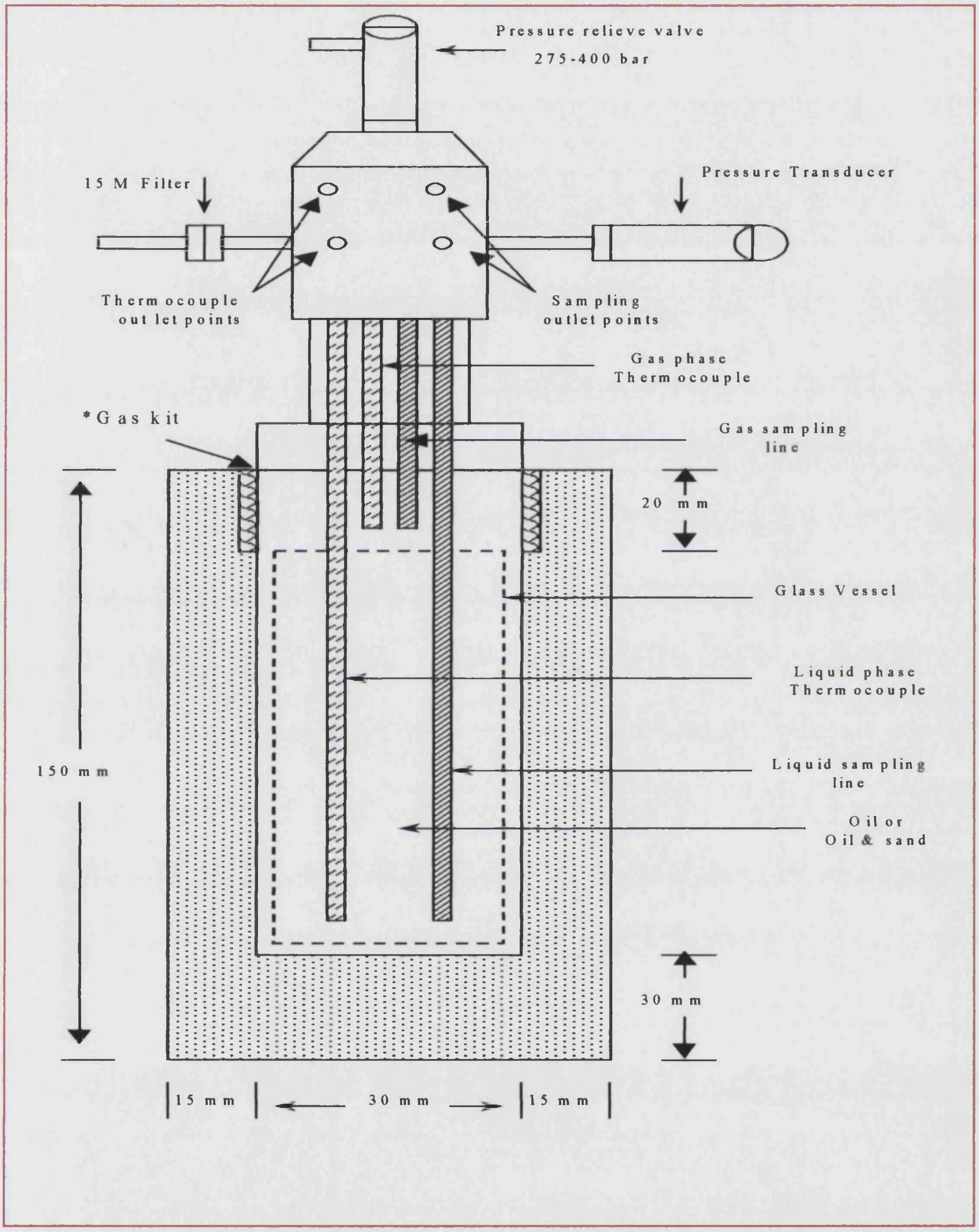

* The Gas kit was supplied by Bristol valve UK, it is made of Flouro-elastermer material

Figure 4.2: Schematic diagram of Small Batch Reactor

4.2.3 Sand Pack Preparation

Used Material

Crushed core D was used for all the experiments. This was a sandstone core from a North Sea reservoir. The properties of crushed core are given below.

Table 4.2: Properties of crushed core sand

Grain density:	2.31 g/cc
Particle size:	70% < 300μ 30% < 600μ

The amount of crushed core sand was used in all of the SBR experiments occupying a bulk volume of 34.4 cc in the SBR.

Stock tank oils were used in the research. The efficiency of light ends (C1 - C4) in the crude oil was not considered to have a significant effect on the LTO reaction. In the reservoir, the light ends are displaced ahead of the reaction zone by the air or flue gas. Distilled water was used instead of connate water, to reduce corrosion effect and eliminate possible catalytic effect of the steel wall.

The weight of crushed sand and the volume of oil and water needed to simulate the required oil and water saturation were calculate based on the above given properties.

An example of calculation of the combination of crushed sand, oil and water mixed to achieve desired oil and water saturations is given in Appendix A.2 and A.3.

Mixing Procedure

In order to closely simulate a water wet system, the crushed core sand was first mixed with distilled water at the required water saturation and left for one hour to ensure water wettability. The crude oil was added to the sand water mixture at the required saturation. Then all of the mixture sand, water, and oil were mixed together to obtain a uniform distribution of oil in the mixture. The oil, water and sand mixture was then packed in 10g aliquots into the glass vessel. Each 10g was packed to the same volume to ensure uniform porosity for each experiment. The glass vessel was then inserted into the main body of the reactor.

4.2.4 Operating Procedure

In the experiments, the glass holder in the reactor was charged with a known volume of the reactant, either oil alone, single pure organic component, or crushed sand, oil, and water mixture. The glass tube holder was inserted into the main body of the SBR and the top head of the reactor with the two thermocouples and sampling line connection was connected to the main body. The reactor head was torqued down to ensure a perfect seal. The SBR was then charged with reactant gas (air or depleted air) at the required pressure (100-150 bar). The free volume in the reactor (46.6 cc) was therefore full of air at the experiment pressure, including some of the initial gas in the pores of the matrix. The reactor was left for 2-3 hours to allow pressure stabilization. The reactor was mounted vertically in the electric furnace. The annulus between the SBR and the inner of the furnace was filled with vermiculite granules, to provide good insulation. The pressure transducer and the thermocouples were connected to the input card of the data acquisition system. The temperature of the electric furnace was then set to the desired run temperature and adjusted manually so as to ensure that the average temperature inside the reactor was within ± 1 °C of the required temperature. No shaking or stirring of the reactor occurred during the experiment.

For selected experiments (oil alone), oxidised oil and produced gas samples were taken at different periods of the experiment for compositional analysis. The loss of oxygen partial pressure and the oil during this sampling are estimated be approximately ±10% in each case. At the end of an experiment, the final reactor pressure and total oxidation time were recorded. The reactor was then taken out of the furnace and left to cool down to room temperature. The produced gas in the reactor was then discharged through a pressure regulator to the gas analysers, to determine the percentages of CO_2, CO and oxygen. Samples of oxidised oil or the sand oil mixture were stored in glass sampler jars for further analysis. For the experiments with sand and oil, the glass vessel contents were unpacked in sections to allow for visible analysis of the oxidised oil and sand.

4.3 Soxhlet Extraction and Distillation unit

The unit was used to separate asphaltenes and coke from the oxidised crude oil mixture, either from oil alone or from oil sand mixture. The unit is consisted of a condenser, flask, thimble, and electric heater. A photograph of the Soxhlet extractor unit is shown below.

Figure 4.3: Photograph of the Soxhlet Extraction Unit inside Ventilation Cabinet

4.3.1 Crude Oil Extraction

In the case of oil and crushed core small batch reactor experiments, the oxidised oil was extracted from the crushed sand and then subjected to asphaltene analysis. In the standard extraction test, the mixture of oxidised oil and crushed sand is placed in the thimble so that the solvent vapor rises through the mixture, condensed and then refluxed back over the sand oil mixture. This process extracts the oxidised oil.

Dichloromethane was used in first stage due to its low boiling point (36 °C) and Toluene used in the second stage to ensure that all of the crude oil was extracted, including the heavy. The detailed procedure is described in Appendix B.1

4.3.2 Asphaltene and Coke Separation

A standard method (ASTM D 3279-90)[82] was employed for asphaltene and coke precipitation. In this method, the crude oil sample is washed and refluxed with paraffinic solvent (n-heptane) to separate the oil sample into two maltenes (soluble) and the asphaltene and coke (insoluble). The yield and quality of asphaltenes depends on the type and volume of the solvent used per unit volume of sample. The second stage of separation used toluene as the solvent to separate asphaltene from coke. Coke is defined as being insoluble in toluene, whereas asphaltenes are soluble.

Separation Procedure

n-Pentane and toluene were used, as solvent in preference to n-heptane and benzene. Even though n-heptane is more favorable due to volatility constraints and stability of asphaltene, n-pentane was chosen because it has a lower boiling point (38°C) as compared to n-heptane (98.4°C), and is easier to control the heating rate. Since a light crude oil consists of many light hydrocarbons, which are volatile at low temperature, using n-pentane will prevent the lighter hydrocarbons in the maltenes from being vaporized. The separation scheme is shown in Figure 4.4. The detailed procedure is given in Appendix B.2.

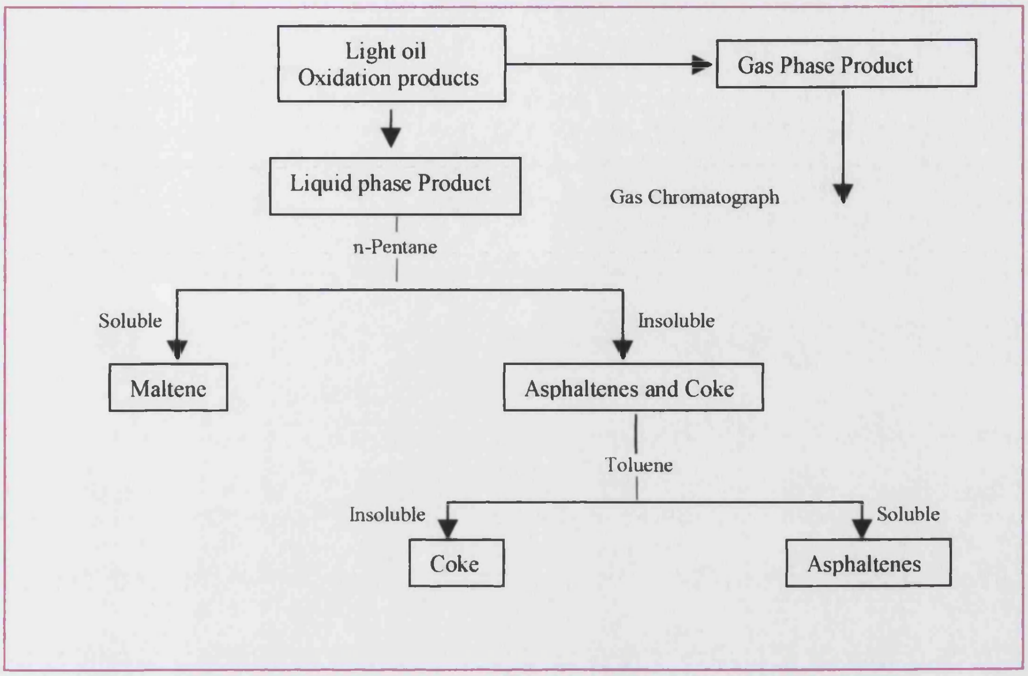

Figure 4.4: Separation Scheme for the oxidation product

4.4 Gas Chromatograph apparatus

Two gas chromatographs were used to analyse the samples of oxidised light crude oils and single organic components. The description and operating procedure for the two gas chromatographs are as follows:

4.4.1 Perkin Elmer Gas Chromatograph Model 8500:

This gas chromatograph was used to analyse the unreacted and oxidised light crude oils. The weight percent of each component in the crude oil was calculated by comparison of the GC trace with an external standard. The physical features of the gas chromatograph are shown in Figures 4.5 and 4.6.

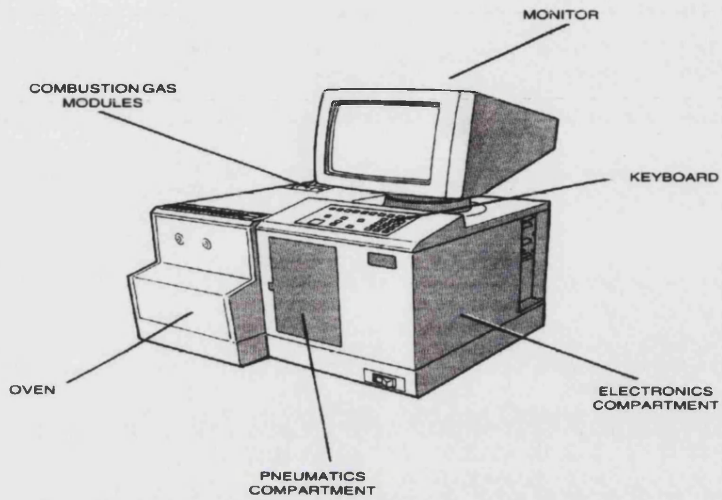

Figure 4.5: Schematic of Perkin Elmer Gas Chromatograph Model 8500

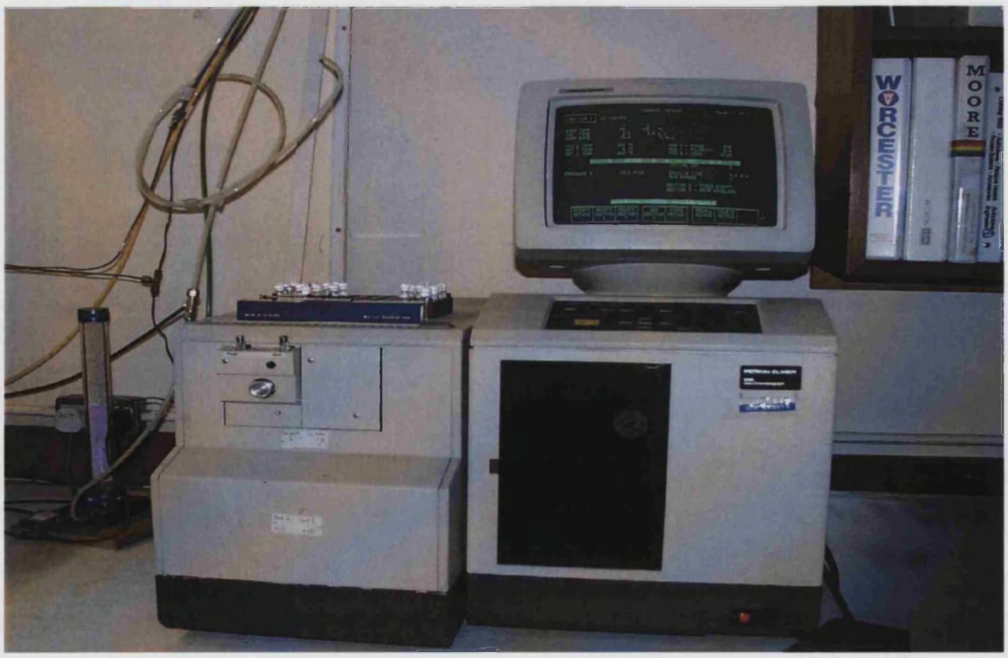

Figure 4.6: Photograph of Perkin Elmer Gas Chromatograph Model 8500

4.4.1.1 Instrument Description

The instrument is made up of three main units; the analyser unit, keyboard unit, and the visual display unit (VDU).

Analyser unit: This unit consists of an analytical oven, an electrical compartment, and a pneumatic compartment. Inside the oven is a column, which is connected to an injector at the top and a detector at the bottom. A sample mixture enters the carrier gas stream via the injector, and moves on the column where the separation takes place. After passing through the column, the sample components enter the detector and produce an electrical signal, which can be used to measure the quantity of each component percent.

Keyboard unit: There are three types of key on the keyboard unit; function keys, soft keys, and numeric keys.

Visual display unit: This unit is used together with the keyboard on the chromatograph to set up the instrument in accordance with the type of analysis required, and to display the resultant chromatograph. The VDU is connected to the chromatograph by a multicore cable but is not mechanically attached.

4.4.1.2 Sample Preparation:

The samples were prepared by diluting 0.1 ml of the standard, unreacted crude oil or oxidised oil with 0.9 ml carbon disulfide in a vial using adjustable pipette. This was sealed with an aluminum crimped septum rubber seal using hand crimper. The mixture was shaken vigorously for 3 min until the mixture was solubilized completely. The carbon disulfide was added to lower the viscosity of the sample mixture and to dissolve high molecular weight materials, it is also miscible with crude oil and has slight response with FID.

Before carrying out the analysis the oven temperature, isothermal time, ramp rate, injection temperature, detector temperature, flow rate, and carrier gas need to be determined. These parameters are shown in Table 4.3.

Table 4.3 Perkin Elmer Gas Chromatographs (Mod. 8500) operating conditions

	Perkin Elmer GC Mod. 8500 *Heavy comp. Method (C_{10} - C_{44})*	*Perkin Elmer GC Mod. 8500* *Light comp. method (C_5 - C_9)*
Sample injection size	1.0 µL	1.0 µL
Dilution ratio	0.1 mL / 0.9 mL	0.1 mL / 0.9 mL
Column	50.8 cm x 0.3175 cm	50.8 cm x 0.3175 cm
Carrier gas	Helium	Helium
Detector	Flame Ionization Detector (FID)	Flame Ionization Detector (FID)
Detector temperature	400 °C	200 °C
Injector temperature	350 °C	150 °C
Temperature program	Start @ 40 °C, isothermal 2 min, 15 °C/min to 350 °C, Isothermal 6 min	Start @ 40 °C, isothermal 10 min, 5 °C/min to 150 °C, Isothermal 6 min

Calibration of the Method;

- An External standard (ASTM D5307 Crude Oil Qualitative Standard) was used to calibrate the generated method and obtaining the response factor of each component.
- The GC standard was supplied by "SUPLECO INC USA".
- The paraffinic components in the standard are C10, C11, ….., C36, C40, C44.
- One µL of diluted standard was injected manually using micrometer syringe; the run key was pressed at the end of injecting the sample to perform the analysis. The chromatograph of each component in the standard appears with its retention time on the screen to the end of the run. At the end of the run, the FID signal returns to the baseline and a report page appears. The relative amount (concentration) of each component in reported page should read the same concentration given in the ASTM Standard.

- When the run finishes the instrument goes into cooling down period, during which time "Cool-Down" is displaced. When the oven temperature has reached the initial oven temperature again, the instrument goes into equilibrium again in preparation for the next run.
- A second method was produced and calibrated for light hydrocarbon standard using same procedure as used for heavy hydrocarbon standard. The retention time and response factor of light hydrocarbon (C5, C6, C7, C8, C9) were obtained.
- For reproducibility and accuracy of the two methods, three samples from each standard were injected and analysed, the average response factor and retention time of the three runs were obtained and saved under a given name for each standard (Light components method and Heavy components method).
- Due to unavailability of the normal gas chromatograph printer, it was connected to a MAC SE PC via serial input port. This unable the analysis data to be printed and saved on floppy disc.

A sample report page of light components standard and heavy components standard is shown in Tables 4.4 and 4.5.

Sample Injection;

The crude oil samples were injected manually using the same procedure as for the GC standards (calibration procedure). The error expected due to the manual injection-using syringe was not known precisely, and the average of three injections was taken instead. A simulated distillation was obtained by assigning paraffinic carbon numbers to those compounds that eluting between Cn and Cn+1, to have a carbon number equal to n+1.

Table 4.4 Reporting page for the heavy components standard (Perkin Elmer GC Model 8500)

RUN 6 1/2/01
11:08

METHOD 1 HEAVY CULATION: EXT STD

RT	AREA	BC	RRT	RF	AMOUNT	NAME	GRP
2.93	1602.564	T	0.338	0.0039	6.25	C10	0
4.36	1736.111	T	0.477	0.0036	6.25	C11	0
5.54	1838.235	T	0.592	0.0034	6.25	C12	0
6.57	2083.333	T	0.693	0.003	6.25	C13	0
7.5	2083.3	T	0.787	0.003	6.2499	C14	0
8.38	1785.714	T	0.874	0.0035	6.25	C15	0
9.2	2083.333	T	0.956	0.003	6.25	C16	0
9.99	1689.189	T	1.035	0.0037	6.25	C17	0
10.73	1736.111	T	1.109	0.0036	6.25	C18	0
12.13	1689.189	T	1.249	0.0037	6.25	C20	0
14.58	1358.674	T	1.494	0.0046	6.2499	C24	0
16.64	1250	T	1.701	0.005	6.25	C28	0
18.45	1201.904	T	1.882	0.0052	6.2499	C32	0
20.04	1116.071	T	2.041	0.0056	6.25	C36	0
21.47	1041.667	T	2.184	0.006	6.25	C40	0
22.78	1096.474	T	2.315	0.0057	6.2499	C44	0

16 MATCHED COMPONENTS 100.00% OF TOTAL AREA
0 UNKOWN UNRETED PEAK TIME 0.00 % OF TOTAL AREA
16 PEAKS AREA/HT REJECT

Table 4.5 Reporting page for the light components standard
(Perkin Elmer GC Model 8500)

RUN 1	1/2/2001 13:19:00 PM						
METHOD 1	LIGHT	CULATION: EXT		STD			
RT	AREA	BC	RRT	RF	AMOUNT	NAME	GRP
0.14	770.1212	T	0.013	0.0099	7.6242	C5	
0.16	723.8	T	0.016	0.0105	7.5999	C5	0
0.22	788.1368		0.022	0.0095	7.4873	C6	0
0.23	743.1359	T	0.022	0.0103	7.6543	C6	
0.37	1030.54	T	0.036	0.0063	6.4924	C7	0
0.38	1579.810 3	T	0.038	0.0058	9.1629	C7	0
0.77	5054.3	T	0.076	0.003	15.1629	C8	0
1.77	3973.289	T	0.177	0.0038	15.0985	C9	
8 MATCHED		COMPONENTS			100.00% OF TOTAL AREA		
0 UNKOWN		UNRETED PEAK TIME			0.00 % OF TOTAL AREA		
8 PEAKS		AREA/HT REJECT					

4.4.2 Perkin Elmer Q-Mass 910 Gas Chromatograph:

The Gas Chromatograph Mass Spectrum was obtained for the oxidised pure organic component, in order to identify what new components were produced by LTO of the saturates and aromatics. It was also used to determine the increase or decrease of oxygenated hydrocarbons in the oxidized light crude oil. Figure 4.7 shows a photograph of the Perkin Elmer Q-Mass 910 system.

Figure 4.7: Photograph of Perkin Elmer Q-Mass 910 Gas Chromatograph

4.4.2.1 Instrument Description

The Perkin Elmer Q-Mass 910 system consists of the following component:

- Q-Mass 910 Bench top mass spectrum
- Perkin Elmer auto system gas chromatograph
- PC compatible DEC
- Q-Mass 910 analytical work station software
- NIST mass spectral data base and search software

4.4.2.2 Sample Preparation

Samples were prepared by diluting 0.2 ml of the unreacted and oxidised single organic component / unreacted crude oil and oxidised crude oil with 1.4 ml carbon disulfide in a vial. This was sealed with an aluminum crimped septum rubber seal using hand crimper. The mixture was shaken vigorously for 3 min until the mixture was solubilized completely. The carbon disulfide was added to lower the viscosity of the sample mixture and to dissolve high molecular weight materials.

4.4.2.3 Operating Procedure and Analysis

The following procedures are the basic steps involved in the operation and analysis of the GC Mass Spectrum:

Tuning the Apparatus

Before starting the analysis, the Perkin-Elmer GC-MS was calibrated. This involved using a standard contained within the MS unit. The calibration produces a specification table, which indicates for a specific range of mass, whether a high or low pass rating is obtained. The specification table for this analysis can be found in Appendix F.

Optimising the GC MS Operation

The operating conditions are given below.

Table 4.6 Gas Chromatographs (Q-Mass 910) operating conditions

	Perkin Elmer Q-Mass 910 GC
Sample injection size	1.0 µL
Dilution Ratio	0.2 mL / 1.4 mL
Column	BP 624, 25 m x 1.2 µm
Carrier gas	Helium
Carrier gas split	40:1
Detector	Q-Mass 910 Mass Spectrum
Detector Temperature	200 °C
Injector Temperature	200 °C
Temperature Program	Start @ 40 °C, isothermal
	10 min, 5 °C/min to 200 °C,

Full-scan Spectrum and GC Trace

Full TIC plot

This allows a full-screen display of the Total Ion Chromatogram of the analysed sample. It shows you where the major peaks are located, how many spectra were collected and the retention time of each spectra.

Peak Identification

A computer library search was used to find the compounds with matching MS spectra. These are then displayed by the computer as a list of up to 20 possible matches with similarity indexes of 0-100, representing how well the MS spectrum of that compound matches the identified peak. A high similarity index compound was used to identify the peak.

Peak Area Calculation

The area under the peak was calculated automatically by clicking on CALC. The calculated area represents the relative abundance of each compound in the sample.

4.5 Viscosity and Density Measurement

A photograph of the Viscosity meter and Density meters is shown in Figure 4.8.

4.5.1 Viscometer

The viscosity of the light crude oils and the oxidised oils was measured using a Brookfield-Digital Viscometer Model DV II.

Operating procedure: The oil sample was placed in the sample tube using a glass syringe. The viscometer was turned on after selecting the unit of measured viscosity (cp). The viscosity of samples was measured at 20 °C using a water bath temperature controlled. However ice was used to lower oil bath temperature. To avoid any errors in the measurements, the oil samples were handled carefully to prevent any contamination.

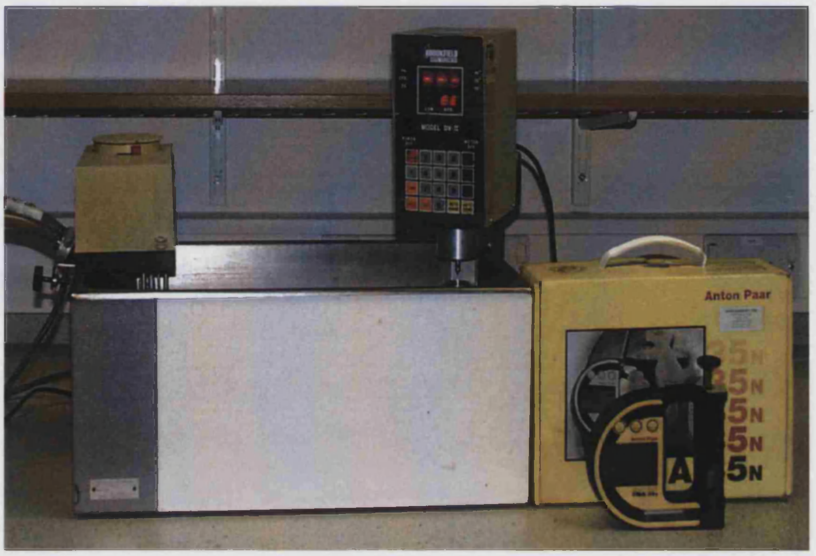

Figure 4.8: Photograph of Viscosity and Density Meters

4.5.2 Density Meter

The DMA 35_N density meter, supplied by Paar Scientific Ltd (U.K) was used to measure the density of the unreacted and oxidised light crude oils.

Operating procedure:

Before the density measurements, the density meter was calibrated using fluid of known density (distilled water). After switching the instrument on, the calibration fluid or oil samples were injected into the inner glass tube using a syringe. At that instant the digital density meter start measuring and displaying the density of the injected sample on the small screen of the density meter. To ensure reproducibility and accuracy, an average of stable reading from three tests for each sample was made. All of the density measurements were carried out at room temperature, which was in the range of 24 to 25 °C.

4.6 CE-440 Elemental Analyzer

The Elemental analyzer was used to carry out an elemental analysis of the unreacted and oxidised light crude oils in-order to determine any changes in C, H, N had occurred duo to LTO. It was not possible to determine S and O with this system. The system was fully automated, and provides high precision analytical data up to ± 0.3 %. The CE-440 is equipped with both static and dynamic combustion, which allow the combustion of a wide range of samples.

The operating and analytical procedures for the CE-440 are given in Appendix C.

In this research, the Elemental Analyzer was only used to determine the carbon and hydrogen content of the samples. A photograph of CE-440 Elemental analyzer is given in Figure 4.9.

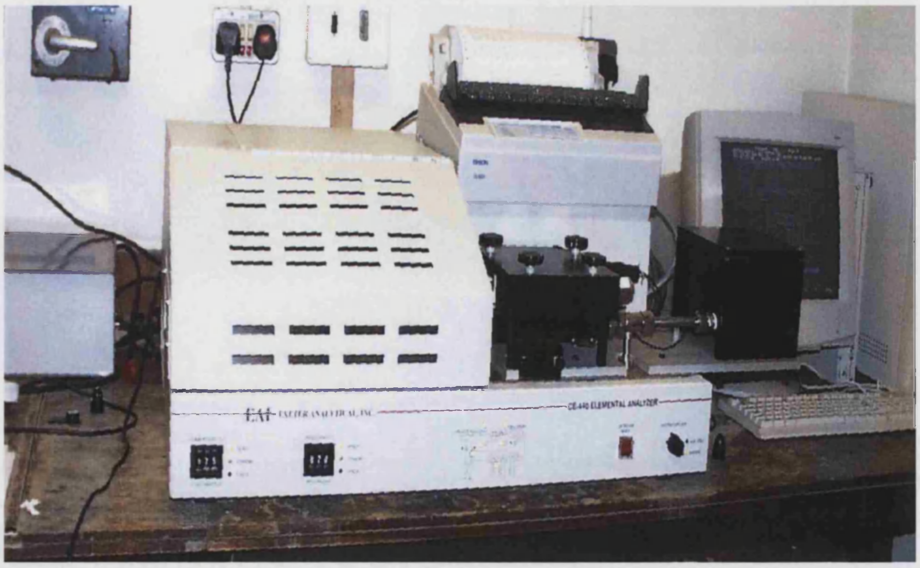

Figure 4.9: Photograph of CE-440 Elemental Analysis

CHAPTER FIVE

EXPERIMENTAL RESULTS AND DISCUSSION

PART I: INTRODUCTION AND GENERAL OBSERVATION

5.1.1 Introduction

Approximately 130 experiments were performed on four different light crude oils and eight single organic compounds using the Small Batch Reactor (SBR). The experiments were designed to simulate the oxidation reactions occurring in the oxidation zone (Figure 3.6).

In each experiment, the light crude oil either alone or in the presence of crushed core together with water (distilled water) were contacted with air injection at reservoir pressure. The reactor temperature was maintained constant throughout the experiment. The parameters that were varied included the reactor temperature, total pressure, oxygen inlet concentration, oil saturation, water saturation, gas residence time, and oil composition.

The effect that each of the above parameter had upon the produced gas composition at the end of experiment, the oxidation kinetics, oxidised oil composition and the autoignition temperature were determined and discussed in this chapter (part III, part IV, and part V).

An example of the analytic analyses of the experimental result is also presented in this chapter (part II).

5.1.2 General observations from SBR experiments

During the low temperature oxidation experiments of light crude oil, a number of interesting observations were made. The most important observations are described below:

1. The temperature control of the SBR was improved when the reactor was surrounded by vermiculite insulation, which also improved the pressure measurement as shown in Figures 5.1 and 5.2.
2. Below 110 °C, the rate of oxygen consumption was too small to measure accurately. Consequently, the data reported in this study are for an oxidation temperature equal of 110 °C, or above.

3. In all the experiments, LTO reaction was evidenced by a drop in reactor pressure due to oxygen consumption and the accompanies changes in the oil composition. In the later stages of reaction, the pressure decline reduced to a very low rate. The residual oil was then non reactive or complete oxygen consumption was achieved as shown in Figure 5.2 and 5.3.
4. The oxidation of light oil in the range 120-200 °C has produces four main products: CO, CO_2, oxygenated hydrocarbons and water. A small percentage of light hydrocarbon gases were also observed as shown in Figure 5.4.

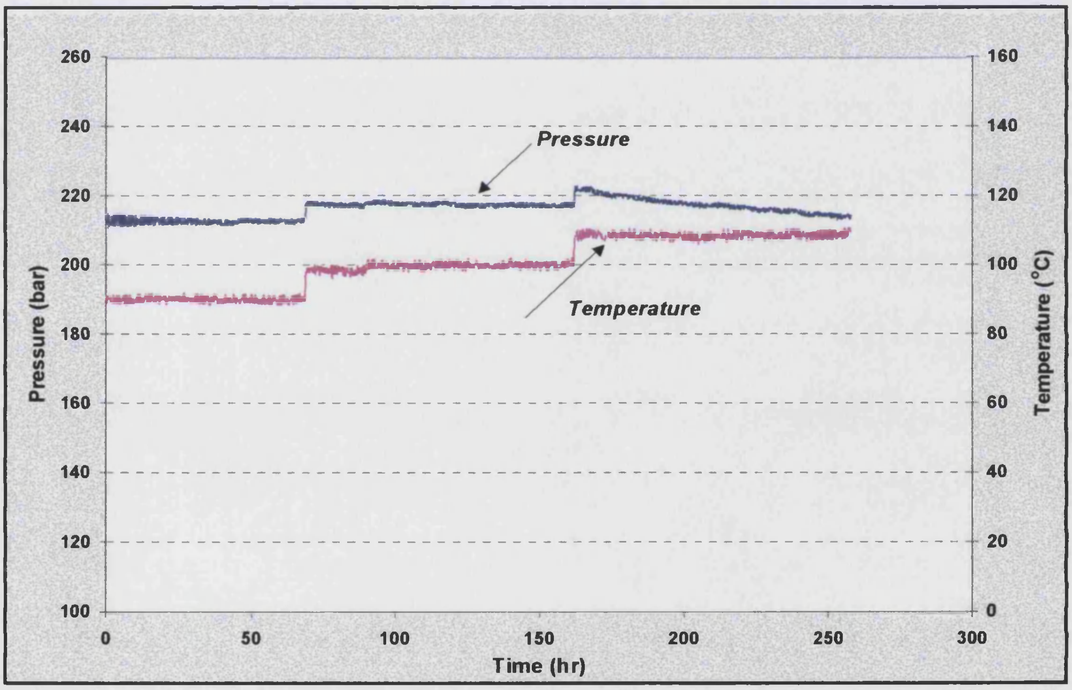

Figure 5.1:Pressure and temperature profile for SBR test with out using vermiculite (Pressure and temperature data recorded every 10 minutes)

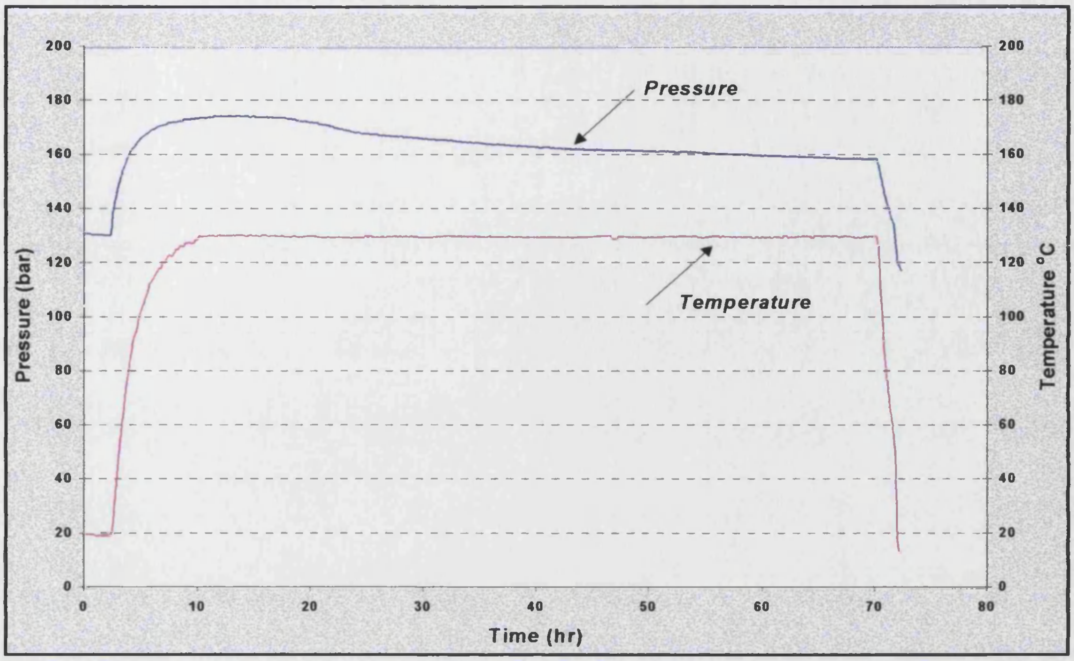

Figure 5.2: Pressure and temperature profiles for SBR test (Run 34) with vermiculite (Pressure and temperature data recorded every 10 minutes)

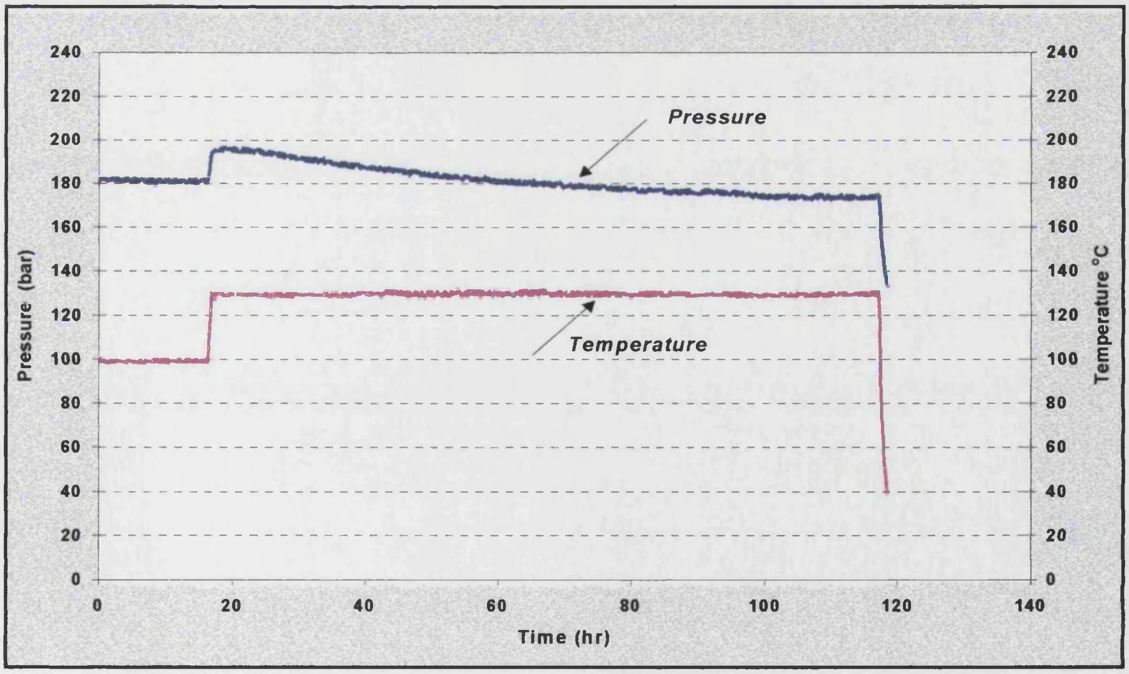

Figure 5.3: Pressure and temperature profile for SBR test (Run 76) (Pressure and temperature data recorded every 10 minutes)

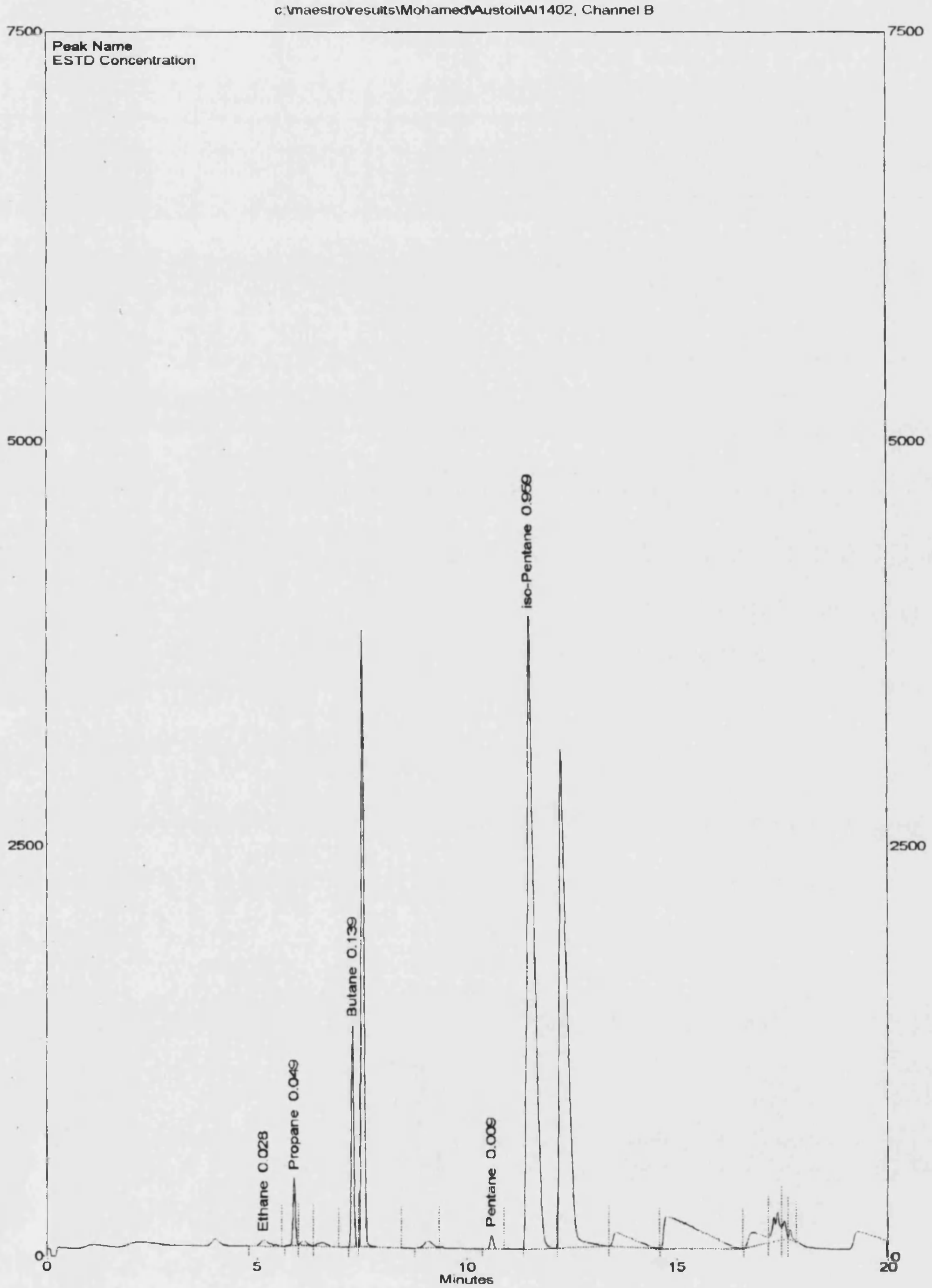

Figure 5.4: Produced light hydrocarbon during LTO reaction

5. The results obtained from the SBR experiments show that the carbon dioxide is one of the main products of the low temperature oxidation. In early stage of reaction , oxygen is incorporated directly into the hydrocarbon chain to form oxygenated products such as carboxylic acids, aldehydes, ketones, alcohols or phenols and also hydroperoxides. Hydroperoxides are unstable and eventually decarboxylate to form carbon dioxide and water, plus some carbon monoxide.
6. The oxygen consumption is always greater than the total produced carbon oxides. The variation of the produced gas composition as function of oxidation temperature is shown in Figure 5.5. Thus, there is a rapid decrease in the oxygen concentration initially (up to 115 °C) occurs at a lower rate beyond 110 °C. Both CO_2 and CO show a gradual increase with increasing temperature. At 140 °C, there is eventually complete oxygen consumption.
7. There is essentially very little difference between the gas phase and oil phase temperature inside the SBR as shown in Figure 5.6 and 5.7. Therefore, the oil phase temperature was used in the analysis of all the SBR experiments.

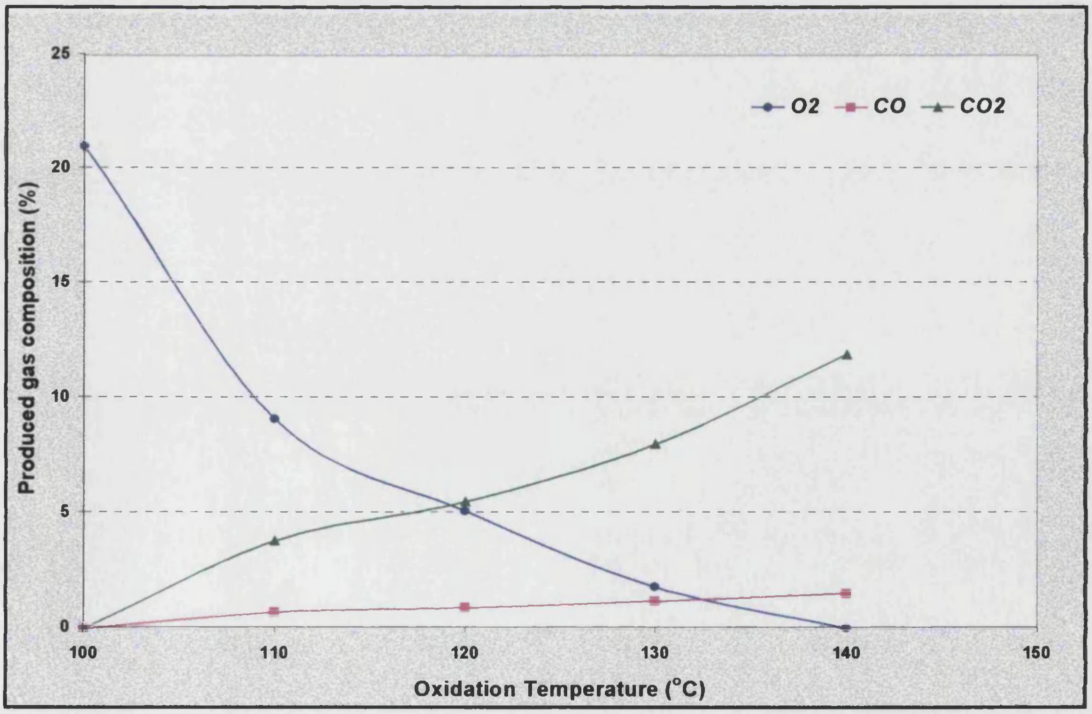

Figure 5.5:Produced Gases versus Oxidation Temperature for oil D (Soi=0.5)

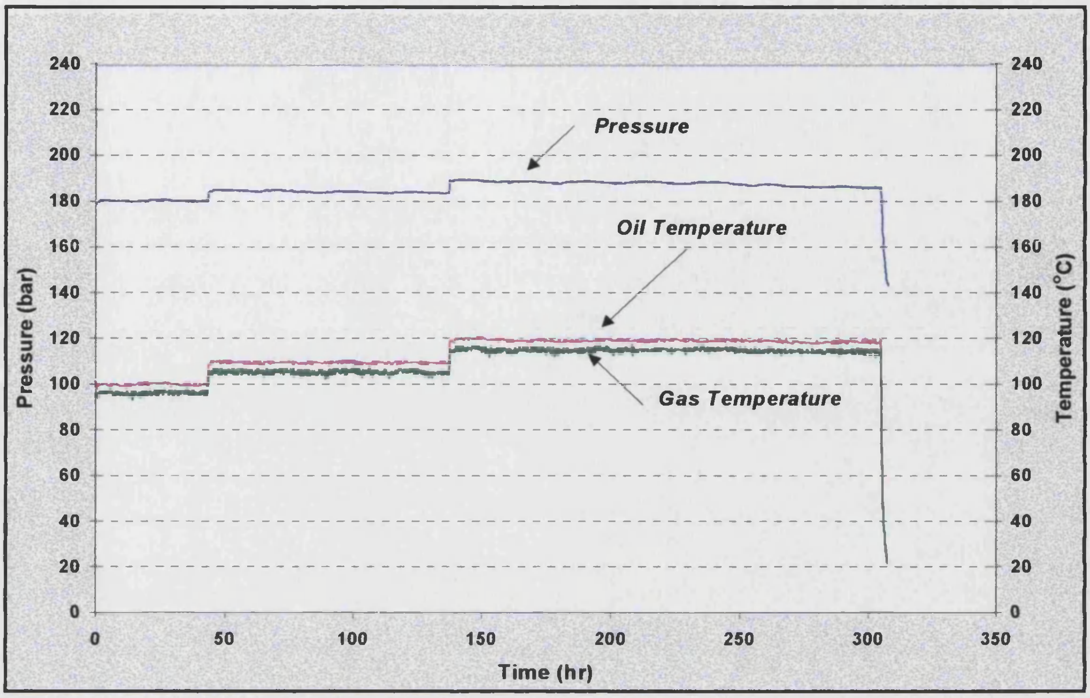

Figure 5.6: Pressure and Temperature Profile for SBR test, Loaded with Oil C alone (Pressure and temperature data recorded every 10 minutes)

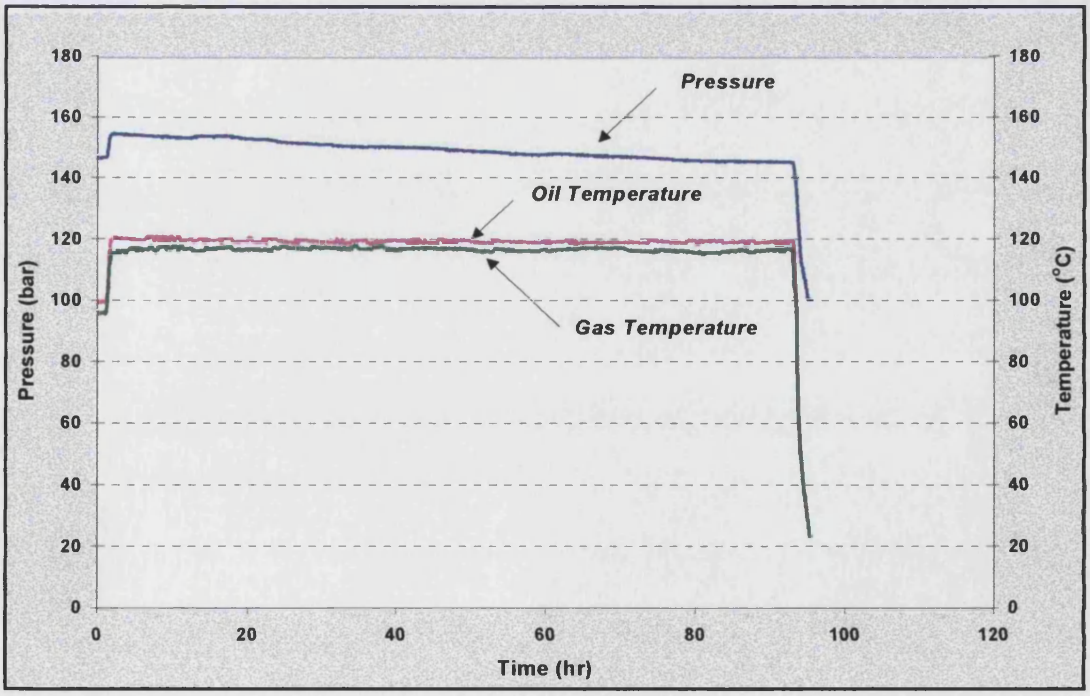

Figure 5.7: Pressure and Temperature Profile for SBR test, Loaded with Oil D alone (Pressure and temperature data recorded every 10 minutes)

8. At high oxidation temperature (>120 °C) and long oxidation periods (> 72 hr), asphaltenes and coke-like residue from the crude oil were deposited on the walls of the glass sample container inside the reactor (Figure 5.8a). This occurred in the case of the oil alone experiments (Runs 1-4, 23-26, 43-47, and 79-83). In experiments where oil and crushed core were used, a hard layer (crust) of asphaltene and coke was precipitated on the top of the packed matrix as shown in Figure (5.8b). The total amount of these heavy residues never exceeded 10% of the oil volume originally charged to the reactor.
9. During the SBR tests, there were several occurrences of corrosion attack of the stainless steel reactor vessel (SS 304). Deep pitting on the internal surface of the reactor tube wall occurred that was not protected by glass sample tube. Corrosion was also observed on the surface of the thermocouples where there was a contact between the thermocouples and oil/sand mixture, and also on the inlet/outlet connection tube (1/4") where sand and condensed liquids may have accumulated (this may have occurred due to gas discharge from a previous run). Severe damage to the thermocouples was observed when water was used with oil and sand as shown in Figure (5.9).

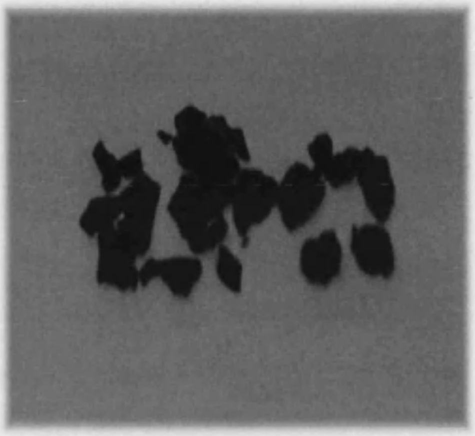

(5.8a)

Figure 5.8a: Residual like coke found on the wall of glass vessel

(5.8b)

Figure 5.8b Residual like coke (hard layer) found on the top of the core matrix

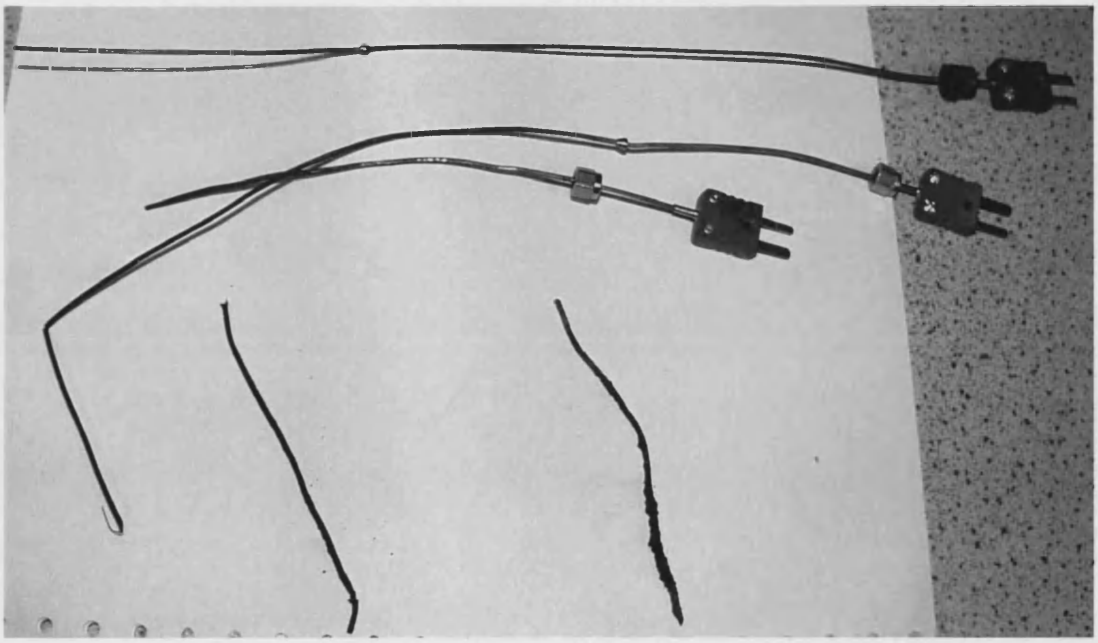

Figure 5.9: Corrosion of thermocouples during LTO reaction

PART II: CALCULATION OF EXPERIMENTAL RESULTS

5.2 Calculation of Experimental Results

The procedure followed in analysing the results of each experiments involved the following assumptions.

- Oxidation of oil occurred under isothermal conditions.
- Reaction took place under steady state conditions, i.e. hydrocarbon component was always in excess during the reaction period and the reaction order with respect to hydrocarbon was therefore equal to zero.
- The reaction order with respect to the oxygen partial pressure was assumed to be equal to one.
- The reaction rate constant is described by an Arrhenius type equation.
- Due to the complexity of the crude oil composition and hence the large number of possible reaction pathways even for a single component, the overall specific reaction rate was calculated for the whole crude. This was used to determine the kinetic parameters.
- It was not possible in the experiments to determine directly the amount of oxygen consumed by the oil to produce oxygenated hydrocarbons. It was therefore assumed that the production of one mole of water during the oxidation was accompanied by the production of one mole of carbon dioxide and one mole of carbon monoxide. A similar assumption was made by Fassihi et al.[51]

The following quantities were determined from the measured experiments data.

- Percent of consumed oxygen, reacted oxygen, and produced carbon oxides.
- Reaction Rate Constant (K) and kinetic parameters (activation energy , Arrhenius constant, and order of reaction with respect to oxygen partial pressure).
- Auto ignition temperature of the light crude oil
- The reaction path way of air injection LTO process.
- The change in composition of the oxidized crude oil.

The data for a total of 131 SBR experiments is tabulated in Appendix D (Table D.1 to D.27). Run number 67 (Table D.14) was selected to demonstrate the experimental calculation.

5.2.1 Calculation of Gas Composition

The initial fluid saturation of run 67 (150 °C and 205 bar) are:

Soi = 15%, Swi = 0.0%, Sgi = 85%

Total pore volume of sand pack = 17 cc (refer to Appendix A for more detail)

Oil density = 0.845 g/cc (measured by density meter)

Volume of free space in SBR = 46.4 cc (Refer to Figure 4.2)

Therefore :

Volume of oil = 2.55cc

Weight of oil = 2.55 x 0.845

= 2.155 g

Total air charged into SBR (ambient)= free gases volume in SBR + initial gas saturation

= 46.4 + 14.45 cc

= 60.85 cc

Initial oxygen partial pressure = 205.08 x 0.21

= 43.067 bar

Final produced gases (mole %)

O_2 = 1.8

CO_2 = 7.3

CO = 1.99

Final oxygen partial pressure @ 150 °C $= 186.36 \text{ x} \frac{1.8}{100}$

$= 3.36$ bar

Appling the ideal gas low

$$n = \frac{PV}{zRT} \quad \ldots\ldots\ldots\ldots\ldots\ldots\ldots\ldots \quad (5.1)$$

$$\text{Charged oxygen (mole)} = \frac{(60.85)(43.067)}{(83.14)(150+273.15)}$$

$= 0.07449$ mole

Oxygen consumed (mole) = final volume x Δp_{O2}

$$\Delta n = \frac{(p^1_{O2} - p^2_{O2}) - (V_1 - V_2)}{R(T_1 - T_2)(z_1 - z_2)} \quad \ldots\ldots\ldots \quad (5.2)$$

As the oxidation reaction occurs at isothermal condition (constant temperature), and drop in oxygen partial pressure is small (< 50 bar). Therefore, it is assumed that there is no change in the compressibility factor (z) during the oxidation. Consequently equation 5.2 can be written as:

$$\Delta n = \frac{(p^1_{O2} - p^2_{O2}) * (V)}{R(T)} \quad \ldots\ldots\ldots\ldots\ldots\ldots \quad (5.3)$$

$$\text{Oxygen consumed (mole)} = \frac{(43.07 - 3.36)(60.85)}{(83.14)(150+273.15)}$$

$= 0.06869$ mole

$$\text{Oxygen consumed (\%)} = \frac{0.06869}{0.07449} x100$$

$$= 92.21\ \%$$

$$\text{Reacted oxygen} = \frac{(consumed\ O_2\ x\ 32)}{charged\ of\ oil\ (g)}$$

$$= \frac{(0.06869x32)}{2.155}$$

Reacted oxygen $= 1.0199$ g O_2 / g oil

$$CO_2 \text{ produced (mole)} = \frac{(gases\ volume)(discharged\ pressure)(produced\ CO_2)}{(83.14)(discharged\ temperature + 273.15)}$$

$$= \frac{(60.85)(130.66)(7.3/100)}{(83.14)(24.6 + 273.15)}$$

$= 0.02345$ mole

$$CO \text{ produced (mole)} = \frac{(gases\ volume)(discharged\ pressure)(produced\ CO)}{(83.14)(discharged\ temperature + 273.15)}$$

$$= \frac{(60.85)(130.66)(1.99/100)}{(83.14)(24.6 + 273.15)}$$

$= 0.00639$ mole

Oxygen reacted to produce carbon oxides $= \dfrac{(mole\ of\ CO_2 + 1/2\ mole\ of\ CO)}{(total\ consumed\ oxygen)}$

$$= \frac{(0.02345) + (0.00639x0.5)}{(0.068688)} \text{ x } 100$$

$$= 38.79\ \%$$

Oxygen reacted to produce water $= \dfrac{(mole\ of\ CO_2 + mole\ of\ CO)}{(mole\ of\ consumed\ oxygen\ x\ 2)}$

$$= \frac{(0.02345) + (0.00639)}{(0.068688\ x\ 2)} \text{ x } 100$$

$$= 21.72\ \%$$

5.2.2 Calculation of Reaction Rate Constant

Generally, the oxidation of crude oil in a porous medium can be described by type rate equation:

$$\text{Ro} = -\frac{dn_{O2}}{dt} = \text{K } p_{O2}^{n} C_o^{m} \ldots\ldots\ldots\ldots\ldots\ldots\ldots\ldots \quad (5.4)$$

Where:

Ro = Reaction rate of oxygen

dn_{O2} = Change in number of oxygen moles per time

K = Reaction rate constant

p_{O2} = Oxygen partial pressure (bar)

C_o = Oil concentration

m,n = reaction orders

By assuming that the fuel (oil) is in excess i.e. the hydrocarbon availability is essentially constant (not depleted) during the reaction, and the reaction order with respect to the oxygen partial pressure is equal to one, equation (5.4) can be written as:

$$\frac{dp}{dt} * \frac{V}{RT} = \text{K } p_{O2} \text{ [oil] [sand]}$$

Where the quantities in the brackets are concentration term (oil and sand)

$$\int_1^2 \frac{dP_{o2}}{P} = \int \frac{k[oil][sand]}{V/RT}\, dt$$

$$\ell n \frac{Po_{2i}}{Po_{2f}} = \frac{K[oil][sand]}{V/RT} (t_2 - t_1)$$

$$\therefore K = \ell n \frac{Po_{2i}}{Po_{2f}} * \frac{V}{RT} * \frac{1}{[oil][sand][t_2 - t_1]} \quad \ldots\ldots\ldots\ldots\ldots (5.5)$$

Where:

K = Reaction Rate Constant (mole O2/bar.hr.cc.g sand)

p_{O2i} = Initial oxygen partial pressure (bar)

p_{O2f} = Final oxygen partial pressure (bar)

V = Volume of charged air (cm^3)

T = Absolute oxidation Temperature (^oK)

R = Universal gas constant (83.14 J/mole)

t_2 = Final oxidation time (hr)

t_1 = Initial oxidation time (hr)

[oil] = Initial volume of oil in the reactor (cm^3)

[sand] = Weight of sand (gm) (constant)

The reaction rate constant for Run 67 is determined as following:

$$K = \ell n \frac{Po_{2i}}{Po_{2f}} * \frac{V}{RT} * \frac{1}{[oil][sand](t_2 - t_1)}$$

$$= \ell n \frac{43.067}{3.354} * \frac{60.85}{83.14 * (150 + 273.15)} * \frac{1}{2.55 * 61.6 * 81}$$

$$= 3.47 \text{ E-07} \quad \frac{(mole\ O_2)}{(bar)(h)(cc)(g\ sand)}$$

The same procedure was made to analysis all of the SBR experiment, and the calculated results are reported in Appendix D (Tables D1 to D27).

5.2.3 Calculation of Reaction order with respect to oxygen partial pressure

The pressure decline data from a number of SBR experiments were analysed to determine the reaction order with respect to the oxygen partial pressure.

A typical example of the decline in total pressure in the reactor versus time (Run 67), as oxygen is consumed by low temperature oxidation (LTO) reaction is shown below.

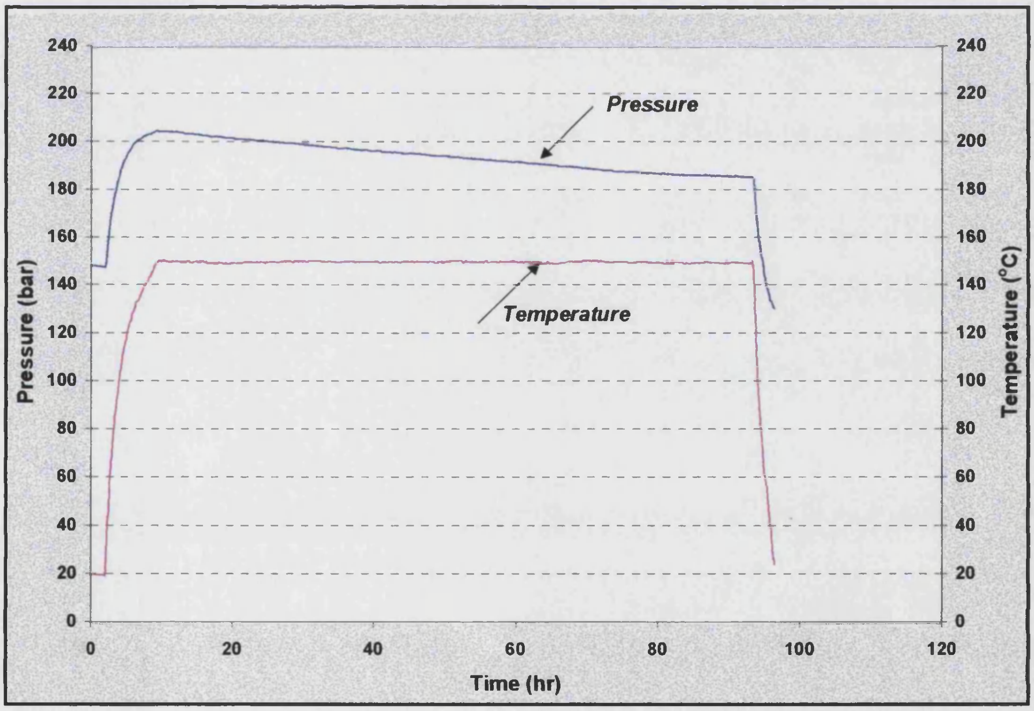

Figure 5.10: Pressure and Temperature Profile of Run 67
(Pressure and temperature data recorded every 10 minutes)

The oxygen consumption rate was calculated at different oxygen partial pressures for different assumed reaction orders (0.25 to 1.1), using Equation 5.8, derived below.

The molar rate of oxygen been consumed in the oxidation reaction is:

$$\frac{dn}{dt} = -kP^n \quad \text{.........................} \quad (5.6)$$

Assuming that the Ideal Gas Law applies and that solubility of oxygen in the liquid is negligible and constant reactor volume.

$$\frac{V}{RT} \times \frac{dP}{dt} = -kP^n \quad \text{..................} \quad (5.7)$$

Integrating for n not equal to one, the above equation can be written as:

$$\frac{KRT}{Vt} = \frac{(p_{O2}^{0})^{1-n} - (p_{O2}^{t})^{1-n}}{(1-n)} \quad \text{.....................} \quad (5.8)$$

For n=1, equation 5.7 can be written as:

$$\frac{KRT}{Vt} = \ell n \frac{(p_{O2}^{0})}{(p_{O2}^{t})} \quad \text{....................} \quad (5.9)$$

Where:

V = Gas volume

K = Rate constant

T = The absolute temperature

R = Gas constant

p_{O2}^{0} = Oxygen partial pressure at time equal zero

p_{O2}^{t} = Oxygen partial pressure at given time

t = Time of oxidation (hour)

n = Reaction order

As an example, the reaction order with respect to the oxygen partial pressure is calculated for Run 67 as follows. The pressure and temperature profile of Run 67 is shown in Figure 5.10. The reaction order with respect to the oxygen partial pressure data for Run 67 is given below.

Table 5.1 Reaction order with respect to the oxygen partial pressure data for run 67

Time	Pressure	O2 %	P_{O2}	n = 0.25	n = 0.5	n = 0.75	n =0.9	n=1.0
0	205.08	21.00	43.0668	0.0000	0.0000	0.0000	0.0000	0.0000
5	203.91	19.83	40.4403	1.0333	0.4065	0.1599	0.0914	0.0629
10	202.34	18.27	36.9588	2.4293	0.9663	0.3844	0.2211	0.1529
15	201.17	17.10	34.3963	3.4779	1.3954	0.5600	0.3239	0.2248
20	199.8	15.73	31.4305	4.7162	1.9125	0.7759	0.4517	0.3150
25	198.24	14.17	28.0990	6.1428	2.5234	1.0375	0.6090	0.4270
30	197.07	13.01	25.6322	7.2264	2.9994	1.2467	0.7367	0.5189
35	196.09	12.03	23.5871	8.1447	3.4118	1.4318	0.8512	0.6021
40	194.73	10.67	20.7806	9.4381	4.0079	1.7066	1.0239	0.7287
45	193.55	9.49	18.3756	10.5817	4.5517	1.9653	1.1895	0.8517
50	192.19	8.14	15.6381	11.9302	5.2160	2.2926	1.4036	1.0130
55	191.02	6.97	13.3126	13.1228	5.8278	2.6064	1.6138	1.1740
60	189.65	5.60	10.6243	14.5691	6.6061	3.0253	1.9028	1.3996
65	188.28	4.23	7.9735	16.0887	7.4776	3.5254	2.2611	1.6866
70	187.5	3.46	6.4810	16.9994	8.0335	3.8648	2.5136	1.8939
75	186.72	2.68	5.0007	17.9566	8.6526	4.2654	2.8221	2.1532
80	186.18	2.14	3.9829	18.6562	9.1336	4.5962	3.0864	2.3807
85	185.84	1.80	3.3451	19.1174	9.4671	4.8374	3.2850	2.5552

The steps used to calculate the above reaction order date are as following:

1. The relation ship between pressure drop and oxygen consumption in the SBR is assumed to be linear during the LTO reaction.
2. The oxygen consumption rate at a given time is calculated from the initial and final oxygen concentrations.

$$\frac{d[O_2]}{dP} = (20 - 1.8)/(205.08 - 189.65)$$

$$= 0.9979 \quad O_2\ \%\ /\ \text{bar}$$

Oxygen concentration @ 5 hr of oxidation $= (21 - (205.08\text{-}203.91)*0.9979)$

$= 19.83\ \%$

The oxygen concentration later time is given in Table 5.1

3. The oxygen partial pressure at different assumed orders of reaction was calculated by first assuming a reaction order (n) and using this in Equation 5.8.

Thus assuming n = 0.25. After 5 hours:

$$\text{Oxygen partial pressure for n=0.25} = \frac{(43.0668)^{1-0.25} - (40.4403)^{1-0.25}}{(1-0.25)}$$

$$= 1.0333\ \text{bar}^{(1-n)}$$

4. For n = 1, Equation 5.8 can't be used and the oxygen partial pressure for a first order reaction is therefore equal to:

$$\ell n \frac{(p_{O2})_{t=0}}{(p_{O2})_t} \quad \dots\dots\dots\dots\dots\dots\dots (5.10)$$

The oxygen partial pressure calculated for n=1.0 is given in Table 5.1.

5. The variation of oxygen partial pressure is plotted against time for the assumed values of n, as shown in Figures 5.11 to 5.13. Hence, n is calculated by determining the best straight line fit to the variation of oxygen partial pressure with time.
6. From Figures 5.11 – 5.13, it can be seen that a reaction order of 0.25 given best fit of the data for Run 67.

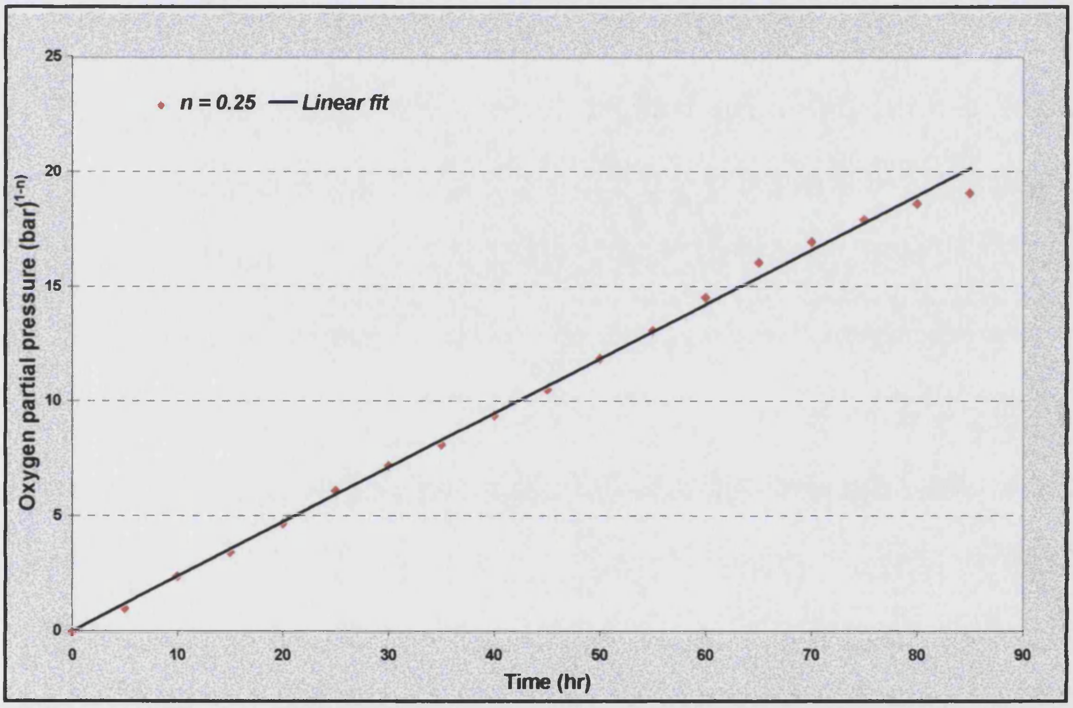

Figure 5.11 Plot of oxygen partial pressure data of Run 67 at n=0.25

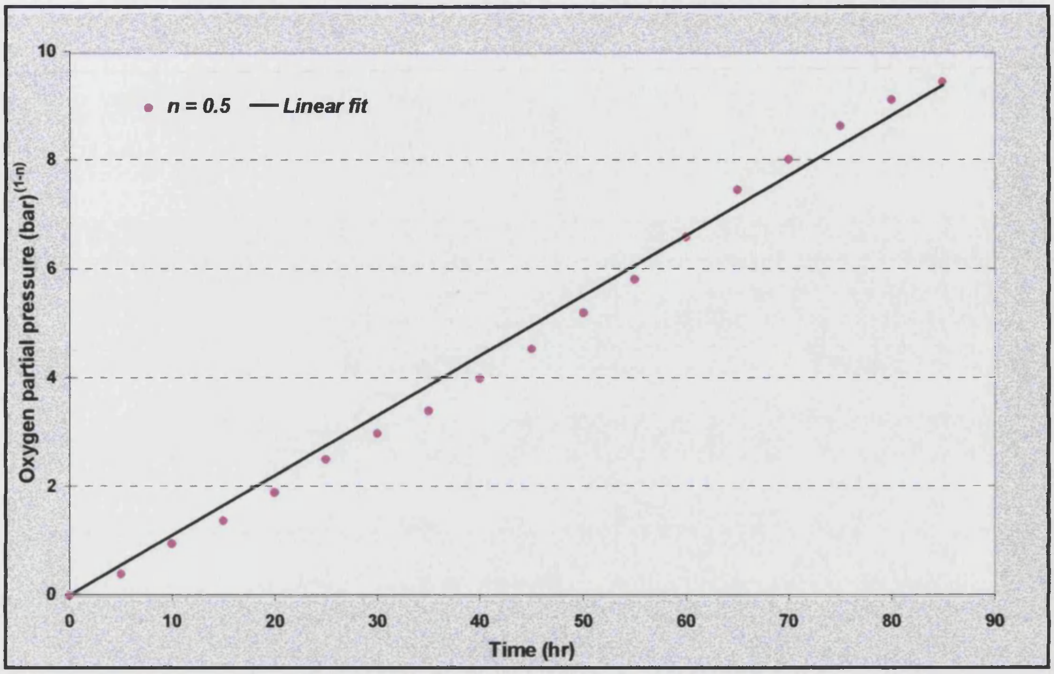

Figure 5.12 Plot of oxygen partial pressure data of Run 67 at n=0.5

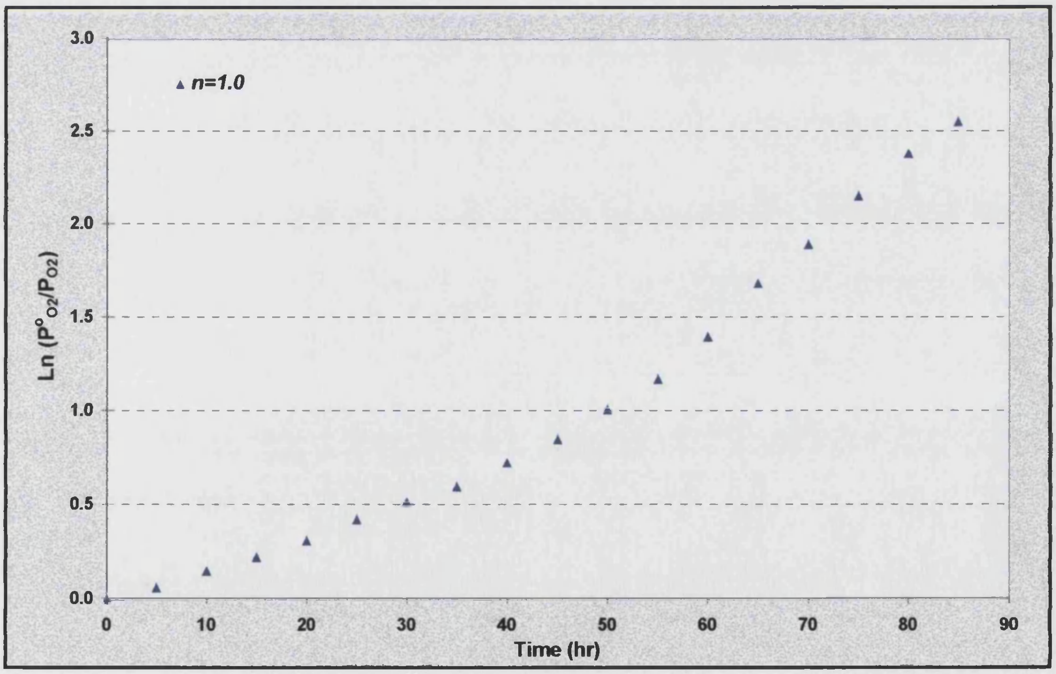

Figure 5.13 Plot of oxygen partial pressure data of Run 67 at n=1.0

PART III: PRODUCED GAS ANALYSIS

5.3 Produced Gas Analysis

Analysis of the produced gases revealed that nitrogen, oxygen, carbon dioxide and carbon monoxide were the main gases produced, together with a very small percentage of light hydrocarbons. The amount of oxygen consumed was always greater than the carbon oxides produced in all runs. The difference between the oxygen consumption and the amount of carbon oxides produced indicates that some of the oxygen is used to produce oxygenated hydrocarbon and water under LTO condition. In addition, the rate of oxygen diffusion into the oil phase is greater than the oxidation reaction rate[28], so that, in the early stage of the reaction oxygen is consumed by this dissolution process.
The main factors effecting the produced gases during air injection LTO process are oxidation temperature, oil saturation, water saturation, reservoir matrix, oxygen partial pressure gas residence time, total pressure and oil composition.

5.3.1 Effect of Oxidation Temperature

Although LTO reaction were taking place below 110 °C, oxygen consumption and carbon oxides formation were not been observed below this temperature . However, as the temperature of the SBR was increased above 110 °C, the production of carbon oxides and the corresponding oxygen utilization became more significant. Infact, the oxidation rate increased rapidly for all of the oils studied. Typically 70 to 100 % oxygen consumption was achieved for oil D and Esso Mix 1 oil at around140 °C, whereas the maximum oxygen consumption achieved for the Australian oil and Oil C at the same temperature was 35% - 60%. Almost complete oxygen consumption was achieved when the reaction at oxidation temperature was 150 °C or higher for all of the different oils investigated. Generally, the amount of oxygen consumed by the crude oil increased with oxidation temperature.
Figures 5.14a – 5.14c show that the oxygen consumption increased very significant as the reaction temperature increases for all of the different oils investigated. However, these figures reveal that, the oxygen consumption depends not only on the oxidation temperature, but also on the initial oil saturation, the type of crude oil, the presence of water and the reservoir matrix.

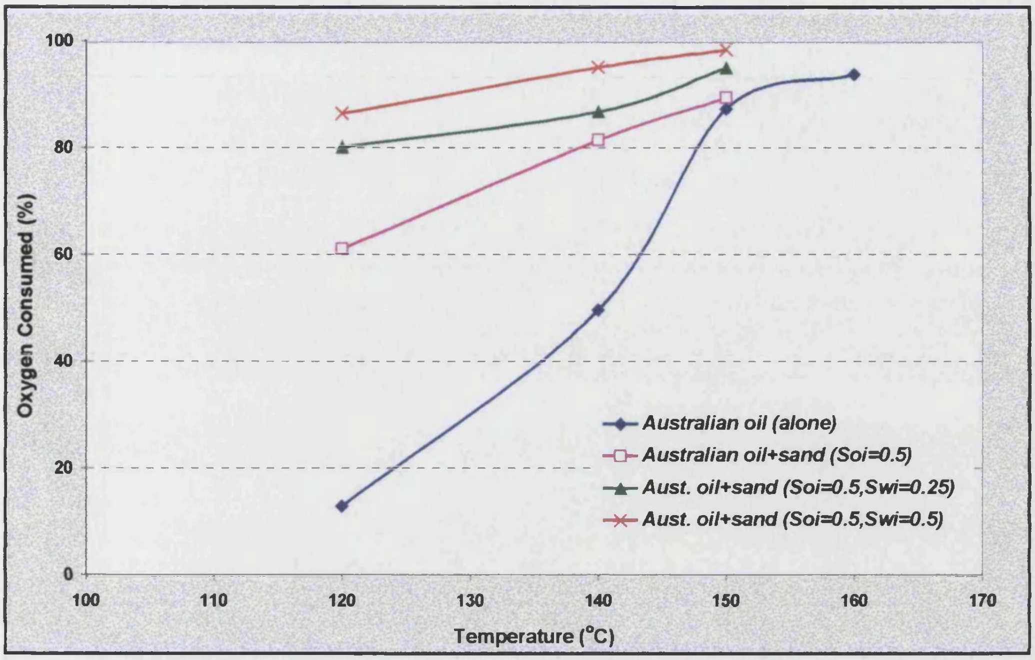

Figure 5.14a: Oxygen consumed versus temperature for Australian oil (Range of reaction pressure 175 – 220 bar)

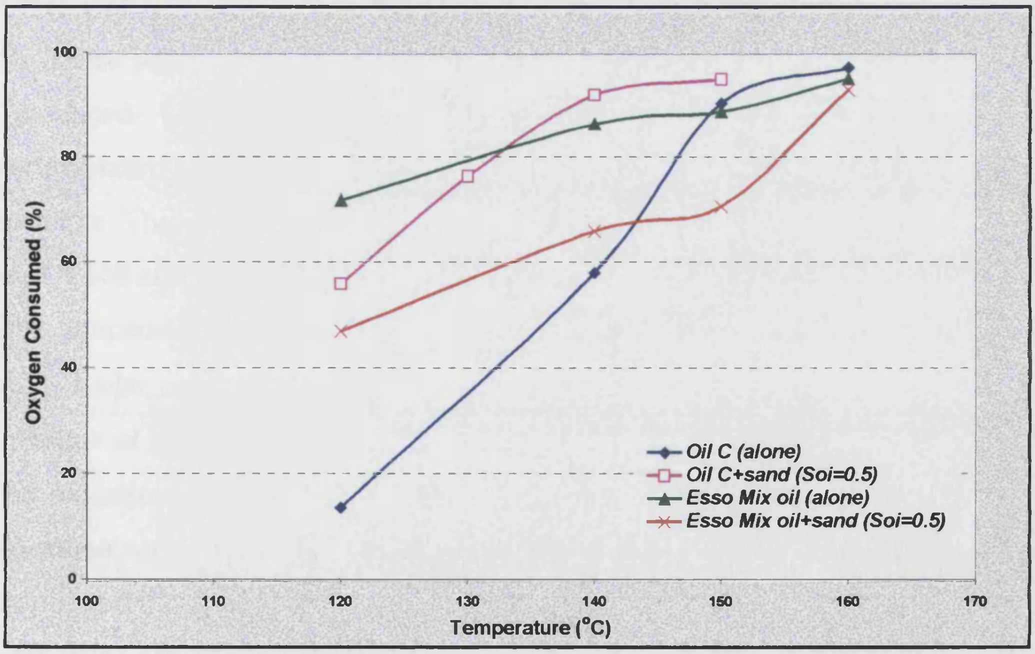

Figure 5.14b: Oxygen consumed versus temperature (Oil C and EssoMix1 oil) (Range of reaction pressure 175 – 220 bar)

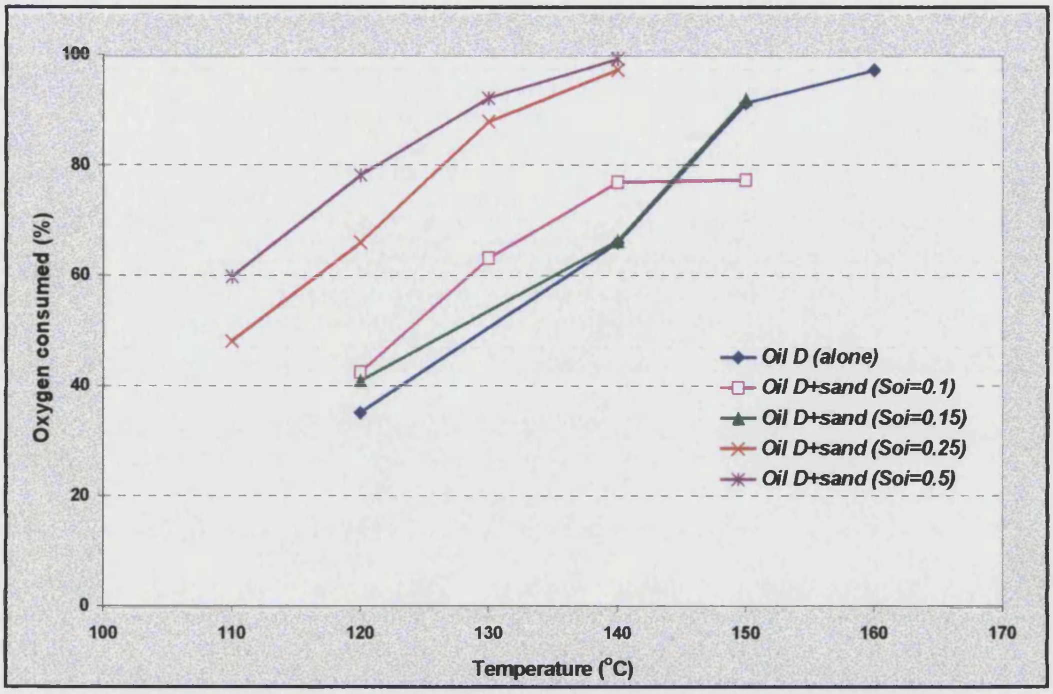

Figure 5.14c: Oxygen consumed versus temperature for Oil D (Range of reaction pressure 175 – 220 bar)

The effect of temperature on carbon oxides production is shown in Figure 5.15a and 5.15b. These plots show that as the oxidation temperature increases more carbon oxide are produced. Therefore the rate at which oxygenated hydrocarbon is decompose (decarboxylate) and the rate of formation of the these compounds also increases with temperature. This result is in agreement with the result reported in the leterature[30,31,54].
Figures 5.16a and 5.16b, show the variation of molar CO/CO_2 ratio of the produced gas against temperature. The plots show clearly that there is a dramatic reduction in the CO/CO_2 molar ratio over the temperature rage 120 – 140 °C, leveling out at higher temperature at around 0.4 –0.75. This indicates that addition CO_2 may be produced by further oxidation of CO, but accelerated decomposition (decarboxylation) of oxygenated hydrocarbon was occurring. No trend was observed between the API gravity of the light crude oils and the CO/CO_2 molar ratio.

The produced gas analysis from the SBR experiments reveals that 30 to 60% of the total oxygen consumed is utilized to produce carbon oxides during low temperature oxidation. This result is very similar to results reported by the EOR Group at the University of Salford[54] for the same crude oils using a temperature ramped reactor. Kisler and Shallcross[34] have also reported the production of carbon oxides during LTO.

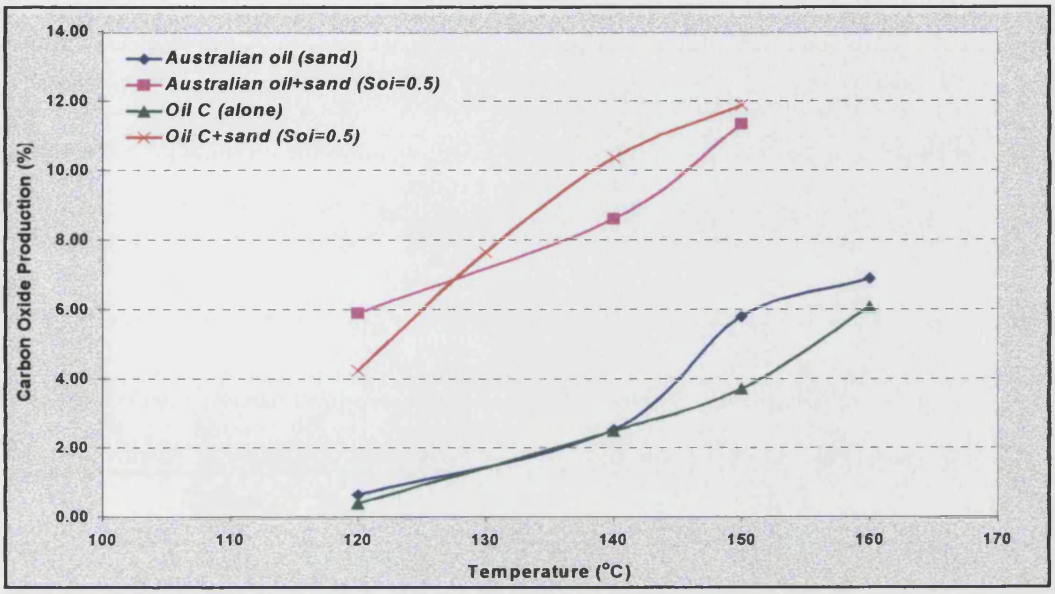

Figure 5.15a: Carbon oxide production versus temperature (Range of reaction pressure 175 – 220 bar)

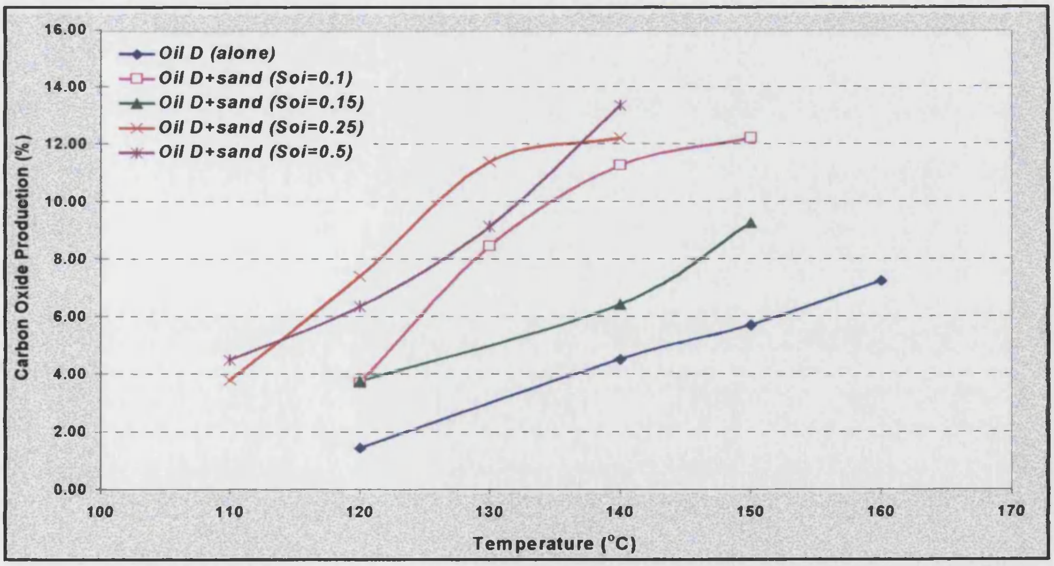

Figure 5.15b: Carbon oxide production versus temperature (Range of reaction pressure (175 – 220 bar)

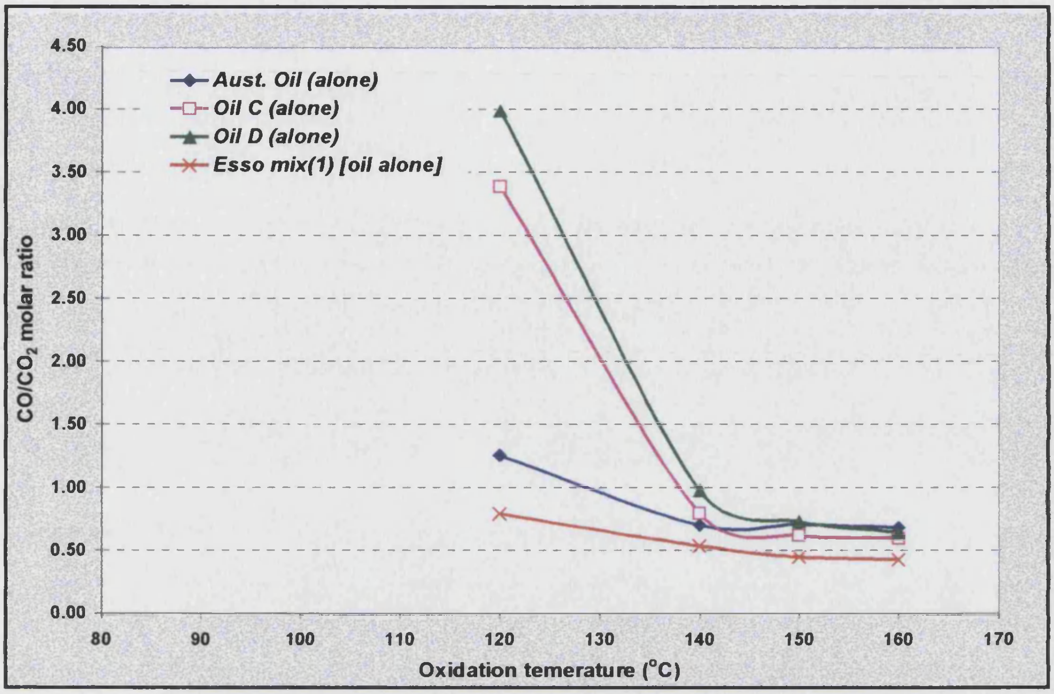

Figure 5.16a: CO/CO_2 molar ratio versus temperature

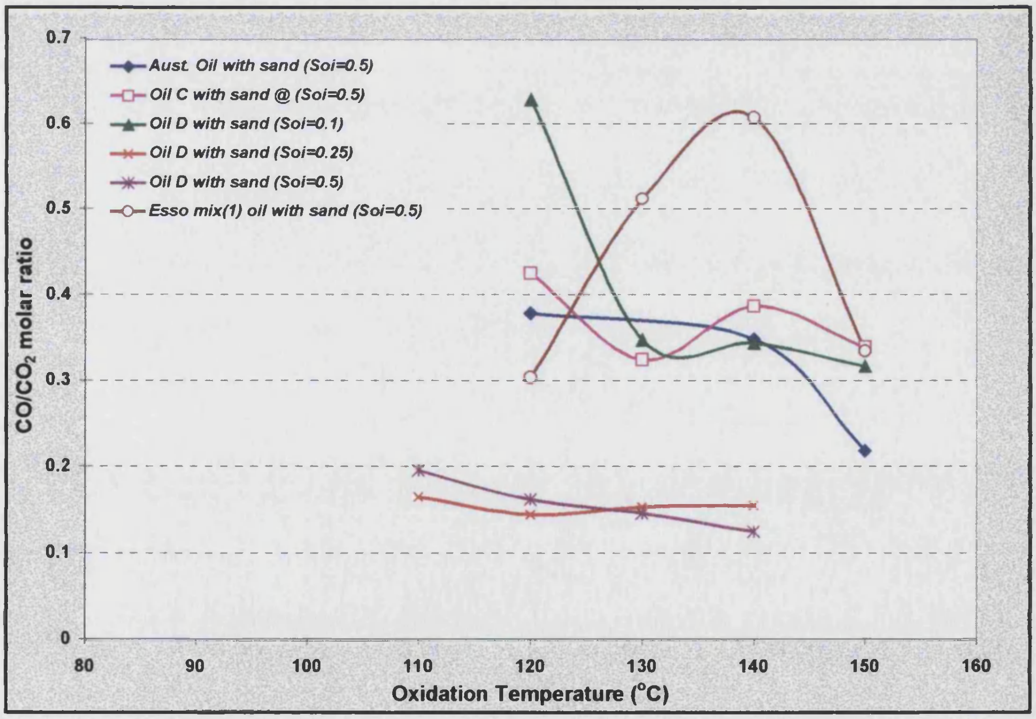

Figure 5.16b: CO/CO_2 molar ratio versus temperature

(Range of reactor pressure 175 -220 bar)

5.3.2 *Effect of Oil Saturation*

The gas discharged from the SBR after each experiment shows that oxygen consumption increases steadily with increasing oil saturation, as shown in Figure 5.17. Oil C shows a decrease in the oxygen consumption, when initial oil saturation increases from 50 to 75 %. The decrease is attributed to difference residence times between the two runs, since at So = 75 %, the residence time was 70 hr, whereas at So = 50 % it was only 37 hr.

The amount of oxygen reacted (g O_2 / g oil) is inversely proportional to the residual oil saturation and it is different depending on the particular crude oil. The decreasing effect may be explained by the fact that in SBR not all the oil is in contacted with the air, and the effect more of a problem when the initial oil saturation is high. This was confirmed during the unpacking of the oil-sand mixture from the reactor. It was found that the lower part of the matrix was not oxidised to the same extent as in the upper part. The color of the upper part of the oil-sand matrix was darker color than in the lower part. Figures 5.18 and 5.19 illustrate the effect of residual oil saturation on the reacted oxygen at two different oxidation temperatures (120 & 140 °C).

The initial oil saturation also affects the production of carbon oxides as shown in Figs. 5.20 and 5.21. The carbon oxides in the produced gases from the SBR steadily increase up to So = 50%, but then decrease beyond this point.

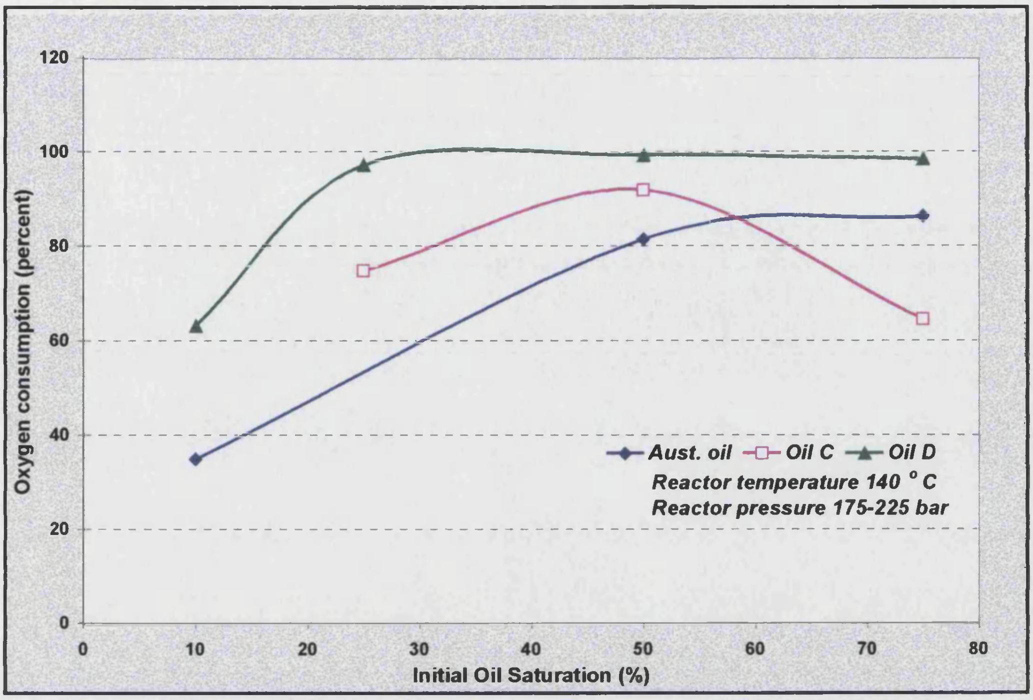

Figure 5.17: Effect of initial oil saturation on oxygen consumption

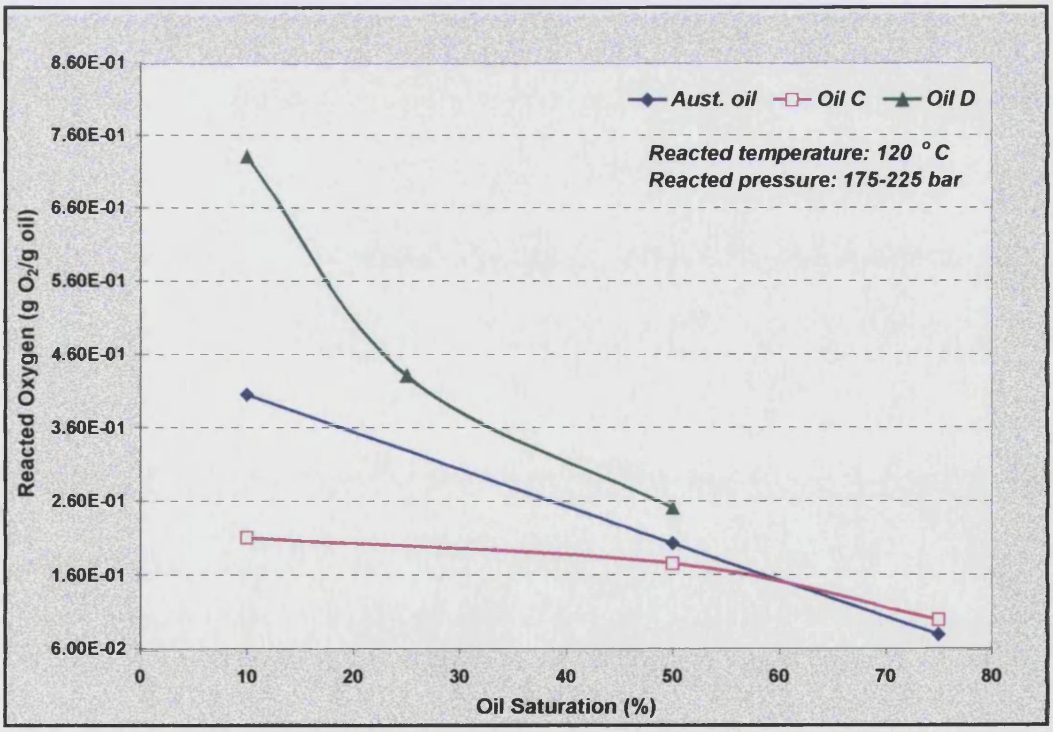

Figure 5.18: Reacted oxygen versus initial oil saturation

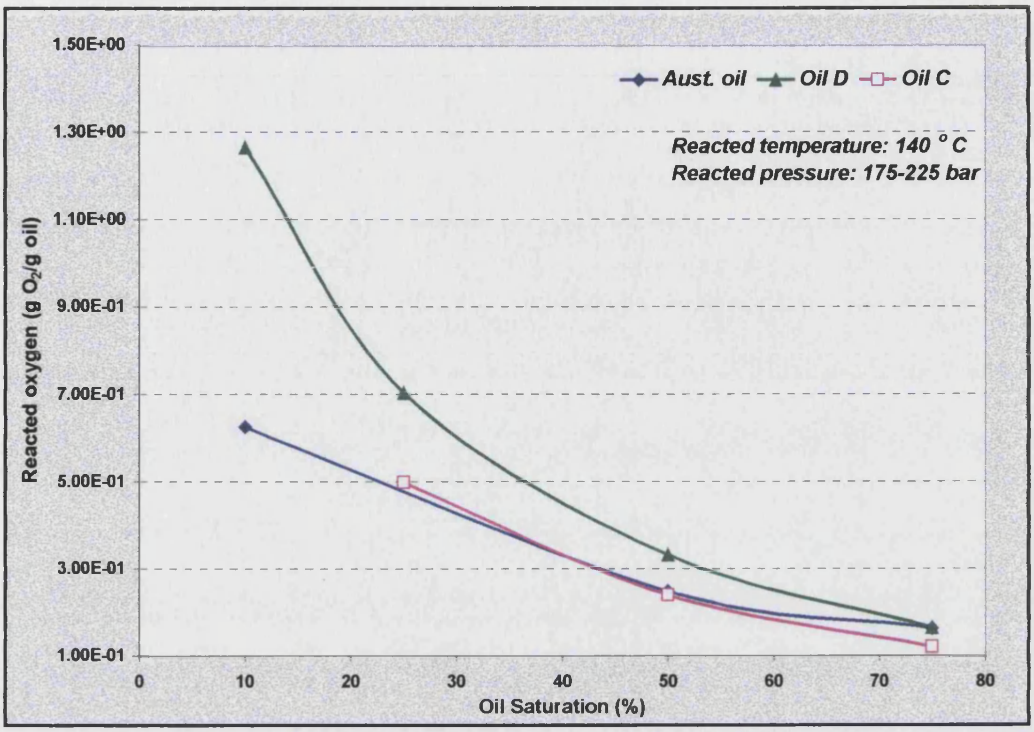

Figure 5.19: Reacted oxygen versus initial oil saturation

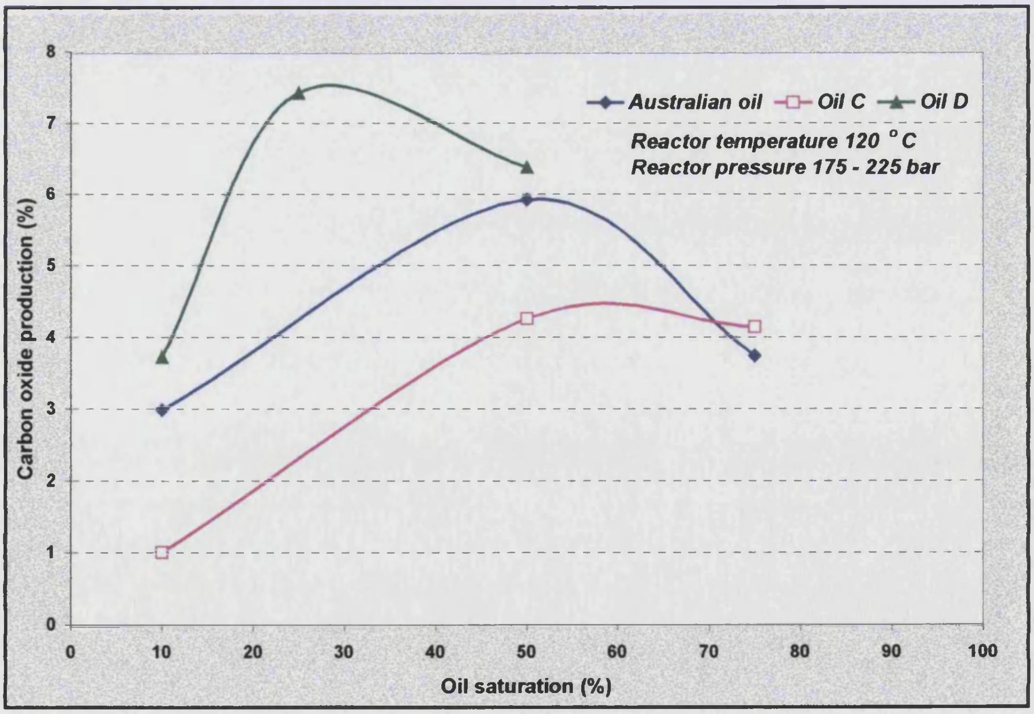

Figure 5.20: Effect of initial oil saturation on carbon oxides production

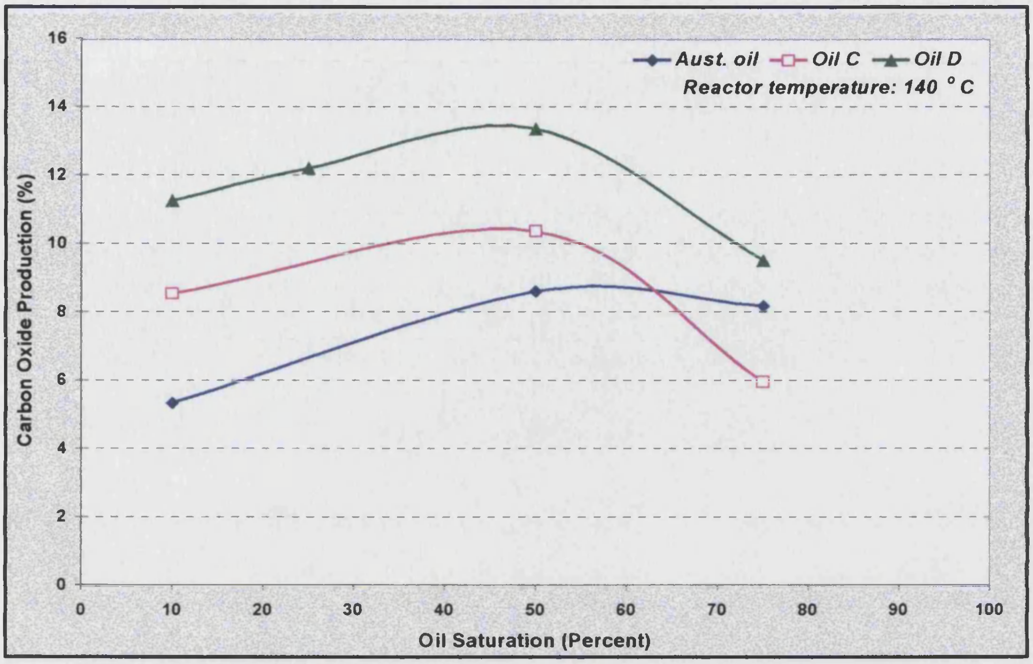

Figure 5.21: Effect of initial oil saturation on carbon oxides production

5.3.3 Effect of Water Saturation

In many light oil reservoirs, which have been watered out an extensive period of 20 years, the water saturation can be quite high (50% or more). A number of experiments were carried out at various water saturations to investigate the effect of water. The results in Table 5.2 show that water in the matrix enhances oxygen consumption by 20 – 40%, and reduces the residence time required to consume the oxygen.

Table 5.2: Effect of water on oxygen consumption

Run No.	*9*	*17*	*33*	*38*	*54*	*55*	*84*	*91*
Light crude oil	Aust. oil	Aust. oil	Oil C	Oil C	Oil D	Oil D	Esso mix	Esso mix
Oil saturation (%)	50	50	50	50	15	15	50	50
Water saturation (%)	0	50	0	50	80	0	0	50
Reactor temperature (^{o}C)	120	120	120	120	120	120	120	120
Reactor pressure (bar)	207.81	203.71	198.44	194.40	176.17	182.45	179.88	176.95
Oxidation time (hr)	51	35	90	87	68	45	123	45
Consumed Oxygen (%)	61.39	86.74	56.24	74.96	54.49	45.05	41.17	45.05

In term of reacted oxygen, as shown in Figure 5.22, the presence of water enhances the reacted oxygen (g O_2/g oil), specially for Australian oil and oil C. For reactive oils such as oil D and Esso Mix1 oil at 120 °C, there is a small decrease in the extent of oxidation due to the presence of water. This small decrease can be explained by the fact that oil D and Esso Mix1 oil have high reactivity, so that the effect of water can not be seen.

Figure 5.23 shows that there is no general trend between the water saturation and extension of oxidation. The only clear trend is for Australian oil at 120 °C, which shows an increase in the amount of oxygen reacted as water saturation increases. At 140 °C, the oxidation effect reverses to the extent that there is a slight decrease overall. Oil C shows both an increasing and decreasing effect at both high and low water saturation value.

If we look at carbon oxides production in Figure 5.24, there is an increase in the carbon oxides for the Australian oil and oil C, compared with oil D and Esso Mix1 oil, when water was used in the SBR experiments. This difference can be attributed to the difference in composition of these light crude oils. The Australian oil and oil C have higher API gravities (39 and 40) compared to oil D and Esso Mix1 oils (37 and 32.5).

The effect of water saturation on carbon oxide production is illustrated in Figure 5.25, the plot shows that the carbon oxide production increases with an increasing in the residual water saturation for Australian oil and oil C at 120 °C.

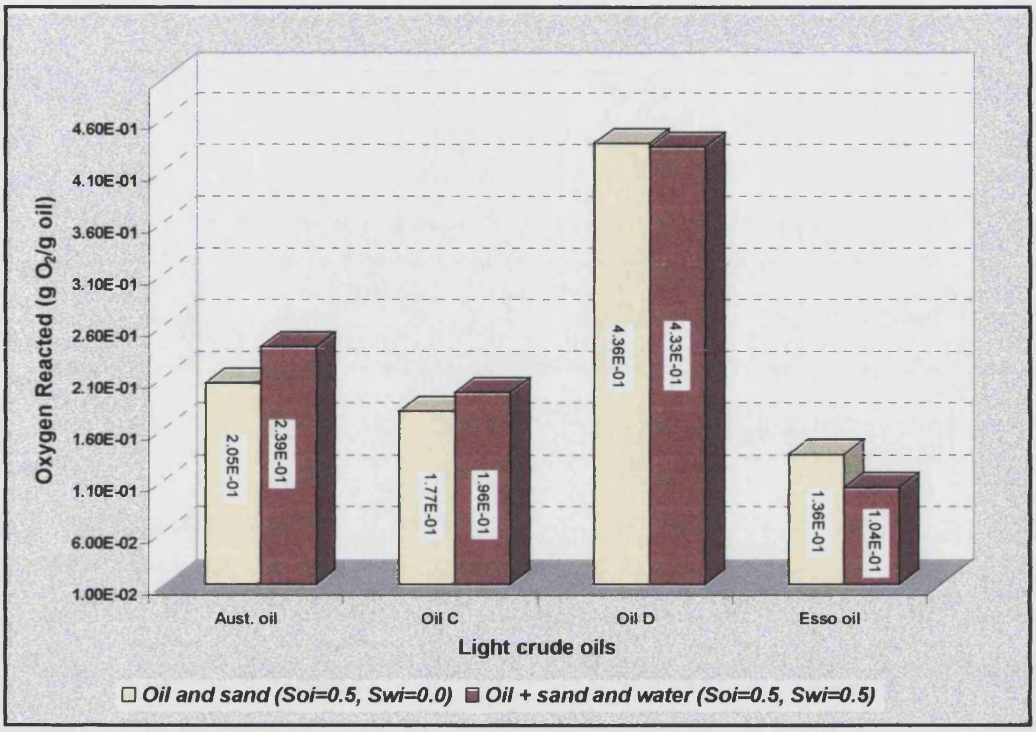

Figure 5.22: Effect of water on amount of oxygen reacted (120 °C, 200 bar)

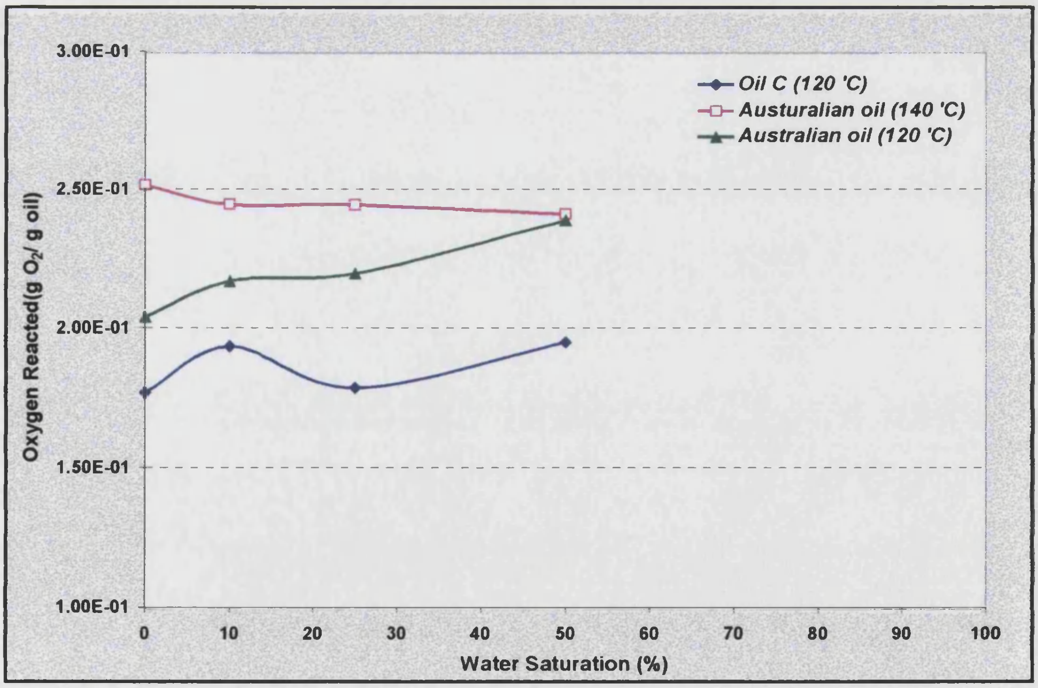

Figure 5.23: Effect of water saturation on reacted oxygen (P= 185-200 bar)

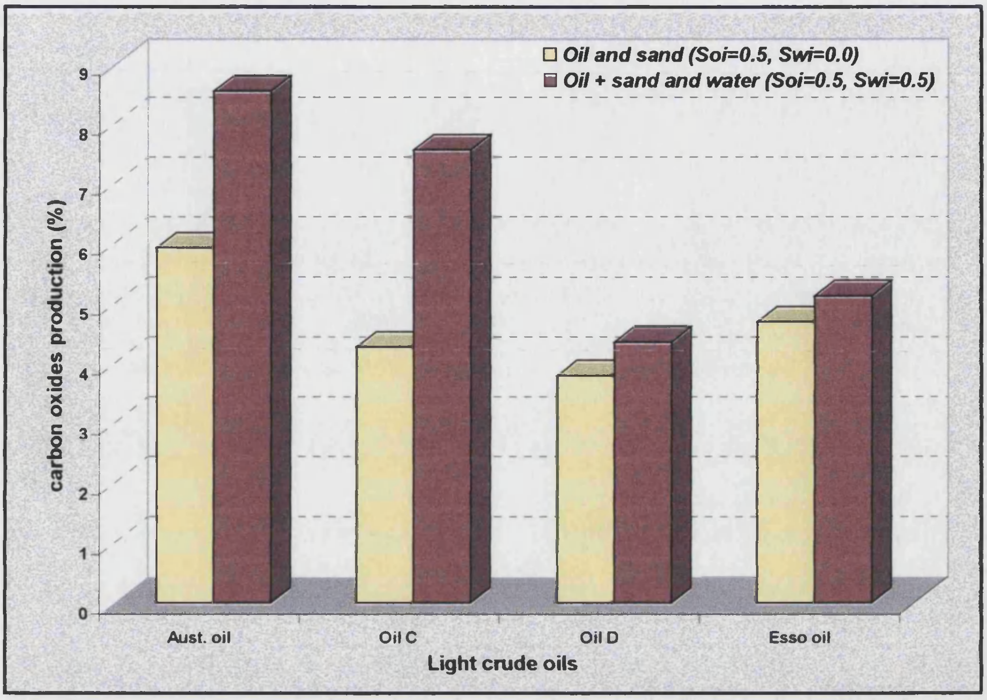

Figure 5.24: Effect of water on carbon oxides production (120 °C, 200 bar)

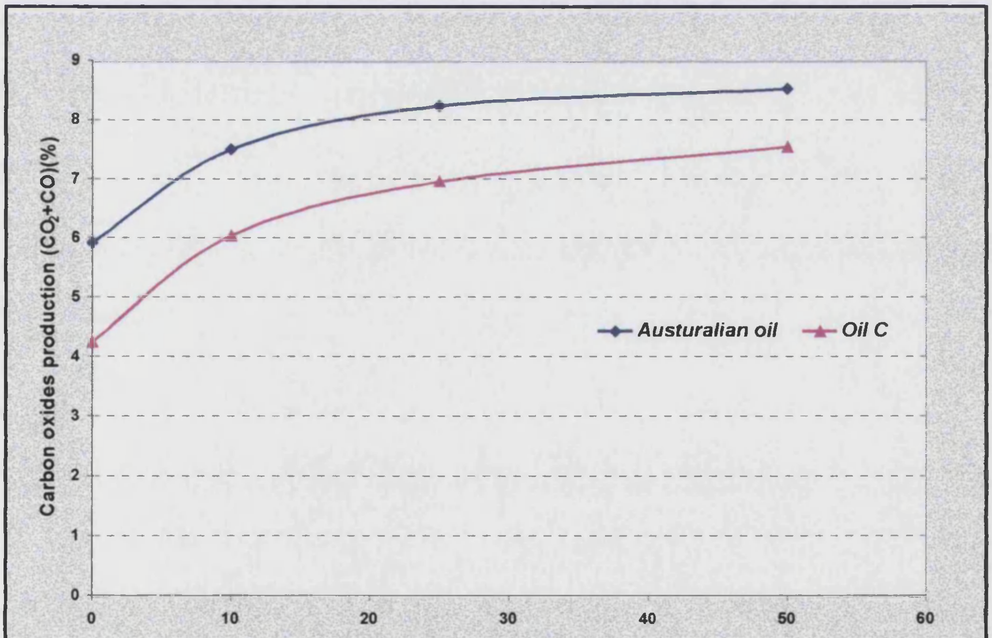

Figure 5.25: Effect of water saturation on carbon oxides production (120 °C, 185-200 bar)

5.3.4 Effect of Crushed Sand

The effect of the sand matrix on the degree of LTO is shown in Figures 5.26 to 5.31. All of the oils show that there is an increase in oxygen consumption, oxygen reacted, and carbon oxides production compared to the case with no sand matrix presence; except for Esso Mix1 oil.

The effect of the sand surface on the rate of oxidation (oxygen consumption) is very clear in Figure 5.26 at temperature of 120 °C. The increase in oxygen consumption various from almost double for oil D to more than four fold for the Australian oil and oil C. However, Esso Mix1 oil shows a reverse effect (decreases by 35%). During unpacking of the reactor after the oxidation tests, Esso Mix1 oil exhibited a hard layer, coke-like deposit on the top of the sand matrix. This obviously reduced the rate of oxygen diffusion from the bulk gas space into the matrix pores and contacting the unreacted oil.

Figure 5.27 shows that there is a less effect of the sand surface at 140 °C, compared to the 120 °C. Australian oil, oil C and D all show an increase of approximate 1.5 folds. Again, Esso Mix1 oil shows a decrease, but it was less than at 120 °C.

The other observation is that, when crushed sand was used with the oil, the fraction of carbon oxides in the produced gases was increased as shown in Figure 5.30. All the oils show an increase of approximate 1.5 to 4.0 folds.

The analyses of the produced gases show that the ratio of CO/CO_2 appears to decrease with the presence of crushed sand as shown in Figure (5.31). This can be explained by the fact that the presence of sand promote the production of carbon dioxide by enhance the oxidation of CO, decomposition of carboxylic acid, and decarboxylation of radicals to produce carbon dioxide.

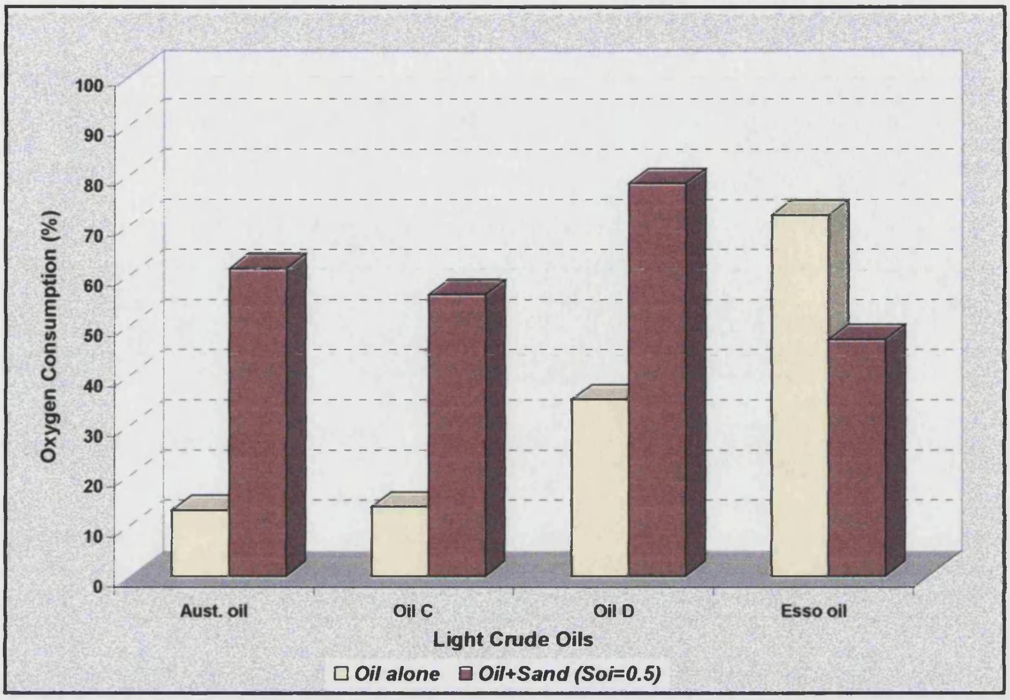

Figure 5.26: Effect of sand on oxygen consumption at 120 °C

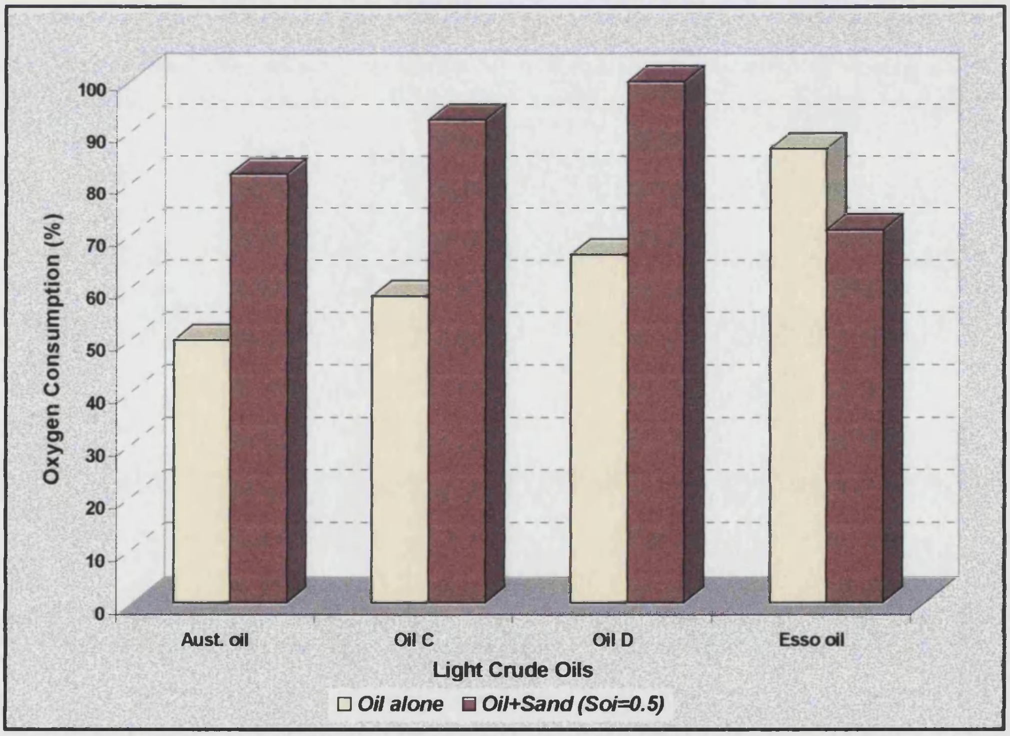

Figure 5.27: Effect of sand on oxygen consumption at 140 °C

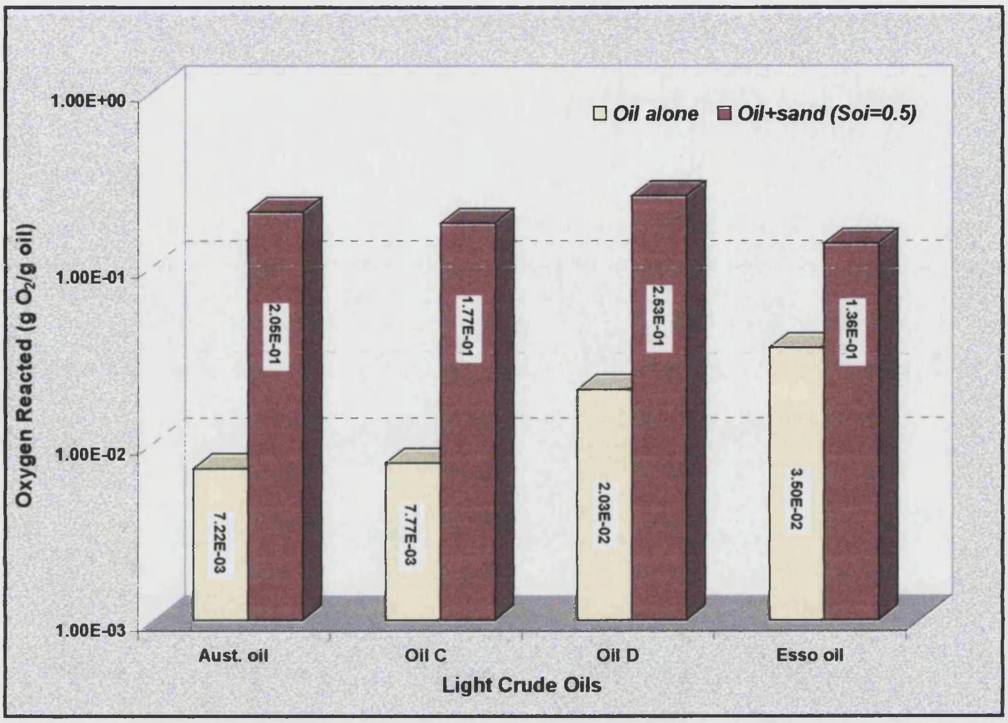

Figure 5.28: Effect of sand on the amount of oxygen reacted at 120 °C

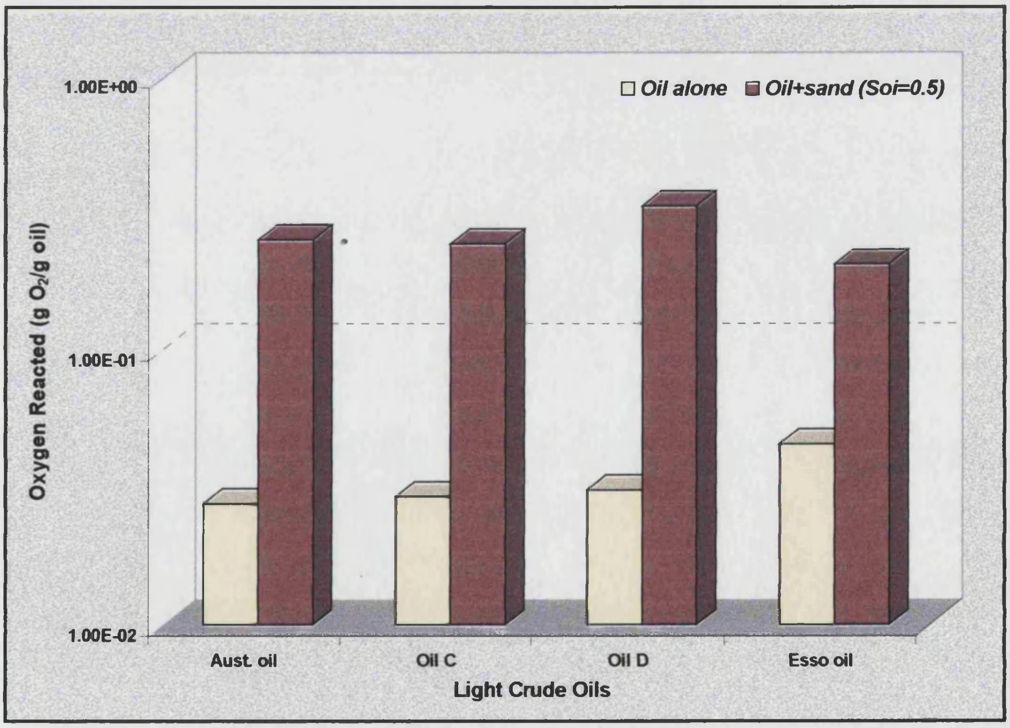

Figure 5.29: Effect of sand on the amount of oxygen reacted at 140 °C

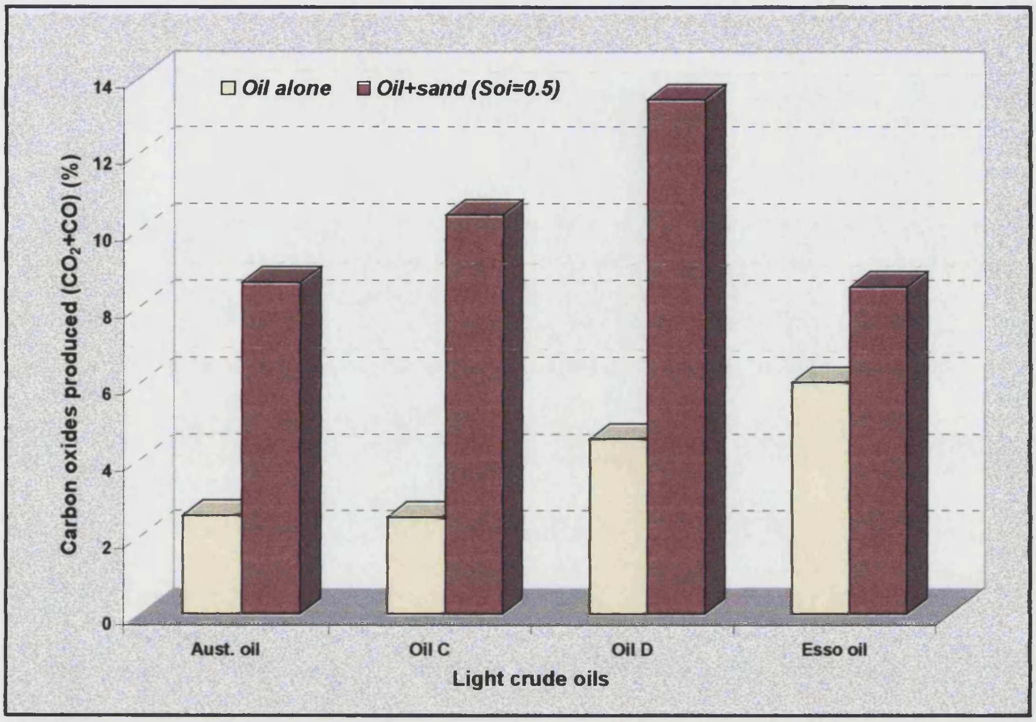

Figure 5.30: Effect of presence of crushed sand on carbon oxide production

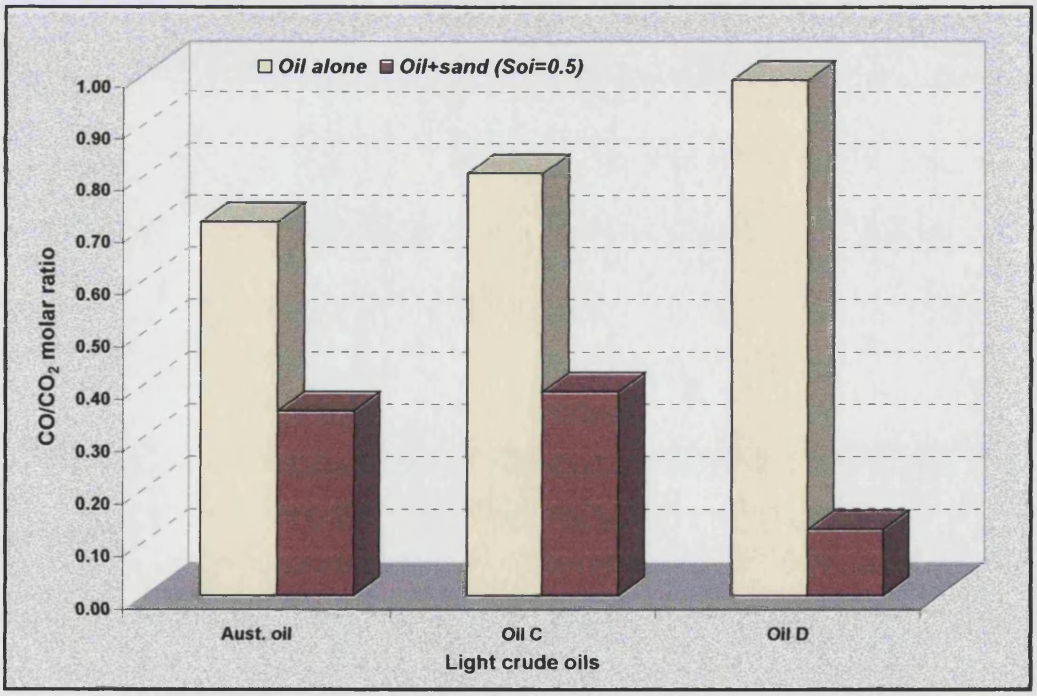

Figure 5.31: Effect of sand on CO/CO_2 molar ratio at 140 °C

5.3.5 *Effect of Oxygen Concentration*

Oil D with crushed core D at low oil saturation (Soi=0.15) and zero water cut was subjected to a set of experiments (Run 55 to 69) to investigate the effect of oxygen concentration (21, 10, and 5%) and vice versa (5, 10, 21%) on the produced gases and reaction rate across the oxidation zone. The pressure profile of Runs 61, 62, 63, 65 is shown in Figure 5.32 and the results of these runs are given in Appendix D (D.12 - D.15).

The important observation drawn from this set of experiments with respect to the produced gases are as following:

1. High percent of oxygen consumption was achieved when virgin oil was contacted with high oxygen concentration, also an increase in the percent of oxygen consumption was observed when the oxidised oil was further oxidised with depleted air as shown in Figure 5.33. In contrary, a reduction in the oxygen consumption was observed when the oxidised oil was further oxidised with higher oxygen concentration.
2. Most of the oxygen which react with oil ends up, eventually, in the gas phase as CO_2 and CO when the oil is oxidised first with air, and then contacted with depleted air (O_2 = 10, 5%). On the other hand, the oxygen ends up in the oil phase as oxygenated hydrocarbons when the oil is contacted first with depleted air (O_2 =5%) and then with higher oxygen concentration (10, 21%) as shown in Figure 5.34.
3. The CO/CO_2 ratio decrease with more oxygen is charged to the reactor and oxidation temperature increases. This agree with the normal expectation that increased oxygen concentration favours the production of CO_2 over CO.

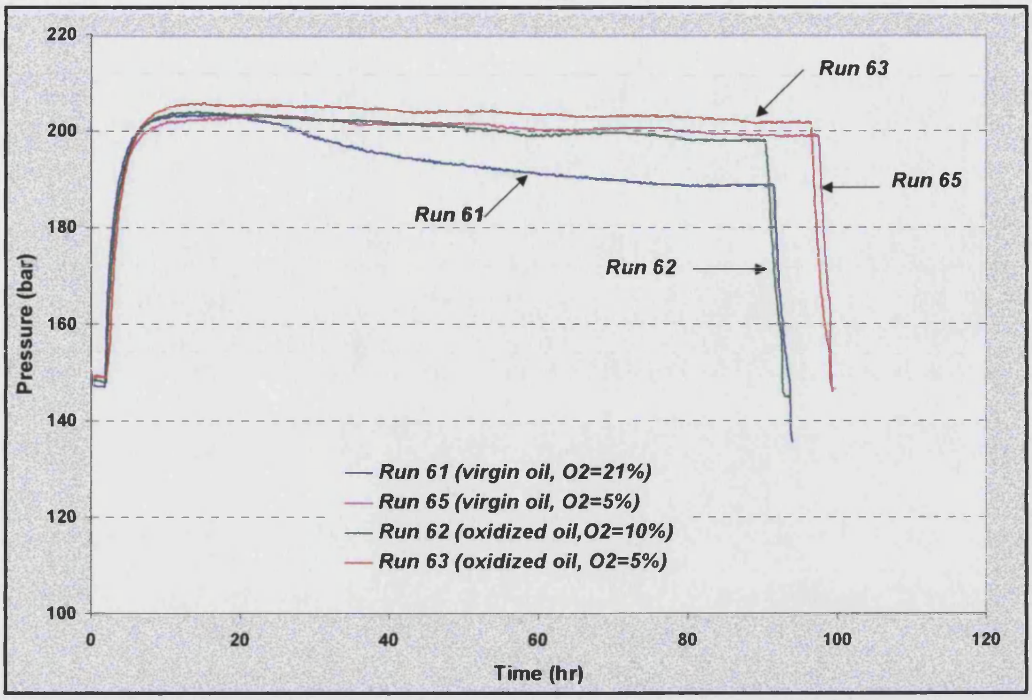

Figure 5.32: Pressure profile of oil D (Soi=0.15, Swi=0.0) at T=140 °C

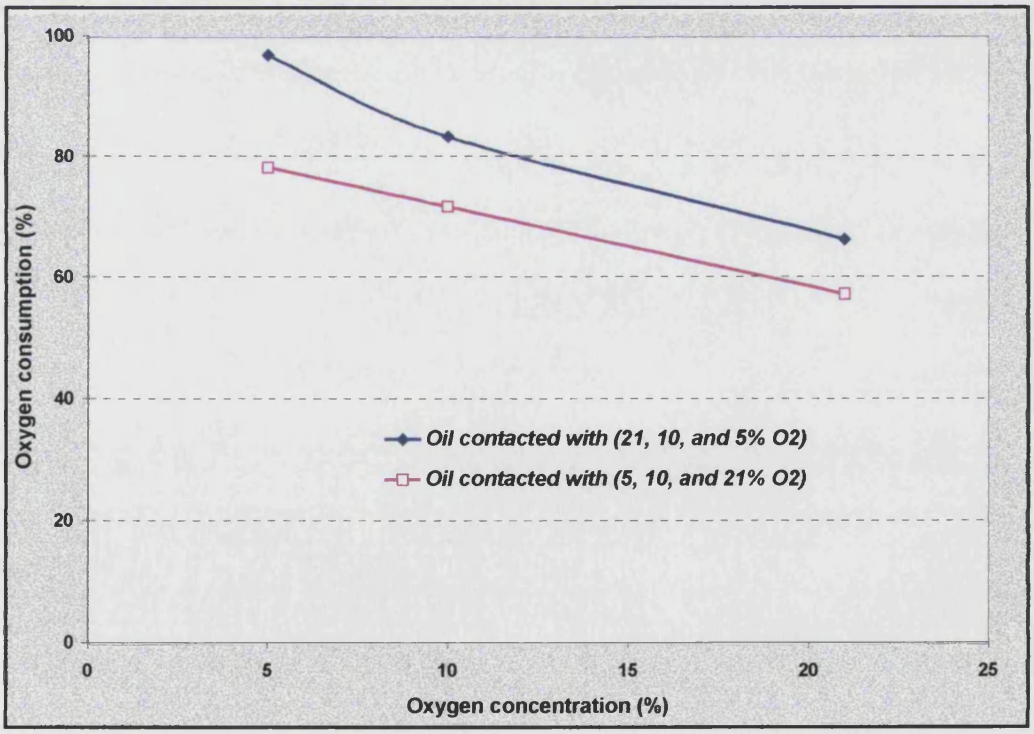

Figure 5.33: Oxygen consumption versus oxygen concentration inlet (T=140 °C)

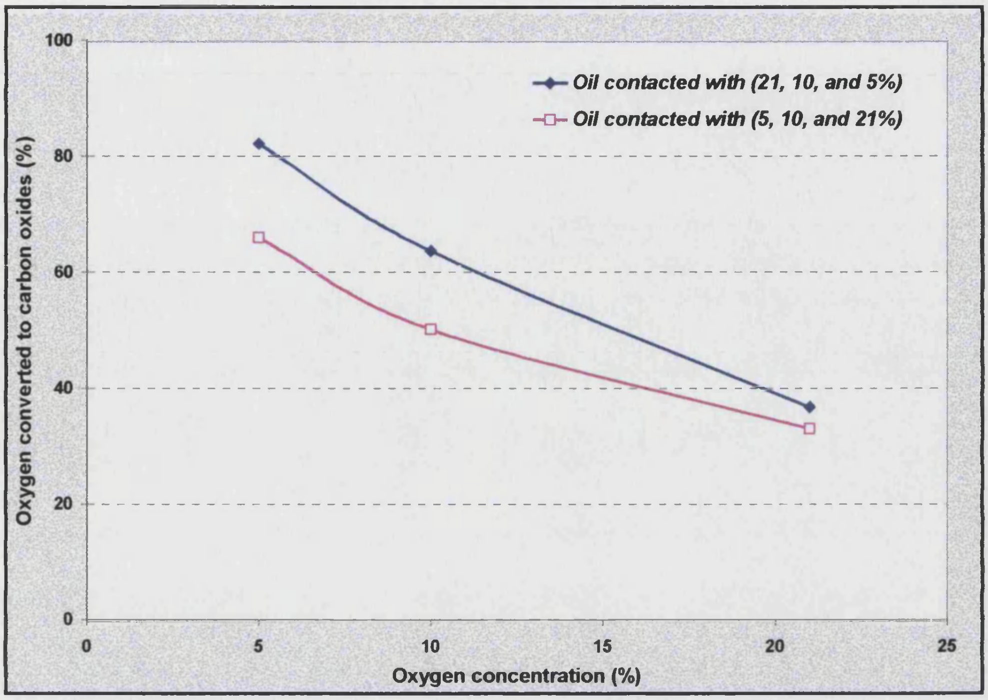

Figure 5.34: Oxygen converted to produce ($CO+CO_2$) versus O_2 concentration

5.3.6 *Effect of Oxidation Time*

The effect of oxidation time on the composition of produced gases was investigated in Runs 7,28, and 50, which were operated at double the oxidation time of Runs 6, 27,49. The results are tabulated in Table 5.3.

The pressure and temperature profiles for Australian oil (Soi=0.1) for oxidation time of 75 and 130 hr are shown in Figures 5.35 and 5.36. The effect of the residence time on the oxygen consumption and carbon oxides production is shown in Figures 5.37 - 5.39. These plots reveal that at a longer oxidation time, both oxygen consumption and carbon oxides produced are increased. These increases are almost double compared to the experiments on half the oxidation time. This effect was reported by Fassihi et al.[29], who used a small packed bed reactor run isothermally.

Table 5.3: Effect of oxidation time on composition of produced gases

Run No.	6	7	27	28	49	50
Initial oil saturation (%)	10	10	10	10	10	10
Water saturation (%)	0	0	0	0	0	0
Initial conc. % of Oxygen	21	21	21	21	21	21
Initial reaction pressure (bar)	203.52	216.21	166.41	168.36	184.57	194.34
Reaction temperature (^oC)	140	140	116	116	120	120
Reaction time (hr)	75	133	85	170	60	125
O_2 % in final reactant gas	14.2	7.2	18.6	14.7	17.2	12.3
CO_2 % in final reactant gas	3.3	6.6	0.6	1.6	1.6	2.3
CO % in final reactant gas	2.09	3.12	0.43	1.2	1.04	1.45
Total percent of O_2 consumed	35.82	68.47	13.92	32.76	20.96	42.72
Reacted oxygen (g O_2/g oil)	0.62579	1.27082	0.21119	0.50268	0.34019	0.73226

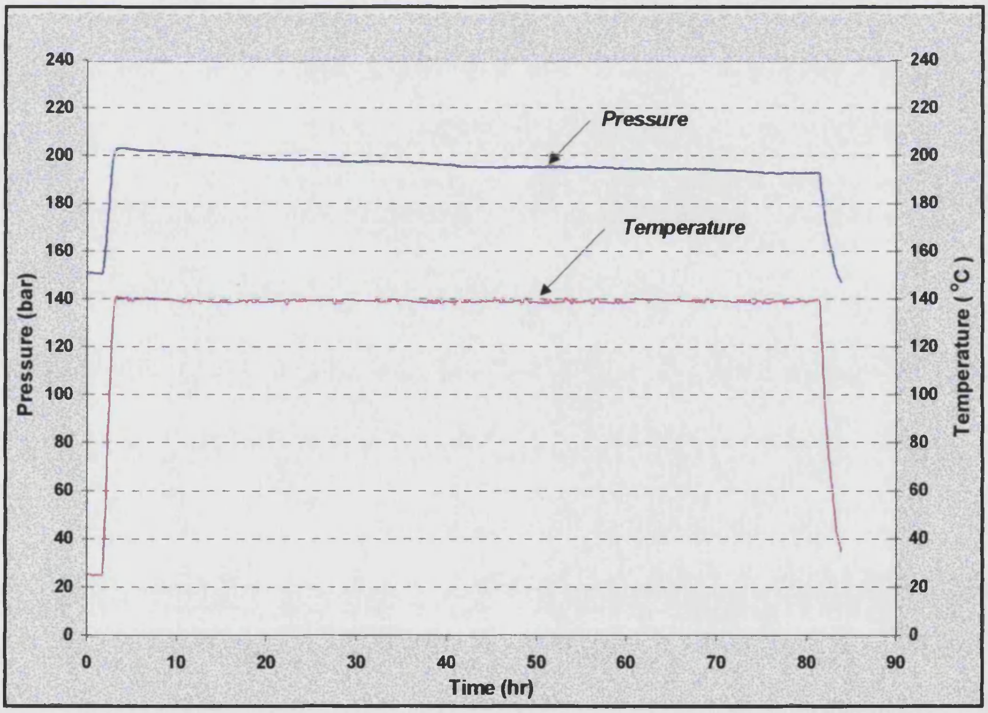

Figure 5.35: Pressure and temperature profiles for Australian oil (Soi=0.1) and crushed core D (Experiment No. 6)

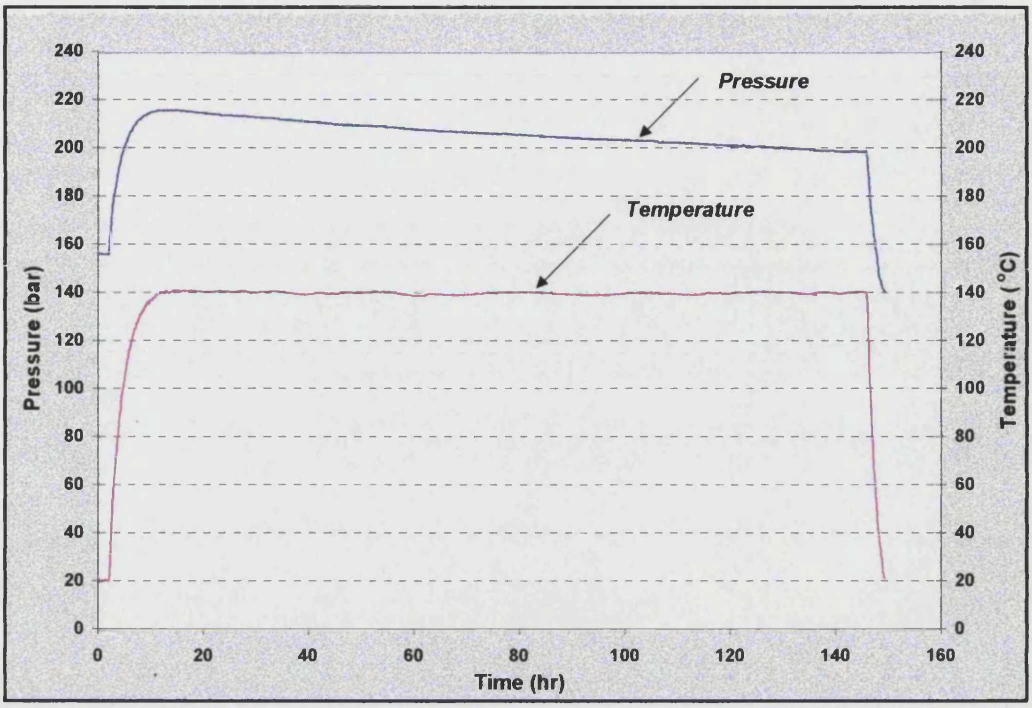

Figure 5.36: Pressure and temperature profiles for Australian oil (Soi=0.1) and crushed core D (Experiment No.7)

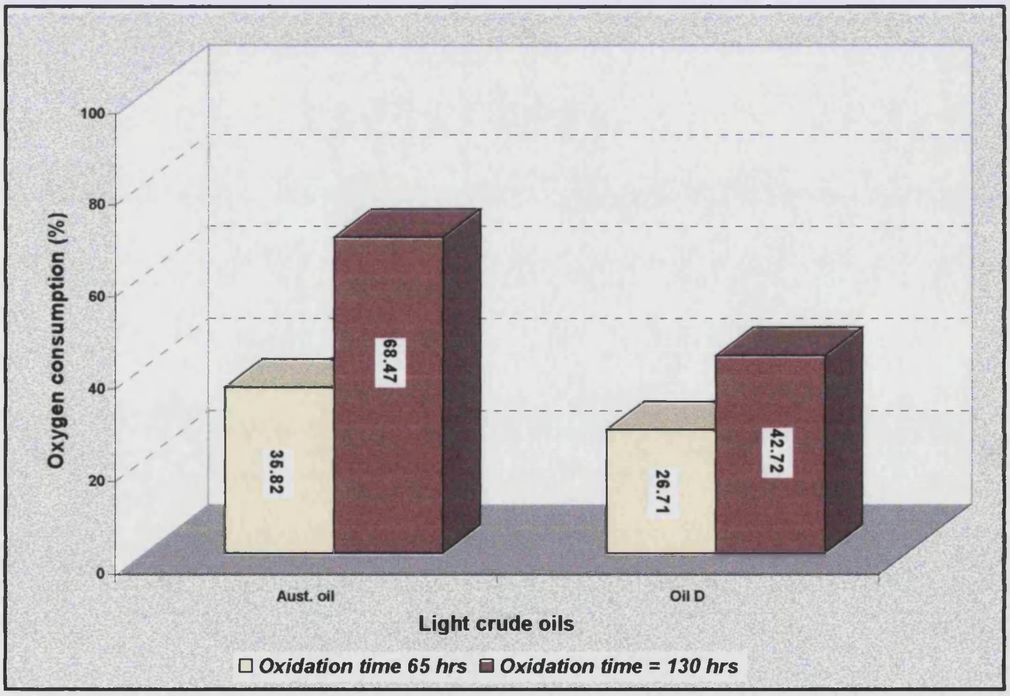

Figure 5.37: Effect of oxidation time on oxygen consumption @ 120 and 140 ℃

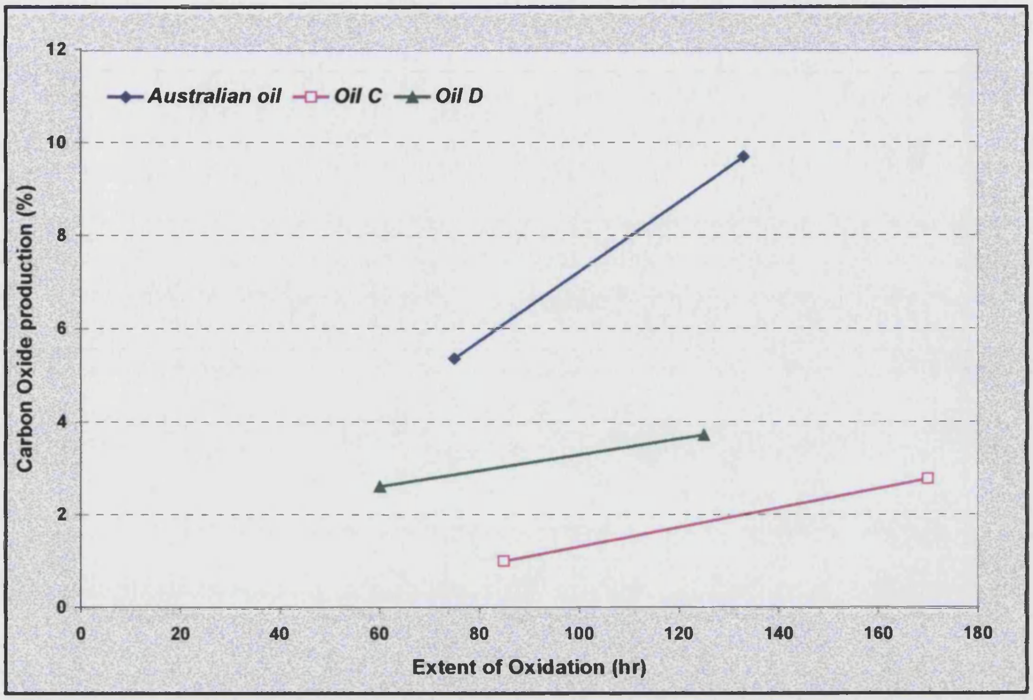

Figure 5.38: Effect of oxidation time on carbon oxides produced at 120 & 140 ℃

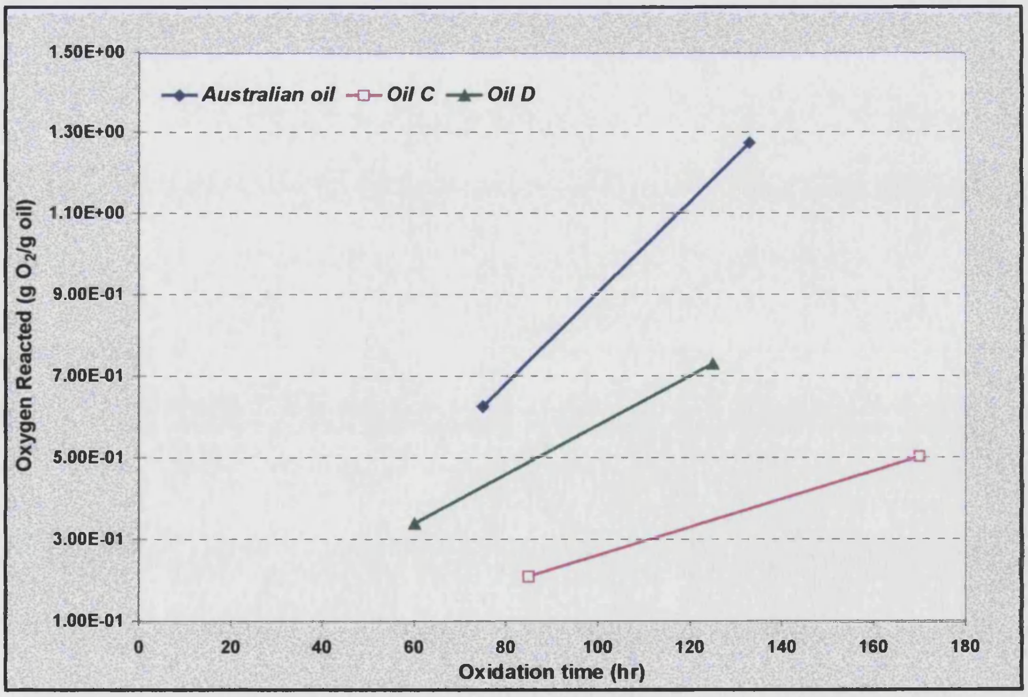

Figure 5.39: Effect of oxidation time on reacted oxygen at 120 & 140 ℃

5.3.7 Effect of Pressure

The pressure is important parameter as it determines the amount of oxygen injected into the process (reactor) and consequently must be consumed by the crude oils in the oxidation zone. The relevant data is reported below.

Table 5.4: Effect of operating pressure on composition of produced gases

Run No.	32	33	48	49	87	88
Oil saturation (%)	50	50	10	10	50	50
Water saturation (%)	0	0	0	0	0	0
Initial percent of Oxygen	21	21	21	21	21	21
Initial reaction pressure (bar)	127.34	198.44	128.52	184.57	133.2	197.09
Reaction temperature (°C)	120	120	120	120	140	140
Reaction time (hr)	86	90	58	60	61	50
O_2 % in final reactant gas	7.2	10.1	15.8	17.2	2.3	6.5
CO_2 % in final reactant gas	3.2	3	1.9	1.6	5.1	5.3
CO % in final reactant gas	1.23	1.28	1.73	1.04	2.18	3.23
Total percent of O_2 consumed	69.66	56.24	26.71	20.96	90.16	70.98
Reacted oxygen (g O_2/g oil)	0.14063	0.17691	0.30276	0.34019	0.17515	0.20404

The interesting feature of this result is that the oxygen consumption increases by 10 to 20 % as the oxygen partial pressure decreased, as shown in Figure 5.40. Therefore, the application of Air Injection LTO process is more effective at lower total pressure or reduced oxygen partial pressure. The other advantage of operating at lower pressure is that, less air would need to be compressed, reducing the operating cost.

Air injection into the West Hackberry field was reported by Gilham[3]. A dramatic oil production response was obtained in the lower pressure part of the reservoir. At the University of Salford[54], a study was carried out on the same four North Sea light crude oils in high pressure DISC reactor (oxidation cell), they concluded that oxygen consumption in the low and high temperature regions decreased as the total pressure was increased. They attributed this to the increase in the oil displacement, providing less oil available for reaction. However in the SBR, which a closed cell operation, the oil is not displaced. This suggests that it may be due to formation of more viscous oxidised oil.

Increases the operating pressure shows that (Fig 5.41) the amount of oxygen reacted increases as where the initial reactor pressure was increased from 100 bar to 150 bar. This represent an increase in the oxygen partial pressure of 10.5 bar, so that more oxygen is available to react with crude oil. However, there is little effect on the carbon oxides production as shown in Figure 5.42.

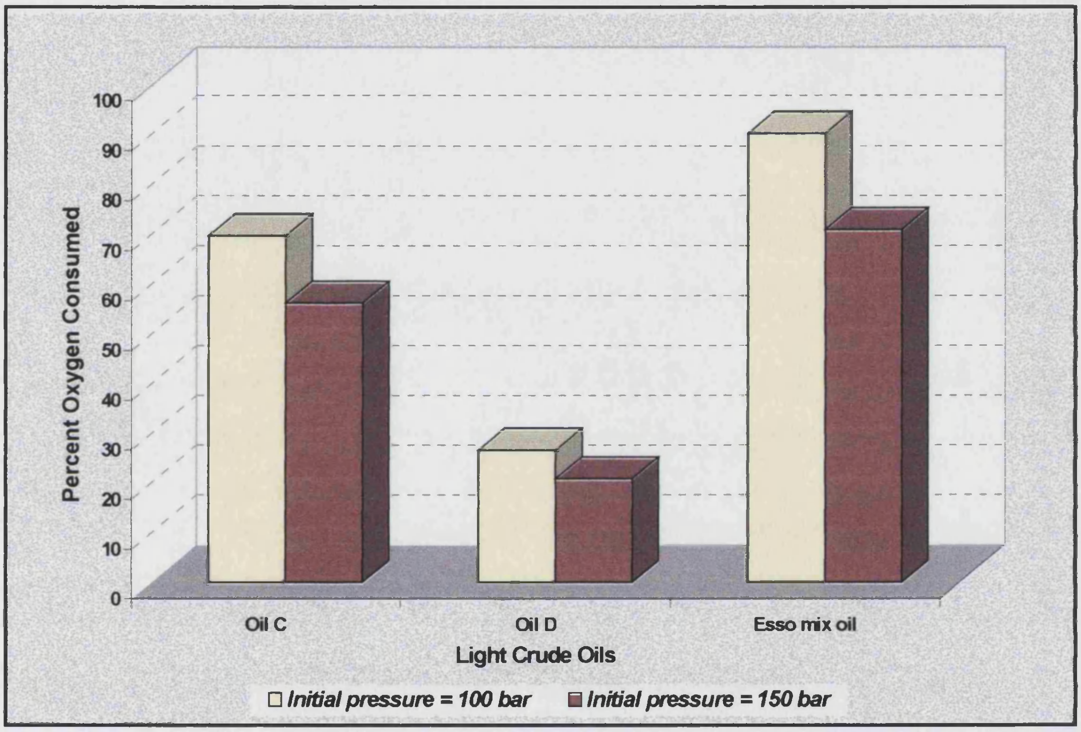

Figure 5.40: Effect of initial reactor pressure on oxygen consumption

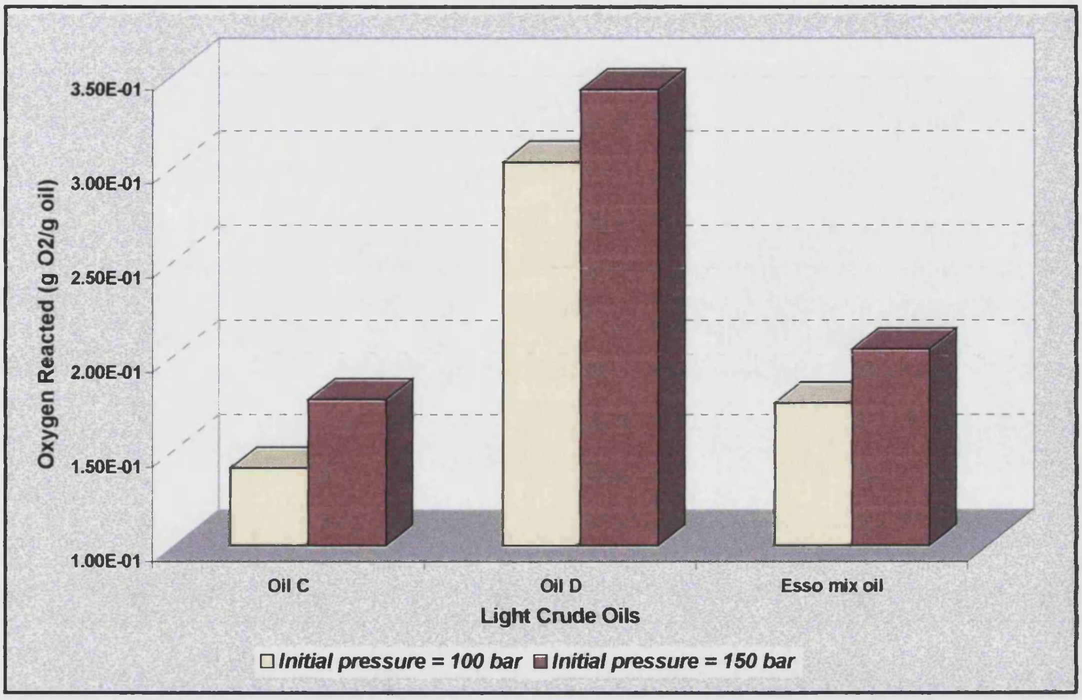

Figure 5.41: Effect of operating pressure on reacted oxygen at (120 & 140 °C)

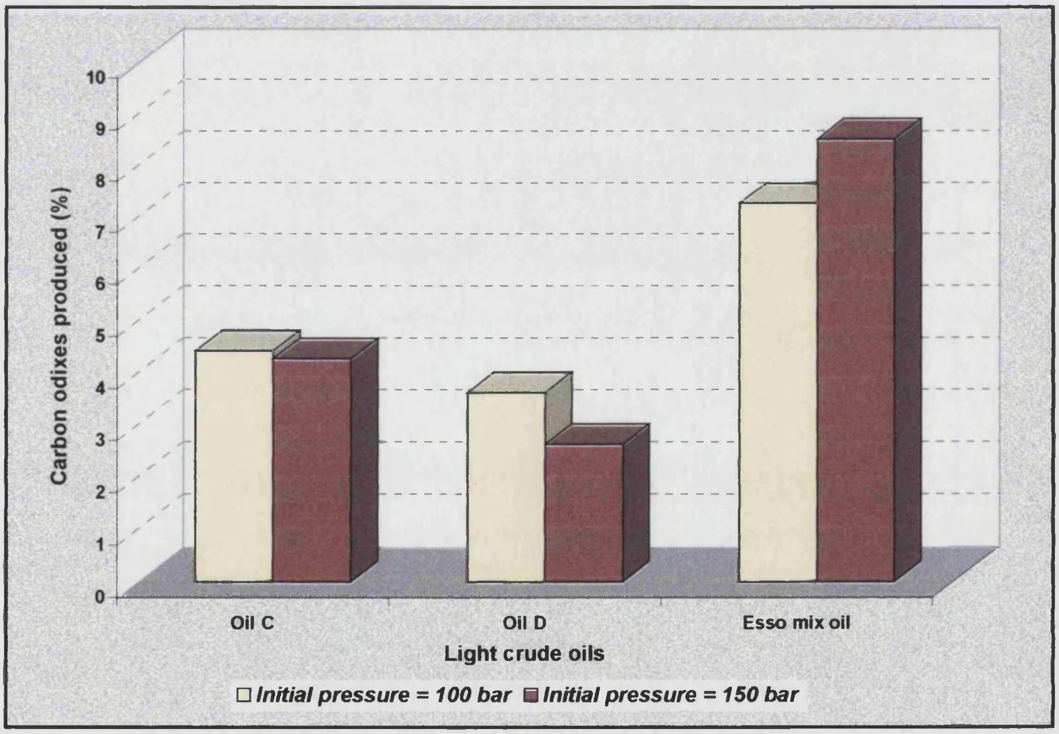

Figure 5.42: Effect of operating pressure on carbon oxides produced at (120 &140 °C)

5.3.8 *Effect of Oil Composition*

A series of experiments was carried out to study the reactivity and produced gas composition using various pure organic compounds. The operating conditions and summary results of these experiments are tabulated in Appendix D (Tables D.20 - D.22). The pure components used were pentane, hexane, toluene, xylene, iso-butylbenzene, n-hexylbenzene, and dodecane. At 140 °C (Fig 5.43), hexane, iso-butylbenzene and dodecane exhibit the same reactivity as regards the percent of oxygen consumed. Pentane and n-hexylbenzene are only slightly less reactive. However, toluene and xylene are much less reactive. Iso-butylbenzene and n-hexylbenzene are aromatics, but have more alkyl group (side chain) than benzene, toluene, and xylene. The alkyl groups are susceptible to low temperature oxidation.

This result is agreed with the results obtained from the oxidation of different light crude oils that have different percent of saturates and aromatic contents. The light crude oil has high percent of saturates are more reactive than the oil which has less percent (oil D more reactive than Australian oil) as shown in Figures 5.44. The saturate and aromatic fractions of Australian oil and oil D are (65, 18%) and (71, 13%) respectively.

The above result also was agree with what it has been reported in the literature[81,83], that saturates are more susceptible (reactive) to LTO reactions, compared to other SARA fractions, particularly aromatics.

Kok and Karacane[47], carried out combustion experiments on SARA fractions of two crude oils (26.12 and 14.95 API) using TGA and DSC techniques. They observed that saturates underwent LTO and gave off the most heat in the LTO region. Verkoczy and Freitag[84] who investigated saturates using TGA, observed that LTO of saturates occurred over the temperature range 125 to 300 °C. The effect of sand on the production of carbon oxide during low temperature oxidation of pure compounds is shown in Figure 5.45. The oxidation of hexane and dodecane produce more carbon oxide than xylene at 140 °C and this effect is increased significantly in the presence of sand matrix, up to 2 and 3 fold compared to xylene.

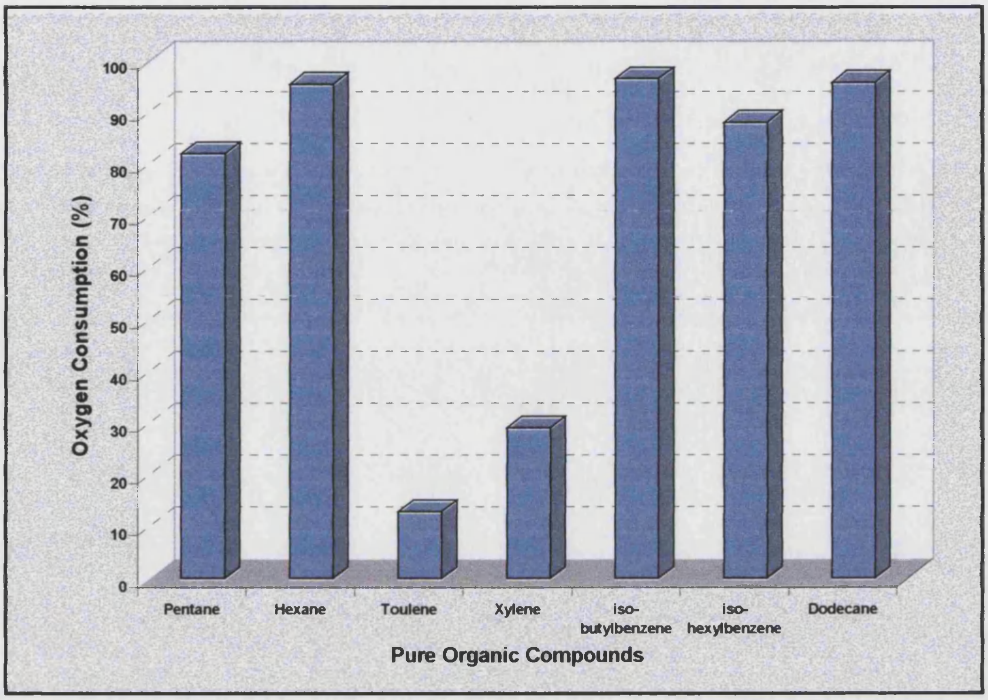

Figure 5.43: Oxygen consumption using pure organic compounds at 140 °C

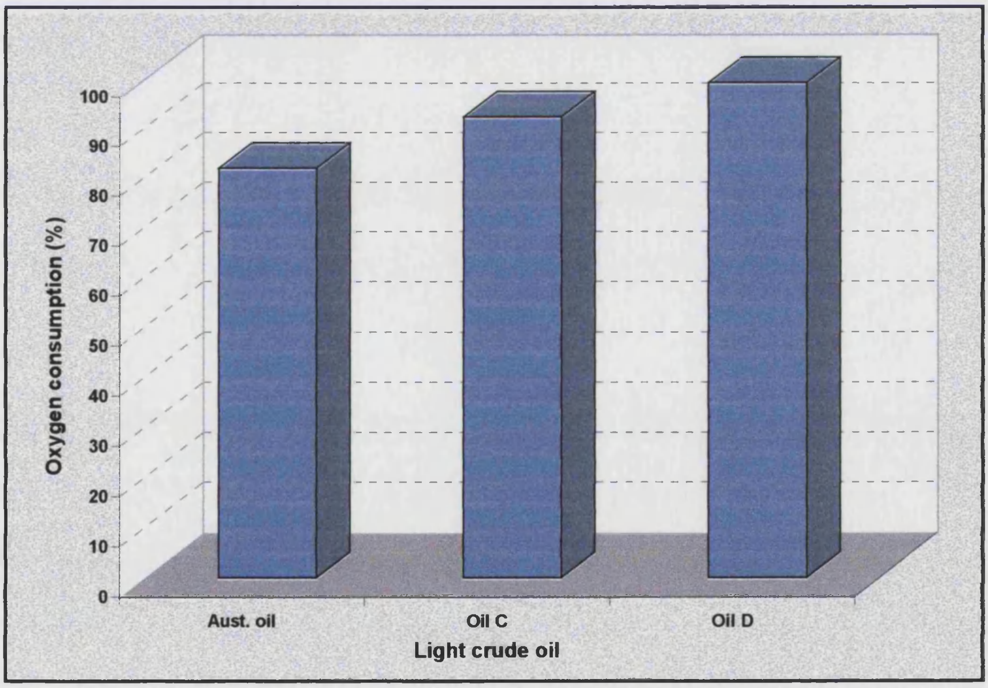

Figure 5.44: Oxygen consumption of Light crude oils (Soi=0.5, Swi=0.0) at 140 °C

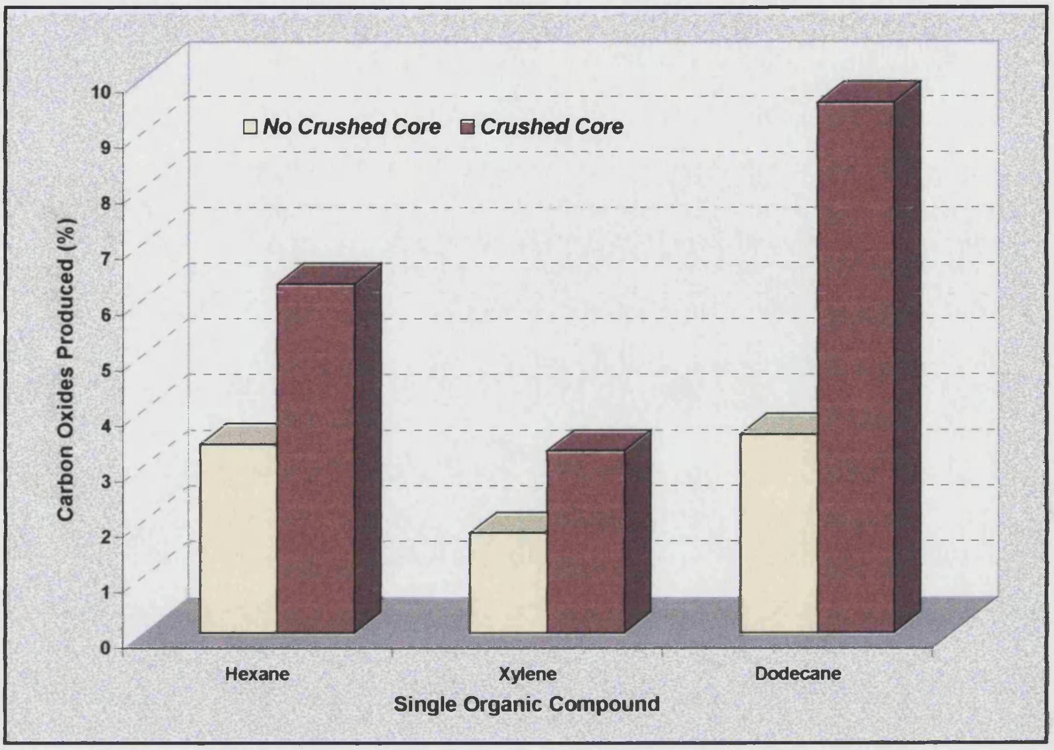

Figure 5.45: Produced carbon oxides using pure organic compounds

PART IV: LTO REACTIONS OF LIGHT CRUDE OIL

5.4 LTO Reactions of Light Crude Oil

This section contains discusses the kinetic data obtained from various SBR experiments. The analysis focused on the following aspects:

- The choice of reaction pathway for oxidation of light crude oils at low temperature (LTO).
- Calculation of the reaction order with respect to the oxygen partial pressure.
- Determination of the reaction rate constant and other kinetic parameters such as Activation Energy and Arrhenius constant (pre-exponential factor).

5.4.1 LTO Reaction Pathway.

The analysis of the pressure profiles obtained from the experiments with oil alone reveal that the LTO reactions of each run can be defined as comprising two main regions, i.e. the LTO reaction involved in two reaction stages occurring at different rates. During the initial period of reaction, the rate of oxidation was high, but then dropped unexpectedly to a lower rate. Two regimes, or stages of reaction are observed as shown in Figures 5.46 – 5.48. The pressure decline curves in these figures exhibit an initial high rate period followed by a long slow decline(Australian oil and oil C). At lower initial oil saturation (Soi=0.15), the pressure decline preceded by a dormant or non reactive period, which is followed by a two-stage higher and lower rate periods (Fig 5.48). This transition in the rate of oxidation may be due more reactive bonds and molecules oxidising first and once these reactions are complete the reaction rate then declines. To investigate this hypothesis, gas samples were taken for analysis from some runs (oil alone) after a certain period of oxidation. The operating conditions and gas sample analyses of these runs are given in Table 5.5. It can be seen that the rate of oxygen consumption is not constant over the oxidation period. For the Australian oil the rate start with 0.0006 mole of oxygen per hour, but in the last stage of the reaction the oxygen consumption rate reduces to 0.0001 mole per hour. The same trend was observed for oil C. In the case of oil C the drop was more due to the fact that oil C contains more higher reactive components (saturates) than the Australian oil and these are consumed at a more rapid rate during the first stage of LTO. The saturates fraction of oil C and Australian oil are 74 and 65% respectively.

This result indicates that at least two type of LTO reactions are involved in the production of oxygenated hydrocarbons, carbon oxides, and water. Furthermore the two reactions occur at different oxidation rates.

Table 5.5: Rate of oxygen consumption

	Australian oil alone			Oil C alone		
	1^{st} Sample	2nd sample	Final sample	1st sample	2^{nd} Sample	Final sample
Oil saturation (%)	100	100	100	100	100	100
Initial % of O_2	21	13.166	11.531	21	12.65	9.05
Initial reactor pressure (bar)	201.56	176.17	151.95	181.89	161.52	135.94
Finial reactor pressure (bar)	197.27	171.68	150.2	181.14	155.86	133.79
Reactor temperature (°C)	140	140	140	140	140	140
Oxidation time (hr)	40	29	10	15	41	21
O_2 percent in gas sample	13.166	11.531	11.166	12.65	9.05	8.2
CO_2 percent in gas sample	tiny	tiny	1.5	tiny	tiny	1.4
CO percent in gas sample	tiny	tiny	1.07	tiny	tiny	1.13
Initial P_{O2} (bar)	42.328	23.195	17.521	38.197	20.432	12.303
Final P_{O2} (bar)	25.973	19.796	16.771	22.914	14.105	10.971
Oxygen consumption (mole)	0.0221	0.0051	0.0012	0.0206	0.0095	0.0022
Oxygen consumed (%)	38.64	14.65	4.28	40.01	30.97	10.83
Rate of oxygen consumption (mole/hr)	0.0006	0.0002	0.0001	0.0014	0.0002	0.0001

Based on the above result, the two step model is to be more representatives of the LTO reaction of light crude oils than a simple one-step model. The two stages of reaction can be represented either by two reactions in series, or in parallel as given by Equation 5.11a and 5.11b respectively:

$$\xrightarrow{\frac{1}{2} O_2} CO$$

Crude oil + O_2 $\rightarrow$ oxygenated hydrocarbon + H_2O ....(5.11a)

$$\xrightarrow{O_2} CO_2$$

Crude oil + O_2 $\rightarrow$ Oxygenated hydrocarbon + H_2O ....(5.11b)

$$CO \longrightarrow CO_2$$

The produced gas and the oxidised oil samples obtained in the early stages of the oxidation process show that there is a very low percentage of carbon dioxide, but a high percentage of oxygenated hydrocarbons. Therefore, the oxidation pathway of light crude oil at reservoir condition can be described by a series oxidation model (5.11a), and the final stable products are CO_2 and H_2O. The oxygenated hydrocarbon and CO are not stable and are directly affected by oxidation temperature. The parallel oxidation model (5.11b) may be become dominant at higher temperature.

Generally, the reaction mechanism of low temperature oxidation of crude oil, which a multi-component mixture is far too complex composition to be, describes in detail. Once oxygenated hydrocarbon radicals are formed, many reaction pathways are possible, such as hydrogen abstraction, and decomposition. The most important concept is that as the temperature increases, different reactions come into play, and new kinds of free radicals are created which then decompose. This process is accompanied by an acceleration in reaction rate and rapid rise in temperature.

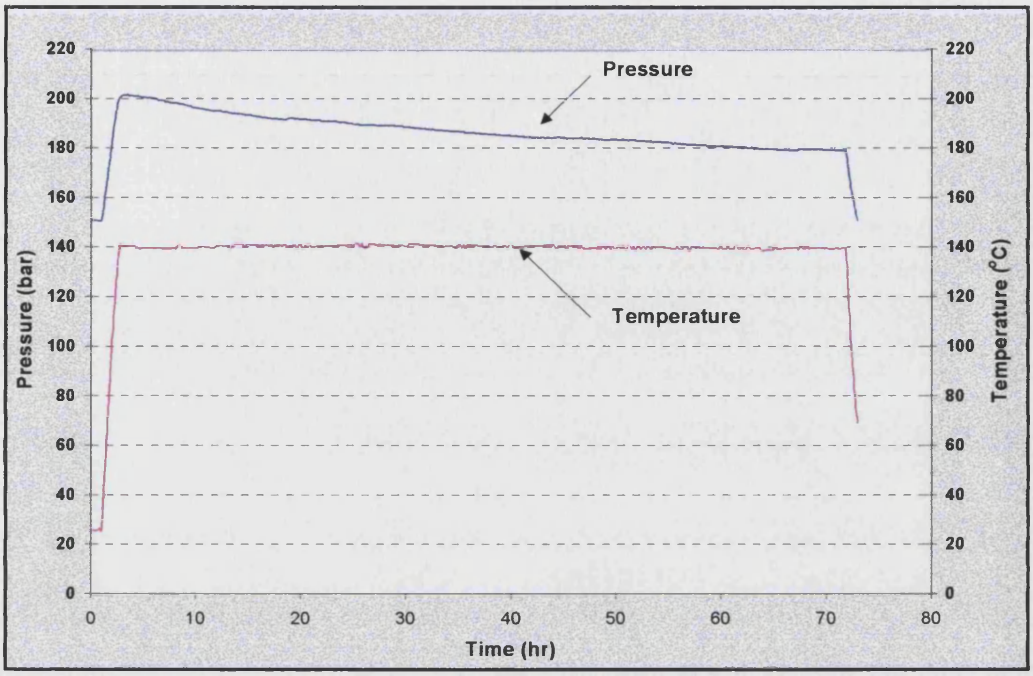

Figure 5.46 Pressure and temperature profiles for SBR (Run 10), Aust. oil (Soi=0.5) And crushed core D. Produced gas: O_2=5.3 %,CO_2 = 6.3 % and CO =3.64 %

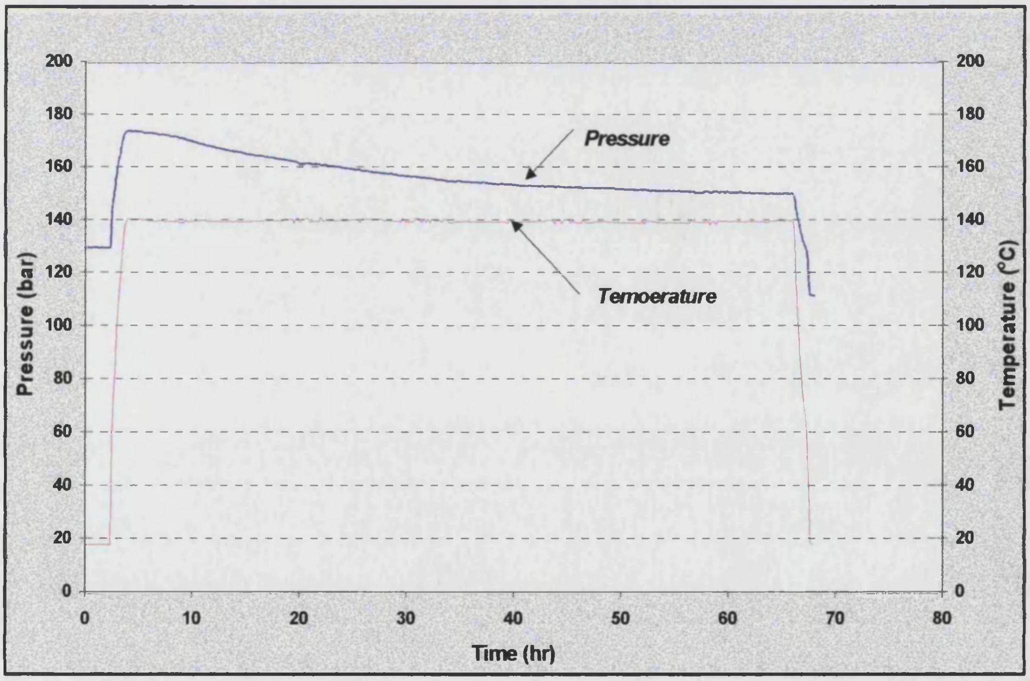

Figure 5.47 Pressure and temperature profile for SBR (Run 35), oil C (Soi=0.5) and crushed core D. Produced gas: O_2= 1.9 %, CO_2 = 7.5 % and CO = 2.91 %

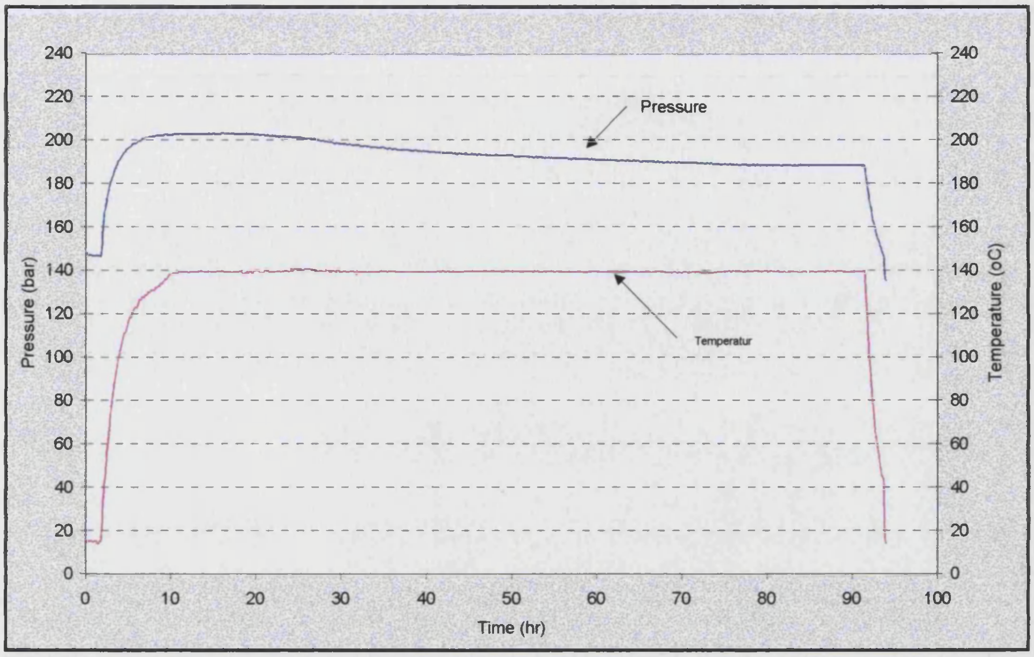

Figure 5.48: Pressure and temperature profiles for SBR (Run 61), oilD (Soi=0.15) and crushed core D. Produced gas: O_2 = 7.6 %, CO_2 = 4.3 % and CO = 2.17 %

5.4.2 Kinetics of LTO Reaction

It is very difficult to determine the kinetic parameters using the two step model with the existing SBR apparatus, this is made more complicated due to the fact that several reaction paths may occur before the final product is formed. As with a number of previous studies reported in the literature[28,46,85], only the overall rate of oxygen consumption is used to calculate the kinetic parameters of the LTO reactions.

Reaction order with respect to oxygen partial pressure

The pressure decline data from a number of SBR experiments were analysed to predict the reaction order with respect to the oxygen partial pressure. The oxygen partial pressure was calculated for assumed different reaction orders (0.25 to 1.1 and plotted against oxidation time. The reaction order, (n) was determined from the best fit (straight line) to the data as shown previously in section 5.2.3 using equations 5.8 and 5.9. These values are given in below.

Table 5.6: Reaction order obtained by fitting oxygen partial pressure data to equation 5.8 and 5.9

Run No.	Crude oil	Soi/Swi	Oxidation Temp. (°C)	$P_{i\,(O2)}$ bar	$P_{f\,(O2)}$ bar	n
10	Aust. Oil	0.50/0.0	140	42.41	7.73	1.1
11	Aust. oil	0.50/0.0	150	43.64	4.67	0.5
15	Aust. oil	0.5/0.25	140	41.96	8.28	0.25
22	Aust. oil	0.75/0.0	140	42.36	14.87	0.5
35	Oil C	0.50/0.0	140	36.62	2.86	1.1
36	Oil C	0.50/0.0	150	36.22	1.72	1.0
42	Oil C	0.75/0.0	140	42.36	14.87	0.25
61	Oil D	0.15/0.0	140	42.82	14.35	1.1
67	Oil D	0.15/0.0	150	43.07	3.35	0.25
71	OilD	0.25/0.0	120	47.46	1.15	0.5
75	OilD	0.50/0.0	120	47.33	0.19	0.9

The value of the reaction order varies depending on the type of crude oil and the operating conditions: temperature, initial and final oxygen partial pressure, and the initial oil and water saturation. The reaction orders in Table 5.6 range between 0.25 and 1.1. Reaction order of 0.3 to 1.0 have been reported previously for LTO reaction of light and heavy crude oils[29,41,56].

Some of the plots of oxygen partial pressure versus time did not exhibit a linear trend for different assumed reaction order values, other experimental results show variable scatter in the plotted points as shown in Figures 5.49 to 5.51.

The failure of certain data to show straight line fitting with equation 5.8 and 5.9 is attributed to the small difference in the initial and final oxygen partial pressure, i.e. low oxygen consumption

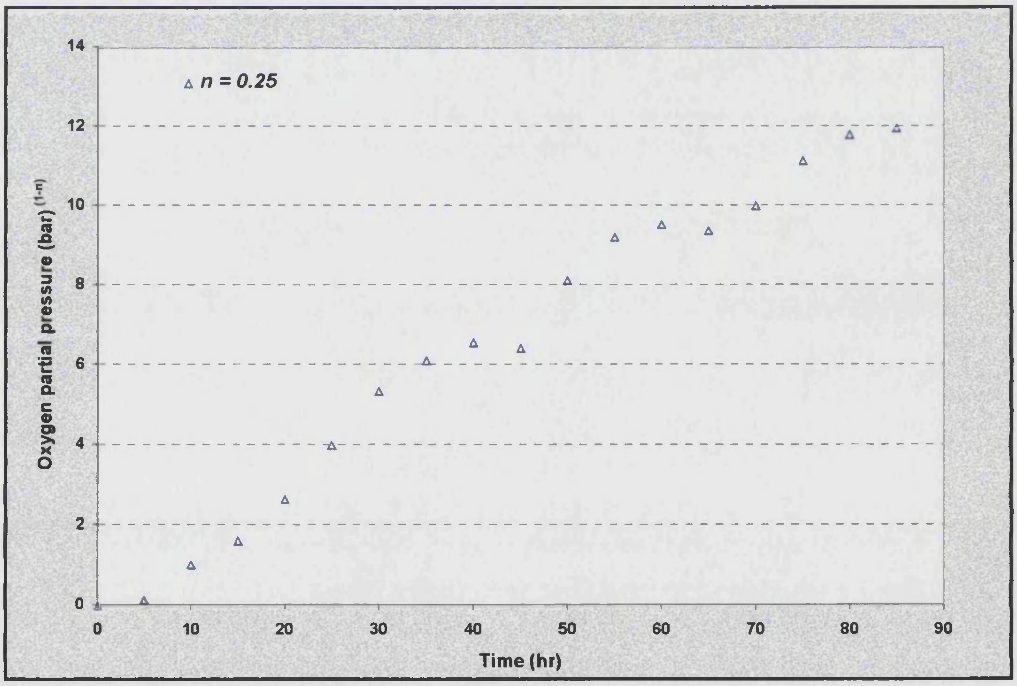

Figure 5.49 Plot of oxygen partial pressure data of Run 86 at n=0.25

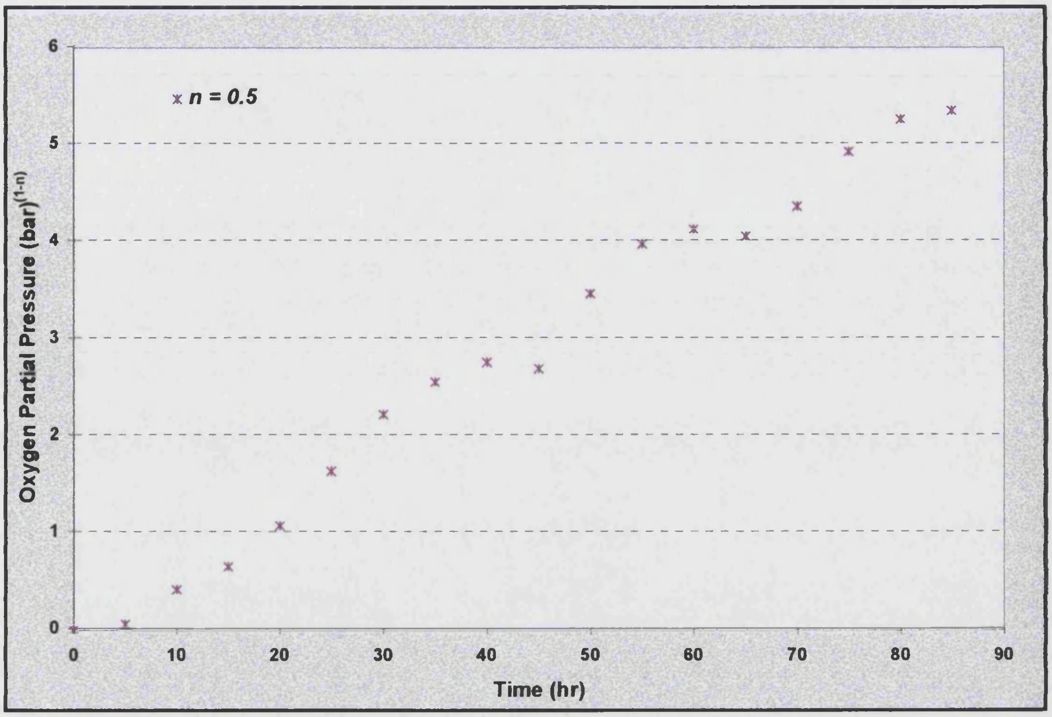

Figure 5.50 Plot of oxygen partial pressure data of Run 86 at n=0.5

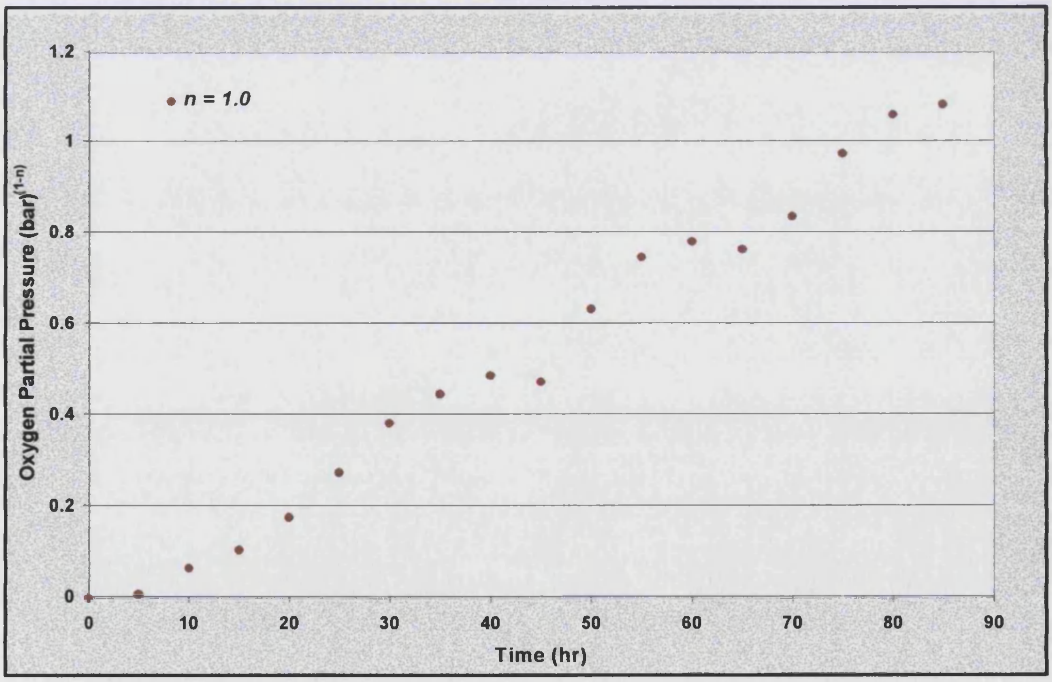

Figure 5.51 Plot of oxygen partial pressure data of Run 86 at n=1.0

LTO Kinetic parameters: Activation Energy and Pre-exponential factor

The relation ship between the reaction rate constant and temperature is given by Arrhenius type below.

$$K = A \exp(-E/RT) \quad \ldots\ldots\ldots\ldots\ldots\ldots\ldots(5.12)$$

where :

K = Reaction rate constant (mole O_2 bar $^{-1}$ hr $^{-1}$ cc $^{-1}$ g sand $^{-1}$)

A = Pre-exponential factor (same unit as reaction rate constant)

E = Activation energy (J mol $^{-1}$ °K $^{-1}$)

R = Universal gas constant (8.314 J mol $^{-1}$)

T = Absolute temperature (°K)

The activation energy (E) and pre-exponential factor (A) for the over-all LTO reaction are determined from a plot of reaction rate constant against the reciprocal of the absolute temperature as shown below.

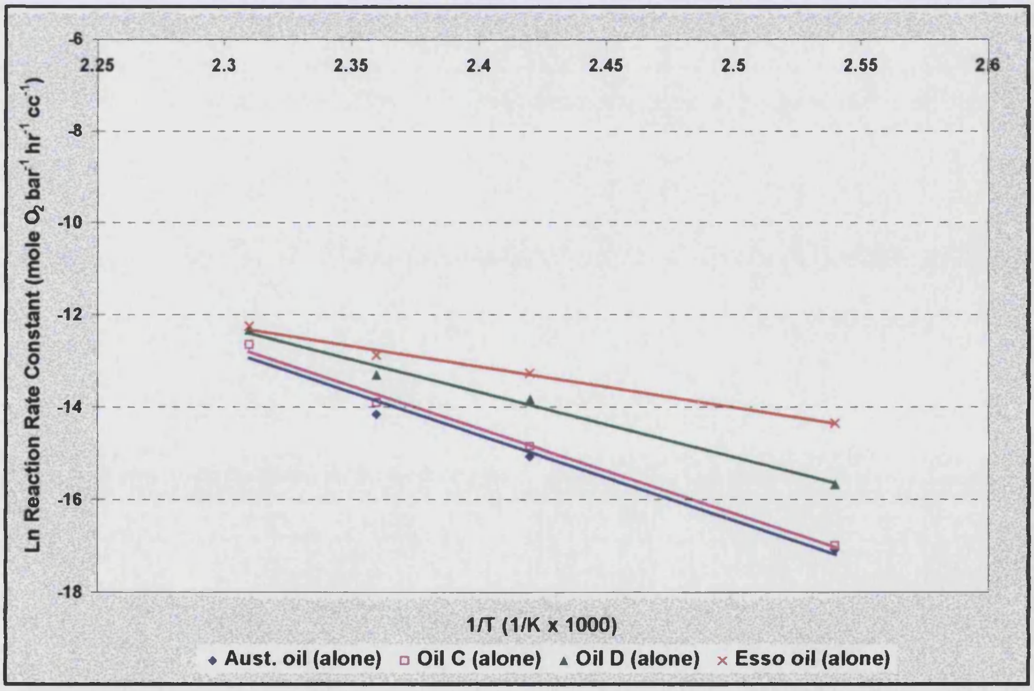

Figure 5.52: Reaction Rate Constant versus Reciprocal Absolute Temperature for light oils

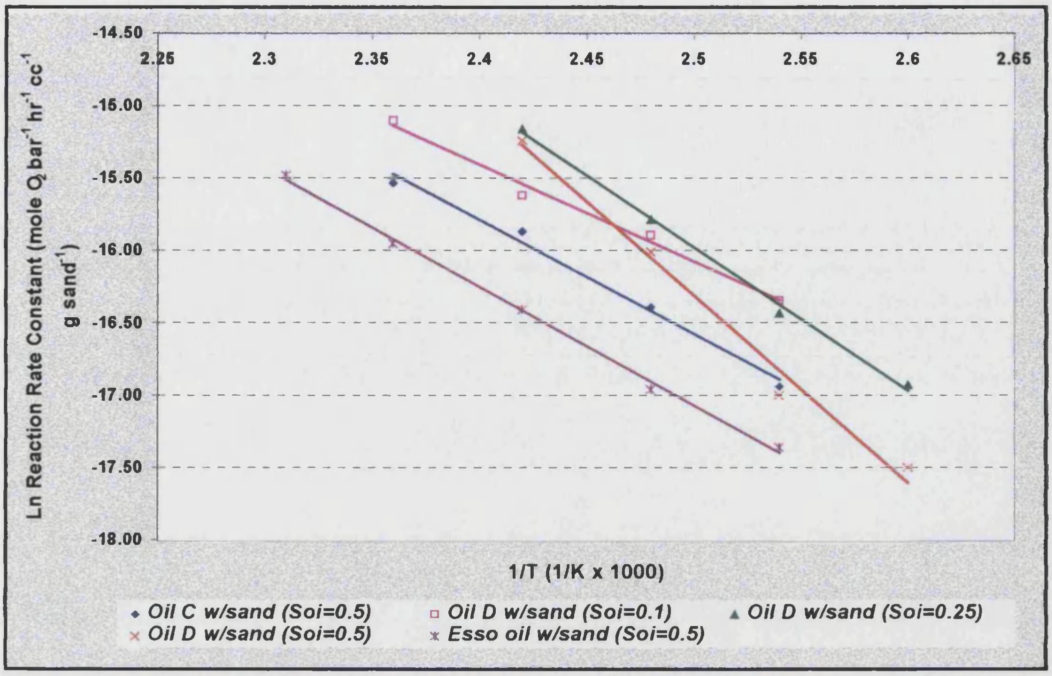

Figure 5.53 Reaction Rate Constant versus Reciprocal Absolute Temperature, for Light Oils with Crushed Core D in SBR Experiments

Table 5.7a and 5.7b summarise the calculated kinetic parameters

Table 5.7a: LTO Kinetic Parameters with and with out matrix

	Activation Energy (kJ mole^{-1})	(A) mole O_2 bar^{-1} hr^{-1} cc^{-1}	Arrhenius Correlation	Reaction Rate Equation
Aust. Oil (alone)	153.78	9.21E+12	Ln R = 29.852 - 18.497/T	R = 9.21E+12 exp (153.78/RT)
Oil C (alone)	153.42	9.30E+12	Ln R = 29.861 - 18.453/T	R = 9.30E+12 exp (153.42/RT)
Oil D (alone)	117.20	5.85E+08	Ln R = 20.188 - 14.097/T	R = 5.85E+08 exp (117.20/RT)
Esso oil (alone)	73.81	3.71E+03	Ln R = 8.2182 - 8.8773/T	R = 3.71E+03 exp (73.81/RT)
Oil C with sand (Soi = 0.50)	65.67	1.48E+03	Ln R = 7.3024 - 7.8994/T	R = 1.48E+03 exp (65.67/RT)
Oil D with sand (Soi = 0.1)	55.45	1.13E+02	Ln R = 4.731- 6.6701/T	R = 1.13E+02 exp (55.45/RT)
Oil D with sand (Soi = 0.25)	82.50	3.09E+05	Ln R = 12.644 - 9.922/T	R = 3.09E+05 exp (82.50/RT)
Oil D with sand (Soi = 0.50)	107.64	4.27E+08	Ln R = 19.872 - 12.945/T	R = 4.27E+08 exp (107.64/RT)
Esso oil with sand (Soi=0.5)	68.25	1.96E+03	Ln R = 7.5809 - 8.2085/T	R = 1.96E+03 exp (68.25/RT)

Table 5.7b: LTO Kinetic Parameter with sand

	(E) KJ $mole^{-1}$	(A) mole O_2 bar^{-1} hr^{-1} cc^{-1} g $sand^{-1}$	Arrhenius Correlation	Reaction Rate Equation
Oil C with sand (Soi = 0.50)	65.65	2.40E+01	Ln RRC = 3.18 - 7.89/T	R = 2.40E+01 exp (65.65/RT)
Oil D with sand (Soi = 0.1)	55.45	1.82E+00	Ln RRC = 0.6103 - 6.67/T	R = 1.82E+00 exp (55.45./RT)
Oil D with sand (Soi = 0.25)	82.47	6.90E+03	Ln RRC = 8.84 - 9.92/T	R = 6.90E+03 exp (82.47/RT)
Oil D with sand (Soi = 0.50)	107.66	9.43E+06	Ln RRC = 16.06 - 12.95/T	R = 9.43E+06 exp (107.66/RT)
Oil D with sand (Soi = 0.15) Inj O2 = 21%	88.96	4.48E+04	Ln RRC = 10.71 - 10.70/T	R = 4.48E+04 exp (88.96/RT)
Oil D with sand (Soi = 0.15) Inj O2 = 5%	88.05	2.46E+04	Ln RRC = 10.11 - 10.59/T	R = 2.46E+04 exp (88.05/RT)
Oxidised Oil D with sand (Soi = 0.15) Inj O2 = 21%	93.22	7.41E+04	Ln RRC = 11.21- 11.213/T	R = 7.41E+04 exp (93.22/RT)
Esso mix(1) oil with sand (Soi=0.5)	68.24	3.18E+00	Ln RRC = 3.46 - 8.2085/T	R = 3.18E+00 exp (68.24/RT)

E = Activation Energy, A = Pre-exponential factor

5.4.3 *Factors Affecting Reaction Kinetics of LTO Process*

LTO kinetics are affected by condition in the oxidation zone, as determined by the temperature, oxygen concentration, reservoir matrix, residence time, initial oil and water saturation, operating pressure, and type of crude oil.

Oxidation Temperature

Most of the light crude oils investigated have sufficient reactivity to initiate spontaneous reaction with oxygen at reservoir temperature but the individual reactivity was found to be different for each oil and this depends on the reservoir temperature. Consequently, the reservoir temperature is a very important parameter which needs to be considered in any air injection process, to ensure spontaneous oxidation occurs between oil and oxygen, there is sufficient increase in the temperature in the oxidation zone to consume all the injected oxygen. The results show that the reaction rate constant is inversely proportional to the oxidation temperature as predicted by Equation 5.12. The variation of reaction rate constant with oxidation temperature for different light crude oils is shown in Figure 5.52 and 5.53.

Oxygen Concentration

Across the oxidation zone, the residual virgin oil and oxidised oil will be contacted by different oxygen concentrations (0 to 21%). To simulate this condition, oil D and crushed core D at Soi=0.15 was subjected to isothermal oxidation at different oxygen concentrations (5, 10, and 21%). For this set of experiments virgin oil and crushed core (sand) were oxidised with 21% O_2, then the oxidised oil was furthered oxidised with 10% O_2. Finally the oxidised mixture from this run was subjected to further oxidation with 5% O_2. A further three runs were made in the same way, but starting with 5% O_2, then 10% O_2 and finally 21% O_2. These tests were run at 120, 140, and 150 °C and the operating pressure and other condition were the same for each run as detailed in Table D.9 to D11. As shown in Table 5.7b that the activation energy is not significantly affected by changing the oxygen concentration. The pre-exponential factor increases when oxidised oil is further oxidised with air compared to oxidation of virgin oil with air. On the other hand the value of pre-exponential factor is doubled when the virgin (residual) oil was oxidised with depleted air (O_2 = 5%), compared to oxidation of virgin oil with air (O_2 = 21%). The relation between reaction constant rate and absolute temperature for oil D (Soi=0.15) at different oxygen concentration is shown in Figure 5.54.

Karen at al.[56] found that as the partial pressure of oxygen in their DTA experiment was increased from 10.1% to 20.9%, the activation energy for LTO reaction of Athabasca bitumen increased from 55 to 63 kJ/kg mole. They also, found that an oxygen partial pressure of greater than 10% O2 favoured exothermic reactions. Hughes et al.[19] in DSC experiments at atmospheric pressure noticed that an increase of oxygen partial pressure caused a reduction in the activation energy of the coke oxidation.

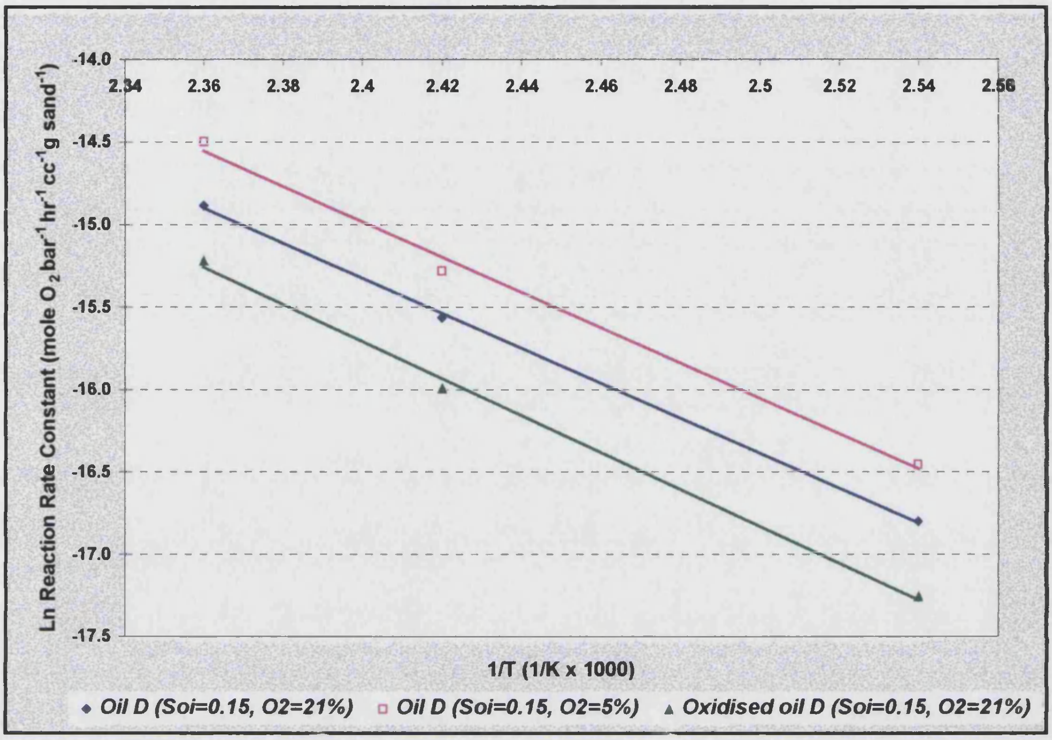

Figure 5.54 Reaction Rate Constant versus Reciprocal Absolute Temperature, for Light Oils with Crushed Core D (Soi=0.15) @ different O_2 Concentration

Effect of Matrix (crushed core)

The oil oxidation reaction is likely to be affected by the presence of reservoir rock. Crushed core D was used in all of the runs. Figures 5.55 and 5.56 show that an increase in the specific reaction rate constant for Australian oil, oil C and oil D with crushed core, compared with oil alone only. This is attributed to the effect of the surface area and possible catalytic effect of the sand surface. A large surface area promotes oxidation reactions and hence lowers the activation energy. Esso Mix1 oil shows a smaller increase due the reduction of the surface area resulting from the precipitation of asphaltene and coke on the top of the sand matrix in the reactor, occurring during the initial stages of oxidation.

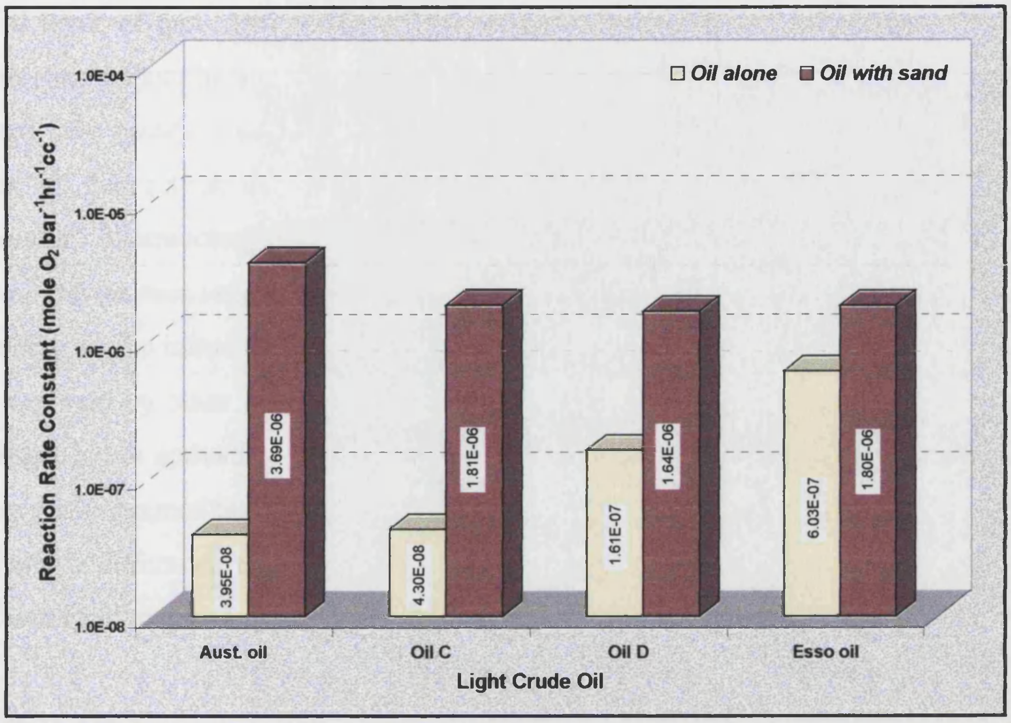

Figure 5.55: Effect of presence of crushed core on reaction rate constant @ 120 °C

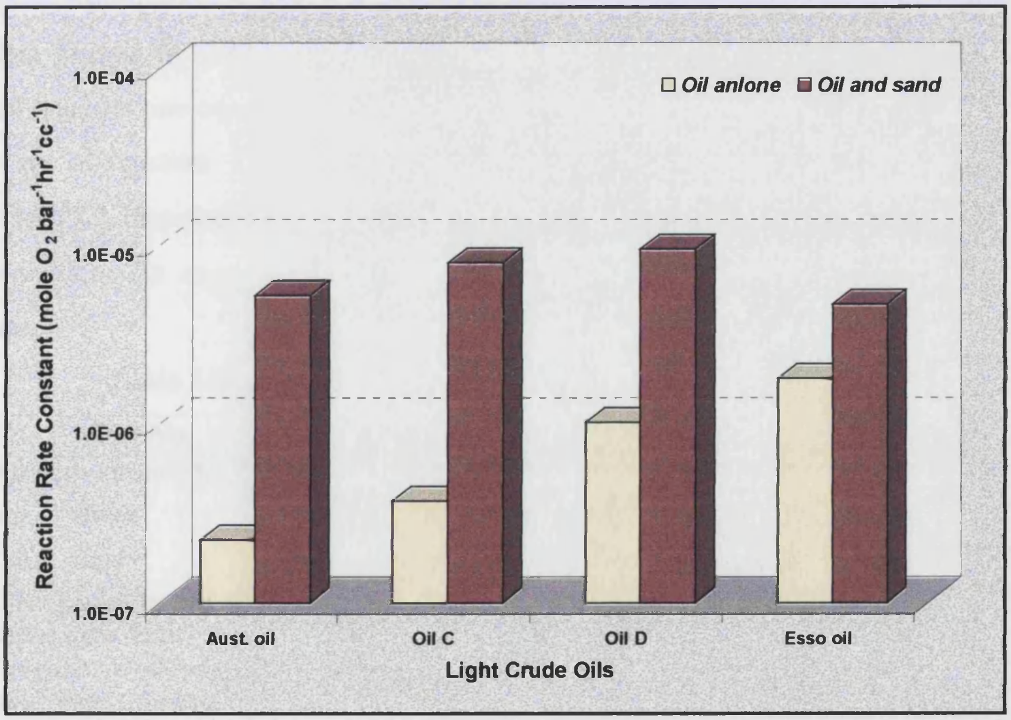

Figure 5.56: Effect of presence of crushed core on reaction rate constant @ 140 °C

A hard layer of fuel (see Fig. 5.8b) was deposited on the top of the sand, when the reactor was unpacked at the end of the experiment. It is clear that the presence of crushed core causes a substantial reduction in the activation energy as shown by the values of the activation energy given in Table 5.7a. Ranjbar[52] found that low temperature thermocatalytic oxidation reactions reduce the activation energy, and increase the reaction velocity. The activation energy values range from 55 – 105 kJ/mole depending on the initial oil saturation. Values of (E) in the range 48 – 98 kJ/mole have been reported by other researchers[28,41,56,85]. Greaves et al.[85] found that when the sand was used, lower activation energy, and higher values of the Arrhenius pre-exponential factors were obtained for LTO reactions of North Sea light oil. Fassihi et al.[55] found that there was a difference in the kinetic parameter values between natural reservoir cores and clean sand material.

Oxidation Time

In section 5.3.6 it was mentioned that the oxidation time has direct effect on the over all oxygen consumption and consequently, the overall reaction rate will be affected. From the data printed in Table 5.8, increases the oxidation time causes an increase in the overall reaction rate constant, although there is a decrease in the oxidation rate during a late stage of reaction. The increase is more higher when the oxidation temperature is high (140 °C). The decrease in oxidation rate is attributed to the fact that at late stage of the oxidation, the oxygen partial pressure is less compared to the early stage of the oxidation.

Table 5.8: Effect of oxidation time on reaction rate constant

Run No.	**6**	**7**	**27**	**28**	**49**	**50**
Initial oil saturation (%)	10	10	10	10	10	10
Initial p_{O2} (bar)	42.73836	45.4041	34.9461	35.3556	38.7597	40.8114
Final p_{O2} (bar)	27.42929	14.31576	30.07992	23.77284	30.63664	23.37492
Reaction temperature °C	140	140	116	116	120	120
Oxidation time (hr)	***75***	***133***	***85***	***170***	***60***	***125***
Total percent of O_2 consumed	35.82	68.47	13.92	32.76	20.96	42.72
Reaction Rate Constant (mole O_2 bar^{-1} hr^{-1} cc^{-1} g $sand^{-1}$)	1.01E-07	1.48E-07	3.20E-08	4.23E-08	7.03E-08	8.02E-08

Residual Oil Saturation

The initial , or residual oil saturation was calculated based on the pore volume of the packed sand (see Appendix A). So was varied from 75 % down to 10 % in order to simulate different stages of recovery from a light oil reservoir, as well as the pre-history pressure maintains (high oil saturation), and water flooding reservoir (high water-cut and low oil saturation). The effect of residual oil saturation on the reaction rate constant is illustrated on Figures 5.57 and 5.58. At 120 °C, Australian oil and oil D first show a very gradual decline up to So = 50% and 25% respectively, and then a much steeper reduction of the reaction rate constant when So is increased to higher values. In contrast, oil C shows a much lower overall effect, which is essentially linear. There are some changes at 140 °C, wherever the oil C and oil D first show an increase then a decrease, albeit at higher values of the rate constant. The IOR Group at University of Salford[54] in (unpublished report) concluded that at low oil saturation, there is a higher reactivity with oxygen compared to a high initial oil saturation condition. This was attributed to the increased oxygen accessibility at lower oil saturation. As shown in Table 5.7b, there is a decrease in the activation energy for oil D when the initial oil saturation is decreased.

Water Saturation

Figures 5.59 shows that with water present, the reaction rate constant increases two fold at 120 °C, compared to the situation with out water. As the water saturation increases, the reaction rate shows a continues increase for Australian oil (Figure 5.60). The relation between the reaction rate constant and absolute oxidation temperature of Australian oil at different water saturation is shown in Figure (5.61). The kinetic data analysis of Australian oil at different water saturation is given in Table 5.9, the analysis shows that the activation energy decreases with an increase in the water saturation in the range of the investigated temperature.

Table 5.9: Overall LTO Kinetic Data of Australian oil at different water saturation

	Activation Energy (KJ/mole)	K_o mole O2/bar. hr.cc.g sand	Arrhenius Correlation	Reaction Rate Equation
Australian oil with Crushed core D (Soi = 0.50)	33.50	1.61E-03	Ln RRC = -6.43 – 4.03/T	RRC = 1.61E-03 exp (33.50/RT)
Australian oil with Crushed core D (Soi=0.50, Swi=0.25)	26.19	2.59E-04	Ln RRC = -8.26 - 3.15/T	RRC = 2.59E-04 exp (26.19./RT)
Australian oil with Crushed core D (Soi=0.50, Swi=0.50)	18.62	4.63E-05	Ln RRC = -9.98 - 2.24/T	RRC = 4.63E-05 exp (18.62/RT)

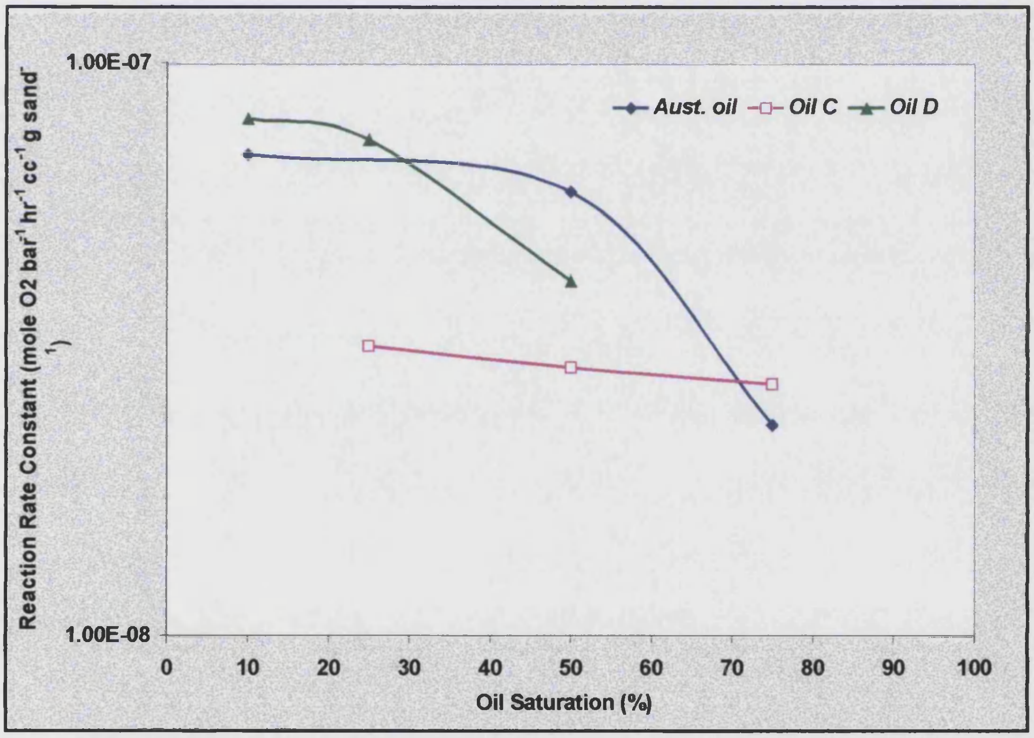

Figure 5.57: Effect of residual oil saturation on reaction rate constant at 120 °C

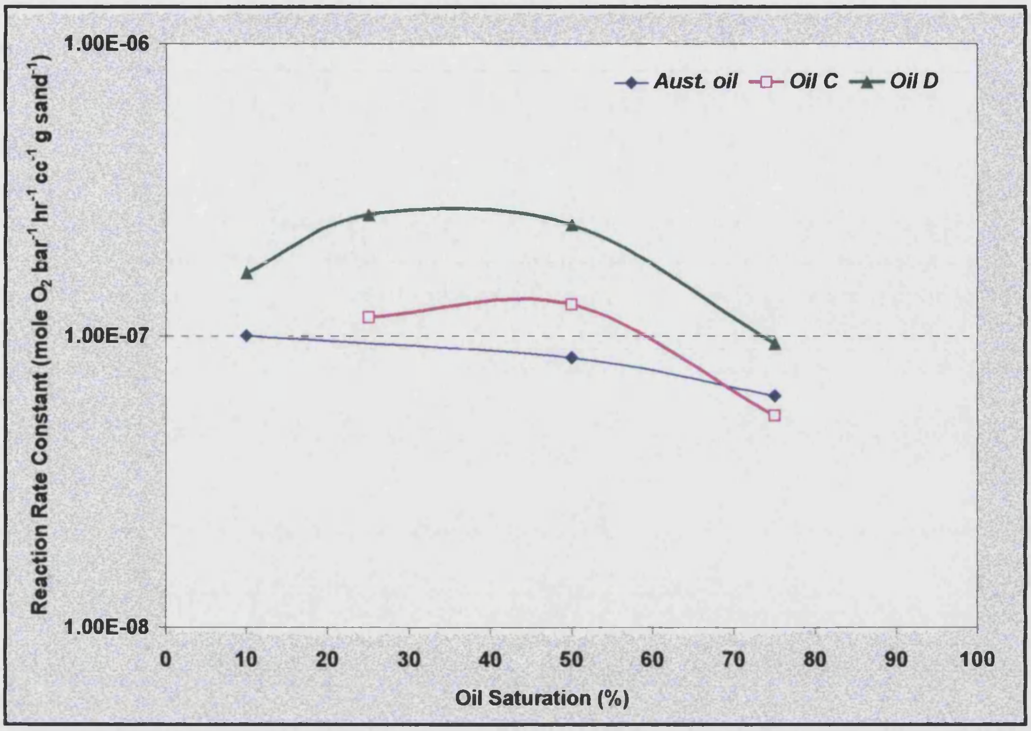

Figure 5.58: Effect of residual oil saturation on reaction rate constant at 140 ℃

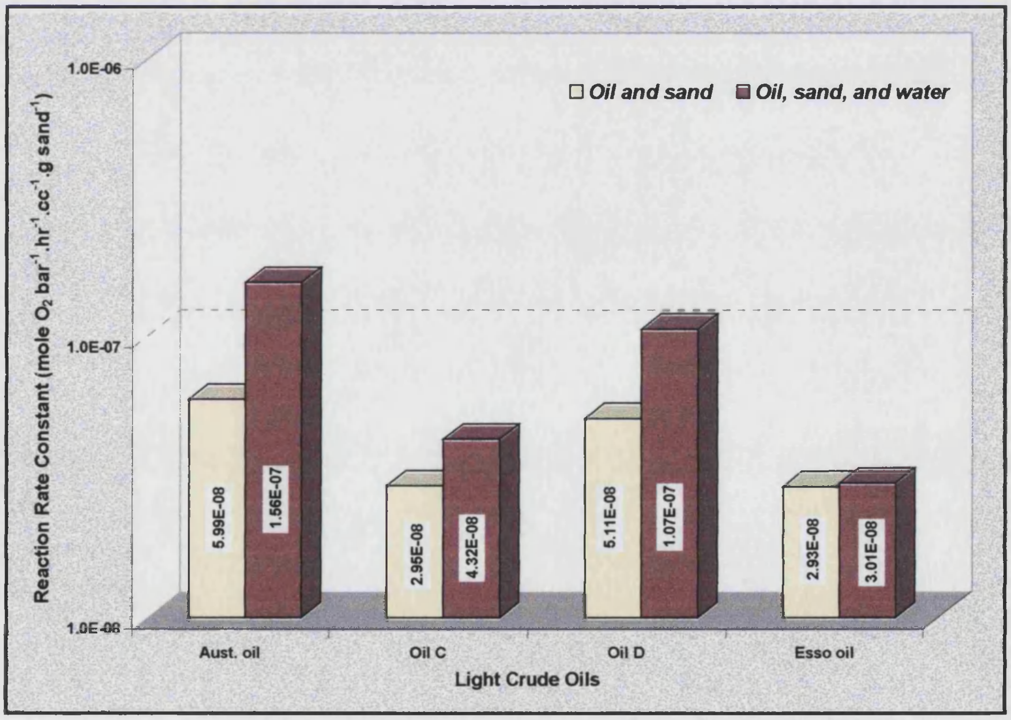

Figure 5.59 Effect of water on reaction rate constant at 120 ℃

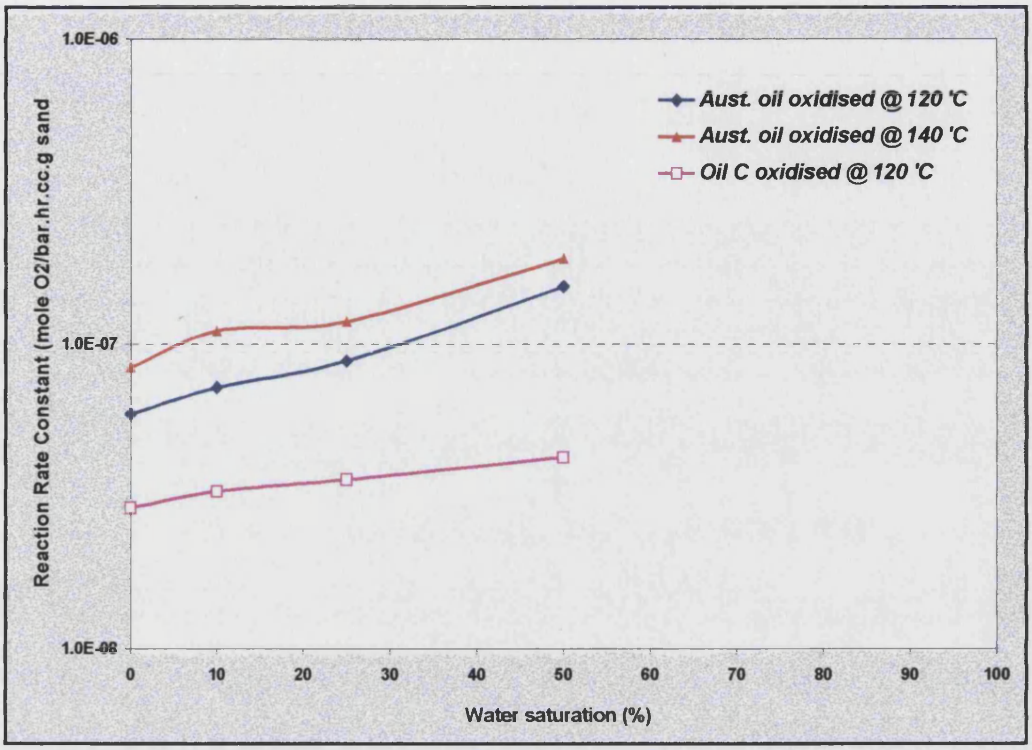

Figure 5.60 Effect of water saturation on reaction rate constant

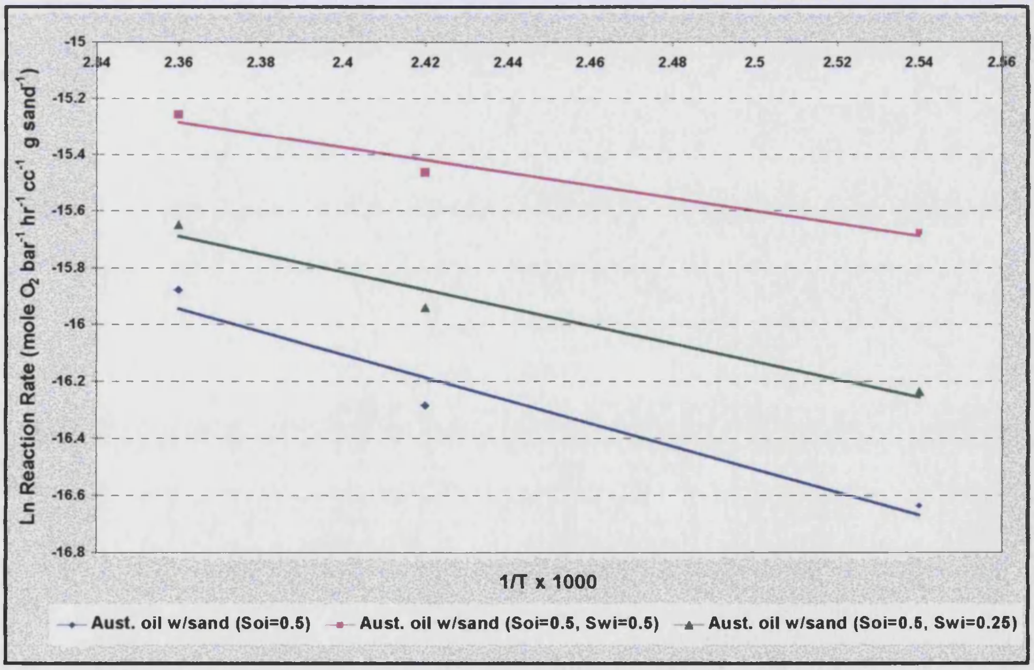

Figure 5.61 Reaction Rate Constant versus Reciprocal Absolute Temperature, for Australian Oil at different water saturation in SBR Experiments

Reactor Pressure

The effect of operating pressure on oil oxidation was investigated by varying the initial pressure of the SBR (Table 5.10). The results (Figure 5.62) show that the reaction rate constant (oxygen consumption) is inversely proportional to the oxidation pressure comparing between 100 bar and 150 bar. Hence, oxygen utilisation increases as the total pressure decreases. This factor has a direct impact on the air injection LTO process from the economic and safety point view. There is not agreement in the literature, however, since some researchers[50,56] have observed an increase in the rate of LTO reaction and exothermicity with increasing pressure, while others[46,85] reported that rate was independent of total pressure under LTO reaction condition. Al-Saffar et al.[50] used consolidated core material in pressurised flow reactor, they found increasing the total pressure results in a decrease in the activation energy of LTO reactions of North Sea light crude oils.

Table 5.10: Effect of reactor pressure on reaction rate constant

Run No.	32	33	48	49	87	88
Initial oil saturation (%)	50	50	10	10	50	50
Initial reaction pressure (bar)	127.344	198.438	128.52	184.57	133.2	197.09
Final reaction pressure (bar)	112.695	180.57	125.19	178.12	119.73	184.77
Reaction temperature (°C)	120	120	120	120	140	140
Initial P_{o2} (bar)	26.7422	41.672	26.9892	38.7597	27.972	41.3889
Final P_{o2} (bar)	8.11404	18.2376	19.7800	30.63664	2.75379	12.01005
Reaction time (hr)	86	90	58	60	61	50
Total Percent of O_2 consumed	69.66	56.24	26.71	20.96	90.16	70.98
Reaction Rate Constant (mole O_2 $bar^{-1} hr^{-1} cc^{-1} g\ sand^{-1}$)	4.44E-08	2.94E-08	9.64E-08	7.03E-08	1.16E-07	7.53E-08

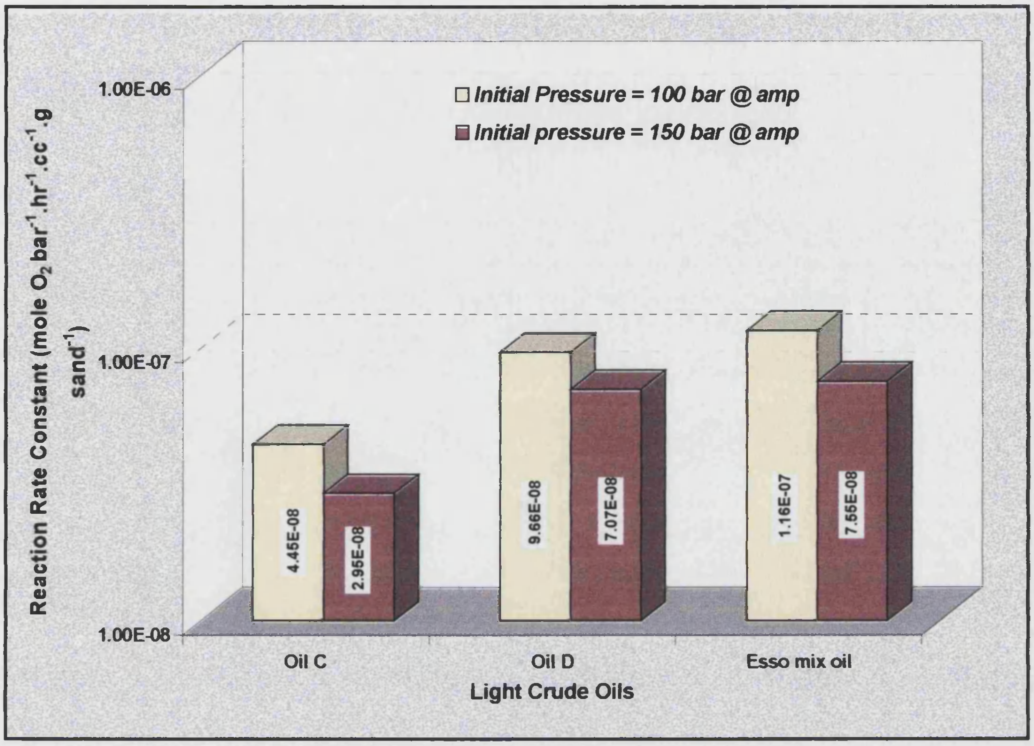

Figure 5.62 Effect of operating pressure on reaction rate constant

5.4.4 Autoignition Temperature

The experiments have been designed in such a way to obtain the ignition temperature of light crude oils, as well as to investigate the effect of different parameters, such as Soi, Swi, Pi, AOR (air to oil ratio) and composition of crude oil.

The operating procedure was modified slightly from previous experiments. The furnace temperature was set at temperature of 200 °C. As the reactor and crude oil heated up and approached 160 °C, the pressure and temperature were recorded every second. In this way the autoignition temperature of the oil could be detected by observing the sharp rise in the oil-sand temperature and the rise in pressure. In addition the oxygen concentration of the produced gas was zero. If there is no sign of ignition, the oxidation temperature inside the reactor will continue to rise until it reaches the isothermal setting temperature (200 °C) and continues at that temperature for a period of time. The results are given in Appendix D (Tables D.23 to D.27). Auto-ignition of light crude oils occur when the temperature and pressure profiles increase (Figure 5.63 and 5.64), demonstrate by two peaks. Autoignition takes place at a temperature between 175 to 187 °C. Another noticeable feature is that when autoignition occurs, the reaction stops and the pressure profile shows no further decline, because of one of the reactants has been exhausted. Since fuel is still present in the SBR at the completion of the experiment, oxygen has been totally consumed (Figure 5.65).

Autocatalytic ignition is a feature of branched chain chemical processes. There is an induction period during which there is build up of intermediate (oxygenated) products produced by LTO reactions at lower temperature (120 to 160 °C). Transition from one reaction state to another is expected with a change in the kinetic parameters[81].

Two types of autocatalytic ignition phenomena have been observed during these experiments. The first shows that at the autoignition point there is a rapid increase in the temperature and pressure, to 330 °C and 400 bar respectively, as shown in Figure 5.63. Other runs culminated in a more explosive effect, in that a detonation noise or bang occurred. In the batch reactor, radicals accumulate in the oil, which accelerate the reaction to a very high rate.

In the second trend, there is only a normal increase in the temperature and pressure inside the SBR, but the oxygen partial pressure is reduced to zero at the end of the experiment (100% oxygen consumption), as given in Appendix D (Table D24 to D26)(Run 112, 114, 115, 120, and 121).

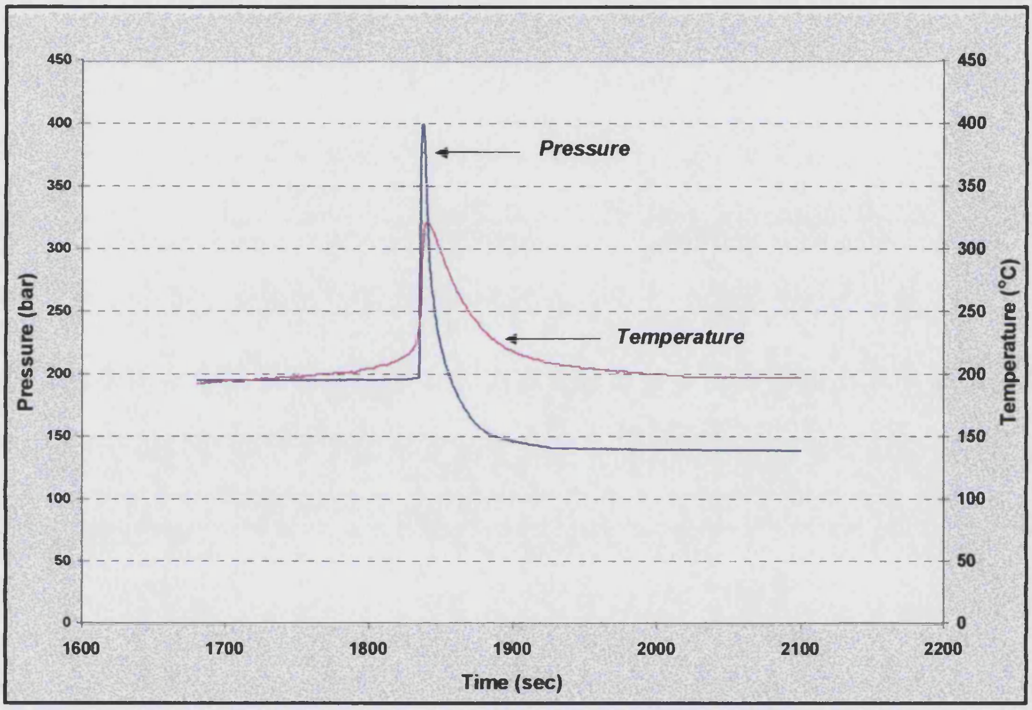

Figure 5.63: Temperature and pressure profiles during autoignition of oil C (Soi=1.0) (Run 123) (Pressure and temperature recorded every second)

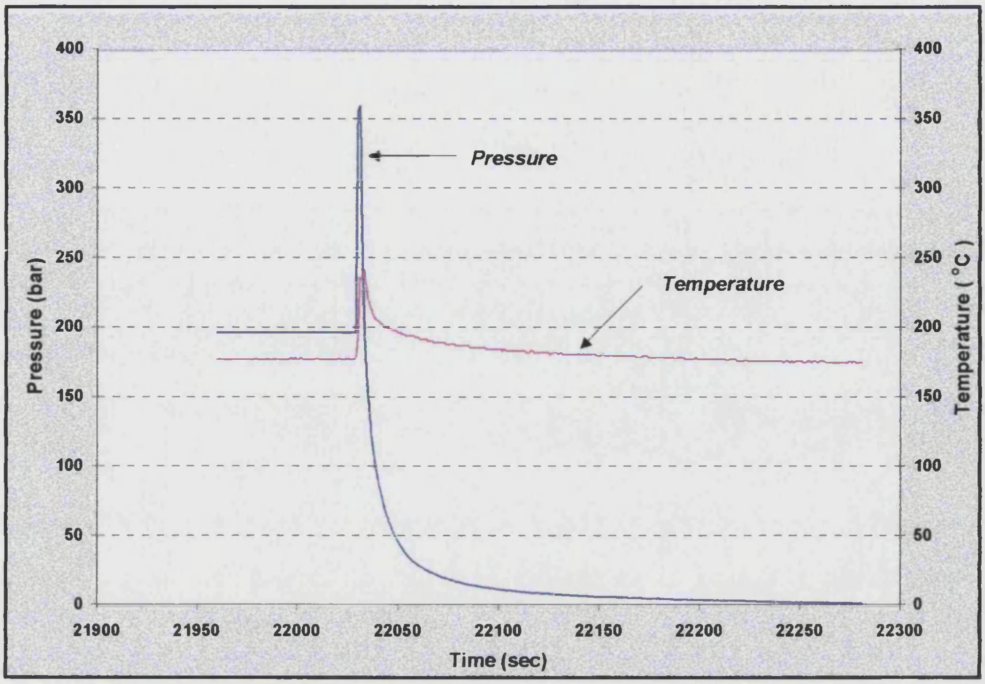

Figure 5.64: Temperature and pressure profiles during autoignition of oil D (Soi=0.5) (Run 126) (Pressure and temperature recorded every second)

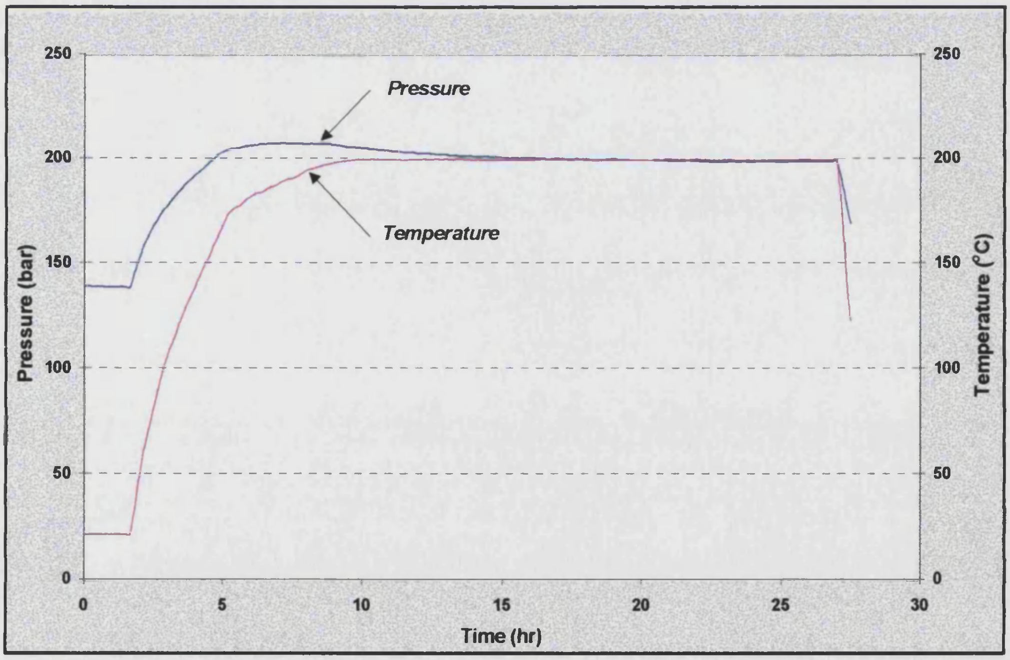

Figure 5.65: Temperature and pressure profiles during autoignition of Australian oil (Soi=0.5) (Run 112)(Pressure and temperature recorded every 10 minutes)

5.4.4.1 Factors Effecting Autocatalytic Ignition

There are many factors affecting the autocatalytic ignition phenomena of light crude oils, including initial oil and water saturation, air oil ratio (strictly air to oil reactor charge), and composition of crude oil.

Oil saturation

The amount of oil charged into the SBR has a very significant effect on the shape of the pressure and temperature peaks, when autocatalytic ignition occurs, as shown in Figures 5.63, 5.66, and 5.67 for oil C. Both of the peaks are higher at higher oil saturation (Soi=1.0). When the oil saturation was decreased to 50% and 25%, the autocatalytic ignition peaks were lower and not observed respectively as shown in Figure (5.66 and 5.67). This is attributed to the smaller amount of free radical components formed during the induction period (120 – 160 °C).

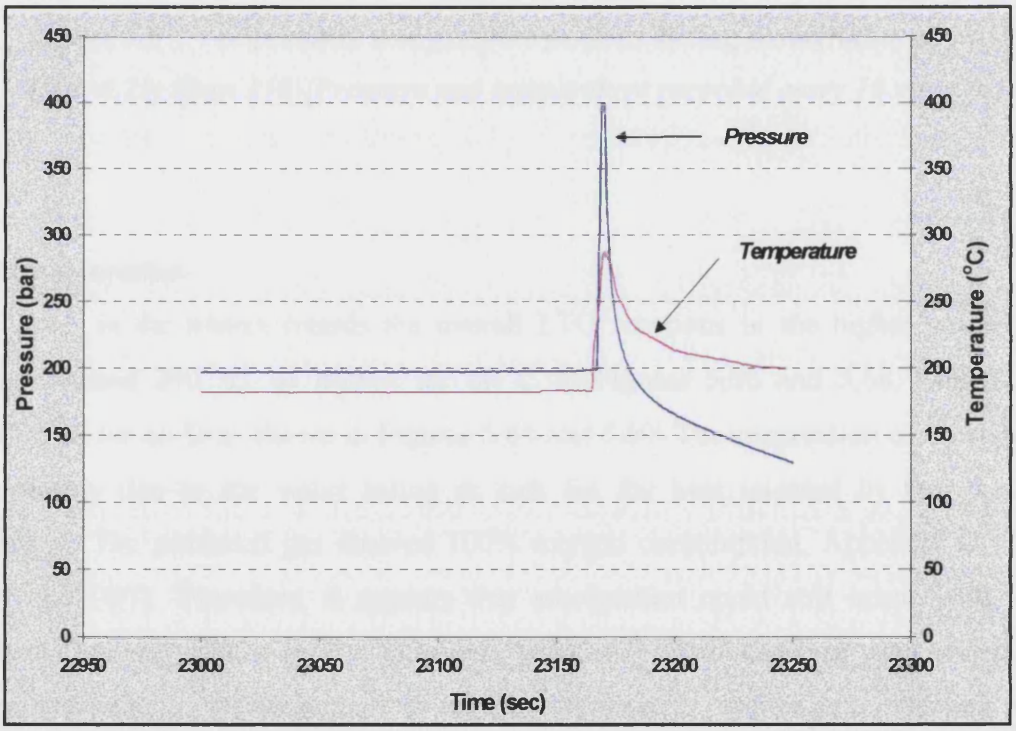

Figure 5.66: Temperature and pressure profiles during auto ignition of oil C (Soi=0.5) (Run 119) (Pressure and temperature recorded every second)

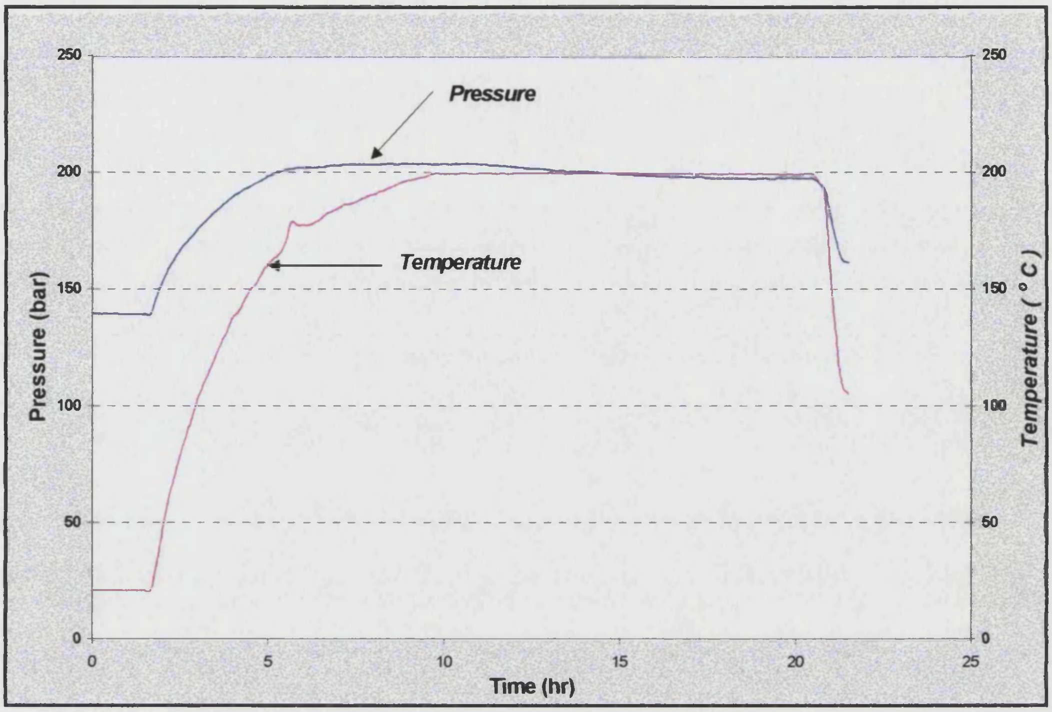

Figure 5.67: Temperature and pressure profiles during autoignition of oil C (Soi=0.25) (Run 118)(Pressure and temperature recorded every 10 minutes)

Water saturation

Water in the matrix retards the overall LTO reactions in the higher temperature range, around 200 °C, as shown for oil C in Figures 5.66 and 5.68. This is also confirmed for oil D as shown in Figures 5.64 and 5.69. The suppression of autoignition is probably due to the water acting as sink for the heat released by the oxidation reactions. The produced gas showed 100% oxygen consumption, Appendix D (Table D26 and D27). Therefore, it appears that autoignition could still occur with water present, but the effect is not detected. Osindero[81] who used an accelerated rate calorimeter found that an increase in the amount of water resulted in a reduction in the self-heat rate during the LTO reaction period.

It is not possible to say whether there is a minimum value of water saturation, above which autoignition will occur. At Swi = 0.25 and 0.5, there is no difference in the temperature and pressure curves, i.e. no spike was observed as shown in Figures 5.68 and 5.70. The absence of a very rapid increase in the pressure and temperature curves may due to the fact that the peroxide reactions are inhibited by the presence of water.

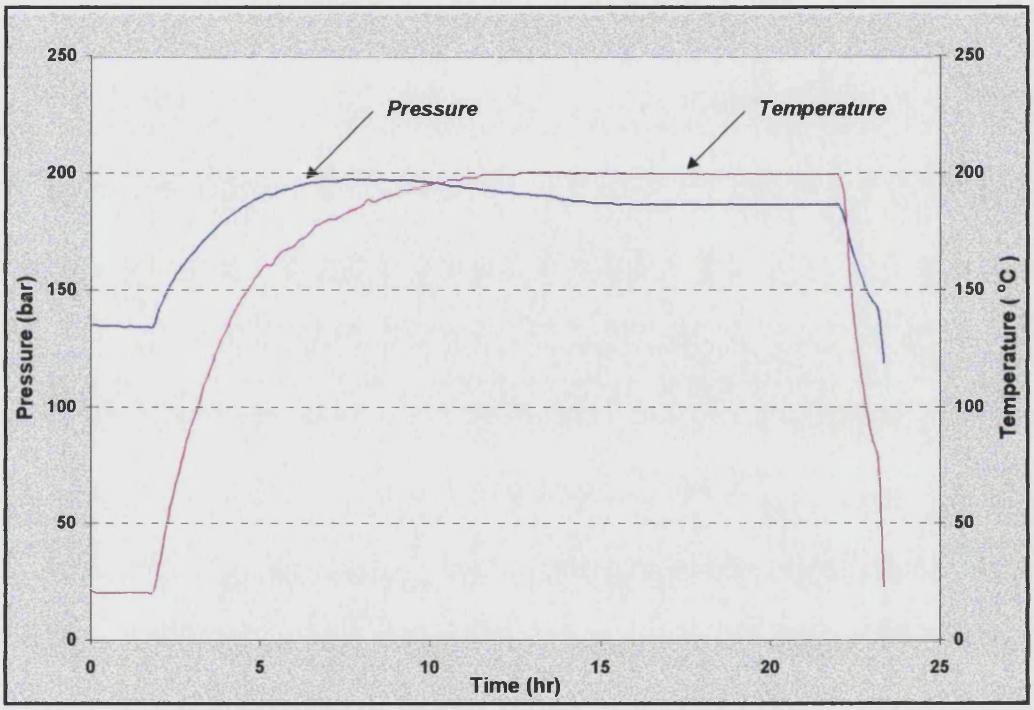

Figure 5.68: Temperature and pressure profiles during autoignition of oil C (Soi=0.5, Swi=0.5) (Run 121)(Pressure and temperature recorded every 10 minutes)

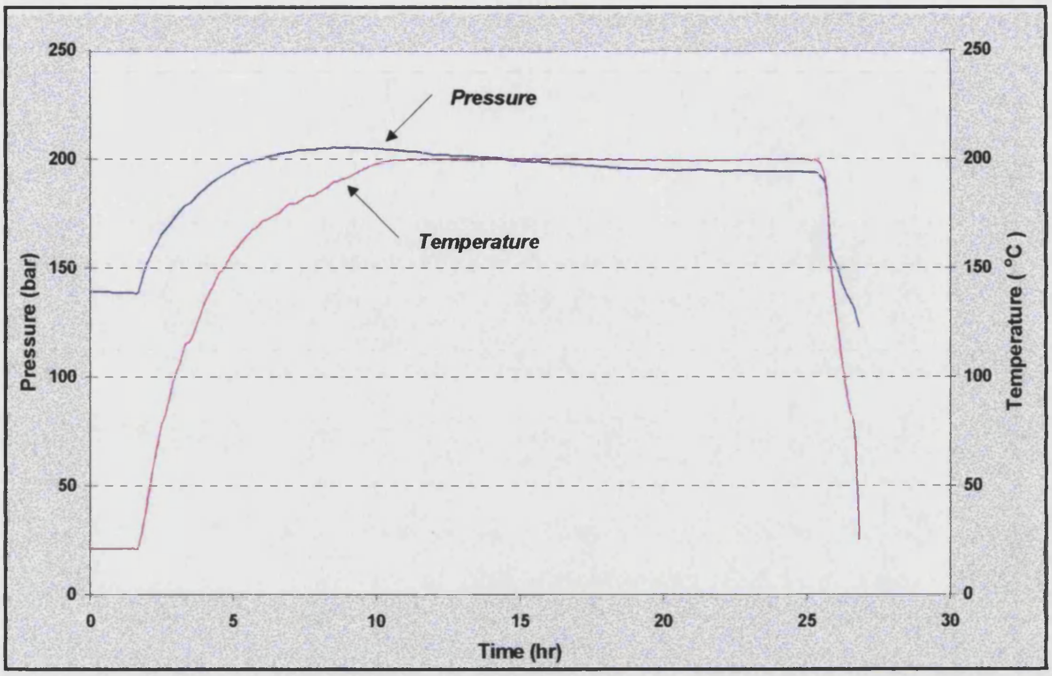

Figure 5.69: Temperature and pressure profiles during autoignition of oil D (Soi=0.5, Swi=0.5) (Run 127)(Pressure and temperature recorded every 10 minutes

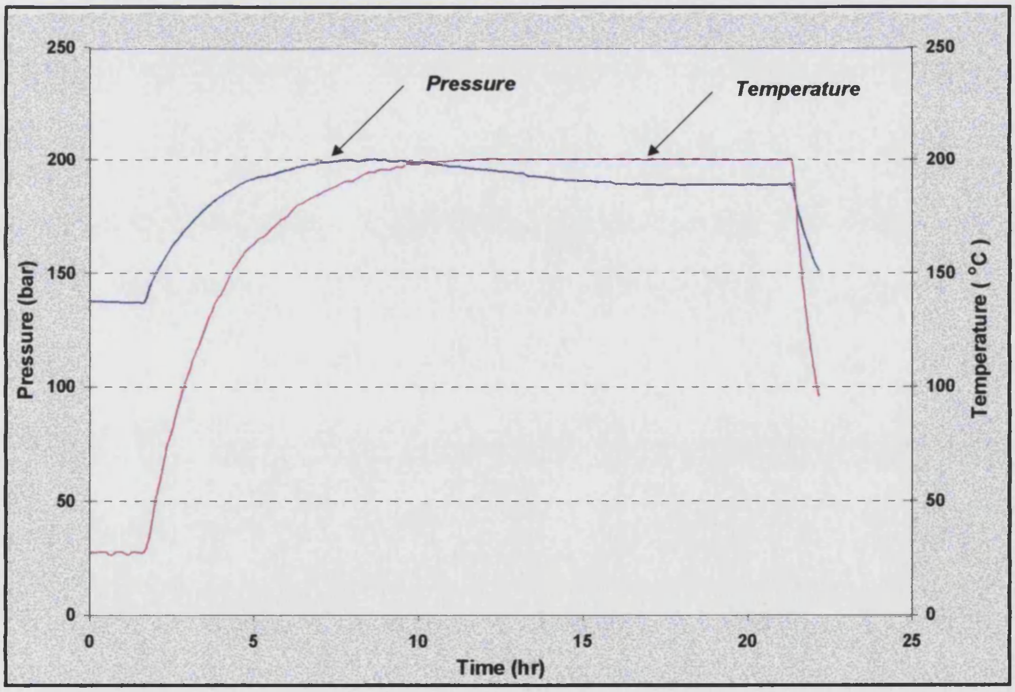

Figure 5.70: Temperature and pressure profiles during autoignition of oil C (Soi=0.5, Swi=0.25) (Run 120)(Pressure and temperature recorded every 10 minutes)

Air oil ratio in SBR

The effect of air oil ratio in SBR on autocatalytic ignition was investigated by varying the volume of oil and air in the SBR (Table 5.11). The results (Figure 5.65 and 5.71) for Australian oil show that the air oil ratio change in the SBR greatly effects the size of the pressure and temperature peaks when no water present (sharp rise in the pressure and temperature peaks). The increased amount of oxygen (mole) in the SBR will increase the formation of free radical components, and hence the likelihood of autocatalytic ignition. However, there is no detectable autoignition when water is present, even at a high AOR as shown in Figure 5.72.

Table 5.11: Effect of air oil ratio in SBR on autoignition of Australian oil

Run No.	112	113	114	115
Initial oil saturation (%)	50	50	50	50
Initial water saturation (%)	0	0	50	50
Initial gas saturation (%)	50	50	0	0
Volume of oil (cc)	8.5	4.25	8.5	4.25
Weight of sand matrix (g)	61.6	30.8	61.6	30.8
Initial volume of air (cc)	54.9	74.9	46.4	66.4
AOR in SBR (scc/cc)	6.459	17.623	5.458	15.623
Initial conc. % of oxygen	21	21	21	21
Initial charged press. (bar)	137.89	143.95	138.67	139.26
Initial p_{O2} (bar)	28.96	30.23	29.12	29.25
Reaction temperature (°C)	200	200	200	200
Reaction Time (hr)	10	6	18	14
Initial O_2 composition (mole)	0.0646	0.0928	0.0549	0.0792
Total percent of O_2 consumed	100	100	100	100
Reacted oxygen (g O_2/gm oil)	0.2939	0.8436	0.2498	0.7196
Observation		Ignition + Explosion		

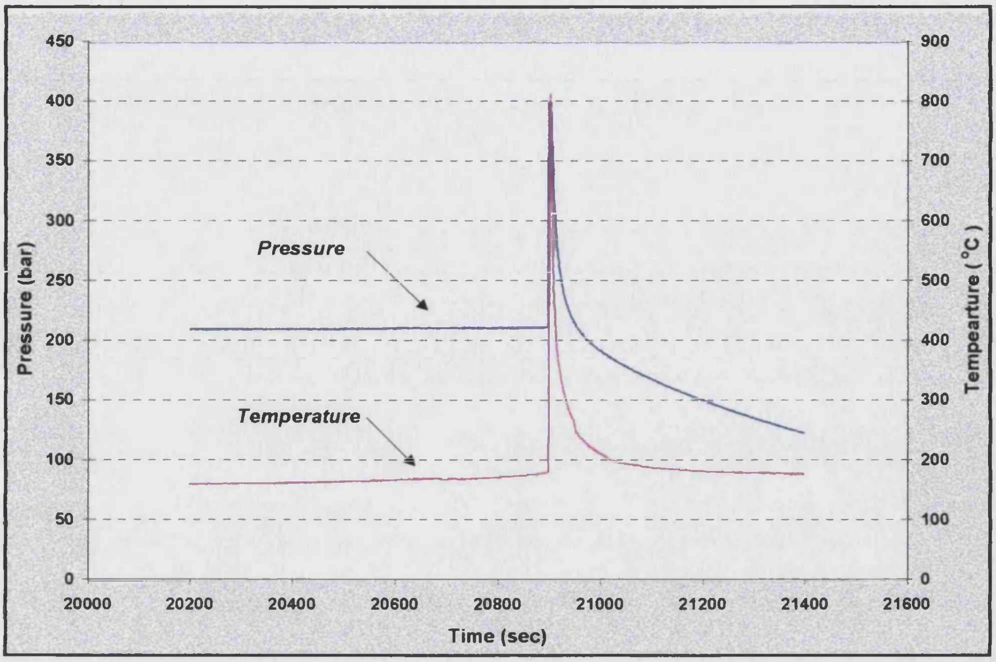

Figure 5.71: Temperature and pressure profiles during autoignition of Australian oil (Soi=0.5) at high AOR (Run 113)

(Pressure and temperature recorded every second)

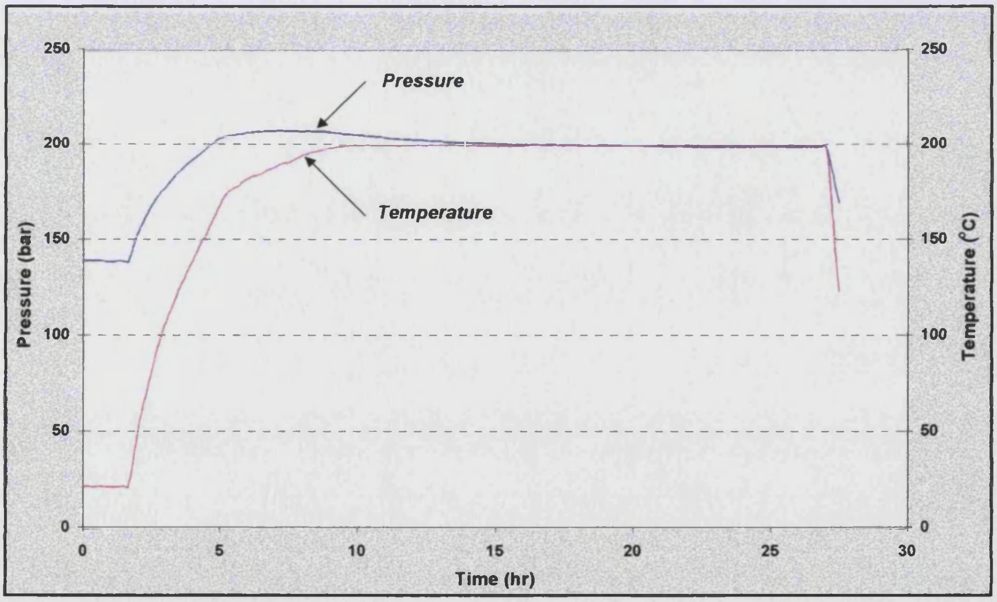

Figure 5.72: Temperature and pressure profiles during autoignition of Australian oil (Soi=0.5, Swi=0.5) at high AOR (Run 115)

(Pressure and temperature recorded every 10 minutes)

Crude oil composition

In Figures 5.64 and 5.66 for oil D and oil C have show high pressure and temperature peaks resulting from autocatalytic ignition. For Australian oil, autoignition was not detected (Figure 5.65). Oil C and oil D contain a high percentage of saturate compounds 75 and 71%, and low percentage of aromatic compounds, 11 and 13%, respectively, according to SARA analysis (Table 4.1). The Australian oil by composition contains 65% saturates and 18% aromatics. It is possible, therefore, that higher saturates content promotes autoignition. This is confirmed by results obtained for the oxidation of single organic compounds (hexane, decane, dodecane, and xylene) subjected to oxidation at 200 °C. This is shown in Figures 5.73 to 5.76. It is clear, that autocatalytic ignition is strongly influenced by the amount of saturates in the oil and less favoured by high aromatics content. This implies that saturates are more reactive to oxygen in the LTO region than aromatics.

It is also noticeable from the pressure and temperature profiles that n-hexane produced a less vigorous reaction than n-decane and n-dodecane (Figure 5.73, 74, and 75). Hence, heavier saturate components, like n-decane and dodecane are more reactive at 200 °C, than lighter component (lower carbon number), like n-hexane.

Heavier saturate components are more reactive at higher temperature, so the oxidation temperature in the reservoir will determine wither C_{10}^{+} saturate are sufficiently reactive to undergo LTO reaction at sufficient rates to remove oxygen.

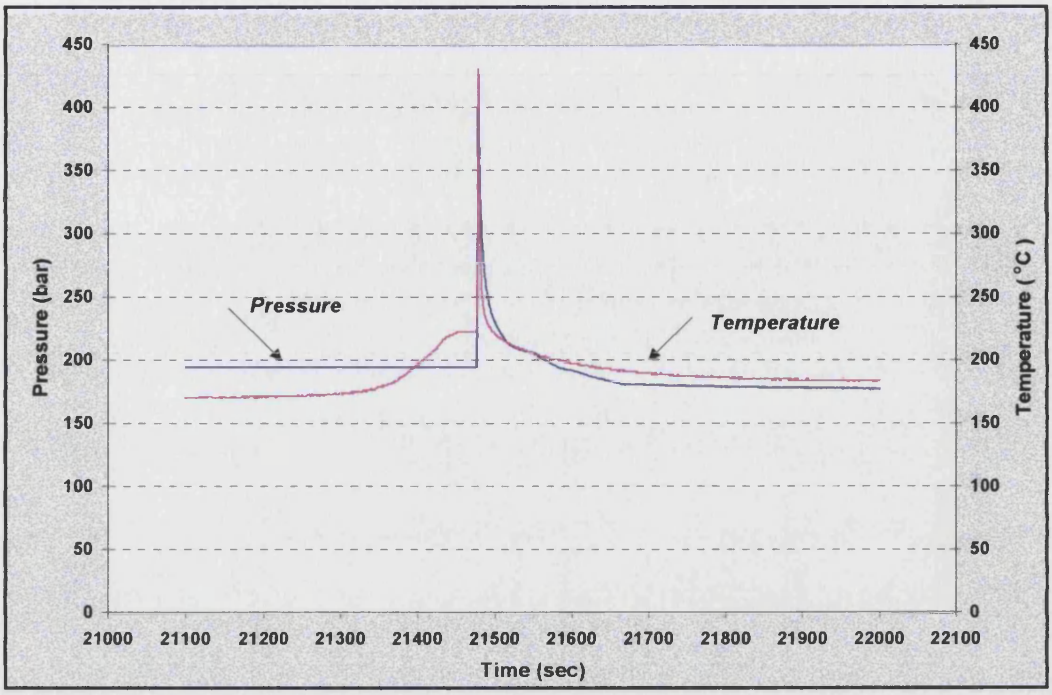

Figure 5.73: Temperature and pressure profiles during auto ignition of n-decane (So=0.5) (Run 130) (Pressure and temperature recorded every second)

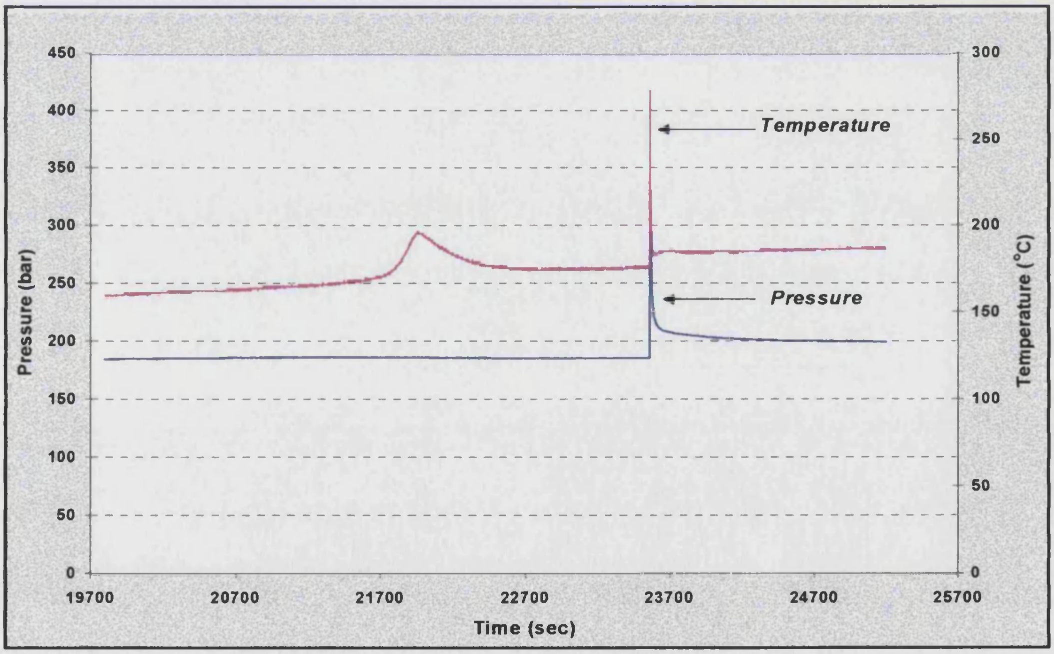

Figure 5.74: Temperature and pressure profiles during auto ignition of n-dodecane (So=0.5) (Run 131) (Pressure and temperature recorded every second)

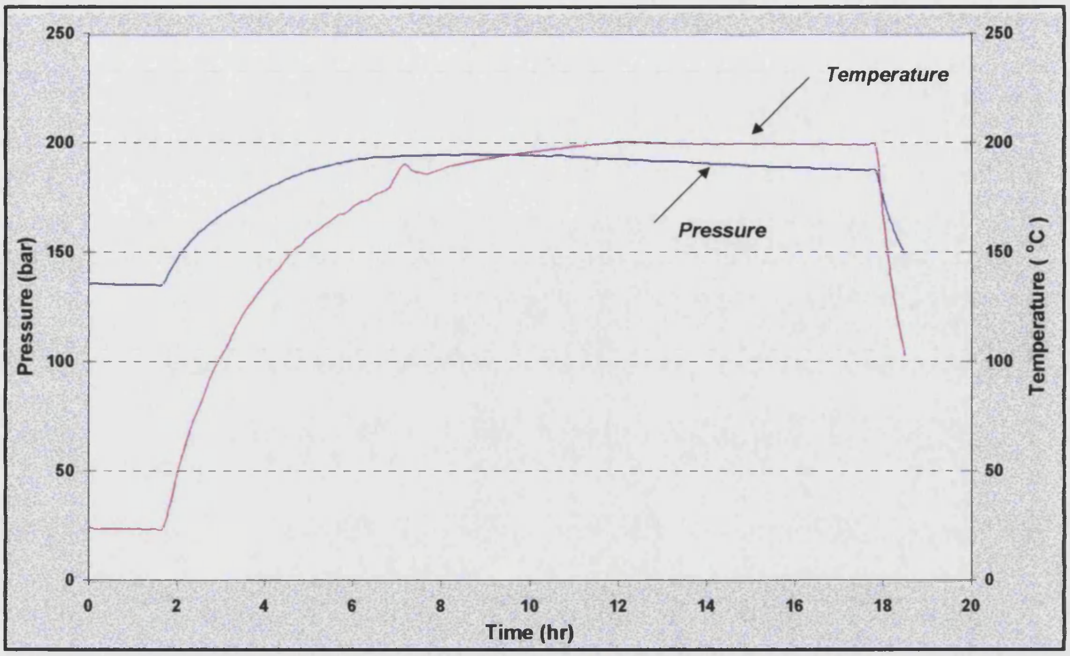

Figure 5.75: Temperature and pressure profiles during auto ignition of hexane (So=0.5) (Run 128) (Pressure and temperature recorded every 10 minuets)

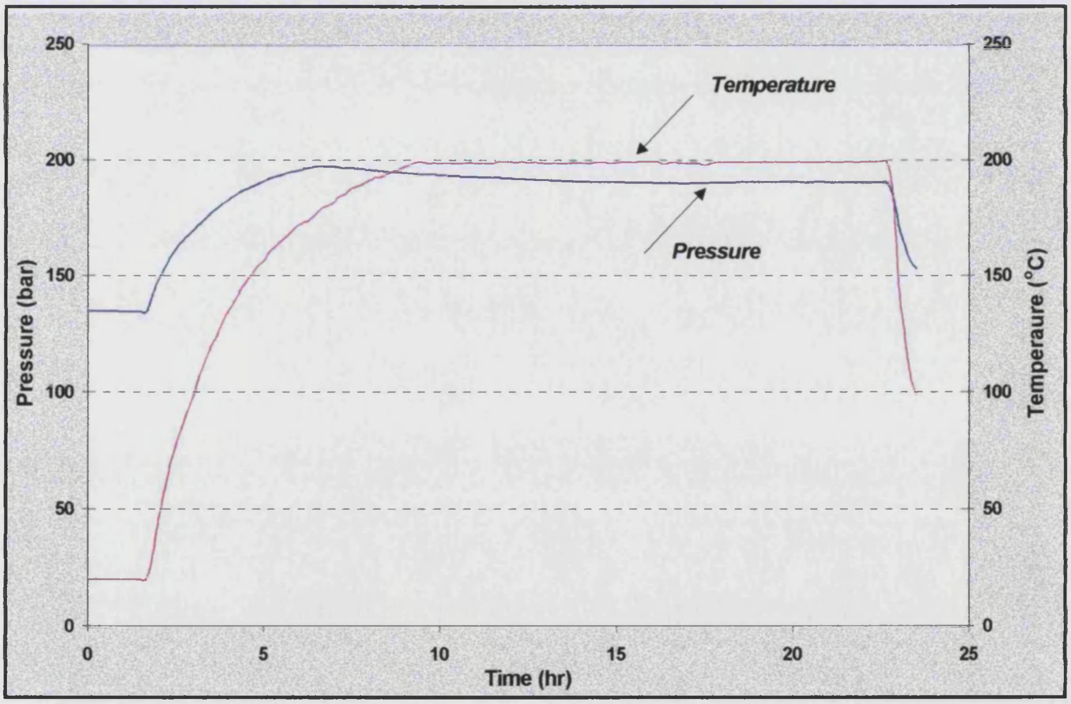

Figure 5.76: Temperature and pressure profiles during auto ignition of xylene (So=0.5) (Run 129) (Pressure and temperature recorded every 10 minutes)

PART V: ANALYSIS OF OXIDISED OILS

5.5 Analysis of Oxidised Oils

During air injection, crude oil undergoes chemical and physical changes. This has a direct impact on the displacement and oil recovery processes from the oxidation zone. Alteration in the composition of the crude oil can have an adverse effect on the produced oil quality. A number of oxidised oil samples were collected from SBR experiments and subjected to detailed compositional analysis. The majority of the samples were taken from experiments involving oil only, at and at temperatures from 120 to 160 °C.

The compositional change occurring in the light crude oils are identified by carrying out comprehensive analysis on the unreacted and oxidised oil samples. This consisted of asphaltene and coke precipitations, viscosity and density measurements, elemental analysis, and simulated distillation using gas chromatography. The analyses are discussed in the follower sections.

5.5.1 Asphaltenes and coke

Several samples of oxidised oil were collected at different oxidation times during each run and subsequently analysed for asphaltene and coke content. In every case, only samples were taken from oil alone experiments because of the increased difficulty of obtaining a sample when sand was present, i.e. low residual quantity. When oil matrix were used, the oxidised oil was extracted from the sand at the end of the run using Soxhelt extraction unit. The original and oxidised oil samples were separated into maltenes and asphaltenes. Asphaltenes are insoluble in pentane, but soluble in toluene. The procedure was carried out in a Soxhlet extraction unit. Figure 5.77 shows a photograph of precipitated asphaltene using n-pentane and also insoluble coke, when the asphaltene dissolves in toluene. After filtering off the asphaltene and coke, the residues were weighted accurately. Figure 5.78 shows a photograph of the residual like coke in the extraction thimble after maltenes and asphaltenes separation.

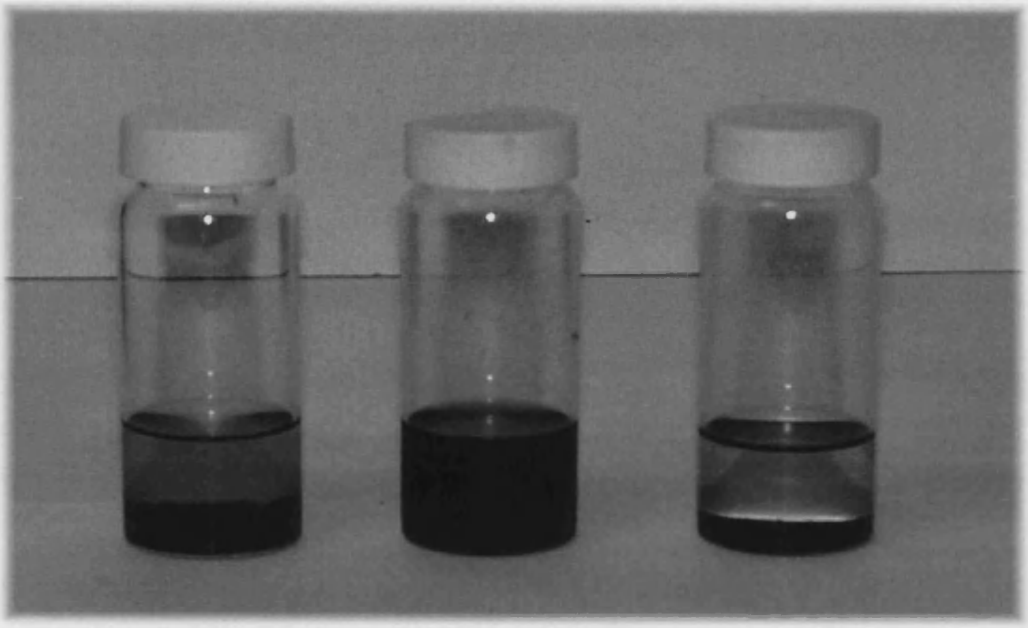

Asphaltene and Coke (Insoluble in n-pentane)	Asphaltene and Coke (in toluene)	Coke (insoluble in toluene)

Figure 5.77: Asphaltene and coke precipitation in solvents

Figure 5.78: Residual like coke in extraction thimble after maltenes and asphaltenes separation

The percentage of asphaltenes and coke in the original and oxidized oil samples are given in Table 5.12 and 5.13.

Contrary to what has been reported in the literature, LTO of light crude oils causes an increase in the asphaltene and coke content. The extent of oxidation (mg O_2/g oil) is plotted against the asphaltene and coke content in Figure 5.79 and 5.80.

Table 5.12: Asphaltene and coke formed in Australian oil and oil C due to LTO

	Original crude oil sample	Aust. oil			Original crude oil sample	Oil C		
		1st sample	2nd Sample	Final sample		1st sample	2nd sample	Final sample
Temperature (°C)	25	120	120	120	25	120	120	120
Oxidation time (hr)	0	68	115	130	0	30	80	130
% maltenes	100.00	100.00	100.00	97.75	100.00	98.97	98.62	98.28
% asphaltenes	0.00	0.00	0.00	0.96	0.00	1.03	1.38	1.56
% coke	0.00	0.00	0.00	1.29	0.00	0.00	0.00	0.16
Temperature (°C)	25	140	140	140	25	140	140	140
Oxidation time (hr)	0	42	70	80	0	20	60	84
% maltenes	100	99.97	99.28	96.92	100	98.87	98.74	96.87
% asphaltenes	0.00	0.03	0.72	0.88	0.00	1.13	1.26	1.62
% coke	0.00	0.00	0.00	2.20	0.00	0.00	0.00	1.51
Temperature (°C)	25	160	160	160	25	160	160	160
Oxidation time (hr)	0	12	22	35	0	12	30	35
% maltenes	100	99.64	99.28	94.63	100	98.17	98.06	94.85
% asphaltenes	0.00	0.36	0.72	2.45	0.00	1.83	1.94	1.79
% coke	0.00	0.00	0.00	2.92	0.00	0.00	0.00	3.36

Table 5.13: Asphaltene and coke formed in oil D and Esso Mix1 oil due to LTO

	Original crude oil sample	Oil D				Original crude oil sample	Esso mix oil		
		1st sample	2nd Sample	Final Sample	With Water		1st sample	Final sample	with Water
Temperature (°C)	25	120	120	120		25	120	120	
Oxid. time (hr)	0	46	78	100		0	21	77	
% maltenes	99.45	98.5	98.12	95.06		98.82	97.50	92.16	
% asphaltenes	0.55	1.50	1.88	2.59		1.18	2.50	3.19	
% coke	0.00	0.00	0.00	2.35		0.00	0.00	4.65	
Temperature (°C)	25			140	140	25	140	140	140
Oxid. time (hr)	0			29	30	0	12	40	37
% maltenes	99.45			94.88	92.79	98.82	98.35	87.93	85.67
% asphaltenes	0.55			2.28	2.94	1.18	1.65	5.56	6.28
% coke	0.00			2.84	4.27	0.00	0	6.51	8.05
Temperature (°C)	25	160		160		25	160	160	
Oxid. time (hr)	0	10		30		0	8	18	
% maltenes	99.45	97.88		91.93		98.82	96.53	84.13	
% asphaltenes	0.55	2.12		3.16		1.18	3.47	4.4	
% coke	0.00	0.00		4.91		0.00	0.00	11.47	

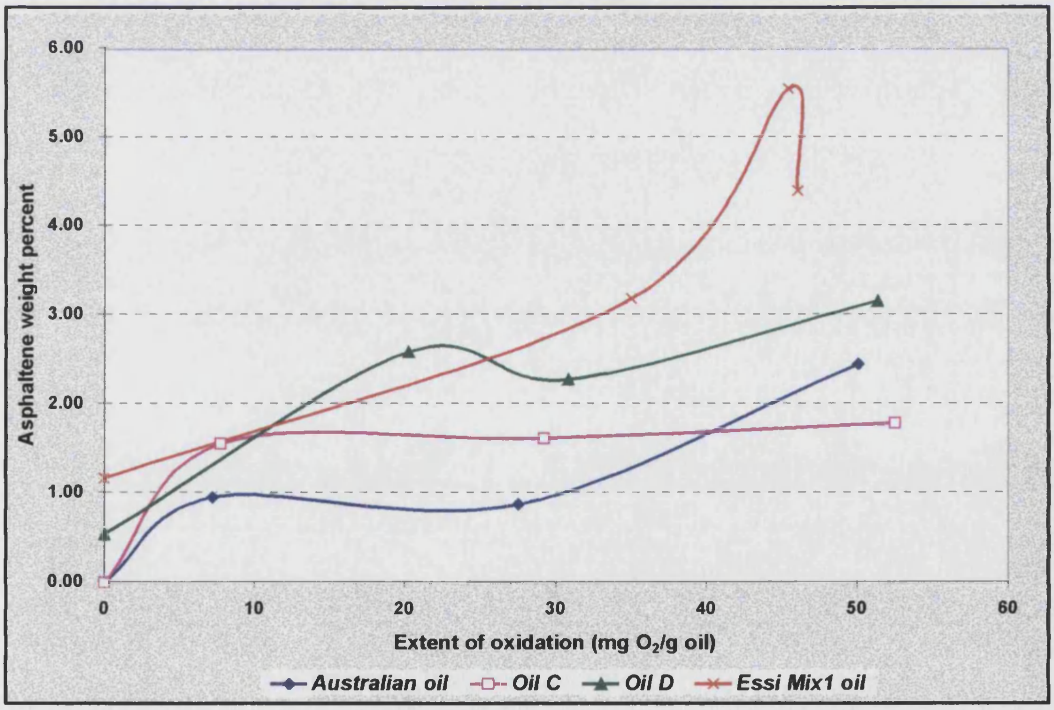

Figure 5.79: Effect of LTO on Asphaltene content as function of extent of oxidation

The main observation that can be drawn from these plots is that the amount of asphaltene and coke in oxidised oil increases with increasing oxidation. A slight decrease in the asphaltene content was observed for oil D between 20 and 30 mg O_2/g oil, and beyond 30mg O_2/g it increases again. The decrease is possibly due to the difference between the rates of conversion and production of asphaltene during the oxidation period. Esso Mix1 oil also shows a decrease in asphaltene content, but at a late stage of oxidation. This decrease can be explained by the fact that the light crude oil has limited ability to solubilize asphaltenes[51]. As additional asphaltenes are formed with increasing oxidation, they precipitate as coke as shown below.

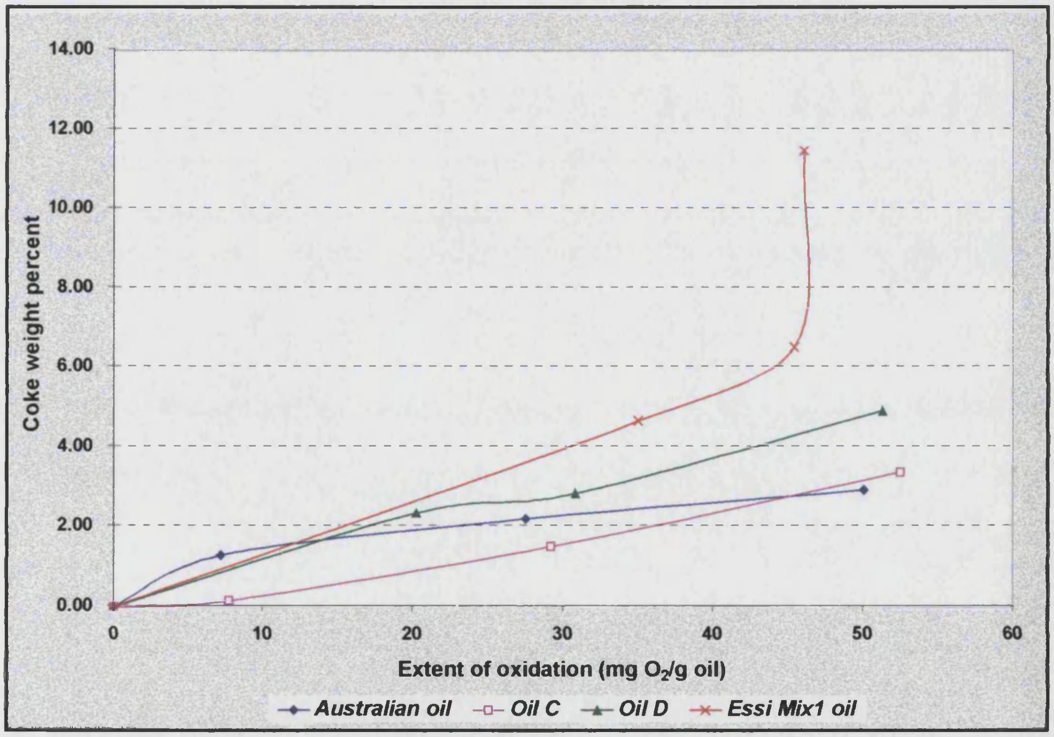

Figure 5.80: Effect of LTO on coke content as function of extent of oxidation

The formation of asphaltene and coke as function of oxidation temperature is shown in Figure 5.81. It can be seen that in general, the amount of asphaltene and coke increases with increasing the temperature from room temperature to 160 °C. Australian oil and oil D show a slight decrease in asphaltene content at 140 °C, but beyond 150 °C, it increases again. The decrease is attributed to the different rates of conversion of asphaltene to coke and the rate of asphaltene production at 140 °C.

The amount of asphaltene and coke was higher for oxidised oil D and Esso Mix1, compared with Australian oil and oil C. The main reason is the fact that oil D and Esso Mix1 oil have higher initial asphaltene contents 0.55 and 1.08 % respectively.

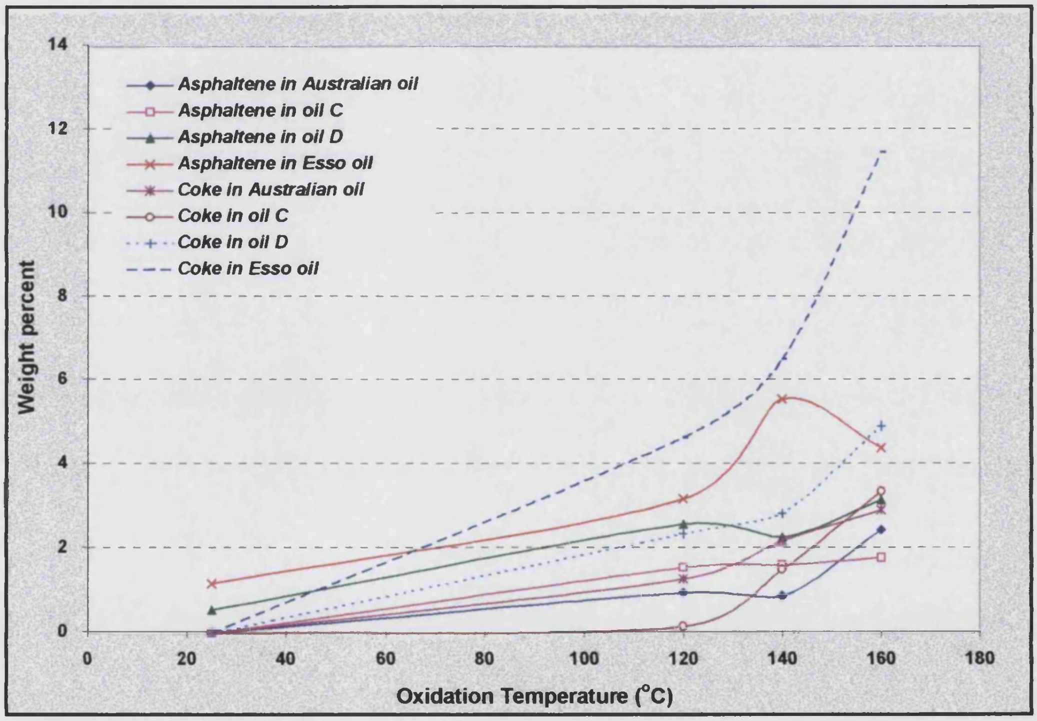

Figure 5.81: Asphaltene and coke precipitation as function of oxidation temperature of light crude oil

Generally, the oxidised oil always contains a higher asphaltene content than the dead crude oil, even if the initial asphaltene content is zero. The greater the original asphaltene content of the crude oil, the higher the increase in the asphaltene concentration accompanying the LTO of light crude oil.

The maximum asphaltene and coke contents occuring during the LTO of the four light crude oils, over the temperature range of 120 to 160 °C, was 6 and 10 weight percent, respectively. Fassihi et al.[51] found about 4% of asphaltenes and high amount of solid were formed during LTO of a light 31.1°API gravity oil. Lakatos et al.[86] found that the ultimate amount of asphaltenes formed by thermal treatment approaches a limiting value of 26-28%. Consequently, they conclude that the physical and chemical properties of the crude oil will only be slightly influenced by air injection.

The effect of oxidation time on asphaltene and coke content in the oxidised oil at 140 °C is shown below.

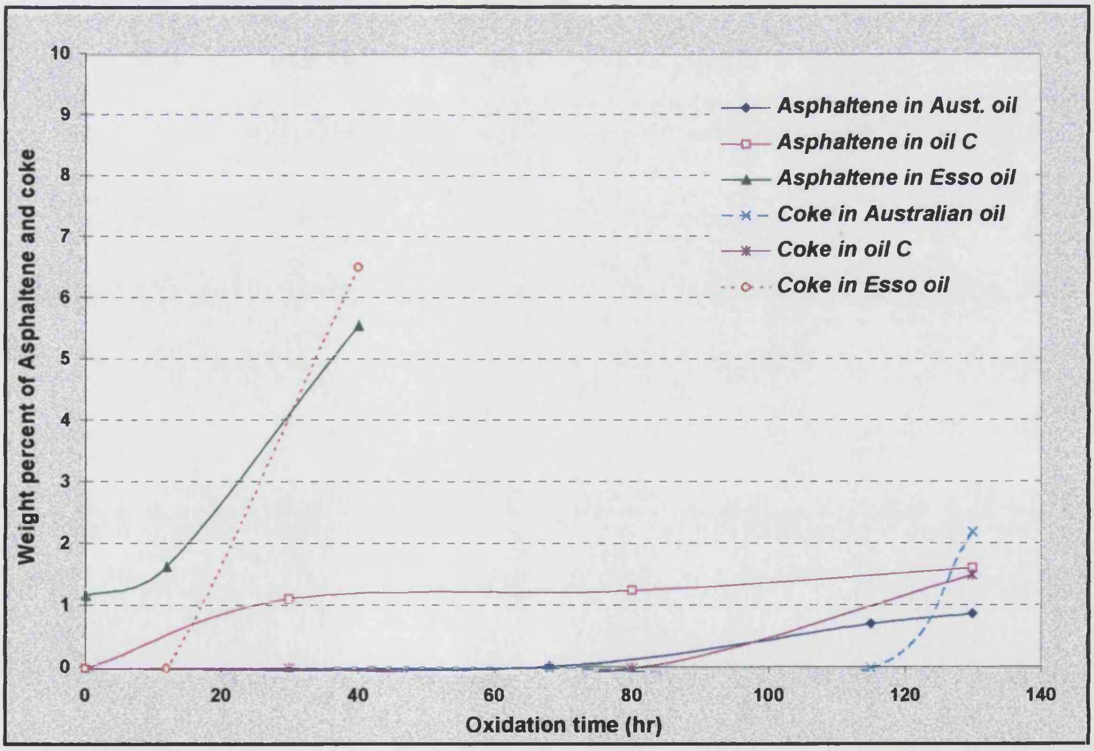

Figure 5.82: Formation of asphaltene and coke as a function of oxidation time at 140 °C

The crude oil having the lowest API gravity (Esso Mix1 oil) requires less time to produce asphaltene and coke compared with a higher API gravity crude oil, at same oxidation temperature.

The effect of water on the production of asphaltene and coke during LTO process was investigated by equal quantities of oil, specifically 20 cc of each. All the other experimental conditions, initial pressure, oxidation temperature, and oxidation time, were identical to the previous experiments with oil only. The result (Table 5.13) shows that amount of asphaltene and coke increased by 29 and 50% respectively, for oil D, whereas for Esso Mix1 oil the asphaltene increased by 17% and the coke was increased by 28%. Figure 5.83 shows the influence of water on asphaltene and coke formation during LTO of light crude oil.

The influence of the matrix on coke formation was also investigated. Figure 5.84 shows an increase in the coke deposited when crushed core was used compared to oil alone. This result is contrary with the result observed by Babu and Cormack[87] for the ultimate coke residue formed from LTO of Athabasca bitumen in the presence of sand, this is probably due to the different composition of light and heavy oils. Verkoczy[88] investigated the affect of surface activity of core minerals on the coke residue formed from heavy crude oils. He found that a low mineral surface activity inhibits coke/residue formation even when the surface area is very large. Conversely, high surface activity leads to an increase in the coke residue, even when the surface area is small.

Visual inspection of the rock after the run was complete showed differences in the colour between the unreacted oil/sand mixture and the oxidised oil/sand mixture. The oxidised oil/sand mixture was darker due to the formation of oxygenated hydrocarbons, in other words heavy components (asphaltene/coke), as shown in Figures 5.85 and 5.86. The colour of the oxidised oil/sand mixture was darker at higher temperature.

The runs with sand at 150 °C or higher formed a crust at the top of the packed sand (Fig. 5.8b). Some free oil was present as a film on the glass container at low temperature (< 140 °C) and high Soi. The residual like coke in the matrix due to LTO after the extraction of maltenes and asphaltene compared to the extracted sand from unreacted oil and burned sand is shown in Figure 5.87 and 5.88

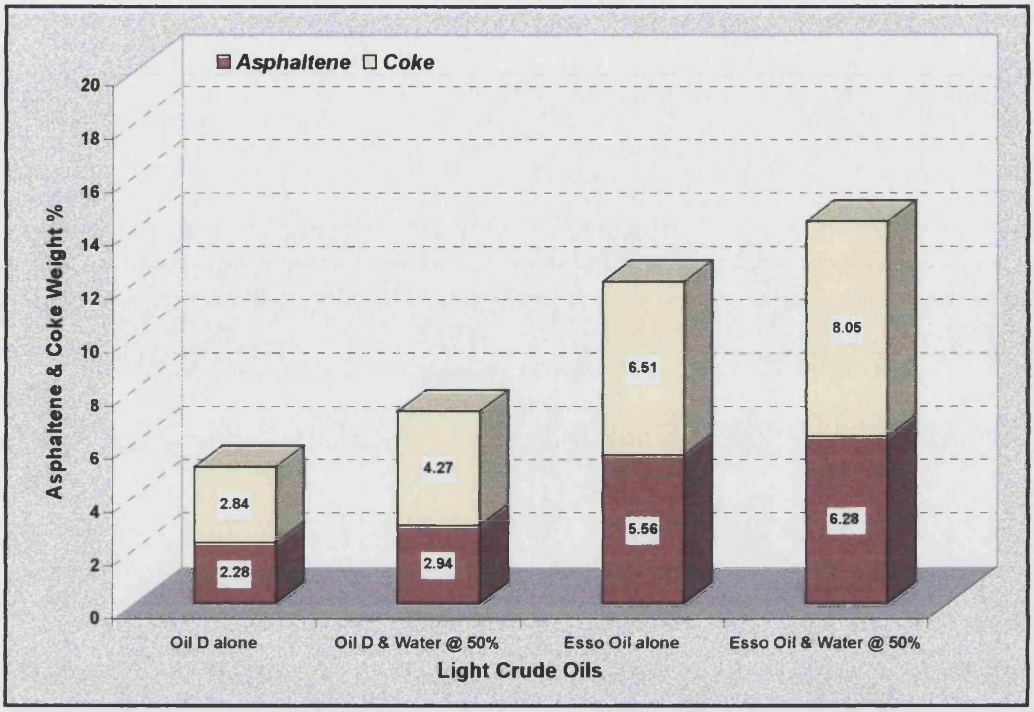

Figure 5.83: Effect of water on asphaltene formation during LTO of light crude oil (T=140 ℃)

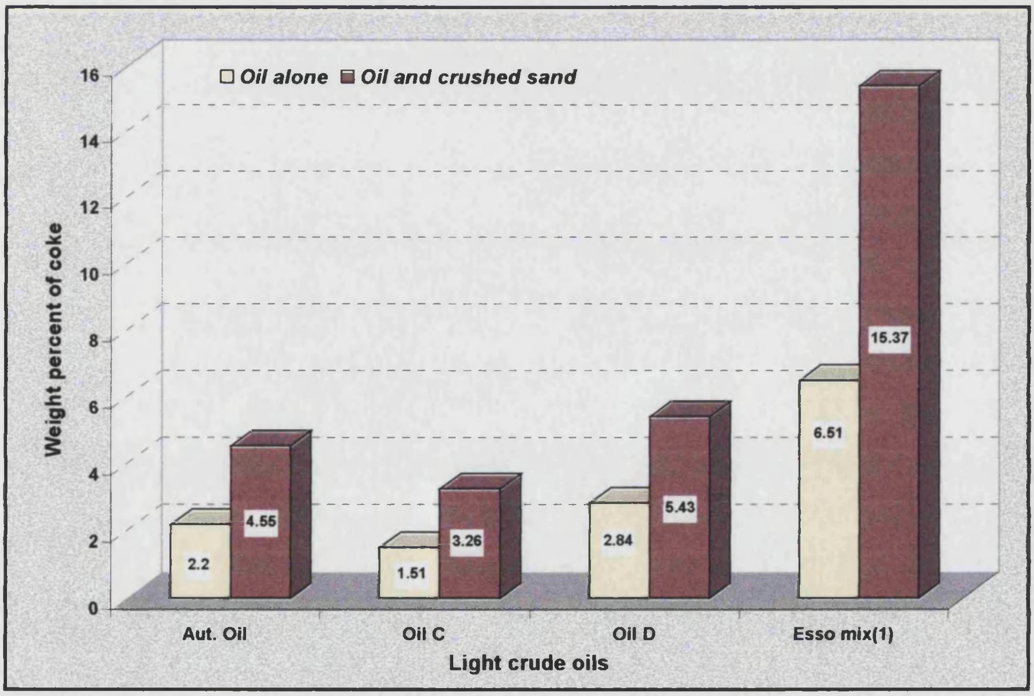

Figure 5.84: Effect of presence of crushed core on coke formation during LTO of light crude oil (T = 140 ℃)

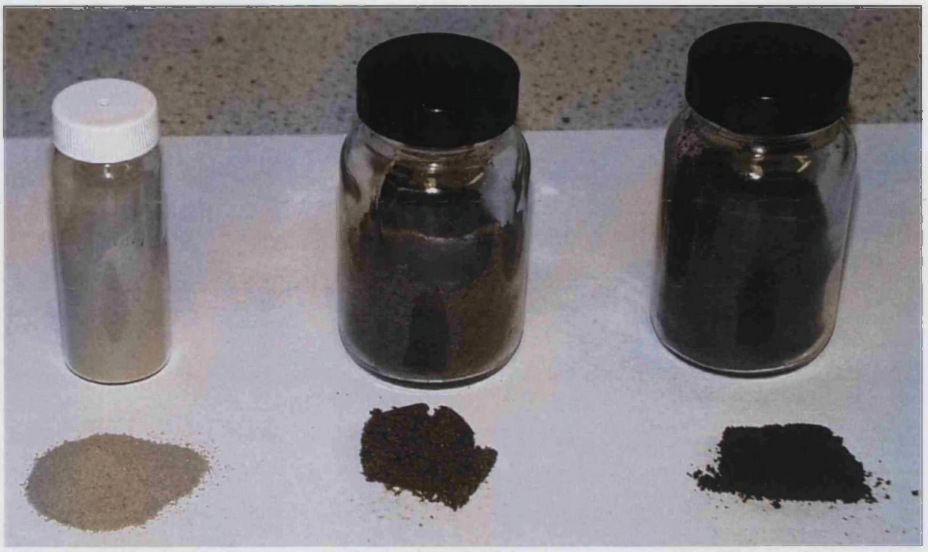

Clean crushed core D | Oil C mixed with crushed core D | Oxidised oil C with crushed core D

Figure 5.85: Comparison between unreacted oil/sand mixture and oxidised oil/sand mixture for oil C (T=140 °C)(Run 35)

Clean crushed core D | Oil D mixed with crushed core D | Oxidised oil D with crushed core D

Figure 5.86: Comparson between unreacted oil/sand mixture and oxidised oil/sand mixture for oil D (T = 140°C)(Run 77)

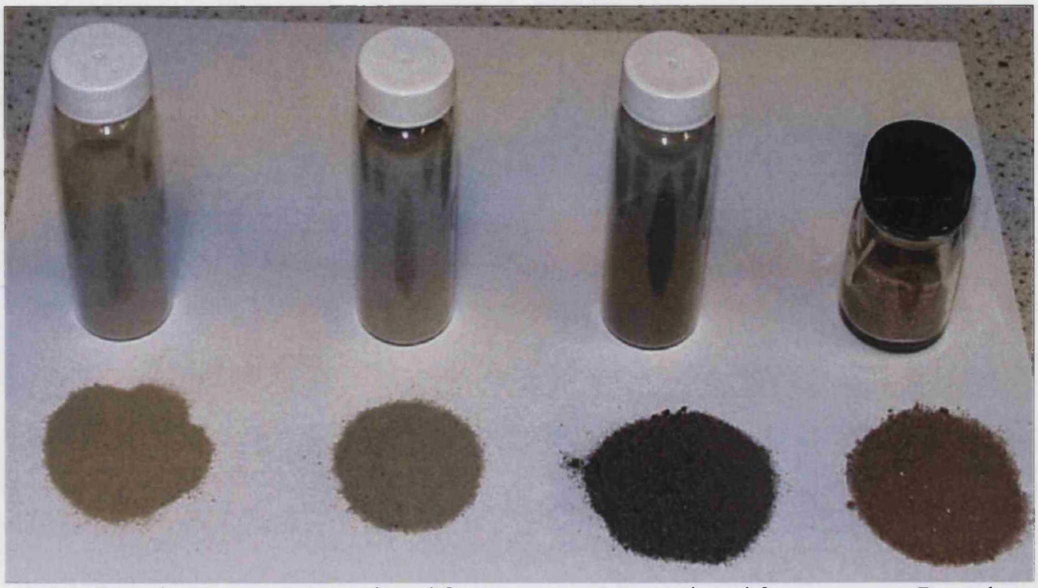

Original crushed Core D | Extracted sand from unreacted oil/sand mixture | Extracted sand from oxidised oil/sand mixture | Burned sand

Figure 5.87: Sand matrix after LTO of oil D (T = 140°C)(Run 77)

Original crushed Core D | Extracted sand from unreacted oil/sand mixture | Extracted sand from oxidised oil/sand mixture | Burned sand

Figure 5.88: Sand matrix after LTO of Esso mix1 oil (T = 140°C)(Run 87)

Two runs were conducted using pure nitrogen as the charge gas, instead of air, for oil D and Esso Mix1 oil. The SBR pressure data showed that there was no change in pressure as shown in Figures 5.89 and 5.90. The unaffected pressure profile when pure nitrogen is used means no reaction occurred with the crude oil at the existing operating condition. Analysis of the oils in the presence of pure nitrogen revealed no increase in either asphaltene or coke content. Hence the increase in the asphaltene fraction in the oxidised oil is due to the increase in the oxygen in the oxidised oil, rather than an effect of the presence of nitrogen.

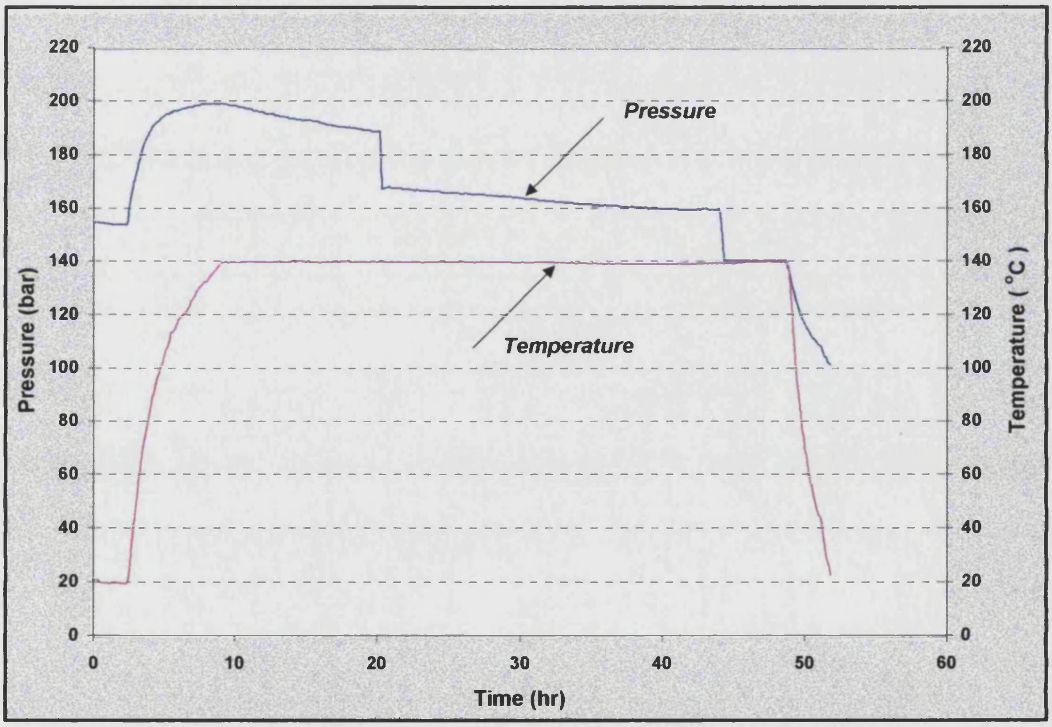

Figure 5.89: Pressure and temperature profile of Esso oil in SBR charged with air (Pressure and temperature recorded every 10 minutes)

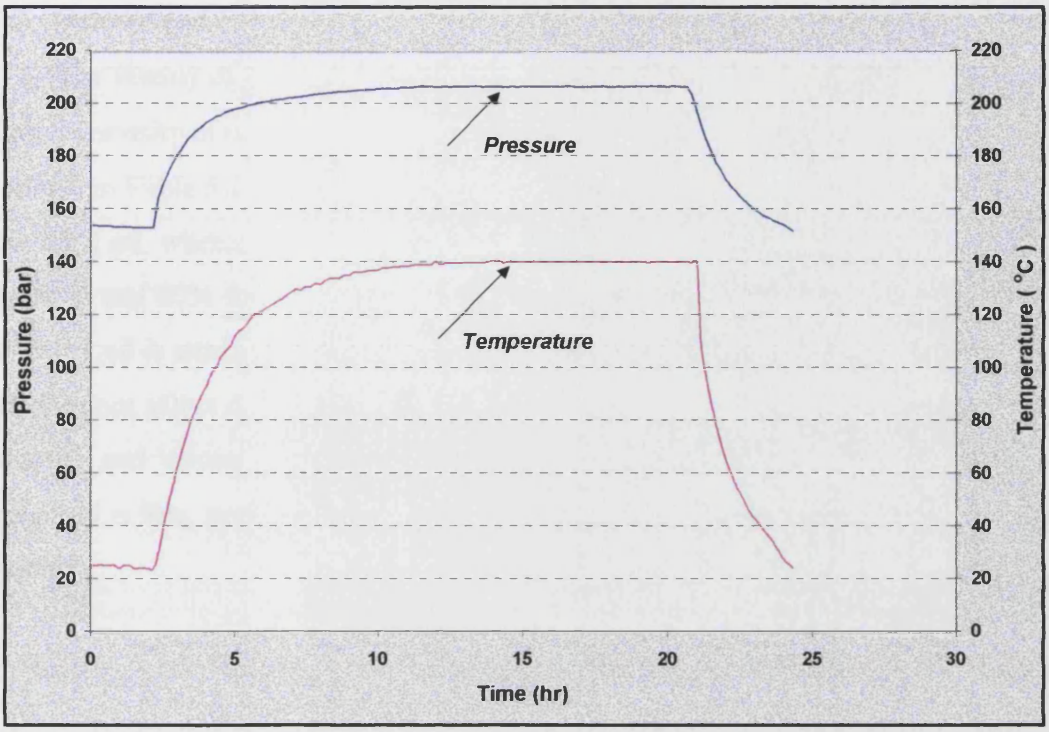

Figure 5.90: Pressure and temperature profile of Esso oil in SBR charged with nitrogen (Pressure and temperature recorded every 10 minutes)

It is clear that LTO of oil D and Esso Mix1 oil increased the amount of heavy fractions in the oxidised oil and consequently, these two oils would have increased ability to sustain an in situ combustion front through the reservoir. In the other hand the Australian oil did not produce a high percentage of asphaltenes and is likely to be suitable only for air injection LTO process. It is postulated that the asphaltene content in the oxidised oil is a key screening tool to determine if light oil is a good candidate for air injection for full ISC or LTO. Also, a high percentage of asphaltenes in the oxidised oil may not be desirable for a LTO process. Thus the asphaltene content of the oxidised oil affect the decision as to whether to design an air injection process for LTO or full ISC for light oil reservoirs.

5.5.2 Density and Viscosity measurement

The density of unreacted and light oils oxidised at 120 to 200 °C were measured initially, viscosity of unreacted and oxidised oil at 150 °C was also measured.

As shown in Table 5.14 the density of oxidised oil increases by 2 to 9 percent compared to the dead oil, whereas the viscosity increased by 20 to 35 % for Australian oil, Oil C, and Oil D and 80% for Esso Mix1. The large increase in the viscosity of the oxidised Esso Mix1 oil is attributed to the asphaltene content of the crude oil.

LTO does not affect density as dramatically as it does viscosity. Normally, the changes in density and viscosity accompanying LTO occurs in the oxidation zone where the residual oil is low, perhaps down to Soi = 10%, or less, depending on the displacement efficiency.

Table 5.14: Density and viscosity ratio of oxidised light crude oils, comparing oxidised and unoxidised oil

Oxidation	Density Ratio at 25 °C						Viscosity Ratio
Temperature °C	120	140	150	160	180	200	150
Australian oil	1.013	1.1157	1.084	1.0155	1.0121		1.200
Oil C	1.011	1.005	1.0374	1.0629	1.0388	1.0216	1.306
Oil D	1.023	1.0247	1.0445	1.0896	1.0227	0.9953	1.347
Esso Mix1 oil	1.035	1.0649	1.0698	1.0515	1.0486		1.848

Viscosity measurement was at 20 °C

The effect of oxidation temperature on the density of the oxidised light crude oils is plotted in Figure 5.91. The density of the oxidised oil increases with increasing oxidation temperature up to 150 –160 °C, and starts to decrease at higher temperature. The decrease in the density beyond 160 °C is attributed to the fact that the autoignition temperature of these light crude oils starts in this range of temperatures.

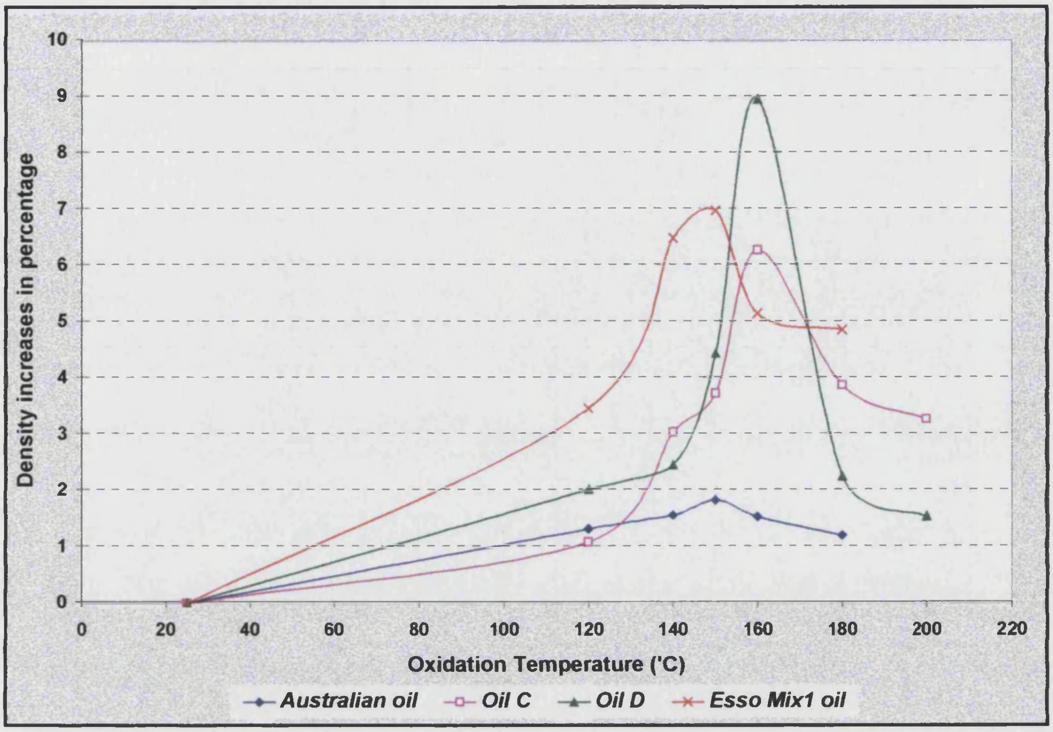

Figure 5.91: Density increases of light crude oils accompany LTO Process

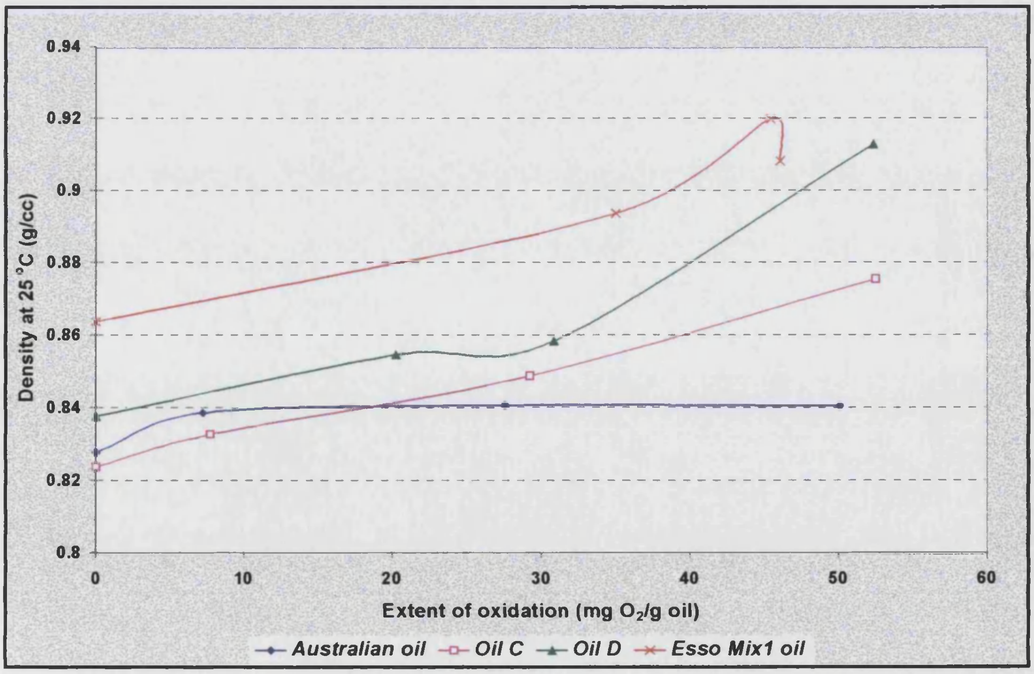

Figure 5.92: Density of oxidised light crude oils as function of extent of oxidation

In Figure 5.92, the densities of oxidised oil C, oil D, and Esso Mix 1 oil show an increase in density as the extent of oxidation increases. However, the Australian oil does not exhibit any significant increase in density except in the early stages of oxidation.

Comparing unreacted and oxidised oils at temperature of 150 'C (Figure 5.93), viscosity increases by 20 to 85 percent. It is considered that the asphaltene content of the oil is a primary contributor affecting the increase in viscosity.

The ratio of the viscosities of the oxidised and unoxidised oils is plotted versus the asphaltene content in Figure 5.94. Thus, the viscosity ratio increases with increasing asphaltene content, a result, which agrees with that, reported by Fassihi et al.[51] and Babu et al.[48].

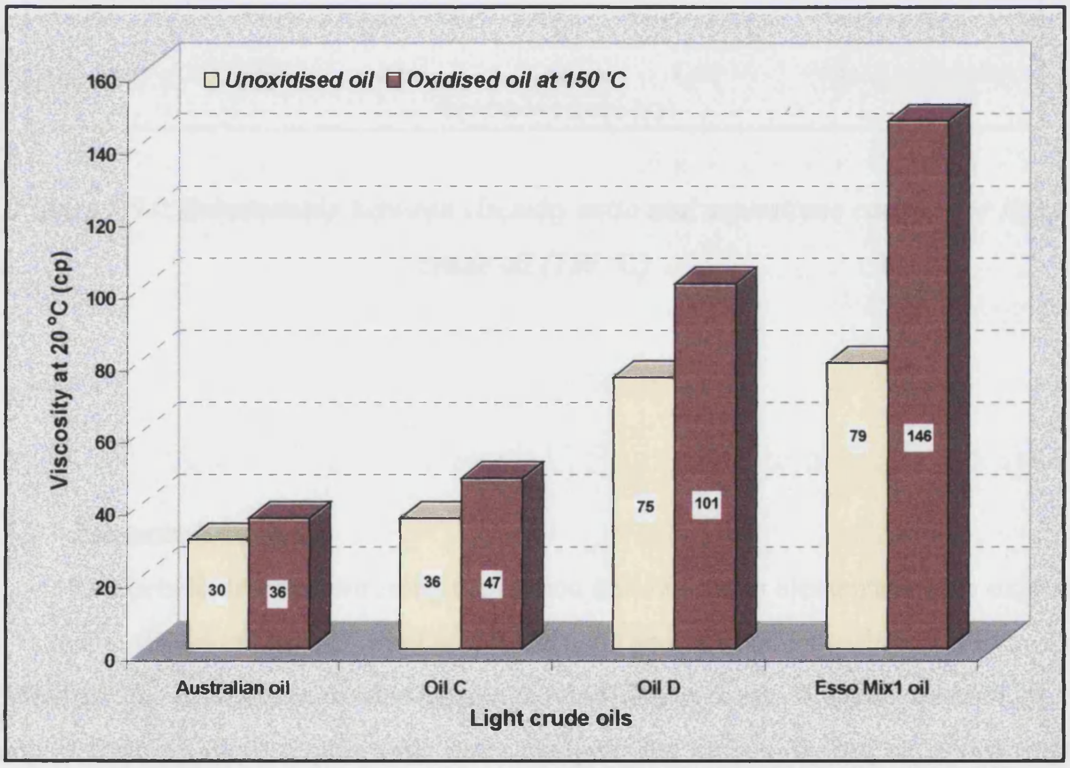

Figure 5.93: Effect of LTO process on viscosity of light crude oils

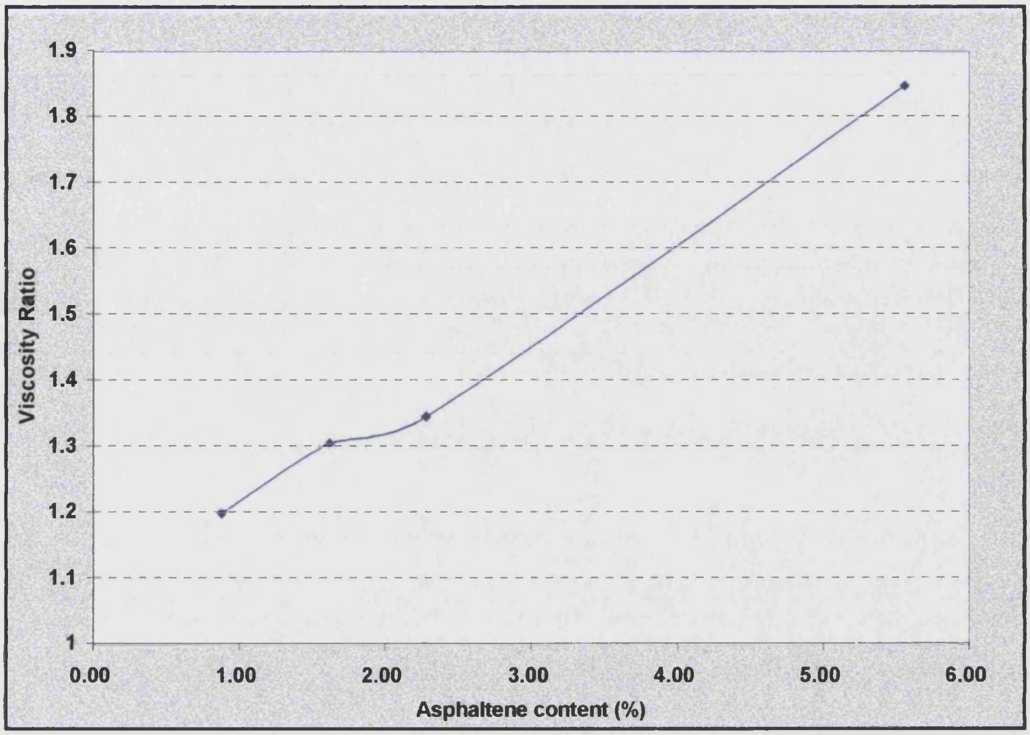

Figure 5.94: Relationship between viscosity ratio and asphaltene content for light crude oil (150 °C)

5.5.3 Elemental Analysis

The benefit from determining the carbon and hydrogen elemental in the oxidised oil is that it allows analysis of what effect the LTO process has on carbon and hydrogen content of the light oil reservoirs accompanying this process. A small number of oil samples from oil alone experiments were analysed for carbon, hydrogen, and nitrogen content using CE-440 Elemental Analyser.

The change in the molar H/C ratio of the oxidised oil is reported in Table 5.15, see Appendix C for calculated values.

Table 5.15: Elemental Analysis of oxidised light crude oils

Oxidation Temperature and crude oil	C	H	N	H/C
Australian oil (alone)				
Unreacted oil	83.86	11.90	1.06	1.70
120	83.68	11.97	0.95	1.72
140	83.39	11.88	0.91	1.71
160	81.40	11.60	0.80	1.71
Oil C (alone)				
Unreacted oil	86.43	12.82	0.82	1.78
120	83.63	12.29	0.91	1.76
140	83.64	12.21	0.72	1.75
160	82.85	12.32	0.70	1.78
Oil D (alone)				
Unreacted oil	85.10	12.34	0.91	1.74
120	84.40	13.35	0.93	1.90
140	80.20	11.00	0.84	1.65
160	81.68	11.22	0.87	1.65
Esso Mix1 oil (alone)				
Unreacted oil	85.36	11.74	1.01	1.65
120	85.16	12.84	0.93	1.81
140	84.09	12.98	1.08	1.85
160	83.81	11.59	1.04	1.66

There is a clear trend for C content, decrease with increasing temperature, and this is consistent with the production gas analysis (see section 5.4), exhibiting increased CO_2. This agrees with Fassihi et al.[51] observation of the LTO of 31.1° API gravity crude oil. On the other hand, there is no general discernable trend for the hydrogen content, which shows both addition and removal, depending on the crude oil. The variation of H/C in Figure 5.95 shows that oils D and Esso Mix1 are most affected, that both exhibit a dramatic reduction beyond about 120 °C.

Fassihi et al.[51] attributed the decrease in the atomic H/C ratio to the production of unsaturated compounds and aromatization of naphthenes.

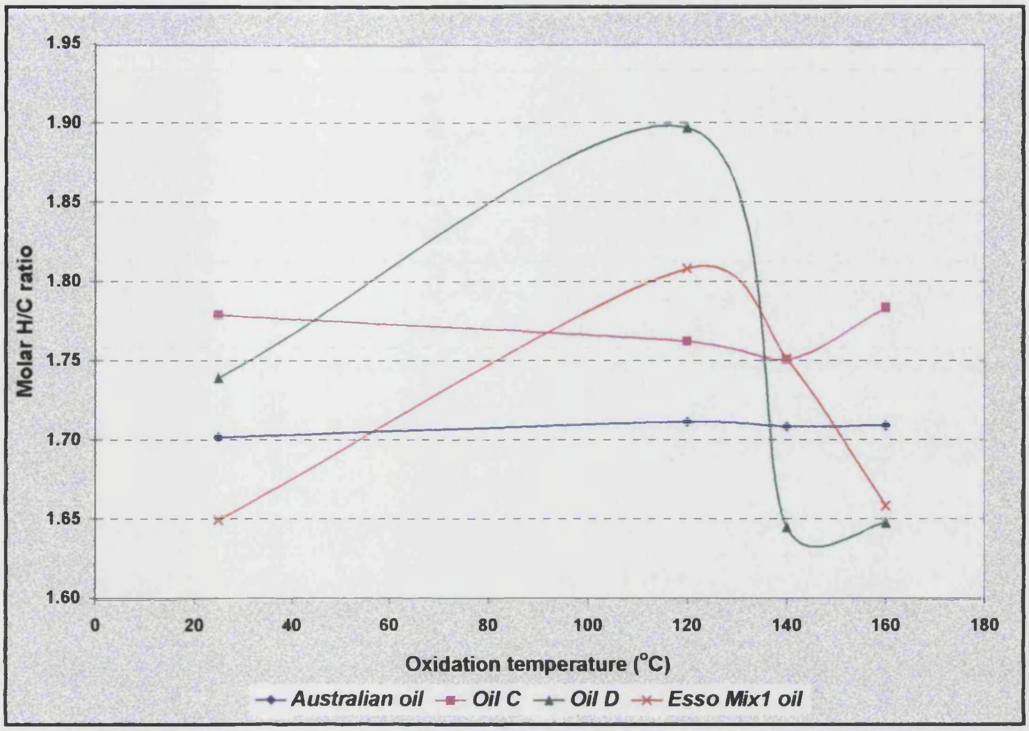

Figure 5.95: Effect of oxidation temperature on molar hydrogen carbon ratio of oxidised light crude oil

5.5.4 Gas Chromatography Analysis

Two types of gas chromatography were used to analyse the oxidised light crude oils and pure organic compound. The objective was to investigate the change in carbon number distribution accompanying LTO, also what the increase in the oxygenated hydrocarbons was, and to ascertain which fraction of the light crude oil (saturates or aromatics) was most important in the LTO process.

5.5.4.1 Single Organic Compounds

The oxidised organic compounds were analysed using Perkin Elmer 8500 Gas Chromatograph and Perkin Elmer Q-Mass 910 Gas Chromatograph (see section 4.4 for operating condition).

Figure 5.96 shows that there is a higher percentage of new products formed during the oxidation of hexane and dodecane compared to aromatic components. Therefore, the saturates components have a higher reactivity compared to the aromatics. Correspondingly, more of the saturates components were consumed during low temperature oxidation. This is in agreement with Kok and Karacan[47], who reported that the saturates components in a 26.12 ° API gravity oil showed a huge weight loss during LTO reaction compared to the other oil fractions, especially aromatics. They also, found that the weight loss of various crude oils at different stages of oxidation was very close to the value obtained by aggregation the SARA fraction values. They suggested that the oxidation of single component in combustion is almost independent of other component in the oil and that they follow their own oxidation pathway.

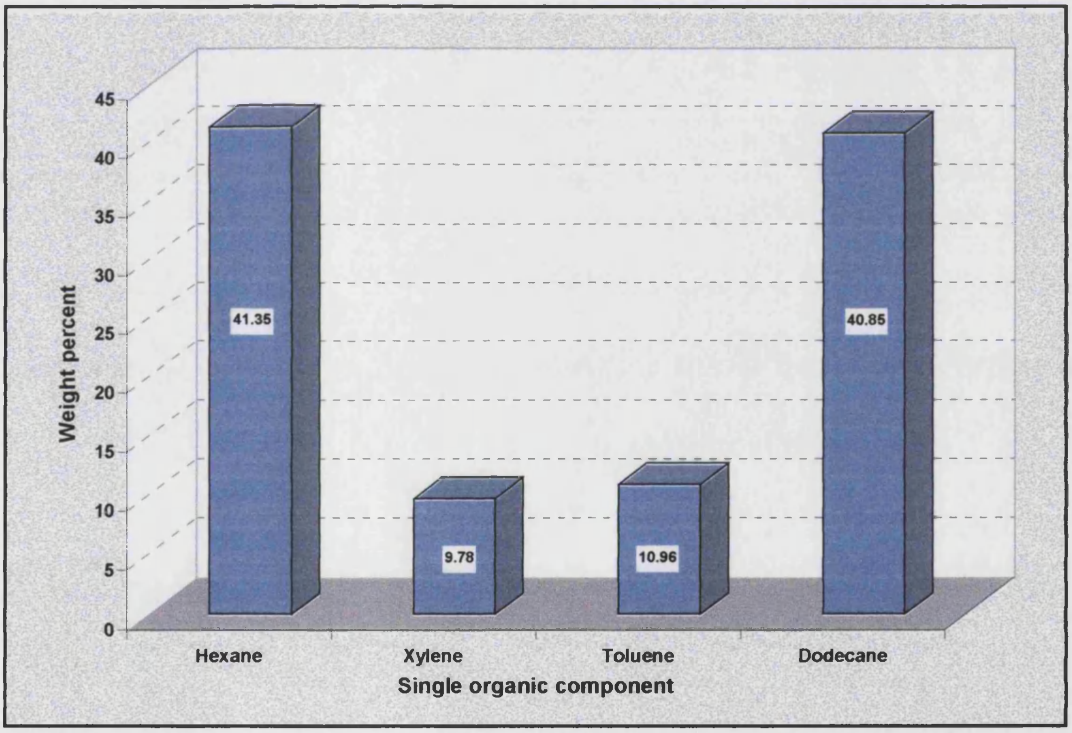

Figure 5.96: New products formed in the oxidised single organic components at 140 °C

In order to identify the new components produced during oxidation of pure organic components, the GC-MS technique was used. When a saturated pure compound hexane or dodecane is oxidised at low temperature (140 °C), the resulting oxygenated hydrocarbons is a ketone, whereas in the case of pure aromatic compounds toluene or xylene, the product is an aldehyde. GC spectrums for the unreacted and oxidised pure components are shown in Figures 5.97 and 5.98 for toluene and dodecane, respectively. A summary of the compound identified in the MS spectrums of toluene and dodecane is given in Tables 5.16.

The detailed analyses of the single organic compounds using GC MS are given in Appendix E.

Table 5.16: Main components in oxidised toluene and dodecane at T=140 °C using GC-MS

Date of GC-MS run:	22/03/01
Time of GC-MS run:	14.09
Sample:	Oxidised Toluene and Dodecane
Oxidation temperature:	140 °C
Dilution:	Carbon Disulfide
Injection Size:	1μL
Carrier Gas Split:	40:1
Carrier gas head pressure:	8 p.s.i.
Oven Temperature:	Initial temperature = 40C for 10 minutes Increasing at 8 °C per minute hold at 140 °C for 30 minutes
Filament Delay:	3 minutes
Filament Total Run Time:	80 minutes
Column:	BP624, 25m, 1.2μm

GC-MS Analysis of Oxidised Toluene:

Compound Name	Formula	S.I.	Retention Time	Peak Area
Toluene	C_7H_8	90	11.99	148616640
Benzaldehyde	C_7H_6O	92	22.46	1886297
Dodecane	$C_{12}H_{26}$	92	28.69	100151565

SI: Similarity Index

GC-MS Analysis of Oxidised Dodecane:

Compound Name	Formula	S.I.	Retention Time	Peak Area
Undecane	$C_{11}H_{24}$	91	25.35	2518353
Dodecane	$C_{12}H_{26}$	90	29.02	171985696
Tridecane	$C_{13}H_{28}$	90	31.83	71841680
Dodecanone	$C_{12}H_{24}O$	80	34.85	6870606
Dodecanone	$C_{12}H_{24}O$	92	35.32	3085882
Dodecanone	$C_{12}H_{24}O$	87	35.58	2562810

SI: Similarity Index

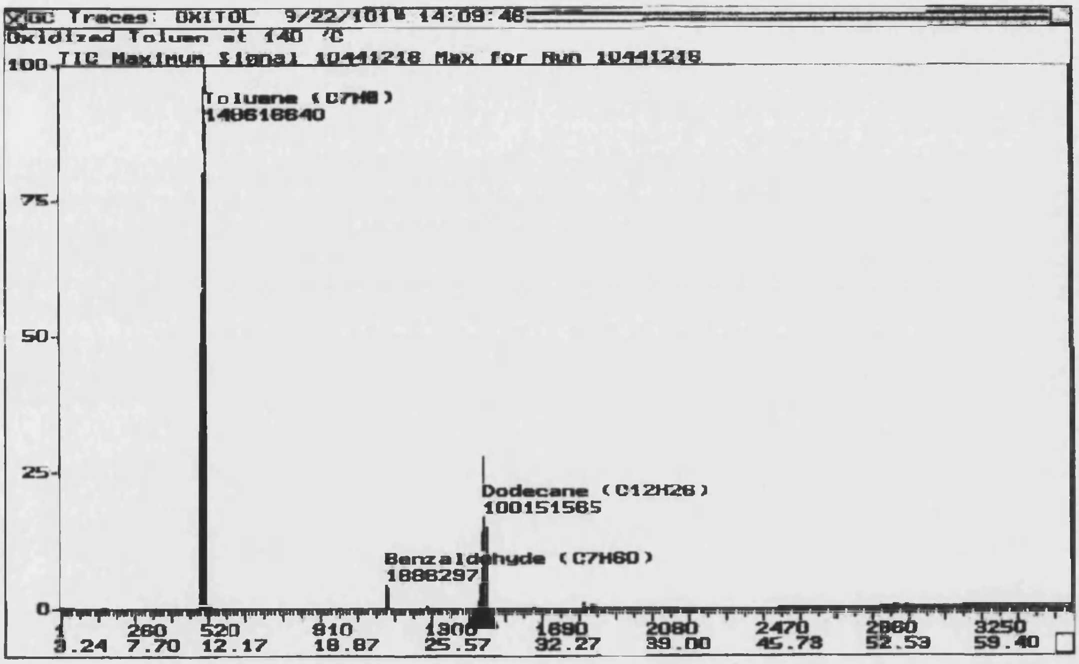

Figure 5.97: GC-MS spectrum for oxidised Toluene

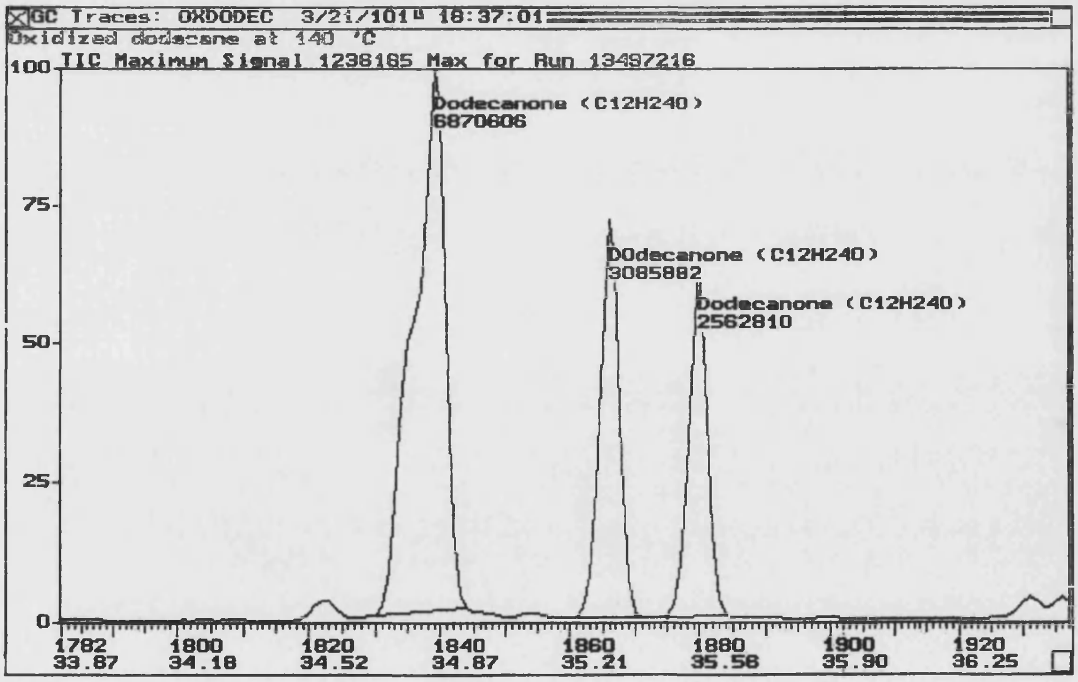

Figure 5.98: GC-MS spectrum for oxidised dodecane

5.5.4.2 Light Crude Oils

GC-MS spectrum analysis was used to determine what oxygenated hydrocarbon products were produced by low temperature oxidation of light crude oil. Figure 5.99 shows the general trend for the production of the oxygenated hydrocarbons as the oxidation temperature increases. Beyond 140 °C the oxygenated hydrocarbons start to decrease, but they are high compared to the original crude oil. This effect tend to support the reaction scenario that intermediate oxygenated hydrocarbons, such as carboxylic acids decompose at higher temperatures to produce carbon dioxide and stable oxygenated hydrocarbons. The fact that Oil D shows a continuous increase in oxygenated hydrocarbons beyond 140 °C, is attributed to the high rate of formation of polar component compared to the rate at which they decompose.

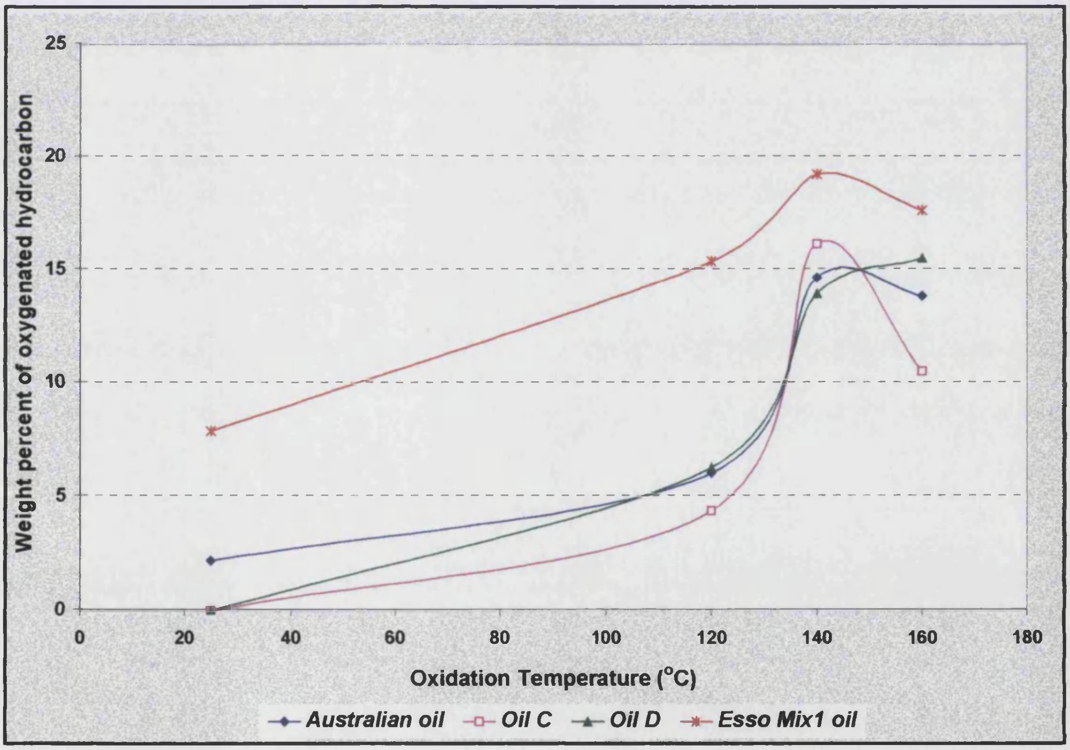

Figure 5.99: Effect of oxidation temperature on oxygenated hydrocarbon products

The GC-MS spectrums for oil D at 120 °C are shown in Figures 5.100 to 5.103. There is little change in the light and heavy molecular weight components after 48 hours, at 78 hour, there are less light components. This is identified from the increase in the medium molecular weight components as shown in Figure 5.102. At longer oxidation time (100 hours), there is now a slight increase in the low molecular weight components, but large reduction in the medium molecular weight components and an increase in the heavier molecular weight components, as shown in Figure 5.103. From this analysis, it is concluded that the LTO pathway, is that, during the early stages of oxidation, the low molecular weight components are converted to medium molecular weight components. Further oxidation, converts a small percentage of their compounds to lighter components. The majority of crude oil is converted (degraded) to higher molecular weight components. Thus, during the early stages of light oil oxidation, more oxygenated hydrocarbons are produced and these decompose at later times to produce stable oxygenated hydrocarbons and carbon oxide. These stable oxygenated hydrocarbons have lower molecular weight relative to the oxygenated hydrocarbons from which they formed.

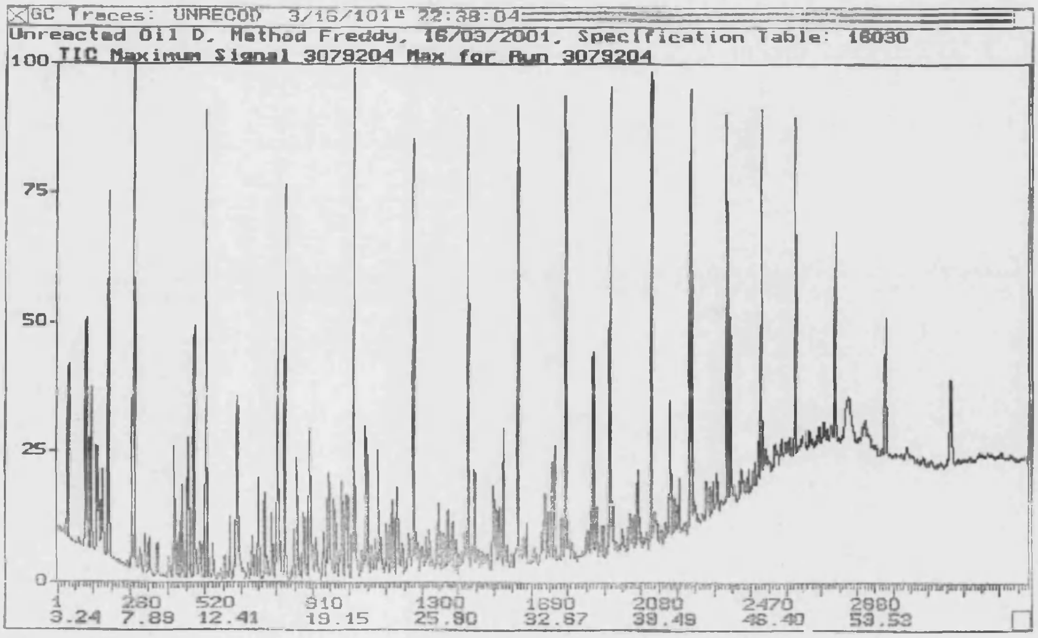

Figure 5.100: GC-MS spectrum for oil D

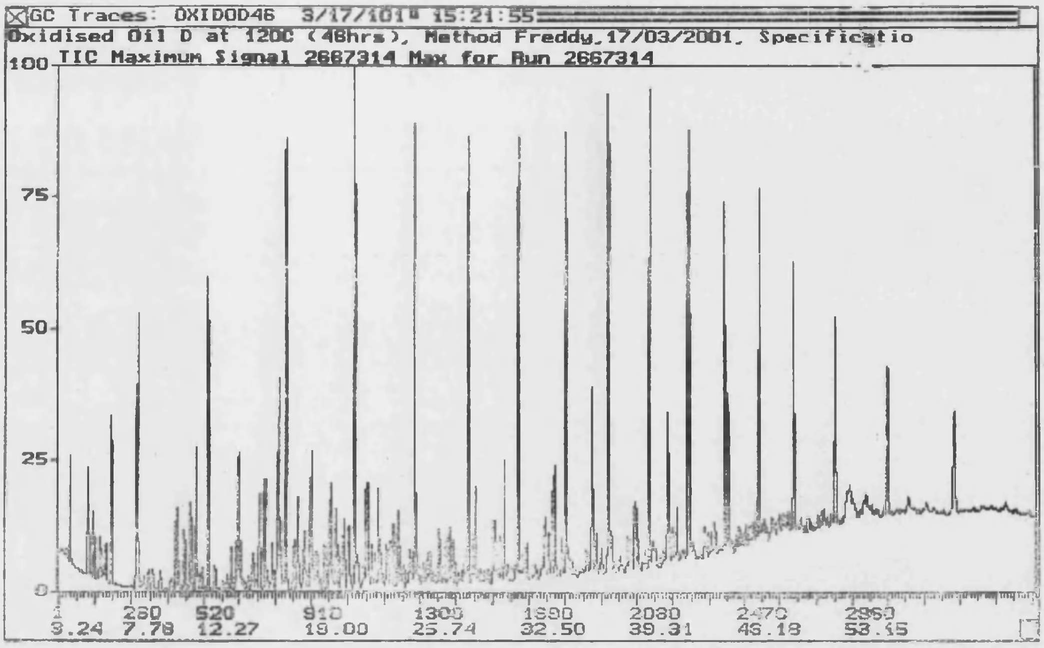

Figure 5.101: GC-MS spectrum traces for oxidised oil D after 48 hrs at 120 °C

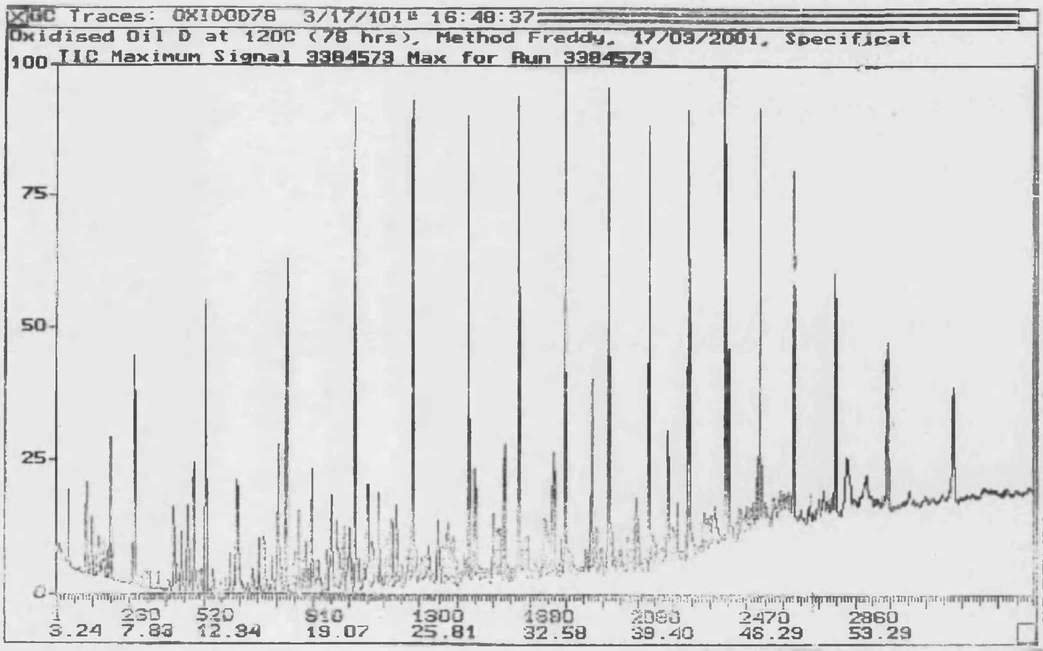

Figure 5.102: GC-MS spectrum traces for oxidised oil D after 78 hrs at 120 °C

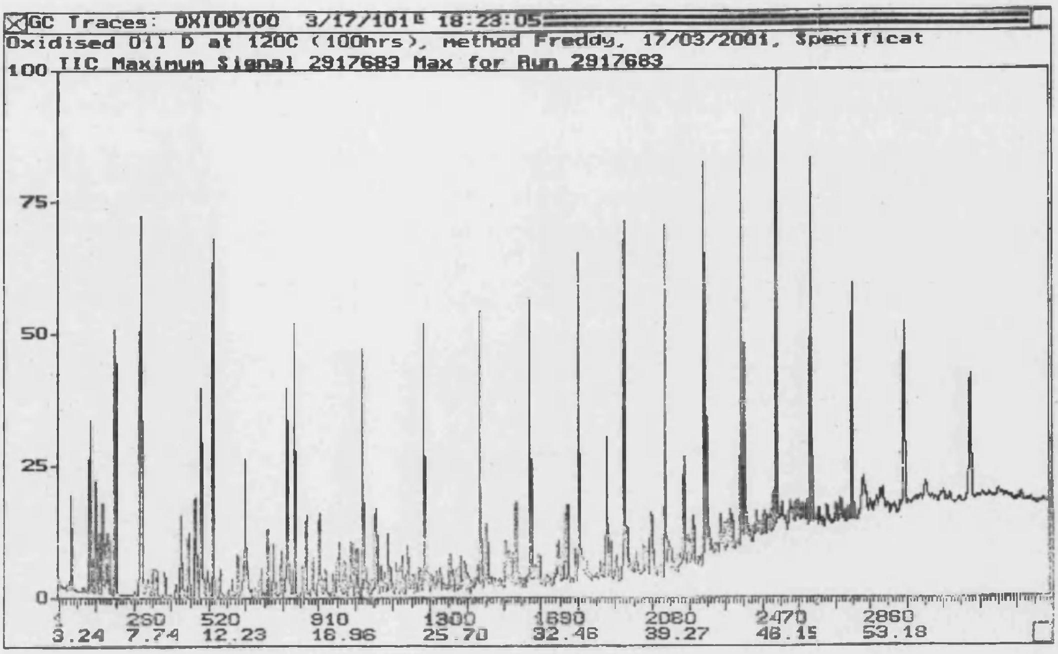

Figure 5.103: GC-MS spectrum traces for oxidised oil D after 100 hrs at 120 °C

In order to investigate the effect of LTO reaction on carbon number distribution, quantitatively via a simulated distillation, Perkin Elmer 8500 Gas Chromatograph was used. Three different plots are generated from the simulated distillation data.

(i) The first type compares the carbon number distributions of the unreacted oil and the oxidised oils as shown in Figures 5.104 to 5.107. The plots mainly show that there is an increase in components having carbon number greater than 10 (Australian oil) or 17 to 44 for oil C, oil D and Esso Mix1 oil.

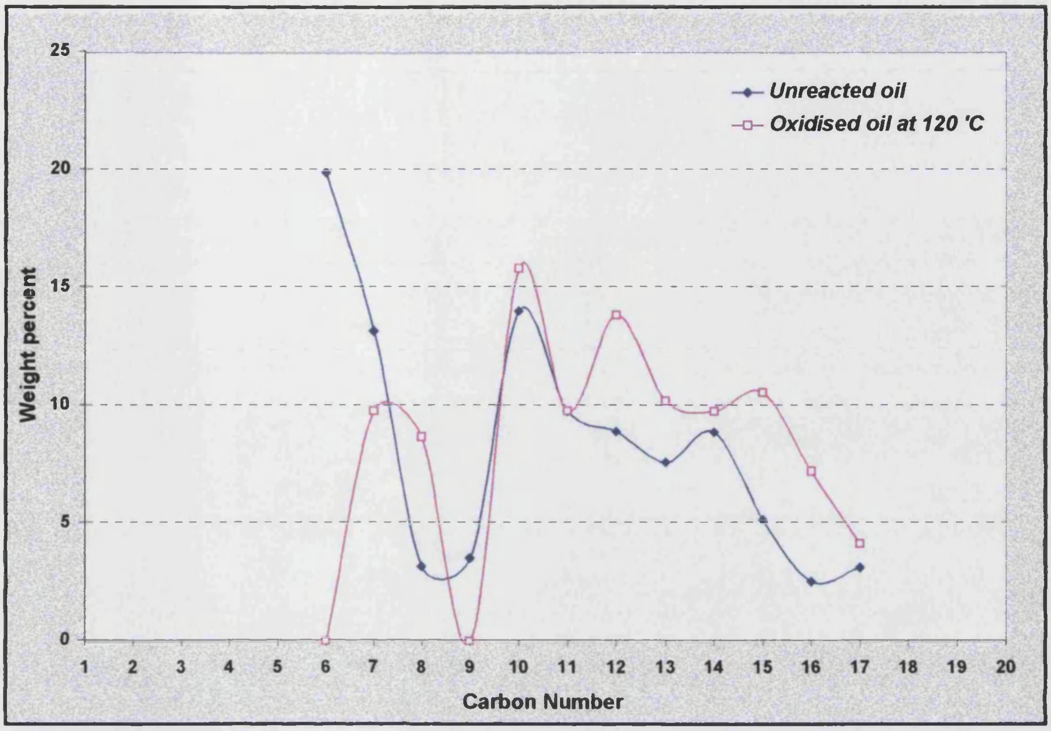

Figure 5.104: Change in carbon number distribution for Australian oil, Run 1

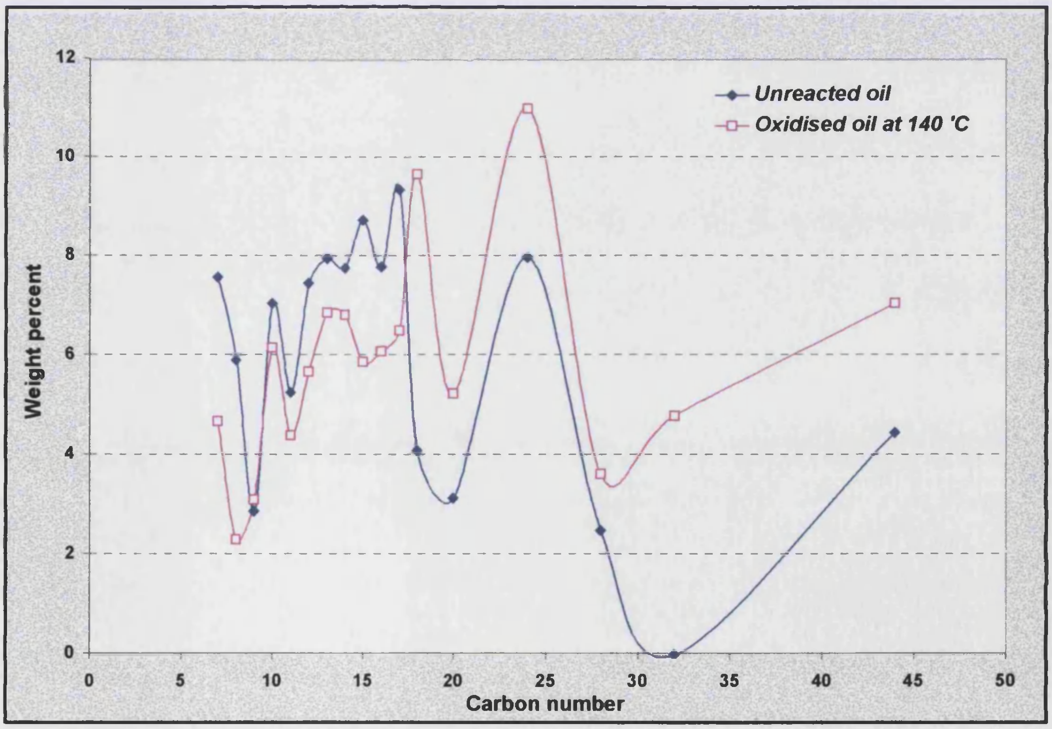

Figure 5.105: Change in carbon number distribution for oil C, Run 24

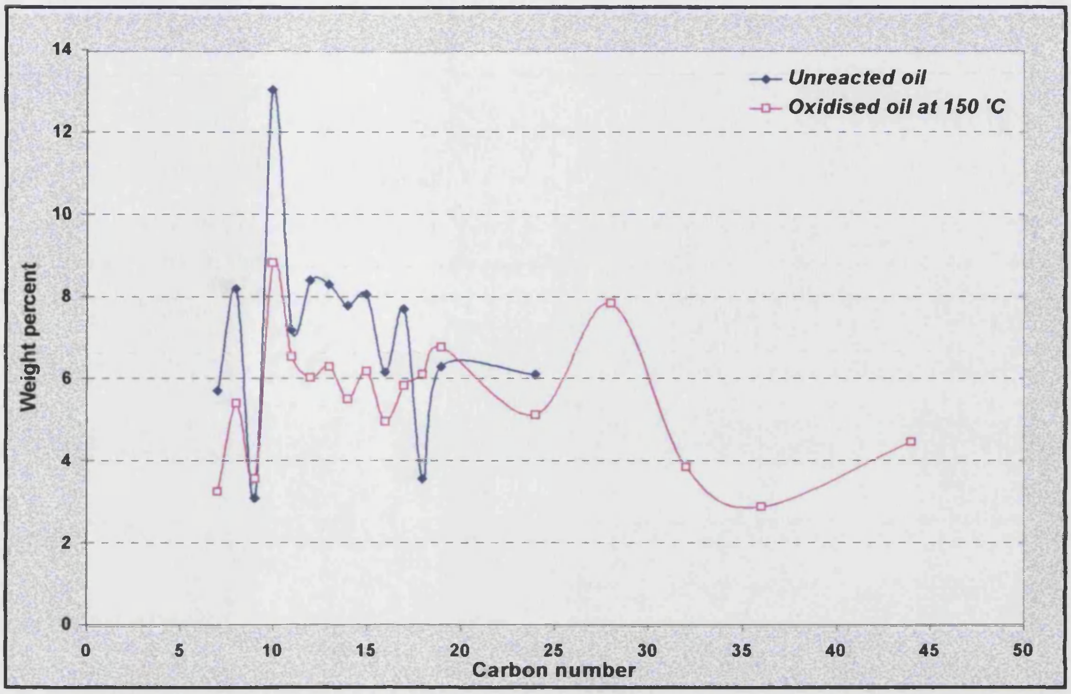

Figure 5.106: Change in carbon number distribution for oil D, Run 45

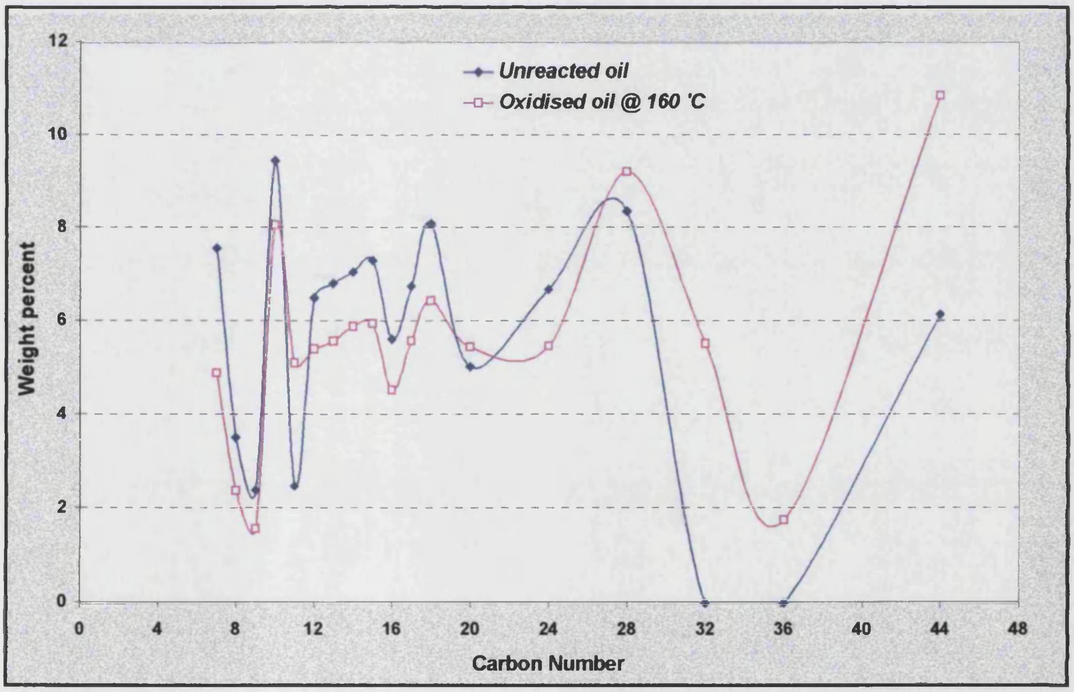

Figure 5.107: Change in carbon number distribution for Esso mix(1) oil, Run 82

(ii) The second plot illustrates the total weight change for each carbon number, comparing oxidised and unreacted oils as shown in Figures 5.108 to 5.111. Australian oil and oil C both show a loss in $C_7 - C_8$ and $C_{11} - C_{14}$ fractions with a gain in the C_9 - C_{10} and C_{15+} fractions. Oil D and Esso Mix1 oil show a consumption of the C_6 - C_{15} fraction, while C_{16} - C_{20+} are produced. The greatest increase in the C_{18} - C_{21+} fraction was observed for oil C, and the greatest decrease in C_6 - C_{10} fraction was observed for the Australian oil. This observation is attributed to the high and low weight percent of these fractions in the unreacted oil samples, respectively.

(iii) The third plot generated illustrates the effect of temperature on the weight percent of classified carbon number fraction; namely, low molecular weight hydrocarbons (C_6 – C_{10}), medium molecular weight hydrocarbons (C_{11} – C_{20}), and heavy molecular weight hydrocarbons (C_{21+}), as shown in Figures 5.112 to 5.115. Table 5.17 gives the composition changes at different oxidation temperatures for the four oils.

Table 5.17: Simulated distillation results for light crude oils

	C6-C9	C10-C13	C14-C16	C17-C20
	Weight %	Weight %	Weight %	Weight %
Unreacted Australian oil	39.86	40.38	16.62	3.14
Oxidised Oil at 120 °C	18.49	49.75	27.61	4.15
Oxidised Oil at 140 °C	24.75	52.99	14.01	8.25
Oxidised Oil at 150 °C	16.52	44.48	22.96	16.04
Oxidised Oil at 160 °C	21.34	50.73	24.29	3.64
Unreacted Oil C	23.45	37.22	24.39	14.94
Oxidised Oil at 120 °C	20.67	32.64	23.04	23.65
Oxidised Oil at 140 °C	16.28	29.69	27.52	26.51
Oxidised Oil at 150 °C	19.41	30.74	21.73	28.12
Oxidised Oil at 160 °C	19.55	23.36	28.09	29
Unreacted Oil D	30.15	39.87	23.84	6.14
Oxidised Oil at 120 °C	23.7	40.99	19.19	16.12
Oxidised Oil at 140 °C	20.75	33.91	21.23	24.11
Oxidised Oil at 150 °C	21.18	30.71	23.79	24.32
Oxidised Oil at 160 °C	16.16	31.08	23.38	29.38
Unreacted Esso Mix1 oil	22.98	30.24	25.55	21.23
Oxidised Oil at 120 °C	18.41	33.2	24.49	23.9
Oxidised Oil at 140 °C	18.12	27.39	20.73	33.76
Oxidised Oil at 150 °C	15.57	27.37	22.8	34.26
Oxidised Oil at 160 °C	16.98	28.03	22.08	32.91

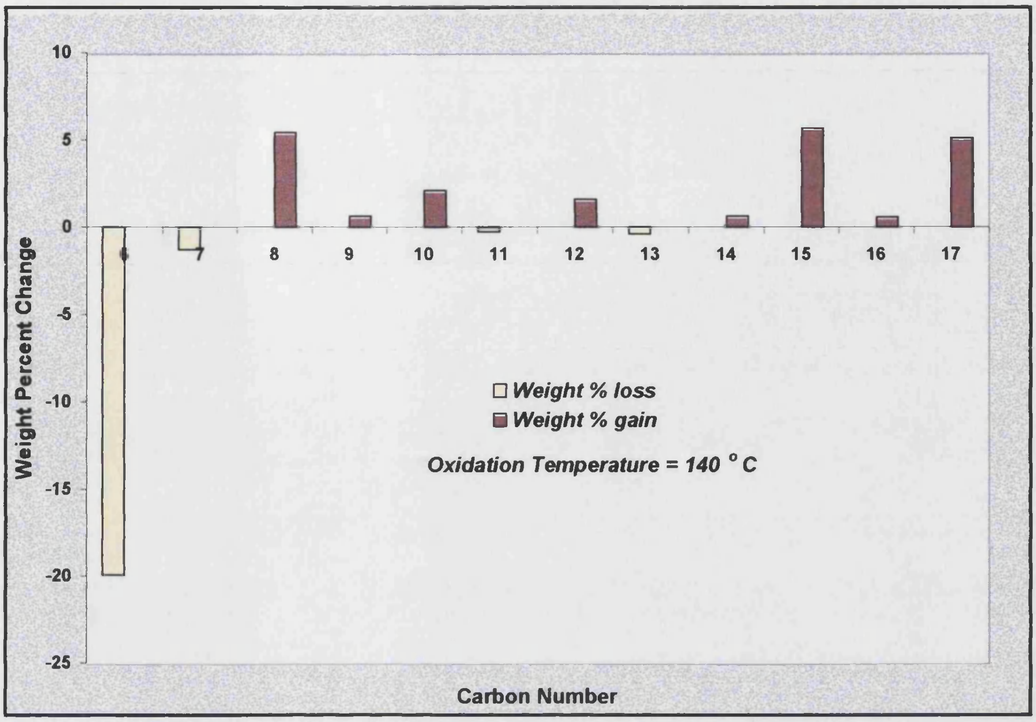

Figure 6.108: Weight percent (gain or loss) of each carbon number due to LTO of Australian oil (Run 2)

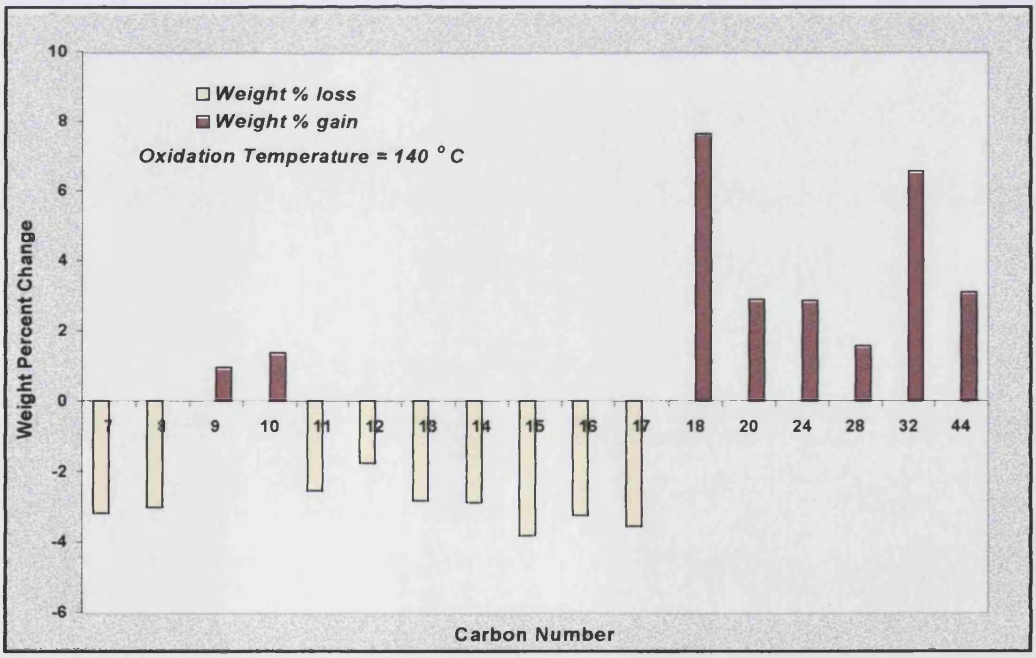

Figure 6.109: Weight percent (gain or loss) of each carbon number due to LTO of oil C (Run 24)

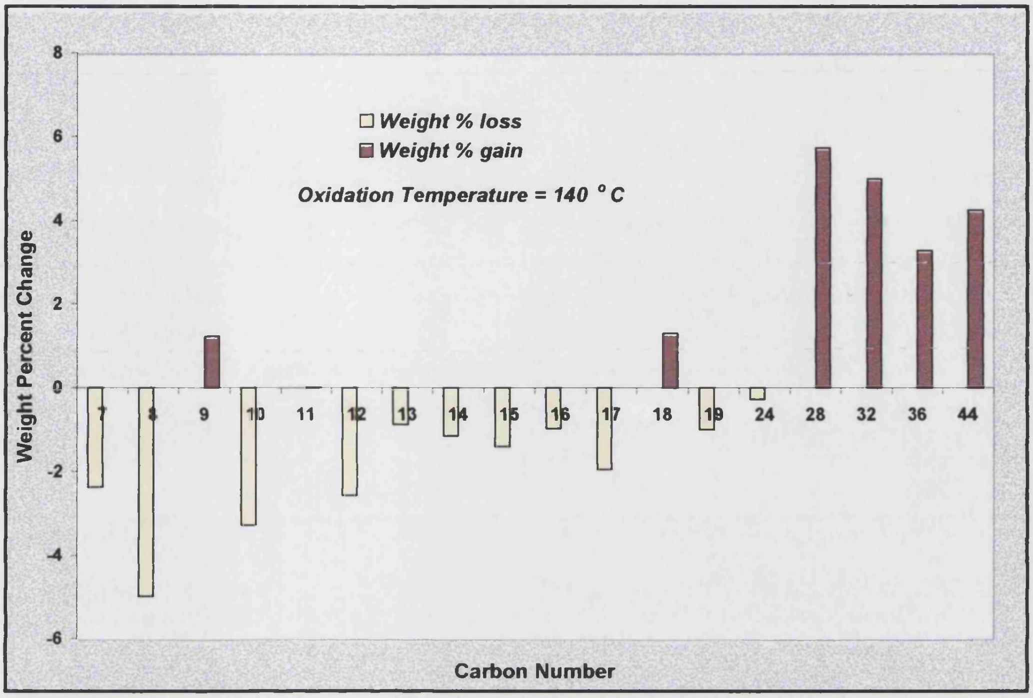

Figure 5.110: Weight percent (gain or loss) of each carbon number due to LTO of oil D (Run 44)

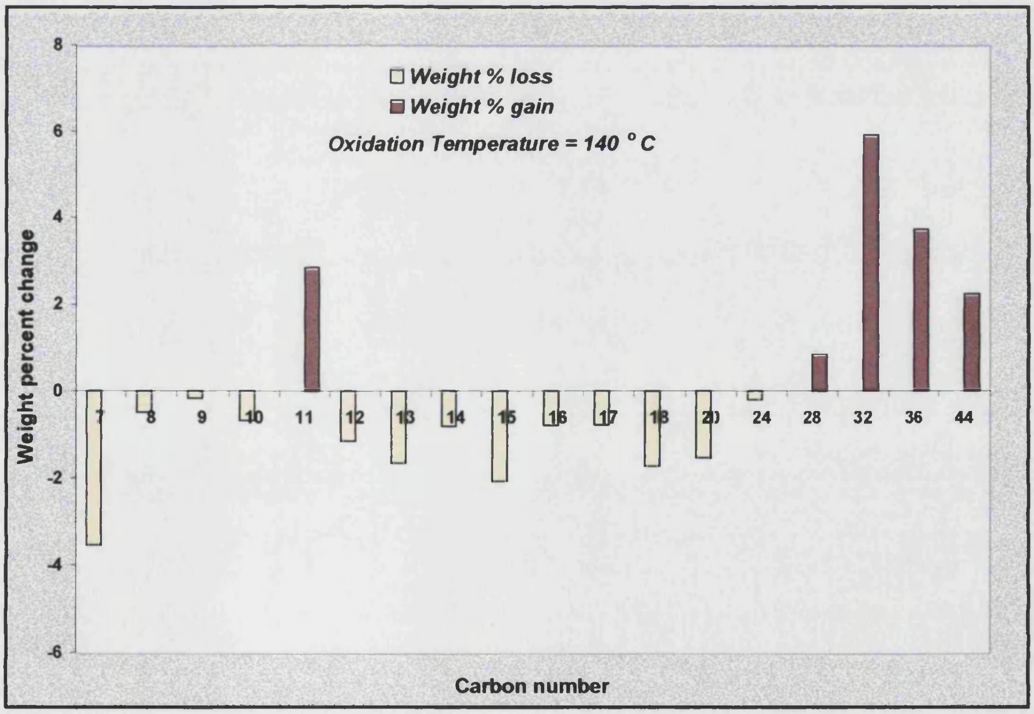

Figure 5.111: Weight percent (gain or loss) of each carbon number due to LTO of Esso Mix1 oil (Run 80)

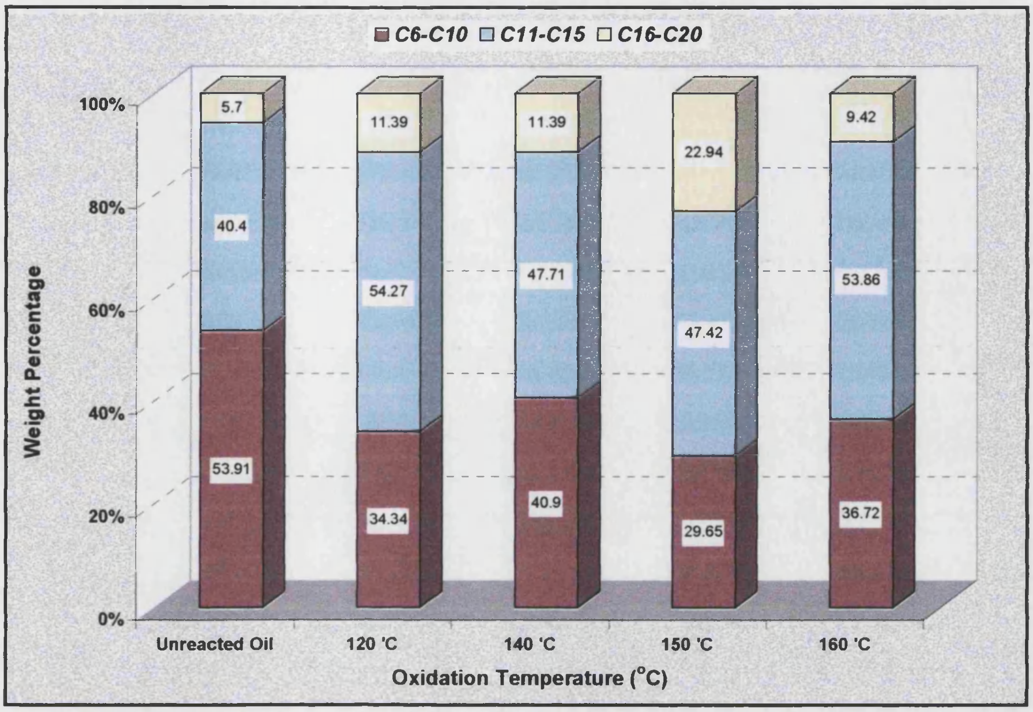

Figure 5.112: Effect of LTO process on carbon number of Australian oil

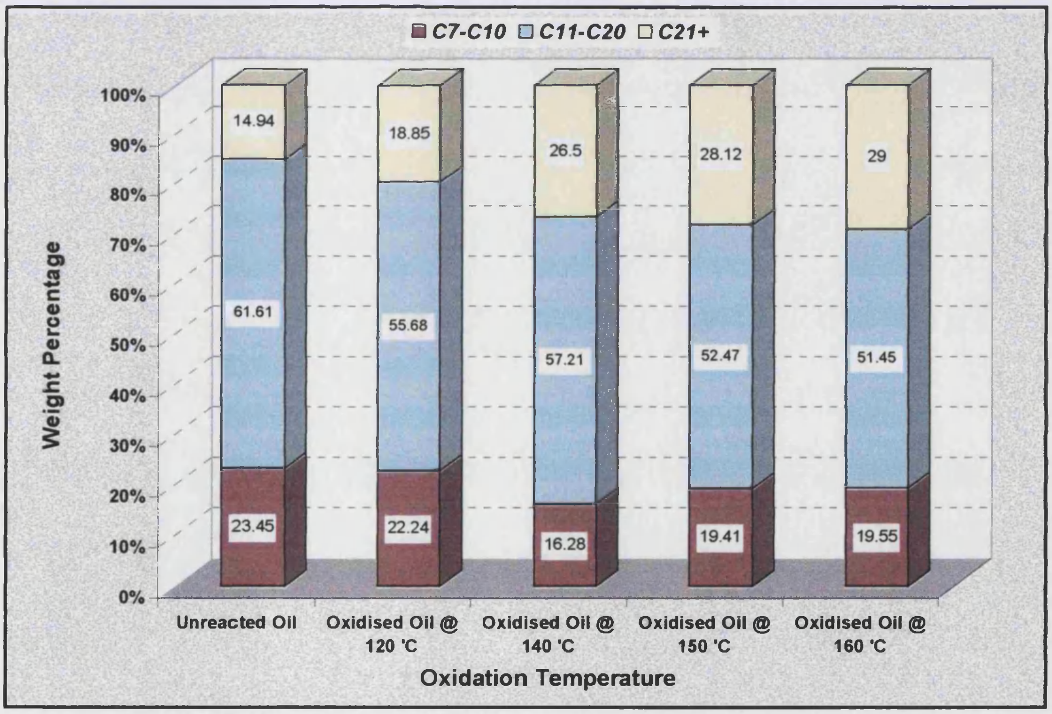

Figure 5.113: Effect of LTO Process on Carbon number of oil C

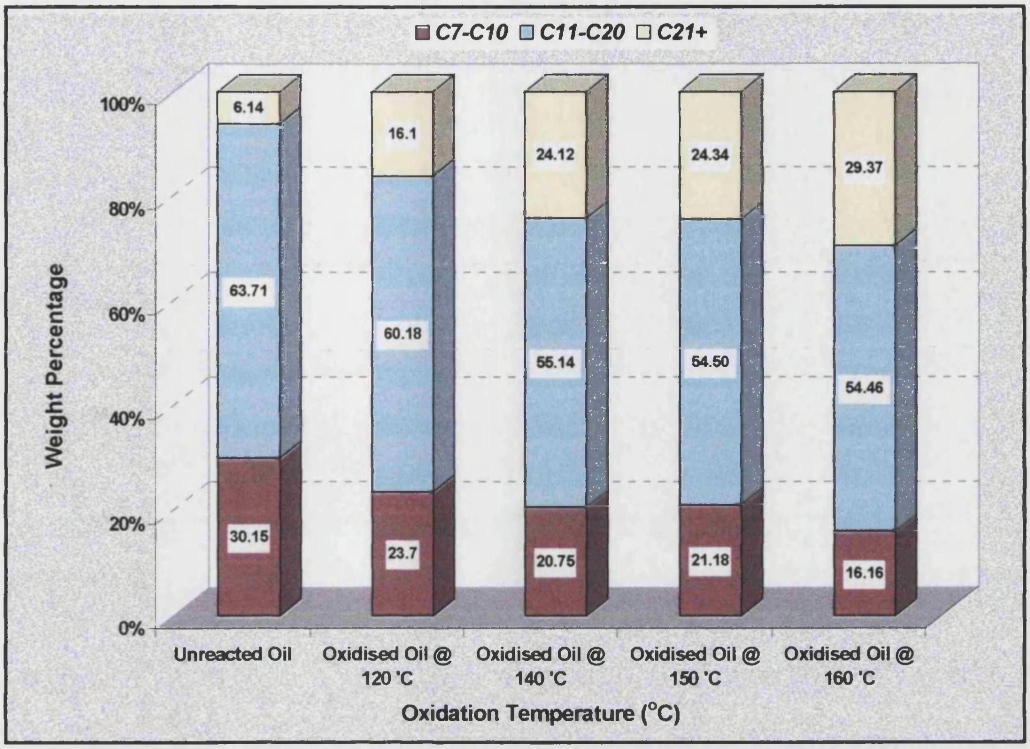

Figure 5.114: Effect of LTO process on carbon number of oil D

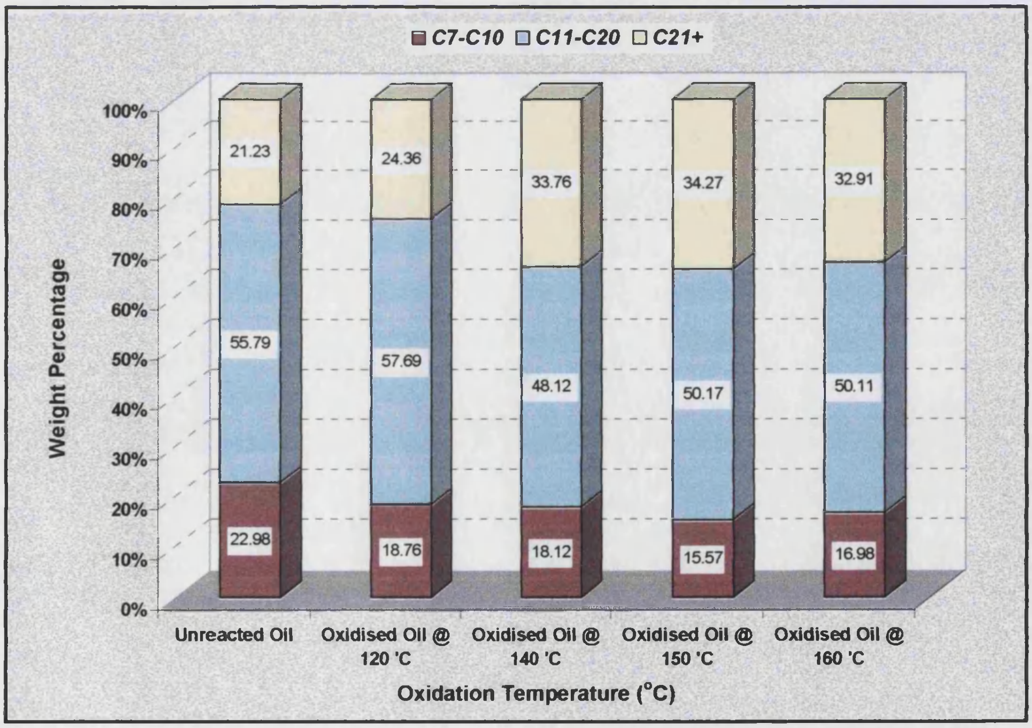

Figure 5.115: Effect of LTO process on carbon number of Esso Mix1 oil

LTO of light crude oil in the temperature range 120 to 150 °C causes low molecular weight hydrocarbon components (C_6-C_{10}) to decrease overall with a corresponding increase in the amount of high molecular weight hydrocarbon components (C_{21+}). Above 150 °C, there is a small increase in light components (C_6-C_{10}) for the Australian Oil and oil C and a decrease in the high molecular weight hydrocarbon components (C_{21+}). Generally the percentage of light components (C_6-C_{10}) at a temperature of 160 °C is still less than the original oil, as are the medium heavy fraction (C_{11}-C_{20+}). However, the heavy fraction (C_{21+}) is increased greatly by 200 to nearly 500%. The increase in high molecular weight components in the light crude oil is attributed to the high reactions of the saturates fraction to oxidation, forming polar oxygenated hydrocarbon.
Sakthikumar et al.[2], used combustion tube to simulate air injection in tertiary conditions (Soi=0.7, Swi=0.3, P = 200 bar, and T = 80-100 °C). The produced oil initially was relatively clean showing gravity drainage oil production. This oil was progressively followed by thicker oil and water emulsion slugs. Analysis of these terminal slugs indicated that produced oil was strongly oxidized through polar compounds (carboxylic acids, ketones, and alcohols).

The detailed oil analyses using Perkin Elmer 8500 Gas Chromatograph is given in Appendix F.

CHAPTER SIX

Conclusion and Recommendation for Future Work

6.1 Conclusion

The main conclusions arising from the Small Batch Reactor (SBR) oxidation experiments on light crude oils at reservoir pressure are summarised below.

1. The rate of pressure decline, or more precisely, reduction in oxygen partial pressure with time, during SBR oxidation experiments, provides a useful measure of the oxygen consumption rate, which can be used to calculate LTO reaction kinetics parameters. The method has been applied to oil alone, and oil and water in contact with reservoir matrix. The procedure is less good, however, if the oil forms of a viscous layer on the top of the oil, which can restrict the diffusion of oxygen into the oil.

2. Low temperature oxidation of light crude oils in the temperature range 120-160 °C produces four main products: CO, CO2, oxygenated hydrocarbons and water. The amount of oxygen consumed by the oil to produce oxygenated hydrocarbons was always greater than the fraction used to produce carbon oxides, when the temperature was less than 140 °C. At higher temperatures, more carbon oxides are produced, also increasing as the oxidation time and the amount of oxygen charged to the reactor increased.

3. All of the North sea light crude oils show good reactivity and high consumption of oxygen in the temperature of the range 110 to 160 °C, even at low oil saturation (Soi=0.1). The reactivity of the Australian oil was lower by comparison at 110-120 °C, however, above 120 °C the reactivity improved.

4. The overall LTO reaction kinetics for light crude oil is well described by an Arrhenius kinetics of the form:

$$\text{Rate} = A\, e^{-E/RT} \left[P_{O2}\right]^{n} \left[C_O\right]^{m}$$

for the temperature range 110 to 160 °C and operating pressure 175 to 225 bar. This is applicable for oil alone or oil and water in contact with reservoir core (core D).

The calculated reaction order on oxygen partial pressure was varied between 0.25 and 1.1, depending on the particular crude oil.

Activation energy values were calculated to be 75 to 150 kJ $mole^{-1}$ for oil alone, and 65 to 100 kJ $mole^{-1}$ with reservoir matrix present, at Soi = 0.5. For oil D, E was reduced to 82 kJ $mole^{-1}$ (Soi = 0.25) and 55 kJ $mole^{-1}$ (Soi =0.1).

5. For the light crude oils autoignition occurred at temperature of 175 - 180 °C, and operating pressure of 150 bar. This was identified by the very rapid increase in temperature and pressure in the reactor, which was intensified as the Soi increased. The phenomenon is suppressed when water is present in the sand matrix, irrespective of the value of Swi.

6. Asphaltenes/coke formation is strongly affected by the amount of oxygen which reacts with the oil. Esso Mix1 and oil D, which both contained significant amounts of asphaltenes (1.1 and 0.55 wt %) produced 3 to 5.5 wt % asphaltenes, and 5 to 11 wt % coke, respectively. The Australian oil and oil C, which contained no asphaltenes, produced up to 2.5 wt % asphaltenes and 3.0 % coke. The amount of asphaltenes/coke was greatly influenced by the oxidation temperature.

   The coke formation increased doubled, when reservoir core (core D) was used. The presence of water with the oil alone, increased the amount of asphaltenes/coke by 20 - 50 wt % for oil D and Esso Mix1 oil.

The asphaltene content of a light crude oil is a useful screening property for assessing if whether a particular reservoir, which has been selected for air injection, should be operated in the LTO or HTO mode.

7. Saturates compounds (pentane, n-hexane and dodecane) are generally more reactive than aromatics compounds (toluene and xylene), at 140 °C and 180 bar. For pure components, the order of oxidation reactivity was found to be: dodecane > isobutylbenzene > hexane > n-hexylbenzene > pentane > xylene > toluene.

   The amount of oxygenated hydrocarbons (ketones) formed by the oxidation of saturates is greater than the oxygenated intermediates (aldehydes) formed by the oxidation of aromatics.

8. Oxygenated hydrocarbons intermediates formed by the oxidation of light crude oil increase up to 140 °C, but then decrease at higher temperatures. Correspondingly, the formation of carbon oxides increases continuously at higher temperatures. This tends to support the view that the LTO reaction mechanism involves the decarboxylation of oxygenated intermediates.

9. Simulated distillation has revealed that oxidation of light crude oil at temperature of 120 to 160 °C causes a decrease in the lighter hydrocarbon fraction (C_6-C_9), but an increase in the heavier (oxygenated) hydrocarbon fraction (C_{21+}). The effect on the intermediate oxygenated fraction (C_{10}-C_{20}) is less clear, showing both increases and decreases, depending on the composition of the crude oil. The apparent increase in carbon number should be interpreted to mean "oxygen addition", so that lighter hydrocarbons shift to higher molecular weight (oxygenated) compounds, that subsequently decarboxylate, resulting in less lighter compounds, which then undergo further oxidation, and so on.

6.2 Recommendations For Future Work

1. Continuous flow experiments using the Small Batch Reactor should be carried in order to simulate more closely the reservoir condition. This arrangement will also unable the LTO kinetics to be studied at nearly constant oxygen partial pressure, and also allow the effect of oxygen/air flux to be determined.

2. On-line analysis of the effluent gases and the oxidised oil using gas chromatography would allow a more precise of the oxygen consumption and complete gas analysis. Elemental analysis of the oxidised samples especially oxygen analysis should be carried out also.

3. Further SARA analysis of light crude oil in the oxidation zone would be useful for determines the contribution of these fractions on the air injection LTO process.

4. The important effect of the rock minerals and their composition on the reaction kinetics should be investigated, to identify specific mineral effect, such as clays (kaolin), quartz, and metals.

CHAPTER SEVEN

REFERENCE AND NOMENCLATURE

7.1 References

1. D.V. Yannimaras, A.H. Sufi and M.R. Fassihi, "The Case for Air Injection into Deep Light Oil Reservoirs", Proceeding of Sixth European Symposium on IOR, Stavanger, Norway, 21-23 May 1991, pp55-63.
2. S. Sakthikumar, K. Madaoui and J. Chastang, "An Investigation of the Feasibility of Air Injection into a Waterflooded Light Oil Reservoir", SPE Paper 29806, the SPE Middle East Oil Show, Bahrain, 11-14 March 1995, pp 343-356.
3. M.R. Fassihi and T.H. Gillham, "The Use of Air Injection to Improve the Double Displacement Processes", SPE paper 26374, presented at the 68th SPE Annual Technical Conference and Exhibition in Houston, Texas, Oct. 3-6 1993, pp 81-92.
4. D.V. Yannimaras and D.L. Tiffin, "Screening of Oil for ISC at Reservoir condition by ARC", SPE Res. Eng., February 1995, pp 36-39.
5. Christopher C.A., "Air Injection for light and Medium Gravity Oil Reservoir", presented at DTI SHARE meeting (1), London, July 20, 1995.
6. M. Latil, "Enhanced Oil Recovery", Éditions Technip1980, Paris, page 35.
7. Gunits Moritis, "Worldwide EOR Survey", Oil & Gas Journal, 15 April 2002, pp 71-83.
8. R.K. Srivastava, and S.S. Huang, "A Laboratory Evaluation of Suitable Operation Strategies for Enhanced Heavy Oil Recovery by Gas Injection", Journal of Canadian Petroleum Technology, 36 (2), pp 33-40, Feb. 1997.
9. T.A. Nguyen and S.M. Faroug Ali, "Effect of Nitrogen on the Solubility and Diffusivity of Carbon Dioxide into Oil and Oil Recovery by the Immiscible WAG Process", Journal of Canadian Petroleum Technology, 37 (2), pp 24-30, Feb. 1998.
10. A. T. Turta, and A. K. Singhal, "Reservoir Engineering Aspect of Oil Recovery from Low Permeability Reservoir by Air Injection", SPE Paper 48841, Presented at 1998 SPE International Conference and Exhibition in China, .
11. J. Burger, P. Sourieau and M. Combarnous, "Thermal Methods of Oil Recovery", Éditions Technip1985, Paris, pp 248-252.

12. M. Greaves, R.W. Field and M.I. Al-Shalabe, "ISC Studies of North Sea Forties and Maya Crude Oils", Chem Eng Res Des, Vol. 65, January 1987, pp 29-39.
13. L.J. Hvizdos, J.V. Howard, and G.W. Roberts, "EOR Through Oxygen Enriched ISC: Test Results From the Forest Hill Field in Taxas", J Pet Tech, June 1983, pp 1061-1070.
14. J.G. Hansel, M.A. Benning, and J.M. Fernbacher, "Oxygen ISC for Oil Recovery: Combustion Tube Tests", J Pet. Tech., July 1984, pp 1139-1144.
15. G.H. Shahani, and J.G. Hansel, "Oxygen Fireflooding: Combustion Tube Tests with Light, Medium, and Heavy Oils", SPE Reservoir Engineering, November 1987, pp 583-590.
16. G.H. Shahani, and H.H. Gunardson, "Oxygen Enriched Fireflooding", DOE/NIPER Symposium on In Situ Combustion Practices – Past, Present and Future Application", Tulsa, April 21-22, 1994, pp 9-12.
17. P.D. White, and G.D. Farfield, "Oxygen fireflood is source of CO_2", Oil and Gas Journal, July 19, 1982, pp 177-180.
18. M. Greaves, R.W. Field, and V.A Adewusi, "In Situ Combustion Kinetic Studies of Medium Heavy Crude Oil", Chem. Eng. Res. Des., Vol. 66, July 1988, pp 328-337.
19. R. Hughes, V.M. Kamath, and D. Price, "Kinetics of In-Sitiu Combustion for Oil Recovery", Chem. Eng. Res. Des., Vol. 65, January 1987, pp 23-28.
20. Roger M. Butler, "The Potential for Horizontal Well for Petroleum Production", Journal of Canadian Petroleum Technology, 28 (3), pp 39-47, March. 1989.
21. S.D. Joshi, "Horizontal Wells: Successes and Failures", Journal of Canadian Petroleum Technology, 33 (3), Jan. 1989.
22. M. Greaves, A.A. Tuwil, and A.S. Bagci, "Horizontal Producer Wells in ISC Processes", Journal of Canadian Petroleum Technology, 32 (4), pp 58-67, 1993.
23. M. Greaves and O Al-Shamali, " ISC Process Using Horizontal Wells", Presented at Canadian SPE/CIM/CANMET International Conference on Recent Advances in Horizontal Wells Applications, March 20-23, 1994, Calgary, Alberta, Canada, pp 1-6.

24. M. Greaves and A.M. Saghr, "Sleeving-back of Horizontal Wells to Control Downstream Oil Saturation and Improve Oil Recovery", SPE Paper 50428, Presented at 1998 SPE International Conference on Horizontal Well Technology held in Calgary, Alberta, Canada.1-4 November 1998, pp 1-5.
25. A. Turta, "In Situ Combustion-From Pilot to Commercial Application", DOE/NIPER Symposium on In Situ Combustion Practices – Past, Present and Future Application, Tulsa, April 21-22, 1994, pp15-31.
26. B. Thornton, D. Hassan, and J. Eubank, "Horizontal Well Cyclic Combustion Wabasca Air Injection Pilot", Journal of Canadian Petroleum Technology, Vol. 35, No. 9, November 1996, pp 40-44.
27. M. Fassihi, T.H. Gillham, and D.V. Yannimaras, "Field Tests Assess Novel Air Injection EOR Processes", Oil & Gas Journal, May 20, 1996, pp 69-72.
28. M. K. Dabbous and P. F. Fulton, "Low Temperature Oxidation Reaction Kinetics and Effect on The In-Situ Combustion Process", SPE Journal, 14:254-265, June 1974, pp 253-262.
29. M. Fassihi, W. Brigham and Henry Ramey, "Reaction Kinetics of In Situ Combustion: Part 1-Observation", Society of Petroleum Engineers Journal, August 1984, pp 399-407.
30. D.C. Shallcross, "Modifying ISC Performance by the Use of Water-Soluble Additives", SPE Paper 19475, Presented at the SPE Asia-Pacific Conference held in Sydney, Australia, 13-15 September 1989, pp 173-184.
31. A.S. Bagci, M.V. Kok, and E. Okandan, "Combustion Reaction in Limestones Containing Heavy Oil", SPE Paper 15737, the fifth SPE Middel East Oil Show held in Manama, Bahrain, 7-10 March 1987, pp 405-416.
32. D.D. Mamora, "New finding in Low Temperature Oxidation of Crude Oil", SPE Paper 29324, the SPE Asia Pacific Oil & Gas Conference held in Kuala Lumpur, Malaysia, 20-22 March 1995, pp 577-586.
33. D.D. Mamora, and W.E. Brigham, "The Effect of Low Temperature Oxidation on Fuel and Produced Oil During ISC", Paper ISC7, DOE/NIPER International ISC Symposium, Tulsa, Oklahoma, 21-22 April 1994.

34. J.P. Kisler and D.C. Shallcross, "An Improved Model for The Oxidation Processes of Light Crude Oil", Trans IchemE. Vol. 75, Part A, May 1997, pp 392-400.
35. J.G. Burger "Spontaneous Ignition in Oil Reservoir", Soc. Pet. Eng. J. April 1976, pp73-80.
36. D. R. Babu and D. E. Cormack, "Low Temperature Oxidation of Athabasca Bitumen", The Canadian Journal of Chemical Engineering, Vol. 61, August 1983, pp 575-579.
37. J.P. Millour, R.G. Moore, D.W. Bennion, and M.G. Ursenbach, "An Expanded Compositional Model for LTO of Athabasca Bitumen", Presented at the 37th Annual Technical Metting of Pet. Soc. of ICM held in Calgary, 8-11 July 1986, pp 1-19.
38. J.G. Burger, and B.C. Sahuquet, "Chemical Aspects of ISC-Heat of Combustion and Kinetics", Society of Petroleum Technology, October 1972, pp 410-422.
39. M. Greaves, A. Osindero, R.R. Rathbone, "Influence of Reservoir Rock and Fluid son Crude Oil Oxidation using an Accelerating Rate Calorimeter", Trans IchemE, Vol. 78, Part A, July 2000, pp 715-720.
40. S. Vossoughi, and R. Kharrat, "Feasibility Study of the In Situ Combustion Process Using TGA/DSC Techniques", Society of Petroleum Technology, August 1985, pp 1441-1445.
41. I.S. Bousaid, and H.J. Ramey Jr., "Oxidation of Crude Oil in Porous Media", Soc. Pet. Eng. J., June 1968, pp 137-148.
42. S. Vossoughi, G.P. Willhite, W.P. Kritikos, I.M. Guvenir, and Y. El Shoubary, "Automation of ISC Tube and Study of the Effect of Clay on the ISC Process", Soc. Pet. Eng. J., August 1982, pp 493-502.
43. S.K. Nickle, K.O. Meyers and L.J. Nash, "Shortcoming in the Use of TGA/DSC Techniques to Evaluate ISC", SPE Paper 16867, the 62nd Annual Technical Conference and Exhibition held in Dallas, 27-30 September 1987, pp 323-337.
44. J.D. Alexander, W.L. Martin, and J.N. Dew, "Factors Effecting Fuel Availability and Composition During In Situ Combustion", Journal of Petroleum Technology, October 1962, pp 1154-1164.

45. R.G. Moore, J.D.M. Belgrave, Raj Mehta, Matt Ursenbach, C.J. Laureshen, and Kejia Xi, "Some Insight Into the LTO and high Temperature In-Situ Combustion Kinetics", SPE Paper 24174, Presented at the SPE/DOE Eight Symposium on Enhance Oil Recovery held in Tulsa, Oklahoma, 22-24 April 1992, pp 179-190.
46. K.O. Adegbesan, J.K. Donnelly, R.G. Moore and D.W. Bennion, "Low Temperature Oxidation Kinetic Parameters for Is-Situ Combustion: Numerical Simulation", SPE Res. Eng., November 1987, pp 573-579.
47. M.V. Kok, and C.O. Karacan, "Behaviour and Effect of SARA Fraction of Oil During Combustion", SPE Paper 37559, Presented at the 1997 SPE International Thermal Operation & Heavy Oil Symposium, held in Bakersfield, California, 15-18 February 1997, pp 421-431.
48. D.R. Babu and D.E. Cormack, "Effect of Low Temperature Oxidation on the Composition of Athabasca Bitumen", Fuel, Vol. 63, June 1984, pp 858-861.
49. G.C. Wichert, N.E. Pkazawa, R.G. Moore, and J.D.M. Belgrave, "In-Situ Upgrading of Heavy Oils by Low Temperature Oxidation in the Presence of Caustic Additives", SPE Paper 30299, Presented at the International Heavy Oil Symposium held in Calgary, Alberta, Canada, 19-21 June 1995, pp 529-536.
50. H. Al-Saffar, D. Price, A. Soufi, R. Hughes, "Distinguish Between Overlapping Low Temperature and High Temperature Oxidation Data Obtained from a Pressurized Flow Reactor System Using Consolidated Core Material", Fuel Vol. 79, 2000, pp 723-732.
51. M.R. Fassihi, K.O. Meyers, and P.F. Baslle, "Low Temperature Oxidation of Viscous Crude Oils", SPE Reservoir Engineering, November 1990, pp 609-616.
52. M. Ranjbar, "Improvement of Medium and Light Oil Recovery with Thermocatalytic In Situ Combustion", Journal of Canadian Petroleum Technology, Vol. 34, No. 8, October 1995, pp 25-30.
53. M. Greaves, R. Rathbone, and A.O. Osindero, "Air Injection into Light Oil Reservoir-Exothermisty and Kinetics of crude oil Oxidation", Presented at the 10th European Symposium on Improved Oil Recovery, Brighton, UK, 18-20 August 1999, pp 1-10.

54. University of Salford, "The Exothermicity and Oxidative Kinetics of North Sea Light Crude Oils for Air Injection IOR Process", EPSRC Project Report, August 2000.

55. M. Fassihi, W.E. Brigham, and H.J. Ramey, "Reaction Kinetics of In-Situ Combustion: Part 2-Modeling", Society of Petroleum Engineers Journal, August 1984, pp 408-414.

56. Karen S. Yoshiki and Colin R. Phillips, "Kinetics of The Thermo-Oxidation and Thermal Cracking Reaction of Athabasca Bitumen", Fuel, Vol. 64, November 1985, pp 1591-1597.

57. Colin R. Phillip and It-Chin Hsieh, "Oxidation Reaction Kinetics of Athabasca Bitumen", Fuel, Vol. 64, July 1985, pp 985-989.

58. T.H. Gillham, B.W. Cerveny, E.A. Turek, and D.V. Yannimaras, "Keys to Increasing Production Via Air Injection in Gulf Coast Light Oil Reservoirs", SPE Paper 38848, the 1997 SPE Annual Technical Conference and Exhibition held in San Antonio, Taxas, 5-8 October 1997, pp 65-80.

59. V. Zelenko and F. Solignac, "Use of Accelerating Rate Calorimeter in Reservoir Oil Selection for Air Injection Process", 7th Petroleum Conference, South Saskatchewan Section, Petroleum Society of CIM, Regina, 19-22 October 1997, pp 1-13.

60. Lewis F. Hatch, Sami Matar, "From Hydrocarbons to Petrochemicals", Gulf Publishing Company, Houston, 1981, pp 8-38

61. M. Greaves, S.R. Ren, and R.R. Rathbone, "Air Injection Technique (LTO Process) for IOR from Light oil reservoirs: Oxidation Rate and Displacement", SPE Paper 40062, the 1998 SPE/DOE Improved Oil Recovery Symposium, Tulsa, Oklahoma, 19-22 April 1998, pp 479-492.

62. A.B.A. Luka, R. Hughes, and D. Price, "Evaluation of a North Sea Oil Recovery by ISC Using High Pressure Differntial Scanning Calorimetry", Trans IchemE, Vol. 72 Part A, March 1994, pp 163-168.

63. C. Clara, M. Durandeun, and T. Nguyen, "Laboratory Studies for Light Oil Air Injection Projects: Potential Application in Handil Field", SPE Paper 54377,

Presented at the 1999 SPE Asia Pacific Oil and Gas Conference and Exhibition held in Jakarta, Indonesia, 20-22 April 1999, pp 1-15

64. M. Greaves, S.R. Ren, R.R. Rathbone, T. Fishlock, and R. Ireland, "Improved Residual Light Oil Recovery by Air Injection (LTO Process)", the Journal of Canadian Petroleum Technology, Vol. 39, No. 1, January 2000, pp 57-61.
65. D.L. Tiffin and D.V. Yannimaras, "High Pressure Combustion Tube Performance of Light Oils", Presented at 8th European Symposium on Improved Oil Recovery, Vienna, Austria, May 15-17, 1995, pp 265-271.
66. R.G. Moore, M.G. Ursenbach, "Field Observation of In-Situ Combustion in a Waterflooded Reservoir in the Kinsella Field", Journal of Canadian Petroleum Technology, Vol. 32, No. 7, September 1993, pp 34-41.
67. S.A. Abu-Khamsin, A. Iddris, M.A. Aggour, "The Spontaneous Ignition Potential of a Super-Light Crude Oil", Fuel,Vol.80, 2001, pp 1415-1420.
68. H.J Tadema, J. Weijdema, "Spontaneous Ignition of Oil Sands", Oil Gas Journal, 1970, Vol. 68, pp 77-80.
69. J.G. Burger, "Spontaneous Ignition in Oil Reservoirs", Society of Petroleum. Engineering Journal, 1976, Vol. 16, pp 73-81.
70. H.K. Sarma, N. Yazawa, R.G. Moore, S.A. Mehta, N.E. Okazawa, H. Ferguson, M.G. Ursenbach, "Screening of Three Light Oil Reservoir for Application of Air Injection Processes by Accelerating Rate Calorimetric and TG/PDSC Tests", Paper No. 156, presented at Petroleum Society's Canadian International Petroleum Conference 2001, Calgary, Alberta, Canada, pp 1-21.
71. R.G. Moore, S.A. Mehta, M.G. Ursenbach, and C.J. Laureshen, "Strategies for Successful Air Injection-Based IOR Processes", Paper 235 Presented at 7th UNITAR International Conf. On Heavy Crude and Tar Sands, Beijing, October 27-30, 1998.235, pp 2171-2178.
72. M. Greaves, T.J. Young, S. EL-Usta, R.R. Rathbone, "Combustion Tube Studies on West of Shetlands Clair Oil and Light Australian Oil", Trans IchemE, Vol. 78, Part A, July 2000, pp 721-730.

73. J.P. Kisler and D.C. Shallcross, "The Effects of Metallic Catalysts on Light Crude Oil Oxidation", In Situ, Vol. 20 (2), 1996, pp 137-160.
74. P.S. Sarathi, "Nine Decades of Combustion Oil Recovery – A Review of ISC History and Assessment of Geologic Environments on Project Outcome", Paper 235 Presented at 7th UNITAR International Conf. On Heavy Crude and Tar Sands, Beijing, October 27-30, 1998.124, pp 1189-1197.
75. Aruel Carcoana, "Applied Enhanced Oil Recovery", Englewood cliffs, New Jersey: Prentice-Hall, 1992, pp 107-111.
76. G.A. Huffman, J.P. Benton, A.E. El-Messidi, and K.M. Riley, "Pressure Maintenance by In-Situ Combustion, West Heidelberg Unit, Jasper County, Mississippi", Journal of Petroleum Technology, October 1983, pp 1877-1883.
77. M.R. Fassihi, D.V. Yannimaras, E.E. Westfall, and T.G. Gillham "Economics of Light Oil Air Injection Projects", SPE Paper 35393, Presented at the 1996 SPE/DOE Tenth Symposium on Improved Oil Recovery held in Tulsa, OK, 21-24 April 1996, pp 501-509.
78. V.K Kumar, M.R. Fassihi, and D.V. Yannimaras, "Case History and Appraisal of the Medicine Pole Hills Unit Air Injection Project", SPE Reservoir Engineering, August 1995, pp 198-201.
79. M.R. Fassihi, D.V. Yannimaras and V.K. Kumar, "Estimation of Recovery Factor in Light Oil Air Injection Projects", SPE Reservoir Engineering, August 1997, pp 173-178.
80. P. Germain and J.L. Geyelin, "Air Injection into a Light Oil Reservoir: The Horse Creek Project", SPE Paper 37782, the SPE Middle East Oil Show, Bahrain, 15-18 March 1997, pp 233-238.
81. A. Osindero. 2000, "Exothermicity and Oxidative Kinetics of Light Crude Oils for Air Injection Improved Oil Recovery", PhD Thesis, University of Bath.
82. A.W. Drews "Manual on Hydrocarbon Analysis", American Society for Testing and Materials, 6th Edition, 1998, Page 545-546.

83. R. A. Kazi, H. B. Al-Saffar, D. Price, and R. Hughes, "High-Pressure Flow Reactor: Design and Application to Pertinent Oil Recovery Studies", Energy & Fuels, Vol. 14, No. 3, 2000, pp 519-525.
84. B. Verkoczy and N.P. Freitag, "Oxidation of Heavy Oils and their SARA Fractions-Its Role in Modelling In-Situ Combustion", Petroleum Society of CIM, Paper No. 97-167, Presented at the Seventh Petroleum Conference of the Saskatchewan Section, Held in Regina 19-22 October 1997, pp 1-6.
85. M. Greaves, R. Rathbone S.R. Ren, "Oxidation Kinetics of North Sea Light Crude Oils at Reservoir Temperature", Trans IchemE Vol. 77, Part A, June 1999, pp 385-394.
86. I. Lakatos, K.Bauer, J. Lakatos-Szabo, A. Szittr, "The Effect of In-Situ Low Temperature Oxidation on Chemical and Physical Properties of Heavy Crude Oils", Presented at the seventh European IOR Symposium in Moscow, Russia October 27-29, 1993.
87. Dasari Ram Babu and Donald E. Cormack, "Coking of Athabasca bitumen: effect of oxidation and sand", Fuel, Vol 62, March1983, pp 350-352.
88. B. Verkoczy, "Factor Affecting Coking in Heavy Oil Cores, Oil and SARA Fractions Under Thermal Stress", Journal of Canadian Petroleum Technology, Vol. 32, No. 7, 1993, pp 25-33.

7.2 *Abbreviation*

API	American Petroleum Institute
ARC	Accelerating Rate Calorimeter
ASTM	American Society Testing and Material
BOPD	Barrel Oil Per Day
BP	Boiling Point
COFCAW	Combination of Forward Combustion and Water
CT	Combustion Tube
DDP	Double Displacement Process
DSC	Differential Scanning Calorimetry
DTA	Differential Thermal Analysis
EGA	Evolved Gas Analysis technique
EOR	Enhanced Oil Recovery
FCM	First Contact Miscibility
FID	Flammable Ionization Detector
GC-MS	Gas Chromatograph Mass Spectroscopy
GOR	Gas Oil Ratio
HCPV	Hydro Carbon Pore Volume
HTO	High Temperature Oxidation
ID	Internal Diameter
IFT	Interfacial Tension
IOR	Improved Oil Recovery
ISC	In Situ Combustion
LTO	Low Temperature Oxidation
MCM	Multiple Contact Miscibility
MMP	Minimum Miscibility Pressure
MTO	Medium Contact Oxidation
NTC	Negative Temperature Coefficient
NTR	Negative Temperature Region
OD	Outer Diameter

OGJ	Oil and Gas Journal
OOIP	Original Oil In Place
PDSC	Pressurized Differential Scanning Calorimetry
SARA	Saturates, Aromatic, Resin, and Asphaltene
SBR	Small Batch Reactor
SI	Similarity Index
SS	Stainless Steel
TGA	Therogravimeteric Analysis
TIC	Total Ion Chromatogram
VDU	Visual Display Unit
WAG	Water Alternating Gas
WAR	Water Air Ratio
WTM	Wet Test Meter

7.3 *Nomenclature*

A	Arrhenius constant or Pre-exponential factor
C	Carbon
CO	Carbon monoxide
CO_2	Carbon dioxide
C_o	Concentration of fuel
dn_{O2}	Change in number of oxygen moles per time
E	Reaction Activation Energy
hr	Hour
H	Hydrogen
K	Reaction rate constant
m	Reaction order with respect to oil concentration
n	Reaction order with respect to oxygen
N_2	Nitrogen
O_2	Oxygen

P	Total pressure
P_{O2}	Oxygen partial pressure
R	Universal gas constant
Ro	Reaction Rate of oxygen
Rc	Combustion Rate
S	Sulfur
Sgi	Initial gas saturation
Soi	Initial oil saturation
Swi	Initial water saturation
t_1	Initial oxidation time (hr)
t_2	Final oxidation time (hr)
T	Temperature
V	Volume
z	Compressibility factor

7.3.1 Subscripts

f	Final
g	Gas
i	Initial
o2	Oxygen
o	Oil
w	Water

7.3.2 Greek Symbols

μ_o	Oil viscosity
ρ_o	Oil density
ρ_s	Sand density
Φ	Porosity

Appendix A

A-1 Design of a New Small Batch Reactor:

The Small Batch Reactors (SBR) was designed as following:

Operating Condition:

Required volume $\cong$ 100 cc

Inside diameter of reactor = 30 mm

Maximum pressure = 400 bar

Maximum Temperature = 200 °C

Required material stainless steel (SS 304)

Method of calculation:

The formula used to calculate the wall thickness of the cylindrical reactor is:

$$t = \frac{PR}{(SE - 0.6P)}$$

Where

t = Thickness, inches

P = Design pressure, psig

R = Inside radius, inches (Given 0.59 in)

S = Stress value of material, psi

E = Efficiency of welded joints, assumed

The maximum allowable stress for the above operating condition = 12900 psi

No welding will be in the designed reactor, therefore E = 1.0

$$\therefore \quad t = \frac{(58880\ x\ 0.59)}{(12900\ x\ 1) - (0.6\ x\ 5880)} = 0.37 \text{ in}$$

The final reactor wall thickness was decided to be 15 mm ≅ 0.6 in, and the base of the reactor was double of the wall thickness ≅ 30mm (1.2 in).

A.2 Calculation of Required Materials for SBR experiments:

The required material for SBR experiments were calculated based on 43.5 cc of the total volume of the glass vessel filled with crushed sand, crude oil, and water. Where the remaining volume of the small batch reactor (main body and top part) filled with Air (46.4 cc).

The bulk volume required to be filled with crushed sand = 43.5 cc
Weight of crushed sand which filled in the 43.5 cc by hand packing = 61.2 g

Density of Amoco crushed core = 2.31 g/cc (Calculated by Physics Department at Bath University using Helium Picnometer method)

$$\text{Sand grain volume} = \frac{\textit{Weight of packed sand}}{\textit{Density of crushed sand}} = \frac{61.2}{2.31} = 26.5 \text{ cc}$$

$$\text{Therefore Pore volume} = \text{bulk volume} - \text{sand grain volume}$$
$$= 43.5 - 26.5 = 17 \text{ cc}$$

Therefore the required volume of oil and water for each run at given saturation is calculated based on the following equations:

Oil volume = Pore volume x Oil saturation

Water volume = Pore volume x Water saturation

Gas volume = Pore volume x Gas saturation

A-3 Calculation of initial fluid saturation for Run 14, 15, 16, and 38

In these runs, Given Soi = 0.5, Swi = 0.25, and Sgi = 0.25.

Therefore, the initial volume of oil, water and gas in the sand pack for these runs are as following:

Initial oil volume	= 17 x 0.5 = 8.5 cc
Initial water volume	= 17 x 0.25 = 4.25 cc
Initial gas volume	= 17 x 0.25 = 4.25 cc

Appendix B

B.1 Extraction of Oxidised Oil

Sample Preparation

The oxidised oil sand mixture was split into two portions and each portion was placed in a weighed extraction thimble.

Extraction procedure

1) Turn on the cooling water to the condenser unit.
2) Switch on the electrical supply to the heater.
3) Weigh separately an empty distillation flask.
4) Place the thimble that contain oil and crushed sand mixture in the Soxhlet extractor, then connect it to the flask.
5) Washing the sample with 150ml of Dichloromethane. Allow all of the solvent to filter through.
6) Connect the chamber to the rest of the Soxhlet apparatus.
7) Switch-on the heater and allow the temperature of the flask to increase up to the boiling temperature of the solvent. The vapor of the solvent rises through the oil and sand mixture and then is condensed in the condenser to reflux back over the mixture to extract the oil from the sand. The dichloromethane soluble material will be collected in the flask, where the insoluble material heavy molecular weight components, coke, and crushed core will stay in the thimble.
8) After about one hour, when the dichloromethane in the inner tube is observed to be clear in color (no more oil can be extract), switch-off the heater.
9) Disconnect the chamber, lift the extraction thimble, and allow the solvent to drain from it into the chamber. Place the extraction thimble, which contain sand, some heavy molecular weight component and coke in a clean beaker.
10) Reconnect the chamber to the distillation flask and condenser.
11) Distill the remaining solution of dichloromethane and crude oil for about 1hr to distill the dichloromethane.

12) When the level of is ¾ of the height of the inner tube, switch off the heater and allow the apparatus to cool to room temperature.
13) When dichloromethane has cooled, carefully remove the chamber from the system.
14) Drain the dichloromethane or toluene into used dichloromethane bottle to be disposed later on.
15) Decant the extracted oil into small jar for further analysis.
16) Place the thimble that contain heavy molecular weight component and sand in the Soxhlet extractor, then connect it to the flask.
17) Repeat steps 5-15 with using toluene as solvent instead of dichloromethane to extract the heavy molecular component from the sand and coke.

By the end of the extraction process, the crushed core sand and coke will precipitate in the thimble, where all of the oxidised oil will be collected in small jars for further analysis.

B.2 Asphaltenes and Coke Seperation

The separation procedure was as following:

1. Turn on the cooling water to the condenser unit.
2. Switch on the electrical supply to the heater.
3. Weigh separately an empty distillation flask and extraction thimble.
4. Weigh out 3.0-5.0g of oil sample into a beaker.
5. Place the extraction thimble at the top of the Soxhlet chamber.
6. Pour the oil sample into the extraction thimble, washing through with 120-200ml of n-pentane.
7. Allow all of the solvent to filter through, then place the extraction thimble into the Soxhlet chamber.
8. Connect the chamber to the rest of the Soxhlet apparatus.
9. Switch-on the heater and allow the apparatus to separate the oil sample into n-pentane soluble material (maltenes), and insoluble material (asphaltene and coke). The n-pentane and maltenes solution will be collected in the distillation flask, where the asphaltene and coke will precipitate in the thimble.

10. After about one hour, when the n-pentane in the inner tube is observed to be clear in colour, switch-off the heater.
11. Disconnect the chamber, lift the extraction thimble, and allow the n-pentane to drain from it into the chamber. Place the extraction thimble, which contain asphaltene and coke in a clean beaker.
12. Reconnect the chamber to the distillation flask and condenser.

Maltenes Separation;

13. Distill the remaining solution of n-pentane and maltenes for about 1hr (to distill the n-pentane).
14. When the level of n-pentane is ¾ of the height of the inner tube, switch off the heater and allow the apparatus to cool to room temperature.
15. When n-pentane has cooled, carefully remove the chamber from the system.
16. Drain the n-pentane into used n-pentane bottle for disposal.
17. Repeat steps 14-16 until all of the n-pentane has been recovered.
18. Weight the distillation flask to obtain the weight of the maltenes.

Asphaltene and Coke Separation:

19. Place the extraction thimble, which contains asphaltene and coke at the top of the Soxhlet chamber.
20. Wash the extraction thimble with 150ml of toluene.
21. Allow the solvent to filter through, then place the extraction thimble in the chamber, and connect the chamber to the Soxhlet condenser.
22. Switch-on the heater and allow the apparatus to reflux. (to separate asphaltene from coke)
23. After about one hour, when the toluene is observed to be clean in color, switch off the heater.
24. Disconnect the chamber, lift the extraction thimble, and allow the toluene to drain from it into the chamber. Place the extraction thimble in the fume cupboard to vaporize any remaining small drops of toluene and to dry out the extraction thimble.

25. Reconnect the chamber back to the Soxhlet condenser.
26. Distill the remaining solution of toluene and asphaltene for one hour (to distill toluene).
27. When the level of toluene in the inner tube reaches ¾ of the height of the inner tube, switch off the heater and allow the toluene to cool.
28. After cooling, disconnect the chamber from the Soxhlet system.
29. Drain the toluene into the toluene bottle for disposal.
30. Repeat steps 27-29 until all of the toluene has been recovered.
31. Weigh the distillation flask to obtain weight of asphaltene.
32. Leaf the extraction thimble contain coke or coke and crushed core in the ventilation unit over-night to dry and then on the next day Weigh the dried extraction thimble to obtain the weight of the coke in the oxidised oil sample.
33. In the case of coke and crushed core, after drying some of the material is weighted in a crucible, which is then placed in a furnace at 800 °C for 5 to 8 hours. The remaining rock is then weighted and the difference in the weight gives the residual amount of solid (coke) content.

Appendix C

CE-440 ELEMENTAL ANALYSER

The CE-440 Elemental Analysis is capable of determining the Carbon, Hydrogen, Oxygen, Nitrogen and Sulphur content of both liquid and solid samples by use of thermal conductivity detection after combustion and reduction. The CE-440 analyser is fully automated, and is capable of producing high precision analytical data that is accurate to ±0.3 %.

Operating Procedure:

The main operating procedure are as following:

1. Weighting the sample

The weight of the sample must be between 1.5 – 1.8mg in order to obtain an accurate result of the elemental content. The sample should be weighed accurately, for more detail about the procedure used to obtaining an accurate measurement of the weight of the sample, please refer to the Manual.

2. Sealing the sample

In order to prevent any changes in weight between weighting and analysis, it is important to seal each sample using the elemental analyser capsule sealer.

3. Analysing the samples

The samples are analysed using CE-440 Elemental Analyse. Whilst the CE-440 is fully automated once running. The samples must first be manually placed into the instrument injector wheel in the correct order. Conditioners, blanks and standards are also used in the sample run for the following reason:

3.1 Conditioners: Before running any sample, it necessary to run one or more conditioner to coat the walls of the system surface (especially the mixing and sample volume) with water vapour, carbon dioxide and nitrogen in order to simulate actual sample running conditions.

3.2 Blanks: A blank is an empty sealed tin capsule run immediately after a weighted conditioner in order to represent a "true" blank of the instrument.

3.3 Standards: Standards are samples of known composition used to establish the calibration factor for the instrument. The used standard should be close in composition, weight, and molecular structure of the samples to be analysed in order to obtain the most accurate result. The most commonly used standards are as follows:

Standard	Name	% C	% H2	% O2	% N2	% S
1	Acetanilide	71.09	6.71	11.84	10.36	0
2	Benzoic Acid	68.84	4.95	26.20	0	0
3	Chloro-2,4-Dinitrobenzene	35.58	1.49	31.6	13.83	0
4	Cytine	29.99	5.03	26.63	11.66	26.68
5	Stearic	75.99	12.79	11.22	0	0

After placing the samples and standards into the injector wheel, insert the wheel
Into the injector box and follow, the on screen commands. For more detail information, please refer to the CE-440 Elemental Analyser instruction manual.

4. Theory of Operation:

The CE-440 Elemental Analyser is capable of determining the elemental content of both organic and inorganic compounds.

This is done by combustion a weighted sample (typically 1.5 – 1.8mg) in pure oxygen. The combustion occurs in the combustion train under static conditions at approximately 975 °C. The combustion products are then completely flushed from the combustion train into the mixing volume, where the pressure consequently raised to 14.5 pisg.

Whilst the sample gases are mixing, pure helium flows through the sample volume and through the detectors. When the mixing is complete, the sample gas captured in the mixing volume is allowed to expand through the expand volume and reach atmospheric pressure. Consequently, the water, carbon dioxide, and nitrogen concentration are measured by displacing the sample gas through the detectors to the atmosphere. While the sample gas is displaced through the detectors, the output signals are recorded.

At the end of the cycle, the exhaust valves are opened to allow the sample gases to escape to the atmosphere. The computer then prints the results of the analysis, and automatically begins to analyse the next sample in the injector wheel.

The combustion train and analytical system can be seen in Figure.

For more details please refer to the Elemental Analyser Manual.

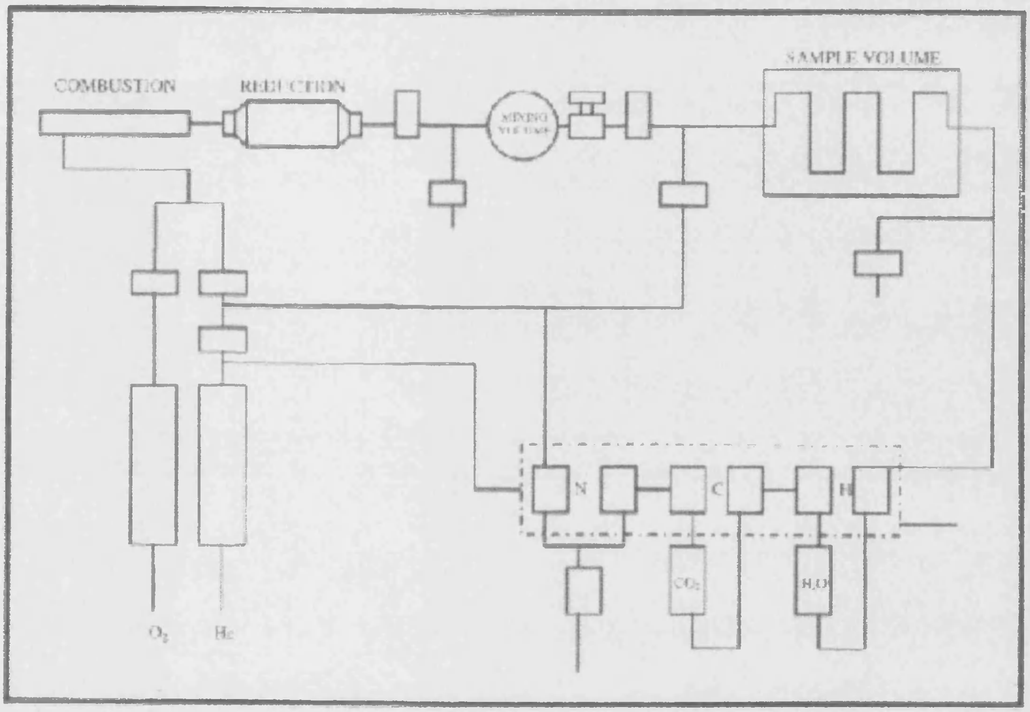

Schematic of the combustion train and analytical system

5. *Result analysis*

The print out of the computer (analsis) will give analyse of Carbon (C), Hydrogen (H), and Nitrogen (N) in the form of percentage based on sample weight.

The analysis of unreacted and oxidised light crude oil samples is given below:

Oxidation Temperature and Type of oil	C	H	N	H/C
Australian oil (alone)				
Unreacted oil	83.86	11.9	1.06	1.70
120	83.68	11.97	0.95	1.72
140	83.39	11.88	0.91	1.71
160	81.4	11.6	0.8	1.71
Oil C (alone)				
Unreacted oil	86.43	12.82	0.82	1.78
120	83.63	12.29	0.91	1.76
140	83.64	12.21	0.72	1.75
160	82.85	12.32	0.7	1.78
Oil D (alone)				
Unreacted oil	85.1	12.34	0.91	1.74
120	84.4	13.35	0.93	1.90
140	80.2	11	0.84	1.65
160	81.68	11.22	0.87	1.65
Esso mix(1) oil (alone)				
Unreacted oil	85.36	11.74	1.01	1.65
120	85.16	12.84	0.93	1.81
140	84.09	12.98	1.08	1.85
160	83.81	11.59	1.04	1.66

Table 6.11: Elemental Analysis of oxidised light crude oils

- ***H/C ration calculation***

To demonstrate the calculation of the hydrogen carbon ratio, one of the samples is taken as an example (Australian oil @ 120 °C)

%C = 83.68

%H = 11.97

Mass of H and C based on 100g

C = 83.68g

H = 11.97g

Mole of H and C based on the above weight:

$$mole\ C = \frac{83.68}{12} = 6.9733$$

$$mole\ H = \frac{11.97}{1} = 11.97$$

$$\therefore \frac{H}{C} = \frac{11.97}{6.9733} = 1.716$$

Appendix D

Table D.1 SBR experimental results for Australian oil

Run No.	1	2	3	4	5
Initial oil saturation (%)	100	100	100	100	10
Initial water saturation (%)	0	0	0	0	0
Initial gas saturation (%)	0	0	0	0	90
Volume of oil (cc)	40	40	70	40	1.7
Weight of oil (gm)	33.13	33.13	57.98	33.13	1.4
Weight of sand matrix (gm)	0	0	0	0	61.6
Initial volume of air (cc)(amt)	46.4	46.4	36.4	46.4	61.7
Initial conc. % of Oxygen	21	21	21	21	21
Initial reaction pressure (bar)	190.43	201.56	178.38	203.91	187.50
Initial p_{O2} (bar)	39.99	42.33	37.46	42.82	39.38
Reaction temperature (^oC)	120	140	150	160	120
Reaction time (hr)	127	79	42	27.5	71
Final reaction pressure (bar)	187.69	191.09	150.5	182.62	178.2
Discharge temperature (^oC)	20.4	15.3	18.2	21.3	22.1
Discharge pressure (bar)	149.42	148.45	108.59	141.45	134.77
O_2 % in final reactant gas	18.5	11.1	3.1	1.4	16.8
CO_2 % in final reactant gas	0.3	1.5	3.4	4.1	1.9
CO % in final reactant gas	0.38	1.07	2.44	2.84	1.11
Final p_{O2} (bar)	34.72	21.21	4.67	2.56	29.94
O_2 consumption (moles) [Equ. 5.3]	0.0075	0.0285	0.0339	0.0519	0.0178
Total percent of O_2 consumed	13.17	49.89	87.55	94.03	23.97
Reacted oxygen (g O_2/gm oil)	0.0072	0.0276	0.0187	0.0501	0.4072
Reaction Rate Constant [Equ. 5.5] (mole O_2 bar^{-1} hr^{-1} cc^{-1})	3.95E-08	2.95E-07	7.33E-07	3.30E-06	4.29E-06
Reaction Rate Constant [Equ. 5.5] (mole O_2 bar^{-1} hr^{-1} cc^{-1} g $sand^{-1}$)					6.96E-08
Total CO_2 produced (moles)	0.0008	0.0043	0.0056	0.0110	0.0064
Total CO produced (moles)	0.0011	0.0031	0.0039	0.0076	0.0037
O_2 converted to carbon oxide (%)	18.46	20.49	22.22	28.53	46.68
O_2 converted to water (%)	12.92	12.94	14.04	17.93	34.79

Table D.2 SBR experimental results for Australian oil

Run No.	6	7	8	9	10
Initial oil saturation (%)	10	10	25	50	50
Initial water saturation (%)	0	0	75	0	0
Initial gas saturation (%)	90	90	0	50	50
Volume of oil (cc)	1.7	1.7	4.25	8.5	8.5
Weight of oil (gm)	1.4	1.4	3.52	7.04	7.04
Weight of sand matrix (gm)	61.6	61.6	61.6	61.6	61.6
Initial volume of air (cc)(amt)	61.7	61.7	46.4	54.9	54.9
Initial conc. % of Oxygen	21	21	21	21	21
Initial reaction pressure (bar)	203.52	216.21	208.02	207.81	202.048
Initial p_{O2} (bar)	42.738	45.40	43.68	43.64	42.43
Reaction temperature (°C)	140	140	140	120	140
Reaction time (hr)	75	133	54	51	61
Final reaction pressure (bar)	193.164	198.83	186.13	195.90	179.88
Discharge temperature (°C)	26.13	18.8	24.3	20.6	25.8
Discharge pressure (bar)	143.163	140.19	136.33	145.12	133.39
O_2 % in final reactant gas	14.2	7.2	1.3	8.6	4.3
CO_2 % in final reactant gas	3.3	6.6	8.3	4.3	6.4
CO % in final reactant gas	2.09	3.12	3.12	1.64	2.25
Final p_{O2} (bar)	27.43	14.32	2.42	16.85	7.73
O_2 consumption (moles) [Equ. 5.3]	0.0275	0.0558	0.0557	0.0450	0.0554
Total percent of O_2 consumed	35.82	68.47	94.46	61.39	81.77
Reacted oxygen (g O_2/gm oil)	0.6285	1.2764	0.5067	0.2045	0.2520
Reaction Rate Constant [Equ. 5.5] (mole O_2 bar^{-1} hr^{-1} cc^{-1})	6.25E-06	9.17E-06	1.70E-05	3.69E-06	5.25E-06
Reaction Rate Constant [Equ. 5.5] (mole O_2 bar^{-1} hr^{-1} cc^{-1} g $sand^{-1}$)	1.01E-07	1.49E-07	2.76E-07	5.99E-08	8.52E-08
Total CO_2 produced (moles)	0.0117	0.0235	0.0212	0.0140	0.0188
Total CO produced (moles)	0.0074	0.0111	0.0079	0.0054	0.0066
O_2 converted to carbon oxide (%)	56.09	52.07	45.25	37.12	39.98
O_2 converted to water (%)	34.79	31.01	26.20	21.53	22.98

Table D.3 Cont. SBR experimental results for Australian oil

Run No.	11	12	13	14	15
Initial oil saturation (%)	50	50	50	50	50
Initial water saturation (%)	0	10	10	25	25
Initial gas saturation (%)	50	40	40	25	25
Volume of oil (cc)	8.5	8.5	8.5	8.5	8.5
Weight of oil (gm)	7.04	7.04	7.04	7.04	7.04
Weight of sand matrix (gm)	61.6	61.6	61.6	61.6	61.6
Initial volume of air (cc)(amt)	54.9	53.2	53.2	50.65	50.65
Initial conc. % of Oxygen	21	21	21	21	21
Initial reaction pressure (bar)	207.23	191.41	199.41	185.16	199.83
Initial p_{O2} (bar)	43.52	40.20	41.88	38.88	41.96
Reaction temperature (°C)	150	120	140	120	140
Reaction time (hr)	53	56	47	54	48
Final reaction pressure (bar)	186.91	174.02	185.83	173.03	187.11
Discharge temperature (°C)	20.6	22.1	22.1	22.4	24.7
Discharge pressure (bar)	145.12	131.05	131.05	131.84	135.16
O_2 % in final reactant gas	2.4	6.2	3.8	4.4	2.9
CO_2 % in final reactant gas	9.3	5.3	6.6	5.9	7.1
CO % in final reactant gas	2.08	2.22	1.19	2.36	2.58
Final p_{O2} (bar)	4.49	10.79	7.06	7.61	5.43
O_2 consumption (moles) [Equ. 5.3]	0.0609	0.0479	0.0539	0.0485	0.0539
Total percent of O_2 consumed	89.69	73.16	83.14	80.42	87.07
Reacted oxygen (g O_2/gm oil)	0.2768	0.2175	0.2451	0.2203	0.2449
Reaction Rate Constant [Equ. 5.5] (mole O_2 bar^{-1} hr^{-1} cc^{-1})	7.87E-06	4.50E-06	6.90E-06	5.51E-06	7.39E-06
Reaction Rate Constant [Equ. 5.5] (mole O_2 bar^{-1} hr^{-1} cc^{-1} g $sand^{-1}$)	1.28E-07	7.30E-08	1.12E-07	8.94E-08	1.20E-07
Total CO_2 produced (moles)	0.0303	0.0151	0.0187	0.0160	0.0196
Total CO produced (moles)	0.0068	0.0063	0.0034	0.0064	0.0071
O_2 converted to carbon oxide (%)	55.38	38.04	37.90	39.71	43.05
O_2 converted to water (%)	30.47	22.31	20.52	23.16	24.83

Table D.4 Cont. SBR experimental results for Australian oil

Run No.	16	17	18	19
Initial oil saturation (%)	50	50	50	50
Initial water saturation (%)	25	50	50	50
Initial gas saturation (%)	25	0	0	0
Volume of oil (cc)	8.5	8.5	4.25	8.5
Weight of oil (gm)	7.04	7.04	3.52	7.04
Weight of sand matrix (gm)	61.6	61.6	30.6	61.6
Initial volume of air (cc)(amt)	50.65	46.4	66.4	46.4
Initial conc. % of Oxygen	21	21	21	21
Initial reaction pressure (bar)	200.59	203.71	204.1	196.48
Initial p_{O2} (bar)	42.12	42.78	42.86	41.26
Reaction temperature (^oC)	150	120	120	140
Reaction time (hr)	52	35	51	41
Final reaction pressure (bar)	183.2	183.04	197.07	173.63
Discharge temperature (^oC)	22.4	137.11	20.3	24.5
Discharge pressure (bar)	131.84	137.49	145.51	129.11
O_2 % in final reactant gas	1.1	3.1	15	1.1
CO_2 % in final reactant gas	9.8	7.5	3.1	7.8
CO % in final reactant gas	2.36	1.05	1.09	2.15
Final p_{O2} (bar)	2.02	5.67	29.56	1.9099
O_2 consumption (moles) [Equ. 5.3]	0.0577	0.0527	0.0270	0.0532
Total percent of O_2 consumed	95.22	86.74	31.03	95.37
Reacted oxygen (g O_2/gm oil)	0.2625	0.2394	0.2456	0.2416
Reaction Rate Constant [Equ. 5.5] (mole O_2 bar^{-1} hr^{-1} cc^{-1})	9.90E-06	9.64E-06	3.48E-06	1.19E-05
Reaction Rate Constant [Equ. 5.5] (mole O_2 bar^{-1} hr^{-1} cc^{-1} g $sand^{-1}$)	1.61E-07	1.56E-07	1.14E-07	1.93E-07
Total CO_2 produced (moles)	0.0266	0.0141	0.0123	0.01888
Total CO produced (moles)	0.0064	0.0019	0.0043	0.00520
O_2 converted to carbon oxide (%)	51.67	28.50	53.43	40.41
O_2 converted to water (%)	28.61	15.18	30.71	22.66

Table D.5 Cont. SBR experimental results for Australian oil

Run No.	20	21	22
Initial oil saturation (%)	50	75	75
Initial water saturation (%)	50	0	0
Initial gas saturation (%)	0	25	25
Volume of oil (cc)	8.5	12.52	12.52
Weight of oil (gm)	7.04	10.37	10.37
Weight of sand matrix (gm)	61.6	61.6	61.6
Initial volume of air (cc)(amt)	46.4	50.5	50.65
Initial conc. % of Oxygen	21	21	21
Initial reaction pressure (bar)	206.64	176.73	200.20
Initial p_{O2} (bar)	43.39	37.11	42.04
Reaction temperature (°C)	150	120	140
Reaction time (hr)	46	52	61
Final reaction pressure (bar)	187.89	170.31	181.03
Discharge temperature (°C)	23.11	20.3	22.4
Discharge pressure (bar)	137.49	129.88	132.42
O_2 % in final reactant gas	0.3	11.9	3.1
CO_2 % in final reactant gas	10.9	2.3	5.9
CO % in final reactant gas	0.98	1.46	2.32
Final p_{O2} (bar)	0.5637	20.2669	5.6119
O_2 consumption (moles) [Equ. 5.3]	0.0565	0.0260	0.0537
Total percent of O_2 consumed	98.70	45.39	86.65
Reacted oxygen (g O_2/gm oil)	0.2568	0.0803	0.1658
Reaction Rate Constant [Equ. 5.5] (mole O_2 bar^{-1} hr^{-1} cc^{-1})	1.47E-05	1.44E-06	3.89E-06
Reaction Rate Constant [Equ. 5.5] (mole O_2 bar^{-1} hr^{-1} cc^{-1} g $sand^{-1}$)	2.38E-07	2.33E-08	6.31E-08
Total CO_2 produced (moles)	0.02038	0.00618	0.01610
Total CO produced (moles)	0.00183	0.00393	0.00633
O_2 converted to carbon oxide (%)	37.71	31.30	35.87
O_2 converted to water (%)	19.67	19.42	20.88

Table D.6 SBR experimental results for oil C

Run No.	23	24	25	26	27
Initial oil saturation (%)	100	100	100	100	10
Initial water saturation (%)	0	0	0	0	0
Initial gas saturation (%)	0	0	0	0	90
Volume of oil (cc)	40	40	70	40	1.7
Weight of oil (gm)	32.96	32.96	57.68	32.96	1.4
Weight of sand matrix (gm)					61.6
Initial volume of air (cc)(amt)	46.4	46.4	36.4	46.4	61.7
Initial conc. % of Oxygen	21	21	21	21	21
Initial reaction pressure (bar)	193.75	182.03	172.85	205.27	166.41
Initial p_{O2} (bar)	40.6875	38.2263	36.2985	43.1067	34.9461
Reaction temperature (^oC)	120	140	150	160	116
Reaction time (hr)	123	80	37	35.5	85
Final reaction pressure (bar)	187.45	173.13	154.88	183.4	161.72
Discharge temperature (^oC)	19.4	24.4	22.1	21.9	17.3
Discharge pressure (bar)	149.17	137.57	114.45	139.9	125.98
O_2 % in final reactant gas	18.7	9.2	2.2	0.6	18.6
CO_2 % in final reactant gas	0.1	1.4	2.3	3.8	0.6
CO % in final reactant gas	0.34	1.13	1.45	2.31	0.43
Final p_{O2} (bar)	35.0532	15.928	3.40736	1.1004	30.0799
O_2 consumption (moles) [Equ. 5.3]	0.008	0.03012	0.03403	0.05412	0.00928
Total percent of O_2 consumed	13.85	58.33	90.61	97.45	13.92
Reacted oxygen (g O_2/gm oil)	0.00777	0.02924	0.01888	0.05255	0.21211
Reaction Rate Constant [Equ. 5.5] (mole O_2 bar^{-1} hr^{-1} cc^{-1})	4.30E-08	3.70E-07	9.45E-07	3.33E-06	1.98E-06
Reaction Rate Constant [Equ. 5.5] (mole O_2 bar^{-1} hr^{-1} cc^{-1} g $sand^{-1}$)					3.21E-08
Total CO_2 produced (moles)	0.00028	0.00361	0.0039	0.01006	0.00193
Total CO produced (moles)	0.00097	0.00292	0.00246	0.00744	0.00138
O_2 converted to carbon oxide (%)	9.61	16.83	15.09	25.45	28.27
O_2 converted to water (%)	7.83	10.84	9.35	16.16	17.86

Table D.7 Cont. SBR experimental results for oil C

Run No.	28	29	30	31	32
Initial oil saturation (%)	10	10	25	25	50
Initial water saturation (%)	0	80	0	75	0
Initial gas saturation (%)	90	10	75	0	50
Volume of oil (cc)	1.7	1.7	4.25	4.25	8.5
Weight of oil (gm)	1.4	1.4	3.5	3.5	7.1
Weight of sand matrix (gm)	61.6	61.6	61.6	61.6	61.6
Initial volume of air (cc)(amt)	61.7	48.1	59.15	46.4	54.9
Initial conc. % of Oxygen	21	21	21	21	21
Initial reaction pressure (bar)	168.36	162.11	202.34	200.39	127.344
Initial p_{O2} (bar)	35.3556	34.0431	42.4914	42.0819	26.7422
Reaction temperature (°C)	116	116	140	120	120
Reaction time (hr)	170	95	78	78	86
Final reaction pressure (bar)	161.72	153.91	189.06	192.38	112.695
Discharge temperature (°C)	20.1	22.8	23.9	23.9	17.5
Discharge pressure (bar)	123.83	120.9	146.09	146.09	81.63
O_2 % in final reactant gas	14.7	13	5.6	14.7	7.2
CO_2 % in final reactant gas	1.6	1.7	6.8	1.8	3.2
CO % in final reactant gas	1.2	0.78	1.78	0.58	1.23
Final p_{O2} (bar)	23.7728	20.0083	10.5873	28.2798	8.11404
O_2 consumption (moles) [Equ. 5.3]	0.02208	0.02087	0.05494	0.01959	0.03129
Total percent of O_2 consumed	32.76	41.23	75.08	32.80	69.66
Reacted oxygen (g O_2/gm oil)	0.50488	0.47692	0.50230	0.17913	0.14102
Reaction Rate Constant [Equ. 5.5] (mole O_2 bar^{-1} hr^{-1} cc^{-1})	2.62E-06	4.89E-06	7.22E-06	1.70E-06	2.74E-06
Reaction Rate Constant [Equ. 5.5] (mole O_2 bar^{-1} hr^{-1} cc^{-1} g $sand^{-1}$)	4.25E-08	7.94E-08	1.17E-07	2.76E-08	4.45E-08
Total CO_2 produced (moles)	0.00501	0.00402	0.02379	0.00494	0.00594
Total CO produced (moles)	0.00376	0.00184	0.00623	0.00159	0.00228
O_2 converted to carbon oxide (%)	31.21	23.67	48.98	29.28	22.61
O_2 converted to water (%)	19.86	14.05	27.32	16.67	13.13

Table D.8 Cont. SBR experimental results for oil C

Run No.	33	34	35	36	37
Initial oil saturation (%)	50	50	50	50	50
Initial water saturation (%)	0	0	0	0	10
Initial gas saturation (%)	50	50	50	50	40
Volume of oil (cc)	8.5	8.5	8.5	8.5	8.5
Weight of oil (gm)	7.1	7.1	7.1	7.1	7.1
Weight of sand matrix (gm)	61.6	61.6	61.6	61.6	61.6
Initial volume of air (cc)(amt)	54.9	54.9	54.9	54.9	53.2
Initial concentration % of Oxygen	21	21	21	21	21
Initial reaction pressure (bar)	198.44	174.61	174.22	171.88	208.79
Initial p_{O2} (bar)	41.67	36.67	36.59	36.09	43.85
Reaction temperature (°C)	120	130	140	150	120
Reaction time (hr)	90	59	60	50	86
Final reaction pressure (bar)	180.57	158.79	150.59	156.05	197.67
Discharge temperature (°C)	19	13.5	18.5	12.2	23.3
Discharge pressure (bar)	132.8	117.77	111.7	110.16	151.83
O_2 % in final reactant gas	10.1	5.4	1.9	1.1	8.8
CO_2 % in final reactant gas	3	5.8	7.5	8.9	4.2
CO % in final reactant gas	1.28	1.89	2.91	3.03	1.86
Final p_{O2} (bar)	18.24	8.58	2.86	1.72	17.39
O_2 consumption (moles) [Equ. 5.3]	0.03936	0.04601	0.05390	0.05365	0.04305
Total percent of O_2 consumed	56.24	76.62	92.18	95.24	60.33
Reacted oxygen (g O_2/gm oil)	0.17739	0.20739	0.24293	0.24179	0.19403
Reaction Rate Constant [Equ. 5.5] (mole O_2 bar^{-1} hr^{-1} cc^{-1})	1.81E-06	4.75E-06	7.99E-06	1.12E-05	2.06E-06
Reaction Rate Constant [Equ. 5.5] (mole O_2 bar^{-1} hr^{-1} cc^{-1} g $sand^{-1}$)	2.95E-08	7.70E-08	1.30E-07	1.82E-07	3.34E-08
Total CO_2 produced (moles)	0.00900	0.01573	0.01896	0.022688	0.013764
Total CO produced (moles)	0.00384	0.00512	0.00735	0.007724	0.006096
O_2 converted to carbon oxide (%)	27.76	39.77	42.02	49.49	39.05
O_2 converted to water (%)	16.32	22.67	24.42	28.34	23.07

Table D.9 Cont. SBR experimental results for oil C

Run No.	38	38	40	41	42
Initial oil saturation (%)	50	50	50	75	75
Initial water saturation (%)	25	50	50	0	0
Initial gas saturation (%)	25	0	0	25	25
Volume of oil (cc)	8.5	8.5	4.25	12.52	12.52
Weight of oil (gm)	7.1	7.1	3.5	10.46	10.46
Weight of sand matrix (gm)	61.6	61.6	30.8	61.6	61.6
Initial volume of air (cc)(amt)	50.65	46.4	66.4	50.65	50.65
Initial concentration % of Oxygen	21	21	21	21	21
Initial reaction pressure (bar)	195.12	194.14	203.13	203.72	201.56
Initial p_{O2} (bar)	40.97	40.77	42.66	42.78	42.33
Reaction temperature (°C)	120	120	120	120	140
Reaction time (hr)	80	87	81	50	37
Final reaction pressure (bar)	182.42	175.98	190.04	194.34	188.48
Discharge temperature (°C)	22.1	25.6	24.7	19.9	19.9
Discharge pressure (bar)	138.28	136.33	126.05	146.87	146.87
O_2 % in final reactant gas	8.4	5.8	8.4	11.1	7.9
CO_2 % in final reactant gas	5.2	5.7	5.4	2.9	5.1
CO % in final reactant gas	1.78	1.87	1.36	1.26	0.89
Final p_{O2} (bar)	15.32	10.21	15.96	21.57	14.89
O_2 consumption (moles) [Equ. 5.3]	0.03975	0.04338	0.05423	0.03286	0.04046
Total percent of O_2 consumed	62.60	74.96	62.58	49.58	64.82
Reacted oxygen (g O_2/gm oil)	0.17915	0.19554	0.49579	0.10054	0.12377
Reaction Rate Constant [Equ. 5.5] (mole O_2 bar^{-1} hr^{-1} cc^{-1})	2.24E-06	2.66E-06	5.80E-06	1.17E-07	2.14E-07
Reaction Rate Constant [Equ. 5.5] (mole O_2 bar^{-1} hr^{-1} cc^{-1} g $sand^{-1}$)	3.64E-08	4.32E-08	1.88E-07	2.75E-08	5.40E-08
Total CO_2 produced (moles)	0.014837	0.014517	0.018251	0.00885	0.015572
Total CO produced (moles)	0.005079	0.004762	0.004597	0.00384	0.002717
O_2 converted to carbon oxide (%)	43.71	38.95	37.90	32.79	41.85
O_2 converted to water (%)	25.05	22.22	21.07	19.32	22.60

Table D.10 SBR experimental results for oil D

Run No.	43	44	45	46	47
Initial oil saturation (%)	100	100	100	100	50
Initial water saturation (%)	0	0	0	0	50
Initial gas saturation (%)	0	0	0	0	0
Volume of oil (cc)	40	40	70	40	20
Weight of oil (gm)	33.8	33.8	58.66	33.8	33.8
Weight of sand matrix (gm)	0	0	0	0	0
Initial volume of air (cc)(amt)	46.4	46.4	36.4	46.4	46.4
Initial conc. % of Oxygen	21	21	21	21	21
Initial reaction pressure (bar)	203.32	173.44	176.17	205.66	177.54
Initial p_{O2} (bar)	42.69	36.42	36.99	43.19	37.28
Reaction temperature (^oC)	120	140	150	160	140
Reaction time (hr)	96	36	21	26	35
Final reaction pressure (bar)	194.46	161.72	150.8	182.23	171.48
Discharge temperature (^oC)	23.2	20.1	23.2	25.3	24.1
Discharge pressure (bar)	127	155.46	116.8	108.01	137.4
O_2 % in final reactant gas	14.2	7.6	2.1	0.6	14.9
CO_2 % in final reactant gas	0.3	2.3	3.3	4.4	1.8
CO % in final reactant gas	1.2	2.27	2.45	2.88	1.11
Final p_{O2} (bar)	27.61	12.29	3.17	1.09	25.55
O_2 consumption (moles) [Equ. 5.3]	0.02141	0.03259	0.03501	0.05424	0.01585
Total percent of O_2 consumed	35.33	66.26	91.44	97.47	31.47
Reacted oxygen (g O_2/gm oil)	0.02027	0.03086	0.01909	0.05135	0.01501
Reaction Rate Constant [Equ. 5.5] (mole O_2 bar^{-1} hr^{-1} cc^{-1})	1.61E-07	1.02E-06	1.73E-06	4.55E-06	7.29E-07
Reaction Rate Constant [Equ. 5.5] (mole O_2 bar^{-1} hr^{-1} cc^{-1} g $sand^{-1}$)					
Total CO_2 produced (moles)	0.00051	0.00673	0.00575	0.00895	0.00462
Total CO produced (moles)	0.00201	0.00665	0.00427	0.00586	0.00285
O_2 converted to carbon oxide (%)	7.05	30.85	22.54	21.90	38.18
O_2 converted to water (%)	5.88	20.52	14.32	13.65	23.59

Table D.11 Cont. SBR experimental results for oil D

Run No.	48	49	50	51	52
Initial oil saturation (%)	10	10	10	10	10
Initial water saturation (%)	0	0	0	0	0
Initial gas saturation (%)	90	90	90	90	90
Volume of oil (cc)	1.7	1.7	1.7	1.7	1.7
Weight of oil (gm)	1.436	1.436	1.436	1.436	1.436
Weight of sand matrix (gm)	61.6	61.6	61.6	61.6	61.6
Initial volume of air (cc)(amt)	61.7	61.7	61.7	61.7	61.7
Initial conc. % of Oxygen	21	21	21	21	21
Initial reaction pressure (bar)	128.52	184.57	194.34	182.6	195.7
Initial p_{O2} (bar)	26.99	38.76	40.81	38.35	41.10
Reaction temperature (°C)	120	120	120	130	140
Reaction time (hr)	58	60	125	140	152
Final reaction pressure (bar)	125.19	178.12	190.04	163.28	167.77
Discharge temperature (°C)	21.1	20	21.6	20	20
Discharge pressure (bar)	97.46	135	131.73	121	122
O_2 % in final reactant gas	15.8	17.2	12.3	8.6	5.6
CO_2 % in final reactant gas	1.9	1.6	2.3	6.3	8.4
CO % in final reactant gas	1.73	1.04	1.45	2.2	2.9
Final p_{O2} (bar)	19.78	30.64	23.37	14.04	9.39
O_2 consumption (moles) [Equ. 5.3]	0.01361	0.01533	0.03291	0.04474	0.05695
Total percent of O_2 consumed	26.71	20.96	42.72	63.38	77.14
Reacted oxygen (g O_2/gm oil)	0.30325	0.34169	0.73345	0.99697	1.26896
Reaction Rate Constant [Equ. 5.5] (mole O_2 bar^{-1} hr^{-1} cc^{-1})	5.95E-06	4.35E-06	4.95E-06	7.77E-06	1.03E-05
Reaction Rate Constant [Equ. 5.5] (mole O_2 bar^{-1} hr^{-1} cc^{-1} g $sand^{-1}$)	9.66E-08	7.07E-08	8.04E-08	1.26E-07	1.67E-07
Total CO_2 produced (moles)	0.00467	0.00547	0.00763	0.01929	0.02594
Total CO produced (moles)	0.00425	0.00355	0.00481	0.00674	0.00896
O_2 converted to carbon oxide (%)	49.94	47.25	30.48	50.67	53.42
O_2 converted to water (%)	32.78	29.42	18.89	29.10	30.64

Table D.12 Cont. SBR experimental results for oil D

Run No.	53	54	55	56	57
Initial oil saturation (%)	10	15	15	15	15
Initial water saturation (%)	0	80	0	0	0
Initial gas saturation (%)	90	5	85	85	85
Volume of oil (cc)	1.7	2.55	2.55(V)	2.55(O)	2.55(O)
Weight of oil (gm)	1.436	2.155	2.155	2.155	2.155
Weight of sand matrix (gm)	61.6	61.6	61.6	61.6	61.6
Initial volume of air (cc)(amt)	61.7	47.24	60.85	60.85	60.85
Initial conc. % of Oxygen	21	21	21	10	5
Initial reaction pressure (bar)	172.852	176.17	182.45	192.77	184.96
Initial p_{O2} (bar)	36.30	36.99	38.3145	19.277	9.248
Reaction temperature (^{o}C)	150	120	120	120	120
Reaction time (hr)	90	68	123	130	100
Final reaction pressure (bar)	156.62	163.48	172.07	183.98	179.1
Discharge temperature (^{o}C)	22	20.78	17	20	15
Discharge pressure (bar)	110	124.68	130	136	135
O_2 % in final reactant gas	5.2	10.3	13.1	4.5	1.7
CO_2 % in final reactant gas	9.3	3.5	2.5	3.1	2.1
CO % in final reactant gas	2.96	0.86	1.3	0.81	0.36
Final p_{O2} (bar)	8.14	16.84	22.54117	8.2791	3.0447
O_2 consumption (moles) [Equ. 5.3]	0.04938	0.02913	0.029364	0.020474	0.011548
Total percent of O_2 consumed	77.56	54.49	41.17	57.05	67.08
Reacted oxygen (g O_2/gm oil)	1.10035	0.43259	0.436032	0.304022	0.171482
Reaction Rate Constant [Equ. 5.5] (mole O_2 bar^{-1} hr^{-1} cc^{-1})	1.71E-05	6.56E-06	3.15E-06	4.75E-06	8.11E-06
Reaction Rate Constant [Equ. 5.5] (mole O_2 bar^{-1} hr^{-1} cc^{-1} g $sand^{-1}$)	2.78E-07	1.07E-07	5.11E-08	7.71E-08	1.32E-07
Total CO_2 produced (moles)	0.02572	0.00844	0.008198	0.010526	0.007201
Total CO produced (moles)	0.00819	0.00207	0.004263	0.00275	0.001234
O_2 converted to carbon oxide (%)	60.38	32.51	35.18	58.13	67.70
O_2 converted to water (%)	34.34	18.04	21.22	32.42	36.52

V: virgin oil (unreacted)

O: previously oxidized oil

Table D.13 Cont. SBR experimental results for oil D

Run No.	58	59	60	61	62
Initial oil saturation (%)	15	15	15	15	15
Initial water saturation (%)	0	0	0	0	0
Initial gas saturation (%)	85	85	85	85	85
Volume of oil (cc)	2.55(V)	2.55(O)	2.55(O)	2.55(V)	2.55(O)
Weight of oil (gm)	2.155	2.155	2.155	2.155	2.155
Weight of sand matrix (gm)	61.6	61.6	61.6	61.6	61.6
Initial volume of air (cc)(amt)	60.85	60.85	60.85	60.85	60.85
Initial conc. % of Oxygen	5	10	21	21	10
Initial reaction pressure (bar)	191.8	188.67	190.23	203.52	204.49
Initial p_{O2} (bar)	9.59	18.867	39.9483	42.74	20.45
Reaction temperature (°C)	120	120	120	140	140
Reaction time (hr)	60	73	135	70	76
Final reaction pressure (bar)	190.02	184.77	183.01	188.87	198.24
Discharge temperature (°C)	21	20	20	15	16
Discharge pressure (bar)	146.5	142	131	136.10	143.30
O_2 % in final reactant gas	3.5	7.1	15.1	7.6	1.7
CO_2 % in final reactant gas	0.2	0.3	0.5	4.3	4.8
CO % in final reactant gas	0.36	0.34	0.31	2.17	1.08
Final p_{O2} (bar)	6.6507	13.11867	27.63451	14.35	3.37
O_2 consumption (moles) [Equ. 5.3]	0.005472	0.010701	0.022924	0.050284	0.030255
Total percent of O_2 consumed	30.65	30.47	30.82	66.41	83.52
Reacted oxygen (g O_2/gm oil)	0.081253	0.158905	0.340398	0.74668	0.44927
Reaction Rate Constant [Equ. 5.5] (mole O_2 bar^{-1} hr^{-1} cc^{-1})	4.45E-06	3.63E-06	1.99E-06	1.08E-05	1.65E-05
Reaction Rate Constant [Equ. 5.5] (mole O_2 bar^{-1} hr^{-1} cc^{-1} g $sand^{-1}$)	7.23E-08	5.90E-08	3.24E-08	1.76E-07	2.68E-07
Total CO_2 produced (moles)	0.000729	0.001064	0.001635	0.01485	0.01741
Total CO produced (moles)	0.001312	0.001205	0.001014	0.00749	0.00392
O_2 converted to carbon oxide (%)	25.31	15.57	9.35	36.99	64.02
O_2 converted to water (%)	18.65	10.60	5.78	22.22	35.25

V: virgin oil (unreacted)

O: previously oxidized oil

Table D.14 Cont. SBR experimental results for oil D

Run No.	63	64	65	66	67
Initial oil saturation (%)	15	15	15	15	15
Initial water saturation (%)	0	0	0	0	0
Initial gas saturation (%)	85	85	85	85	85
Volume of oil (cc)	2.55(O)	2.55(V)	2.55(O)	2.55(O)	2.55(V)
Weight of oil (gm)	2.155	2.155	2.155	2.155	2.155
Weight of sand matrix (gm)	61.6	61.6	61.6	61.6	61.6
Initial volume of air (cc)(amt)	60.85	60.85	60.85	60.85	60.85
Initial conc. % of Oxygen	5	5	10	21	21
Initial reaction pressure (bar)	205.66	202.93	204.10	201.56	205.08
Initial p_{O2} (bar)	10.28	10.15	20.41	42.33	43.07
Reaction temperature (°C)	140	140	140	140	150
Reaction time (hr)	75	74	85	84	81
Final reaction pressure (bar)	202.15	199.41	198.22	191.8	186.36
Discharge temperature (°C)	16.8	17.5	17.8	17.1	24.6
Discharge pressure (bar)	146.32	146.87	144.70	138.48	130.66
O_2 % in final reactant gas	0.15	1.1	2.9	9.4	1.8
CO_2 % in final reactant gas	3.6	2.2	3.1	3.1	7.3
CO % in final reactant gas	0.7	0.65	1	2	1.99
Final p_{O2} (bar)	0.34	2.19	5.75	18.03	3.35
O_2 consumption (moles) [Equ. 5.3]	0.017679	0.014089	0.025973	0.043045	0.06869
Total percent of O_2 consumed	97.05	78.38	71.84	57.41	92.21
Reacted oxygen (g O_2/gm oil)	0.26252	0.20921	0.38568	0.63918	1.01996
Reaction Rate Constant [Equ. 5.5] (mole O_2 bar^{-1} hr^{-1} cc^{-1})	3.26E-05	1.44E-05	1.04E-05	7.06E-06	2.14E-05
Reaction Rate Constant [Equ. 5.5] (mole O_2 bar^{-1} hr^{-1} cc^{-1} g $sand^{-1}$)	5.30E-07	2.33E-07	1.68E-07	1.15E-07	3.47E-07
Total CO_2 produced (moles)	0.01329	0.00814	0.01128	0.01083	0.02345
Total CO produced (moles)	0.00258	0.00240	0.00364	0.00698	0.00639
O_2 converted to carbon oxide (%)	82.52	66.28	50.45	33.26	38.79
O_2 converted to water (%)	44.92	37.41	28.73	20.69	21.72

V: virgin oil (unreacted)

O: previously oxidized oil

Table D.15 Cont. SBR experimental results for oil D

Run No.	68	69	70	71	72
Initial oil saturation (%)	15	15	25	25	25
Initial water saturation (%)	0	0	0	0	0
Initial gas saturation (%)	85	85	75	75	75
Volume of oil (cc)	2.55(V)	2.55(O)	4.25	4.25	4.25
Weight of oil (gm)	2.155	2.155	3.59	3.59	3.59
Weight of sand matrix (gm)	61.6	61.6	45	45	45
Initial volume of air (cc)(amt)	60.85	60.85	59.15	59.15	59.15
Initial conc. % of Oxygen	5	21	21	21	21
Initial reaction pressure (bar)	204.88	208.01	233.2	217.77	239.65
Initial p_{O2} (bar)	10.24	43.68	48.97	45.73	50.33
Reaction temperature (^oC)	150	150	110	120	130
Reaction time (hr)	85	98	143	139	140
Final reaction pressure (bar)	199.11	191.41	223.83	200.59	212.31
Discharge temperature (^oC)	17.5	21	27.8	33.3	29.8
Discharge pressure (bar)	146.87	132.23	171.8	153.9	194
O_2 % in final reactant gas	0.1	2.5	11.3	7.7	2.8
CO_2 % in final reactant gas	2.8	9.7	3.3	6.5	9.9
CO % in final reactant gas	0.54	1.86	0.55	0.95	1.53
Final p_{O2} (bar)	0.199	4.79	25.29	15.45	5.94
O_2 consumption (moles) [Equ. 5.3]	0.0174	0.06728	0.04397	0.05481	0.07832
Total percent of O_2 consumed	98.06	89.05	48.35	66.23	88.19
Reacted oxygen (g O_2/gm oil)	0.25799	0.99902	0.39192	0.48854	0.69813
Reaction Rate Constant [Equ. 5.5] (mole O_2 bar^{-1} hr^{-1} cc^{-1})	3.14E-05	1.53E-05	2.02E-06	3.33E-06	6.34E-06
Reaction Rate Constant [Equ. 5.5] (mole O_2 bar^{-1} hr^{-1} cc^{-1} g $sand^{-1}$)	5.10E-07	2.48E-07	4.49E-08	7.39E-08	1.41E-07
Total CO_2 produced (moles)	0.01035	0.03191	0.01340	0.02322	0.04510
Total CO produced (moles)	0.00199	0.00612	0.00223	0.00339	0.00697
O_2 converted to carbon oxide (%)	65.35	51.98	33.02	45.47	62.04
O_2 converted to water (%)	35.55	28.27	17.78	24.28	33.24

V: virgin oil (unreacted)

O: previously oxidized oil

Table D.16 Cont. SBR experimental results for oil D

Run No.	73	74	75	76	77
Initial oil saturation (%)	25	50	50	50	50
Initial water saturation (%)	0	0	0	0	0
Initial gas saturation (%)	75	50	50	50	50
Volume of oil (cc)	4.25	8.5	8.5	8.5	8.5
Weight of oil (gm)	3.59	7.18	7.18	7.18	7.18
Weight of sand matrix (gm)	45	45	45	45	45
Initial volume of air (cc)(amt)	59.15	54.9	54.9	54.9	54.9
Initial conc. % of Oxygen	21	21	21	21	21
Initial reaction pressure (bar)	224.81	186.33	205.27	196.68	225.19
Initial p_{O2} (bar)	47.21	39.13	43.11	41.31	47.29
Reaction temperature (^oC)	140	110	120	130	140
Reaction time (hr)	127	163	161	98	94
Final reaction pressure (bar)	198.63	171.68	182.42	174.81	199.81
Discharge temperature (^oC)	35.9	23.7	17.13	39.9	27.1
Discharge pressure (bar)	144.5	131.25	133.7	133.9	115.3
O_2 % in final reactant gas	0.58	9.1	5.1	1.8	0.1
CO_2 % in final reactant gas	10.6	3.8	5.5	8	11.9
CO % in final reactant gas	1.66	0.75	0.9	1.18	1.5
Final p_{O2} (bar)	1.15	15.62	9.30	3.15	0.199
O_2 consumption (moles) [Equ. 5.3]	0.07931	0.04051	0.05677	0.06249	0.07526
Total percent of O_2 consumed	97.56	60.07	78.42	92.38	99.58
Reacted oxygen (g O_2/gm oil)	0.70695	0.18055	0.25304	0.27854	0.33544
Reaction Rate Constant [Equ. 5.5] (mole O_2 bar^{-1} hr^{-1} cc^{-1})	1.18E-05	1.14E-06	1.88E-06	5.06E-06	1.09E-05
Reaction Rate Constant [Equ. 5.5] (mole O_2 bar^{-1} hr^{-1} cc^{-1} g $sand^{-1}$)	2.63E-07	2.54E-08	4.18E-08	1.12E-07	2.43E-07
Total CO_2 produced (moles)	0.03526	0.01109	0.01673	0.02259	0.03018
Total CO produced (moles)	0.00552	0.00219	0.00274	0.00333	0.00380
O_2 converted to carbon oxide (%)	47.94	30.09	31.87	38.82	42.62
O_2 converted to water (%)	25.71	16.40	17.14	20.74	22.57

Table D.17 SBR experimental results for Esso Mix1 oil

Run No.	78	79	80	81	82
Initial oil saturation (%)	75	100	100	100	100
Initial water saturation (%)	0	0	0	0	0
Initial gas saturation (%)	25	0	0	0	0
Volume of oil (cc)	12.75	40	40	50	40
Weight of oil (gm)	10.77	34.56	34.56	43.2	34.56
Weight of sand matrix (gm)	61.6	0	0	0	0
Initial volume of air (cc)(amt)	50.65	46.4	46.4	46.4	46.4
Initial conc. % of Oxygen	21	21	21	21	21
Initial reaction pressure (bar)	185.16	176.17	199.8	180.66	192.97
Initial p_{O2} (bar)	38.88	36.99	41.96	37.94	40.52
Reaction temperature (°C)	140	120	140	150	160
Reaction time (hr)	86	75	38	22	20
Final reaction pressure (bar)	165.43	158.98	181.25	154.3	145.16
Discharge temperature (°C)	24.4	23.4	23	21.5	22.5
Discharge pressure (bar)	121.29	125.47	140.76	111.72	105.2
O_2 % in final reactant gas	0.3	6.5	3.1	2.7	1.3
CO_2 % in final reactant gas	6.7	2.2	3.9	4.7	5.1
CO % in final reactant gas	2.85	1.77	2.14	2.16	2.23
Final p_{O2} (bar)	0.496	10.33	5.62	4.17	1.89
O_2 consumption (moles) [Equ. 5.3]	0.05660	0.03784	0.04908	0.04454	0.04978
Total percent of O_2 consumed	98.72	72.07	86.61	89.02	95.34
Reacted oxygen (g O_2/gm oil)	0.16811	0.03504	0.04545	0.03299	0.04609
Reaction Rate Constant [Equ. 5.5] (mole O_2 bar^{-1} hr^{-1} cc^{-1})	5.86E-06	6.03E-07	1.79E-06	2.65E-06	4.94E-06
Reaction Rate Constant [Equ. 5.5] (mole O_2 bar^{-1} hr^{-1} cc^{-1} g $sand^{-1}$)	9.52E-08				
Total CO_2 produced (moles)	0.01664	0.00519	0.01034	0.00994	0.01013
Total CO produced (moles)	0.00708	0.00417	0.00567	0.00457	0.00502
O_2 converted to carbon oxide (%)	35.65	19.25	26.86	27.46	25.39
O_2 converted to water (%)	20.95	12.38	16.32	16.29	15.22

Table D.18 Cont. SBR experimental results for Esso Mix1 oil

Run No.	83	84	85	86	87
Initial oil saturation (%)	50	50	50	50	50
Initial water saturation (%)	50	0	0	0	0
Initial gas saturation (%)	0	50	50	50	50
Volume of oil (cc)	20	8.5	8.5	8.5	8.5
Weight of oil (gm)	34.56	7.344	7.344	7.344	7.344
Weight of sand matrix (gm)	0	61.6	61.6	61.6	61.6
Initial volume of air (cc)(amt)	46.4	54.9	54.9	54.9	54.9
Initial conc. % of Oxygen	21	21	21	21	21
Initial reaction pressure (bar)	198.24	179.88	195.90	194.34	133.2
Initial p_{O2} (bar)	41.63	37.77	41.14	40.81	27.97
Reaction temperature (^oC)	140	120	120	130	140
Reaction time (hr)	42	74	72	78	61
Final reaction pressure (bar)	185.35	168.75	182.42	178.91	119.73
Discharge temperature (^oC)	18.5	22.2	17.7	20.5	22.9
Discharge pressure (bar)	140.43	130.86	143.36	133.79	89.23
O_2 % in final reactant gas	9.9	11.4	11.9	7.7	2.3
CO_2 % in final reactant gas	2.5	3.6	3.8	4.4	5.1
CO % in final reactant gas	1.48	1.1	1.92	2.26	2.18
Final p_{O2} (bar)	18.35	19.24	21.71	13.78	2.75
O_2 consumption (moles) [Equ. 5.3]	0.03144	0.03113	0.03263	0.04428	0.04031
Total percent of O_2 consumed	55.92	49.07	47.23	66.24	90.16
Reacted oxygen (g O_2/gm oil)	0.02911	0.13566	0.14220	0.19295	0.17563
Reaction Rate Constant [Equ. 5.5] (mole O_2 bar^{-1} hr^{-1} cc^{-1})	1.32E-06	1.80E-06	1.75E-06	2.68E-06	7.15E-06
Reaction Rate Constant [Equ. 5.5] (mole O_2 bar^{-1} hr^{-1} cc^{-1} g $sand^{-1}$)		2.93E-08	2.85E-08	4.36E-08	1.16E-07
Total CO_2 produced (moles)	0.00671	0.01053	0.01236	0.01324	0.01015
Total CO produced (moles)	0.00397	0.00321	0.00624	0.00679	0.00434
O_2 converted to carbon oxide (%)	27.69	39.00	47.47	37.57	30.57
O_2 converted to water (%)	17.00	22.08	28.52	22.62	17.97

Table D.19 Cont. SBR experimental results for Esso mix(1) oil

Run No.	88	89	90	91
Initial oil saturation (%)	50	50	50	50
Initial water saturation (%)	0	0	0	50
Initial gas saturation (%)	50	50	50	0
Volume of oil (cc)	8.5	8.5	8.5	8.5
Weight of oil (gm)	7.344	7.344	7.344	7.344
Weight of sand matrix (gm)	61.6	61.6	61.6	61.6
Initial volume of air (cc)(amt)	54.9	54.9	54.9	46.4
Initial conc. % of Oxygen	21	21	21	21
Initial reaction pressure (bar)	197.09	210.35	196.88	176.95
Initial p_{O2} (bar)	41.39	44.17	41.34	37.16
Reaction temperature (°C)	140	150	160	120
Reaction time (hr)	50	67	33	54
Final reaction pressure (bar)	184.77	188.09	181.64	168.75
Discharge temperature (°C)	21.6	21.6	26.2	17.7
Discharge pressure (bar)	133.35	134.77	129.49	130.86
O_2 % in final reactant gas	6.5	1.6	2.6	12.1
CO_2 % in final reactant gas	5.3	9.8	7.3	3.7
CO % in final reactant gas	3.23	3.29	2.37	1.43
Final p_{O2} (bar)	12.01	3.009	4.723	20.418
O_2 consumption (moles) [Equ. 5.3]	0.04695	0.06424	0.05583	0.02376
Total percent of O_2 consumed	70.98	93.19	88.58	45.05
Reacted oxygen (g O_2/gm oil)	0.20460	0.2799	0.24327	0.10355
Reaction Rate Constant [Equ. 5.5] (mole O_2 bar^{-1} hr^{-1} cc^{-1})	4.65E-06	7.36E-06	1.18E-05	1.85E-06
Reaction Rate Constant [Equ. 5.5] (mole O_2 bar^{-1} hr^{-1} cc^{-1} g $sand^{-1}$)	7.55E-08	1.19E-07	1.91E-07	3.01E-08
Total CO_2 produced (moles)	0.01583	0.02959	0.02085	0.00929
Total CO produced (moles)	0.00965	0.00993	0.00677	0.00359
O_2 converted to carbon oxide (%)	44.00	53.79	43.41	46.65
O_2 converted to water (%)	27.14	30.76	24.74	27.10

Table D.20 SBR experimental results for Single Organic Compound

Run No.	92	93	94	95	96
Name of organic compound	*Pentane*	*Pentane*	*Hexane*	*Hexane*	*Toluene*
Structure of organic compound	*C5H12*	*C5H12*	*C6H14*	*C6H14*	*C7H8*
Volume of organic compound (cc)	30	30	30	30	30
Initial fluid density (gm/cc)	0.65	0.658	0.664	0.664	0.867
Weight of organic compound (gm)	19.5	19.74	19.92	19.92	26.01
Initial volume of air (cc)(amt)	56.4	56.4	56.4	56.4	56.4
Initial conc. % of Oxygen	21	21	21	21	21
Initial reaction pressure (bar)	182.20	183.20	170.31	185.94	158.10
Initial p_{O2} (bar)	38.26	38.47	35.76	39.05	33.20
Reaction temperature (^oC)	115	140	110	140	140
Reaction time (hr)	40	25	35	15	20
Final reaction pressure (bar)	174.02	164.32	165.43	148.63	151.95
Discharge temperature (^oC)	11.7	19.4	13.9	20.6	29
Discharge pressure (bar)	131.25	115.5	126.56	110.10	115.01
O_2 % in final reactant gas	19.1	4.2	19.5	1.2	19
CO_2 % in final reactant gas	0.1	1.7	0.1	2.4	0.1
CO % in final reactant gas	0.14	0.66	0.1	1	0.1
Final p_{O2} (bar)	33.24	6.90	32.26	1.784	28.87
O_2 consumption (moles) [Equ. 5.3]	0.00878	0.05184	0.00621	0.06118	0.00711
Total percent of O_2 consumed	13.13	82.06	9.80	95.43	13.04
Reacted oxygen (g O_2/g SOC)	0.01441	0.08403	0.00997	0.09829	0.00875
Reaction Rate Constant [Equ. 5.5] (mole O_2 bar^{-1} hr^{-1} cc^{-1})	2.05E-07	3.76E-06	1.74E-07	1.13E-05	3.82E-07
Total CO_2 produced (moles)	0.00031	0.00455	0.00029	0.00610	0.00026
Total CO produced (moles)	0.00044	0.00177	0.00029	0.00254	0.00026
O_2 converted to carbon oxide (%)	6.05	10.49	7.23	12.04	5.45
O_2 converted to water (%)	4.27	6.10	4.82	7.06	3.63

Table D.21 Cont. SBR experimental results for Single Organic Compound

Run No.	97	98	99	100	101
Name of organic compound	Xylene	Is-butyl benzene	Is-butyl benzene	n-hexyl benzene	Dodecane
Structure of organic compound	C8H10	C10H14	C10H14	C12H18	C12H26
Volume of organic compound (cc)	30	30	30	30	30
Initial fluid density (gm/cc)	0.861	0.85	0.85	0.86	0.752
Weight of organic compound (gm)	25.83	25.5	25.5	25.8	22.56
Initial volume of air (cc)(amt)	56.4	56.4	56.4	56.4	56.4
Initial conc. % of Oxygen	21	21	21	21	21
Initial reaction pressure (bar)	183.79	165.43	167.77	175.51	173.44
Initial p_{O2} (bar)	38.59	34.74	35.23	36.86	36.42
Reaction temperature (^oC)	140	110	140	140	120
Reaction time (hr)	35	30	12	25	35
Final reaction pressure (bar)	175.20	154.49	140.20	147.27	138.67
Discharge temperature (^oC)	23.6	17.3	16.3	16.2	22
Discharge pressure (bar)	130.01	122.50	106.02	107.42	110.11
O_2 % in final reactant gas	15.6	15.1	0.9	3	1.6
CO_2 % in final reactant gas	1.6	0.2	2.9	3.2	2.6
CO % in final reactant gas	0.2	0.18	1.13	1.03	0.5
Final p_{O2} (bar)	27.331	23.328	1.262	4.418	2.219
O_2 consumption (moles) [Equ. 5.3]	0.0185	0.02021	0.05578	0.05326	0.05902
Total percent of O_2 consumed	29.19	32.85	96.42	88.01	93.91
Reacted oxygen (g O_2/g SOC)	0.02291	0.02536	0.06999	0.06606	0.08371
Reaction Rate Constant [Equ. 5.5] (mole O_2 bar^{-1} hr^{-1} cc^{-1})	5.40E-07	7.83E-07	1.52E-05	4.64E-06	4.60E-06
Total CO_2 produced (moles)	0.00475	0.00057	0.0072	0.00806	0.00657
Total CO produced (moles)	0.00059	0.00051	0.00281	0.00259	0.00126
O_2 converted to carbon oxide (%)	27.31	4.11	15.43	17.57	12.21
O_2 converted to water (%)	14.46	2.69	8.97	10.00	6.64

Table D.22 Cont. SBR experimental results for Single Organic Compound

Run No.	102	103	104	105
Name of organic compound (SOC)	Dodecane	n-Hexane	Xylene	Dodecane
Structure of organic compound	C12H26	C6H14	C7H8	C12H26
Organic compound saturation (%)	100	50	50	50
Initial water saturation (%)	0	0	0	0
Initial gas saturation (%)	0	50	50	50
Volume of organic compound (cc)	30	8.5	8.5	8.5
Weight of organic compound (gm)	22.56	5.644	7.3185	6.392
Weight of sand matrix (gm)	0	61.6	61.6	61.6
Initial volume of air (cc)(amt)	56.4	54.9	54.9	54.9
Initial conc. % of Oxygen	21	21	21	21
Initial reaction pressure (bar)	159.57	191.61	190.43	187.66
Initial p_{O2} (bar)	33.51	40.24	39.99	39.41
Reaction temperature (^oC)	140	140	140	140
Reaction time (hr)	13	54	50	61
Final reaction pressure (bar)	130.47	178.91	181.25	177.34
Discharge temperature (^oC)	22	24.8	23.8	19.9
Discharge pressure (bar)	97.12	133.59	131.84	128.71
Final O_2 % in final reactant gas	1.1	7.3	15.3	2.4
Final CO_2 % in final reactant gas	2.8	4.8	2.4	6.8
Final CO % in final reactant gas	0.78	1.48	1.24	2.74
Final p_{O2} (bar)	1.435	13.060	27.731	4.256
O_2 consumption (moles) [Equ. 5.3]	0.05267	0.04344	0.01959	0.05618
Total percent of O_2 consumed	95.72	67.54	30.66	89.20
Reacted oxygen (g O_2/g SOC)	0.07470	0.24628	0.08567	0.28127
Reaction Rate Constant [Equ. 5.5] (mole O_2 bar^{-1} hr^{-1} cc^{-1})	1.33E-05	3.92E-06	1.38E-06	6.86E-06
Reaction Rate Constant [Equ. 5.5] (mole O_2 bar^{-1} hr^{-1} cc^{-1} g $sand^{-1}$)		6.36E-08	2.23E-08	1.11E-07
Total CO_2 produced (moles)	0.00624	0.01421	0.00704	0.01972
Total CO produced (moles)	0.00174	0.00438	0.00364	0.00795
O_2 converted to carbon oxide (%)	13.50	37.76	45.19	42.17
O_2 converted to water (%)	7.58	21.40	27.23	24.62

Table D.23 SBR experimental results for light crude oils @ high temperature

Run No.	106	107	108	109	110
Type of light crude oil	Aust. Oil	Oil C	Oil D	Oil D	Esso Mix1
Initial oil saturation (%)	100	100	100	10	100
Initial water saturation (%)	0	0	0	0	0
Initial gas saturation (%)	0	0	0	90	0
Volume of oil (cc)	40	40	40	1.7	34.56
Weight of oil (gm)	33.12	33.12	33.5	1.42	1.4
Weight of sand matrix (gm)	0	0	0	61.6	0
Initial Volume of air (cc)(amt)	46.4	46.4	46.4	61.7	46.4
Initial concentration % of oxygen	21	21	21	21	21
Initial charged pressure (bar)	157.42	156.64	155.27	132.23	147.07
Initial charged temperature (°C)	21.7	31.5	24.2	21.4	24.9
Initial p_{O2} (bar)	33.06	32.89	32.61	27.77	30.88
Initial O_2 composition (mole)	0.06257	0.06026	0.06119	0.06996	0.05783
Reaction temperature (°C)	180	180	180	180	180
Reaction Time (hr)	20	16	14	42	32
O_2 % in final reactant gas	0.6	0.6	0.5	1.3	0.6
CO_2 % in final reactant gas	5.3	5.3	5.1	10.3	1.41
CO % in final reactant gas	1.77	1.77	1.73	2.87	5.8
Final discharge pressure (bar)	126.76	126.76	125.39	117.38	119.14
Final discharge temperature (°C)	23.3	23.3	26.2	23.4	25.4
Final p_{O2} (bar)	0.76056	0.76056	0.62695	1.52594	0.71484
Final O2 composition (mole)	0.00145	0.00145	0.00076	0.00189	0.00087
Final CO2 composition (mole)	0.01281	0.01281	0.00778	0.03064	0.00205
Final CO composition (mole)	0.00428	0.00428	0.00264	0.00854	0.00843
O_2 consumption (moles) [Equ. 5.3]	0.06112	0.05881	0.06044	0.06807	0.05696
Total percent of O_2 consumed	97.68	97.59	98.75	97.29	98.49
Reacted oxygen (g O_2/gm oil)	0.05906	0.05682	0.05773	1.53393	1.30193
Reaction Rate Constant [Equ. 5.5] (mole O_2 bar^{-1} hr^{-1} cc^{-1} g $sand^{-1}$)	5.56E-06	6.94E-06	8.32E-06	1.03E-06	4.02E-06
O_2 converted to carbon oxide (%)	24.45	25.42	15.06	51.28	11.00
O_2 converted to water (%)	13.98	14.53	8.62	28.78	9.20

Table D.24 Cont. SBR experimental results for light crude oils @ high temperature

Run No.	111	112	113	114	115	116
Type of light crude oil	Aust. oil	Aust. oil	Aust. oil	Aust. oil	Aust. oil	Oil C
Initial oil saturation (%)	10	50	50	50	50	10
Initial water saturation (%)	0	0	0	50	50	0
Initial gas saturation (%)	90	50	50	0	0	90
Volume of oil (cc)	1.7	8.5	4.25	8.5	4.25	1.7
Weight of oil (gm)	1.4	7.04	3.52	7.04	3.52	1.4
Weight of sand matrix (gm)	61.6	61.6	30.8	61.6	30.8	61.6
Initial volume of air (cc)	61.7	54.9	74.9	46.4	66.4	61.7
Initial conc. % of oxygen	21	21	21	21	21	21
Initial charged press. (bar)	142.38	137.89	143.95	138.67	139.26	144.14
Initial charged temp. (℃)	18.5	22.6	20.4	22.6	21.9	20.1
Initial p_{O2} (bar)	29.89	28.96	30.23	29.12	29.25	30.27
Initial O_2 composition (mole)	0.0761	0.0646	0.0928	0.0549	0.0792	0.0766
Reaction temperature (°C)	200	200	200	200	200	200
Reaction Time (hr)	42	10	6	18	14	45
O_2 % in final reactant gas	0.2	0	N/A	0	0	0.1
CO_2 % in final reactant gas	12.2	12.6	N/A	12.8	13.6	13.9
CO % in final reactant gas	4.13	3.32	N/A	3.12	2.87	2.21
Final discharge press. (bar)	128.13	124.8	N/A	124.8	124.02	114.65
Final discharge temp. (°C)	20.8	25.3	N/A	25.3	22.4	23.4
Final p_{O2} (bar)	0.0395	0.0348	N/A	0.0299	0.0456	0.0399
Final O_2 composition (mole)	0.0006	0	N/A	0	0	0.0003
Final CO_2 com (mole)	0.2563	0	N/A	0	0	0.1146
Final CO composition (mole)	0.0134	0.0092	N/A	0.0073	0.0096	0.0063
O_2 consumption (moles) [Equ. 5.3]	0.0754	0.0647	N/A	0.0549	0.0792	0.0763
Total percent of O_2 consumed	99.26	100		100	100	99.62
Reacted oxygen (g O_2/gm oil)	1.7242	0.2939	N/A	0.2498	0.7196	1.7443
Reaction Rate Constant [Equ. 5.5] (mole O_2 bar^{-1} hr^{-1} cc^{-1} g $sand^{-1}$)	1.70E-06	N/A	N/A	N/A	N/A	1.86E-06
O_2 converted to CO_2+CO (%)	61.17	60.90	N/A	60.98	63.65	56.41
O_2 converted to water (%)	35.01	34.00	N/A	33.80	34.86	30.28
Observation			Ignition + Explosion			

Table D.25 Cont. SBR experimental results for light crude oils @ high temperature

Run No.	116	117	118	119	120
Type of light crude oil	Oil C	Oil C	Oil C	Oil C	Oil C
Initial oil saturation (%)	10	10	25	50	50
Initial water saturation (%)	0	0	0	0	25
Initial gas saturation (%)	90	90	75	50	25
Volume of oil (cc)	1.7	1.7	4.25	8.5	8.5
Weight of oil (gm)	1.4	1.4	3.502	7	7
Weight of sand matrix (gm)	61.6	61.6	61.6	61.6	61.6
Initial Volume of air (cc)(amt)	61.7	61.7	59.15	54.9	50.65
Initial concentration % of oxygen	21	21	21	21	21
Initial charged pressure (bar)	144.14	140.04	140.04	136.52	137.89
Initial charged temperature (°C)	20.1	20.5	21.6	20.8	28.3
Initial p_{O2} (bar)	30.27	29.41	29.41	28.67	28.96
Initial O_2 composition (mole)	0.0766	0.07432	0.07098	0.06440	0.05852
Reaction temperature (°C)	200	200	200	200	200
Reaction Time (hr)	45	13	16	3	13.5
O_2 % in final reactant gas	0.1	2.5	0	0	0
CO_2 % in final reactant gas	13.9	9.6	13.4	13.1	12.4
CO % in final reactant gas	2.21	4.83	3.58	2.79	2.82
Final discharge pressure (bar)	114.65	128.32	125.78	119.92	121.09
Final discharge temperature (°C)	23.4	21.6	25.3	24.5	25.5
Final p_{O2} (bar)	0.0399	3.21	0	0	0
Final O2 composition (mole)	0.0003	0.00808	0	0	0
Final CO2 composition (mole)	0.1146	0.03102	0.04017	0.03485	0.03062
Final CO composition (mole)	0.0063	0.01561	0.01073	0.00742	0.00696
O_2 consumption (moles) [Equ. 5.3]	0.0763	0.06625	0.07098	0.06440	0.05852
Total percent of O_2 consumed	99.62	89.10	100	100	100
Reacted oxygen (g O_2/gm oil)	1.7443	1.51417	0.64862	0.29441	0.26752
Reaction Rate Constant [Equ. 5.5] (mole O_2 bar^{-1} hr^{-1} cc^{-1} g $sand^{-1}$)	1.86E-06	2.55E-06	N/A	N/A	N/A
O_2 converted to carbon oxide (%)	56.41	58.60	64.16	59.88	58.29
O_2 converted to water (%)	30.28	35.19	35.86	32.82	32.12
Observation			Ignition	Ignition	

Table D.26 Cont. SBR experimental results for light crude oils @ high temperature

Run No.	121	122	123	124	125
Type of light crude oil	Oil C	Oil C	Oil C	Oil D	Oil D
Initial oil saturation (%)	50	50	100	10	10
Initial water saturation (%)	50	50	0	0	80
Initial gas saturation (%)	0	0	0	90	10
Volume of oil (cc)	8.5	4.25	17	1.7	1.7
Weight of oil (gm)	7	3.502	14	1.42	1.42
Weight of sand matrix (gm)	61.6	30.8	61.6	61.6	61.6
Initial volume of air (cc)	46.4	66.4	46.4	61.7	48.1
Initial conc. % of oxygen	21	21	21	21	21
Initial charged press. (bar)	135.16	137.89	136.33	139.45	148.24
Initial charged temp. (°C)	21.1	21.9	19.9	18.9	25.2
Initial p_{O2} (bar)	28.38	28.96	28.63	29.28	31.13
Initial O_2 composition (mole	0.05383	0.07838	0.05452	0.07441	0.06037
Reaction temperature (°C)	200	200	200	200	200
Reaction Time (hr)	12	8	N/A	38	41
O_2 % in final reactant gas	0	1.4	N/A	0.1	2.4
CO_2 % in final reactant gas	11.4	11.5	N/A	12.4	10.2
CO % in final reactant gas	2.85	2.7	N/A	2.78	1.96
Final discharge press. (bar)	119.34	125.98	N/A	124.15	134.57
Final discharge temp. (°C)	24.5	26.1	N/A	19.8	24.4
Final p_{O2} (bar)	0	1.76	N/A	0.12415	3.22968
Final O_2 composition (mole)	0	0.00471	N/A	0.00032	0.00628
Final CO_2 com (mole)	0.02550	0.03867	N/A	0.03899	0.02669
Final CO composition (mole)	0.00637	0.00908	N/A	0.00874	0.00513
O_2 consumption (moles) [Equ. 5.3]	0.05383	0.07368	N/A	0.0741	0.05409
Total percent of O_2 consumed	100	93.99	100	99.6	90.7
Reacted oxygen (g O_2/gm oil)	0.2461	0.67321	N/A	1.66985	1.21885
Reaction Rate Constant [Equ. 5.5]			N/A	2.15E-06	6.45E-07
(mole O_2 bar^{-1} hr^{-1} cc^{-1} g $sand^{-1}$)	N/A	4.51E-06	N/A	58.53	54.08
O_2 converted to carbon oxide (%)	53.31	58.64	N/A	32.21	29.41
O_2 converted to water (%)	29.62	32.40			
Observation			Ignition + Explosion		

Table D.27 Cont. SBR experimental results for light crude oils @ high temperature

Run No.	126	127	128	129	130	131
Type of light crude oil	Oil D	Oil D	Hexane	Xylene	decane	Dodecane
Initial oil saturation (%)	50	50	50	50	50	50
Initial water saturation (%)	0	50	0	0	0	0
Initial gas saturation (%)	50	0	50	50	50	50
Volume of oil (cc)	8.5	8.5	8.5	8.5	8.5	8.5
Weight of oil (gm)	7.11	7.11	5.644	7.318	6.205	6.392
Weight of sand matrix (gm)	61.6	61.6	61.6	61.6	61.6	61.6
Initial volume of air (cc)	54.9	46.4	54.9	54.9	54.9	54.9
Initial conc. % of oxygen	21	21	21	21	21	21
Initial charged press. (bar)	138.28	139.26	135.74	135.16	133.59	136.52
Initial charged temp. (°C)	24.8	21.8	24.1	20.6	22.1	22.8
Initial p_{O2} (bar)	29.04	29.24	28.5054	28.3836	28.0539	28.6692
Initial O_2 composition (mole	0.06436	0.05533	0.063324	0.063805	0.062743	0.06397
Reaction temperature (°C)	200	200	200	200	200	200
Reaction Time (hr)	N/A	21	14.5	11	5	4.5
O_2 % in final reactant gas	N/A	0	0.2	0.1	0	0
CO_2 % in final reactant gas	N/A	13.8	11.8	11.8	12.5	12.3
CO % in final reactant gas	N/A	2.46	3.87	2.43	3.65	3.12
Final discharge press. (bar)	N/A	123.63	118.36	122.27	115.47	119.14
Final discharge temp. (°C)	N/A	25.6	26.2	23.8	22.5	28.6
Final p_{O2} (bar)	N/A	0	0.23672	0.12227	0	0
Final O_2 composition (mole)	N/A	0	0.000522	0.000272	0	0
Final CO_2 com (mole)	N/A	0.03187	0.030808	0.032083	0.032238	0.03207
Final CO composition (mole)	N/A	0.00568	0.010104	0.006607	0.009413	0.00813
O_2 consumption (moles) [Equ. 5.3]	N/A	0.05534	0.062802	0.063533	0.062743	0.06397
Total percent of O_2 consumed	100	100	99.17	99.58	100	100
Reacted oxygen (g O_2/gm oil)	N/A	0.24905	0.356069	0.277814	0.323574	0.32024
Reaction Rate Constant [Equ. 5.5] (mole O_2 bar $^{-1}$ hr $^{-1}$ cc $^{-1}$ g sand $^{-1}$)	N/A	N/A	8.81E-07	1.32E-06	N/A	N/A
O_2 converted to carbon oxide (%)	N/A	62.73	57.10	55.70	58.88	56.49
O_2 converted to water (%)	N/A	33.93	32.57	30.45	33.19	31.42
Observation	Ignition + Explosion				Ignition + Explosion	Ignition + Explosio n

Appendix E

E.1 Gas Chromatograph Mass Spectrum Traces of Single Organic Compound and Light Crude Oil Samples

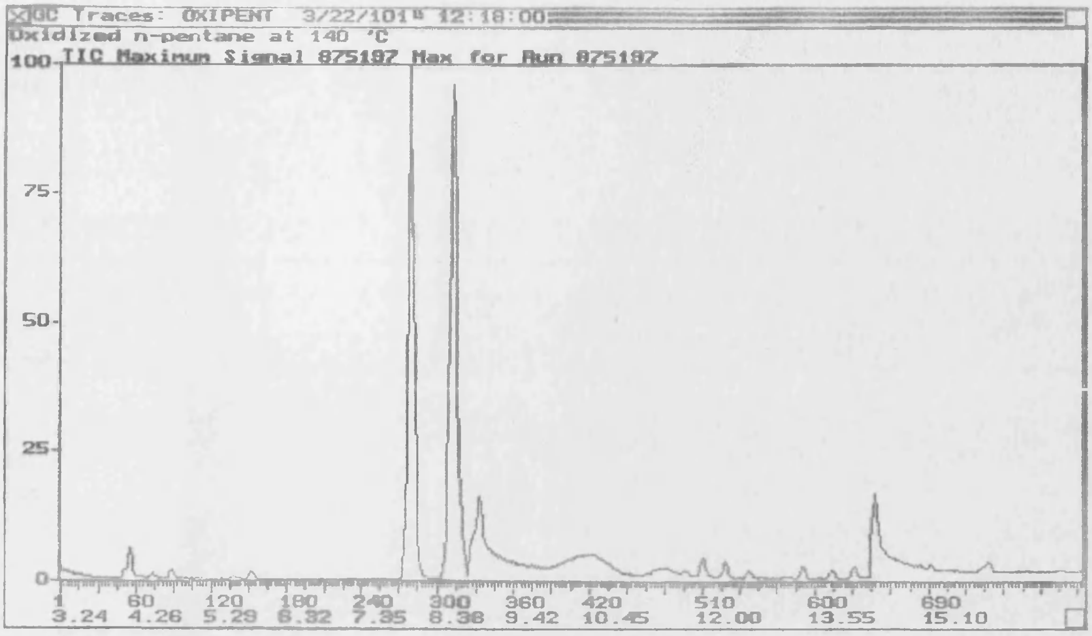

E 1.1: GC-MS spectrum traces for oxidised pentane at 140 °C

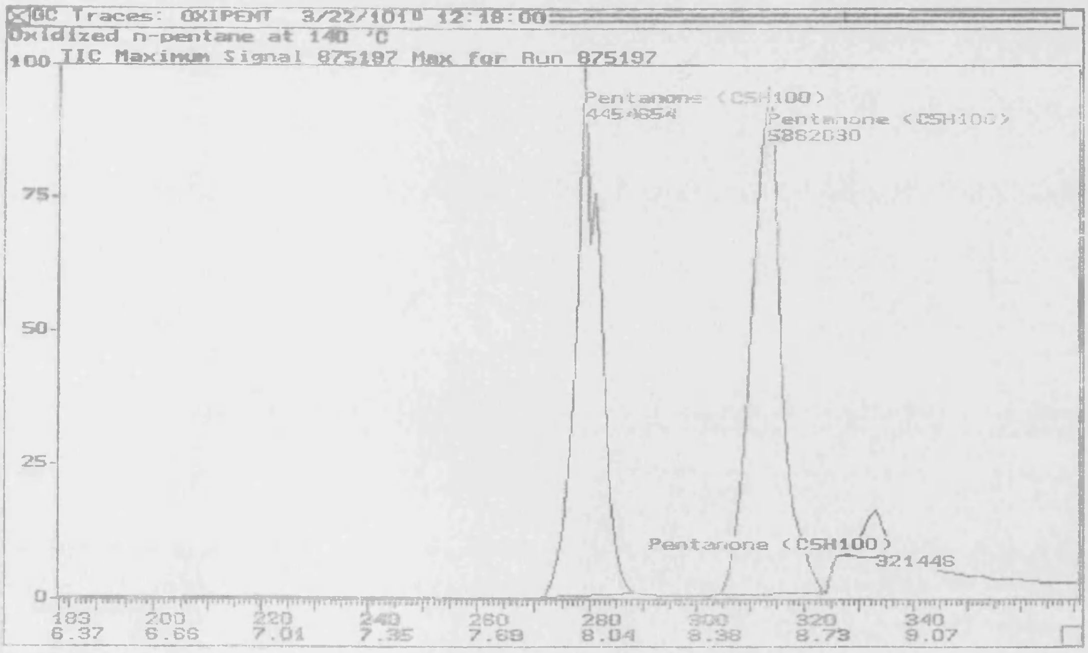

E 1.2: Peak identification of oxidised pentane at 140 °C

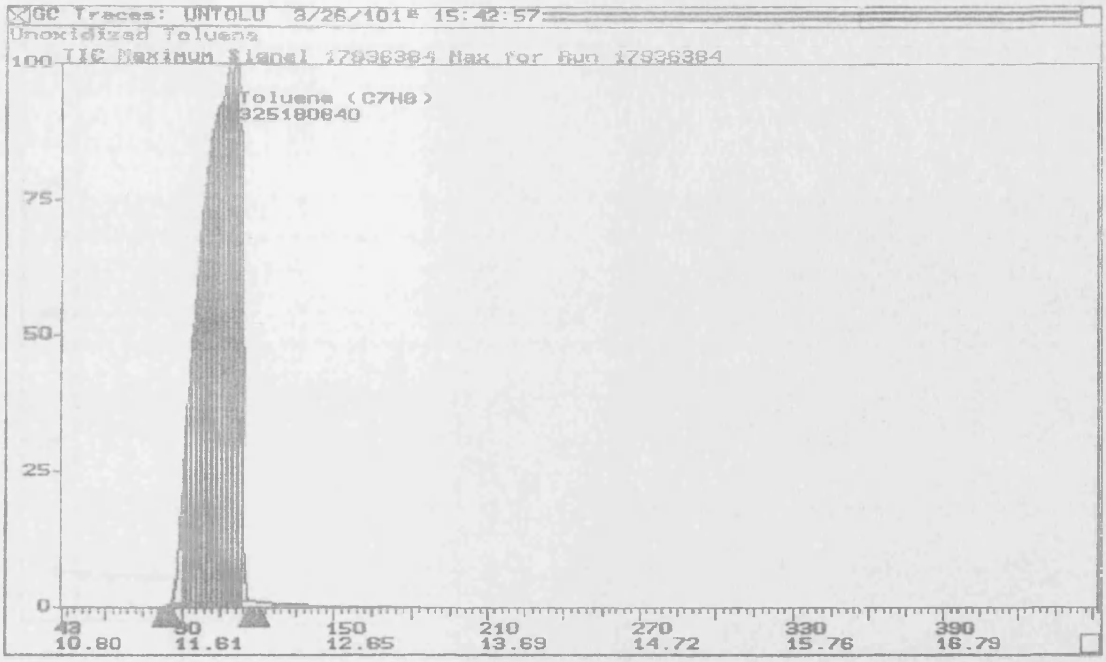

E 1.3: GC-MS spectrum traces for toluene

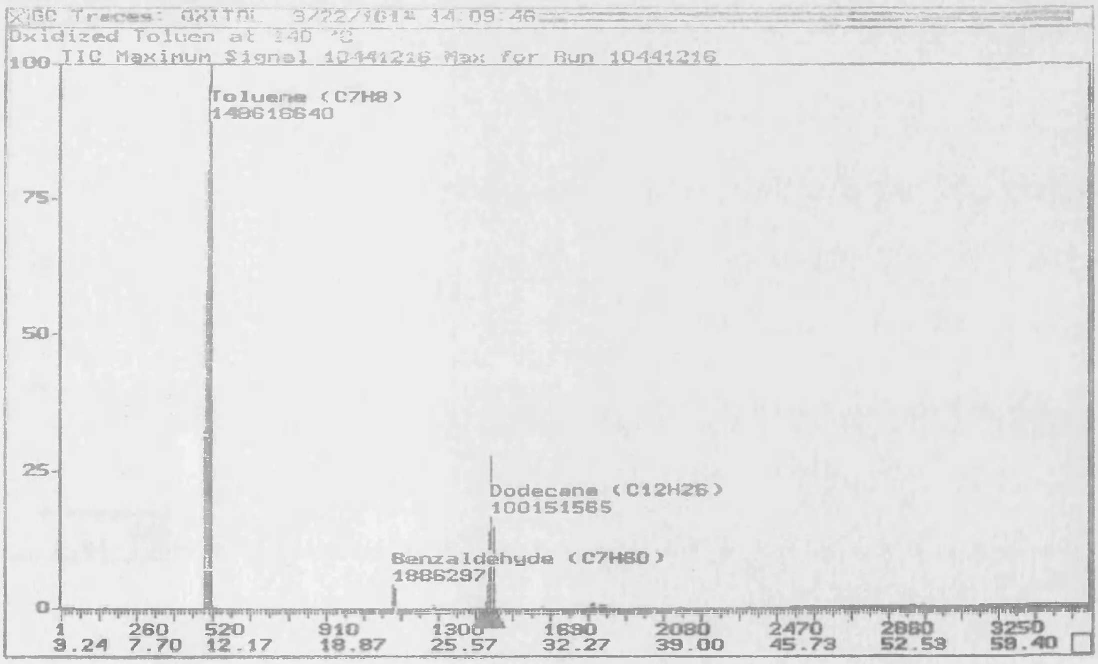

E 1.4: GC-MS spectrum traces for oxidised toluene at 140 °C

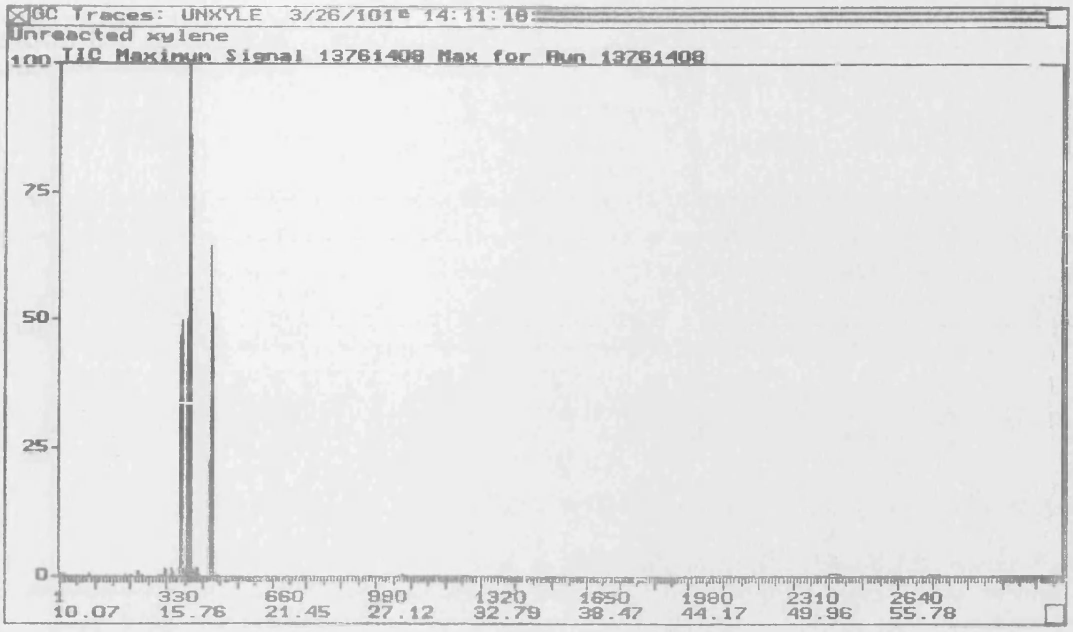

E 1.5: GC-MS spectrum traces for xylene

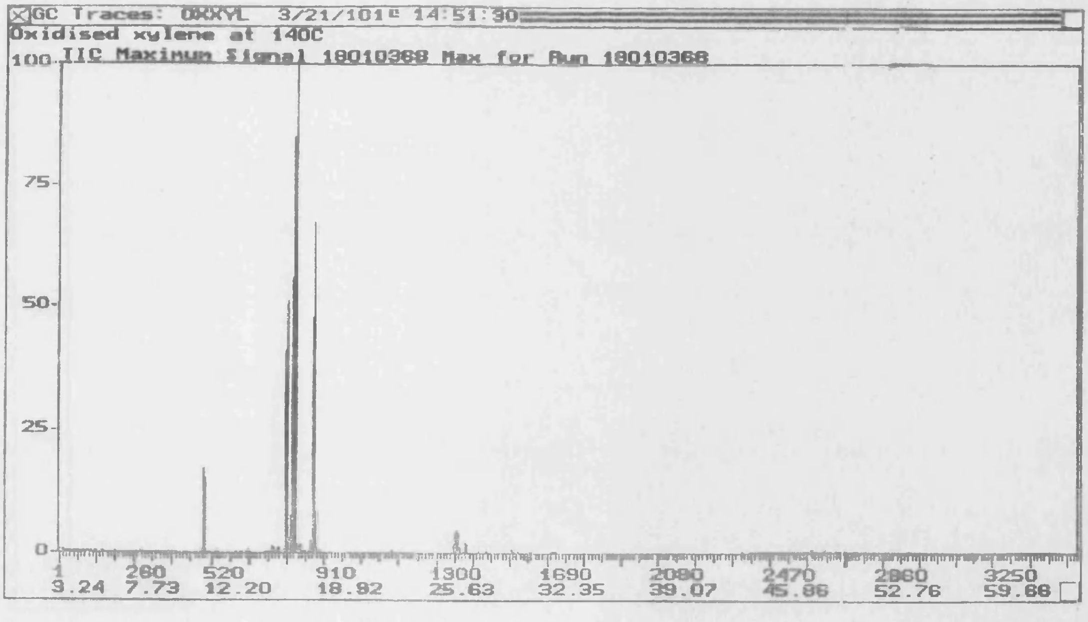

E 1.6: GC-GS spectrum traces for oxidised xylene at 140 °C

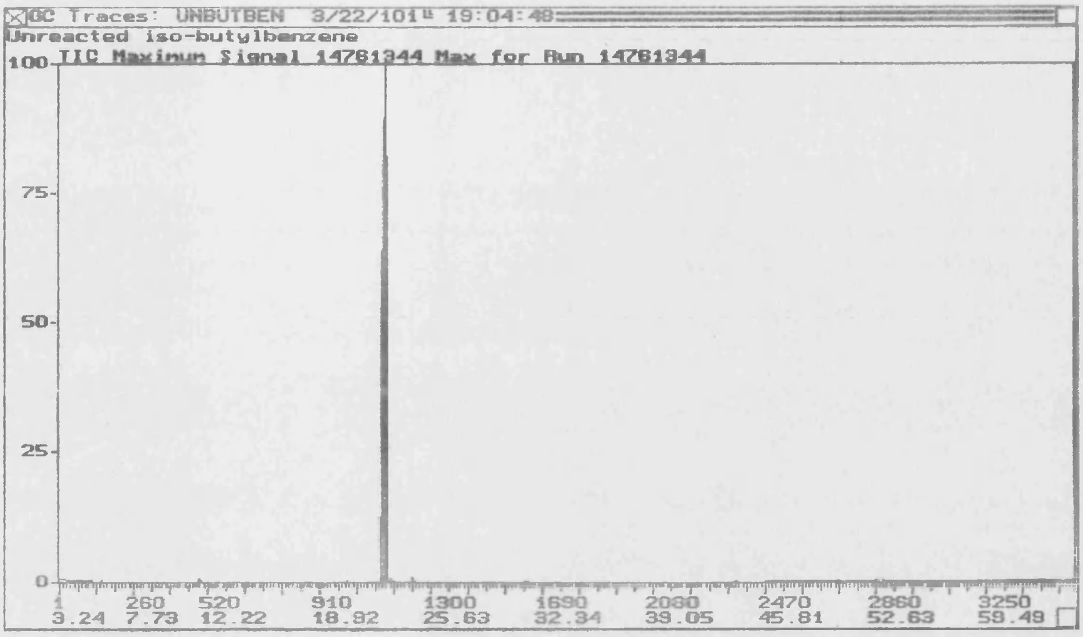

E 1.7: GC-MS spectrum traces for iso-butylbenzene

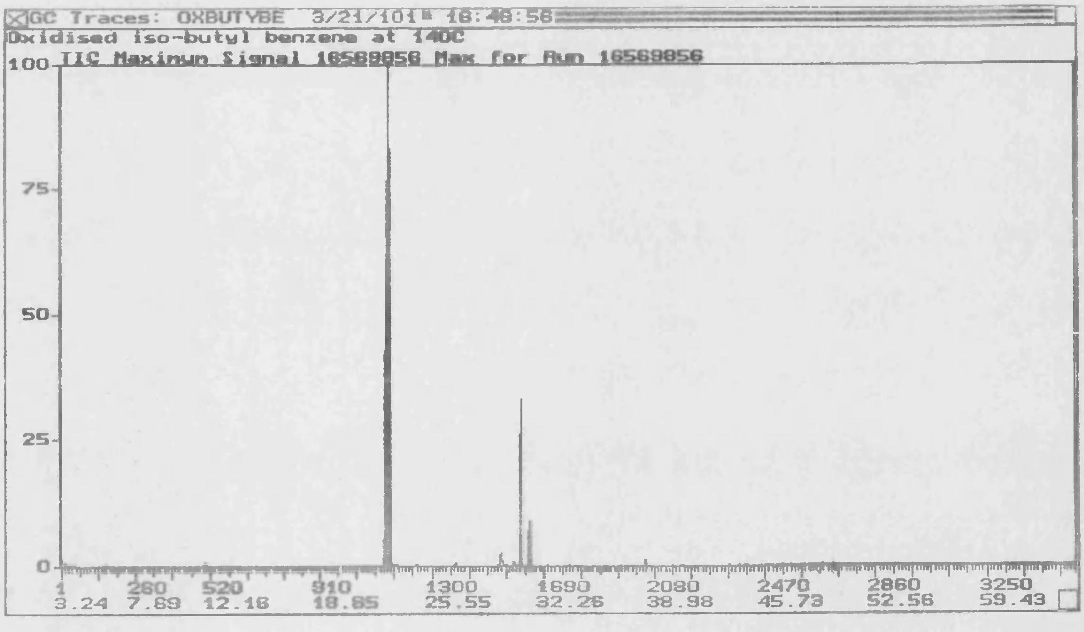

E 1.8: GC-MS spectrum traces for oxidised iso-butylbenzene at 140 °C

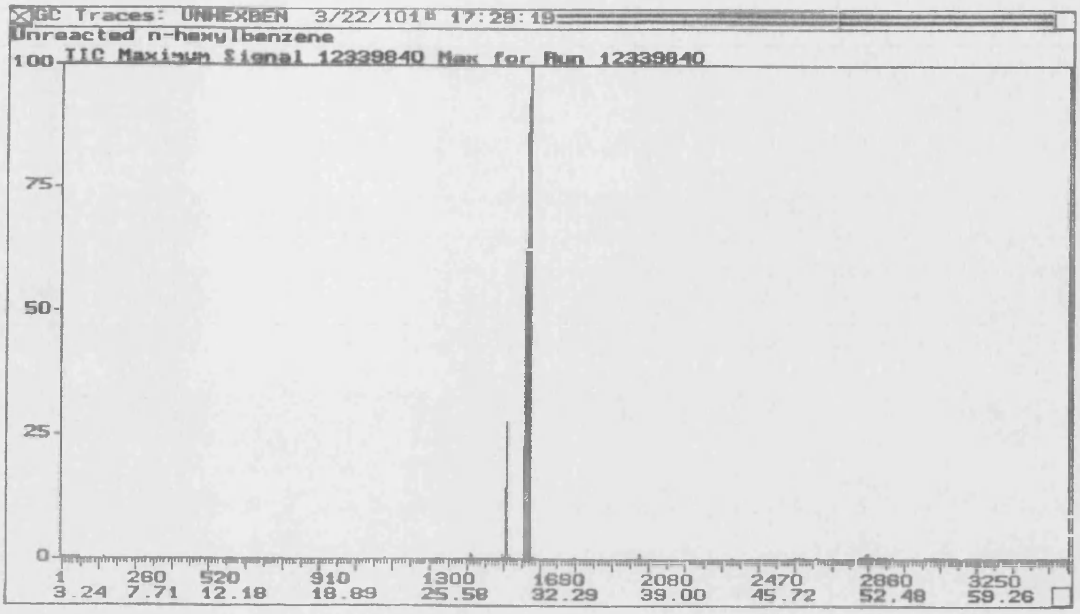

E 1.9: GC-MS spectrum traces for n-hexylbenzene

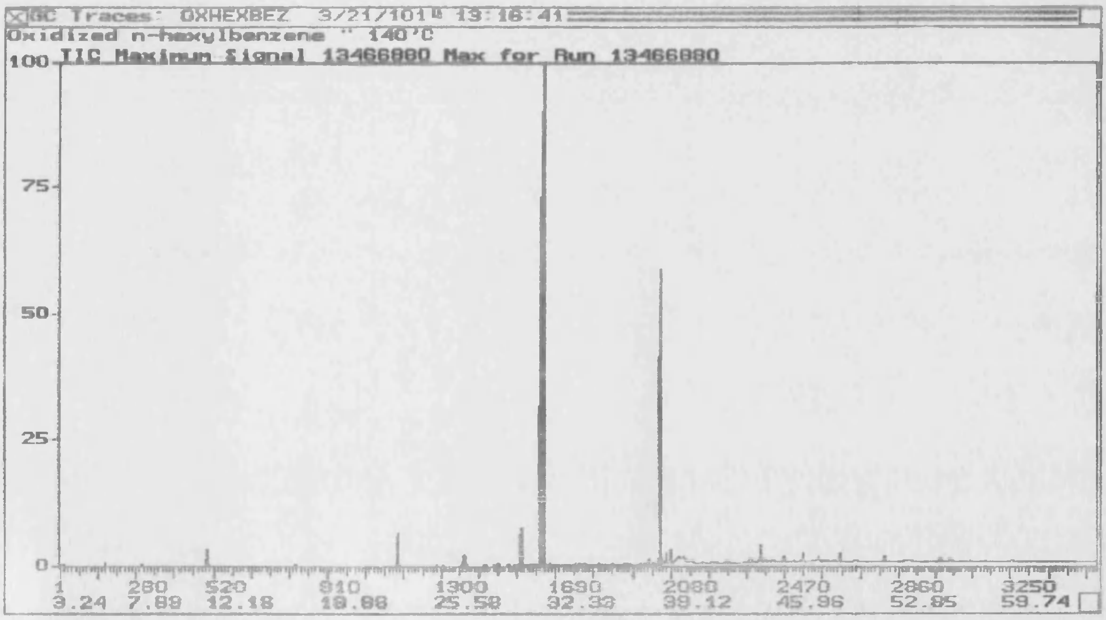

E 1.10: GC-MS spectrum traces for oxidised n-hexylbenzene at 140 °C

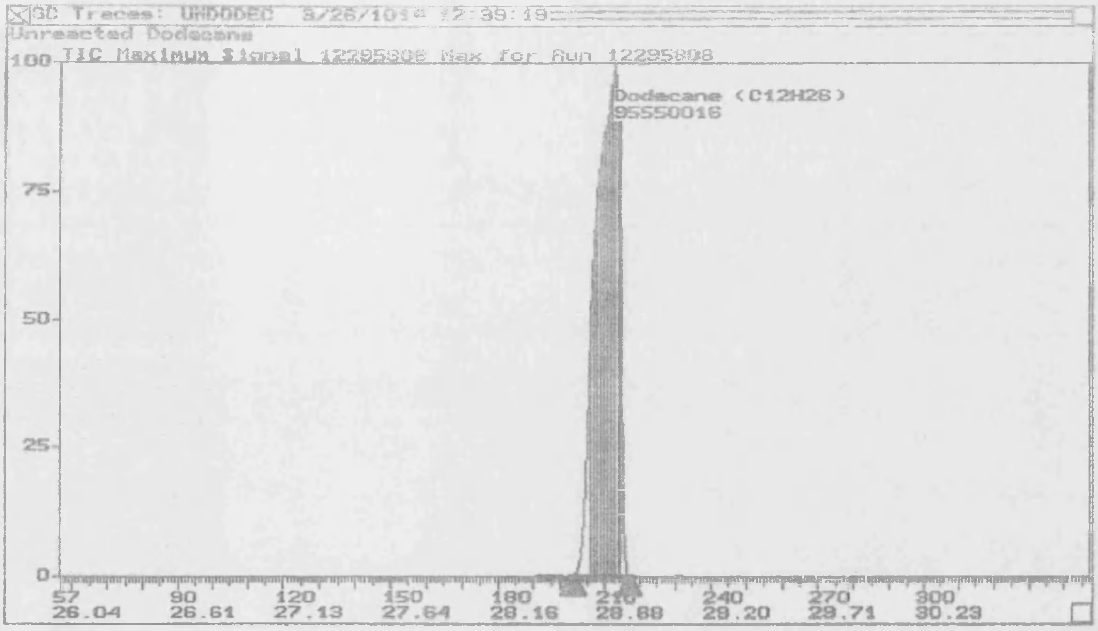

E 1.11: GC-MS spectrum traces for n-dodecane

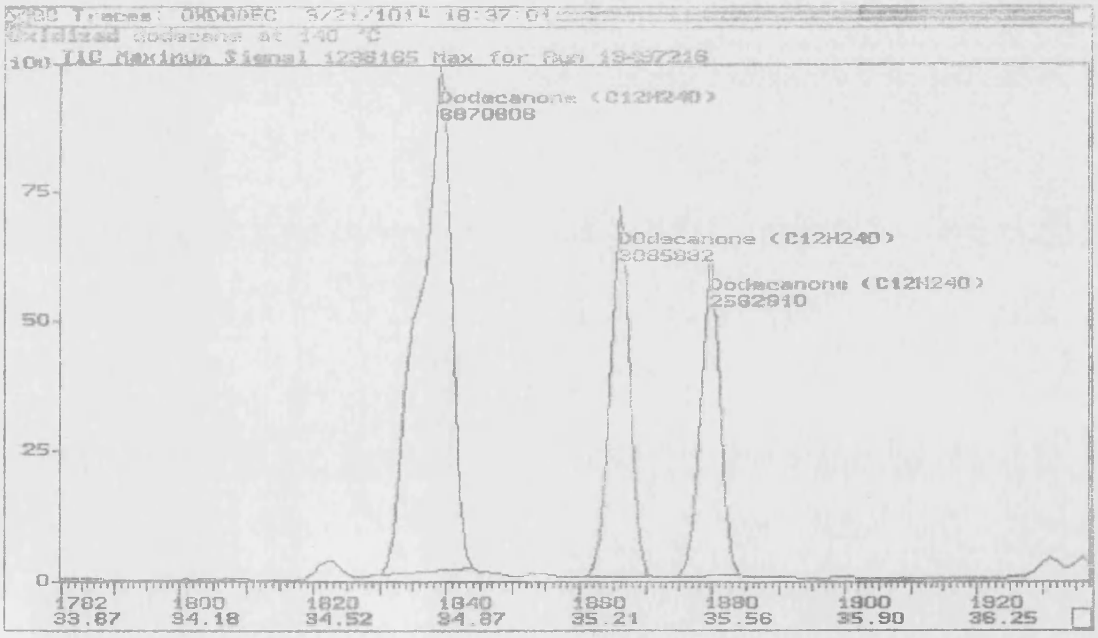

E 1.12: GC-MS spectrum traces for oxidised n-dodecane at 140 °C

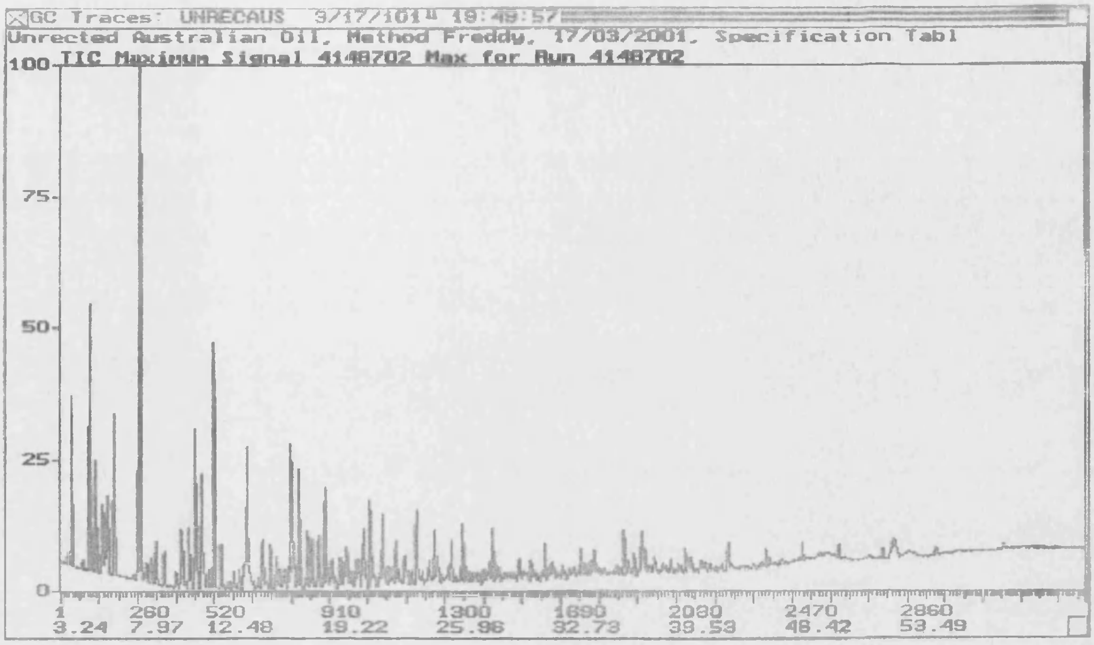

E 1.13: GC-MS spectrum traces for Australian oil

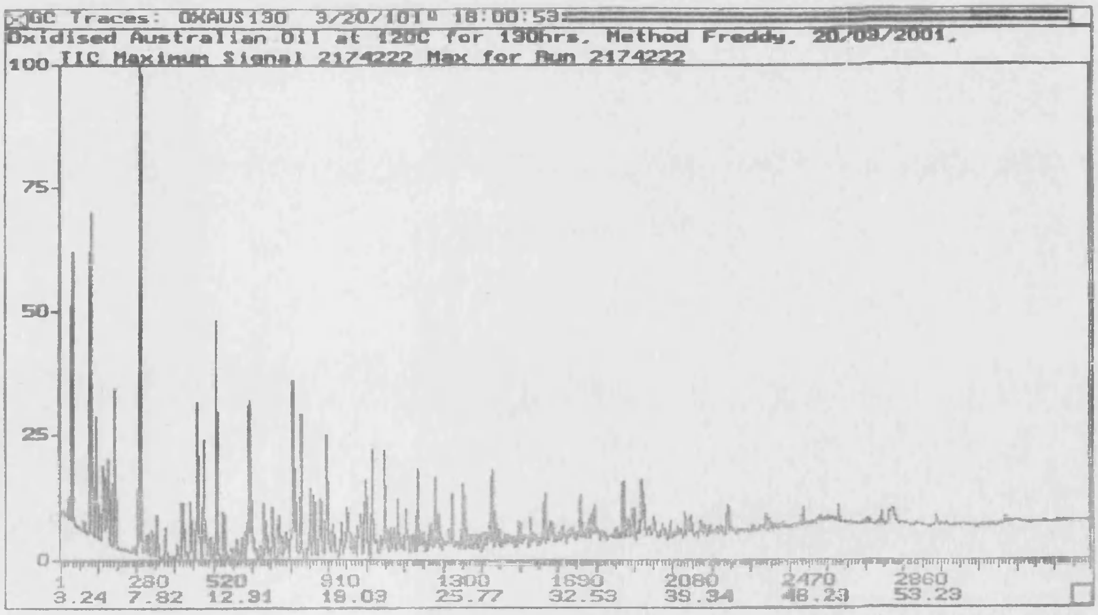

E 1.14: GC-MS spectrum traces for oxidised Australian oil at 120 °C

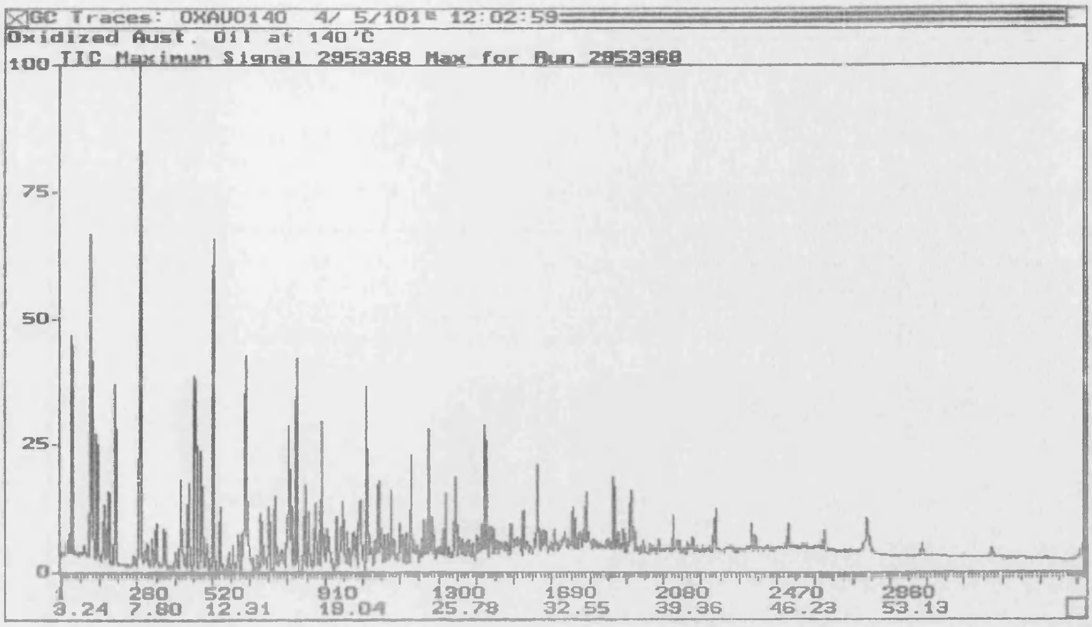

E 1.15: GC-MS spectrum traces for oxidised Australian oil at 140 °C

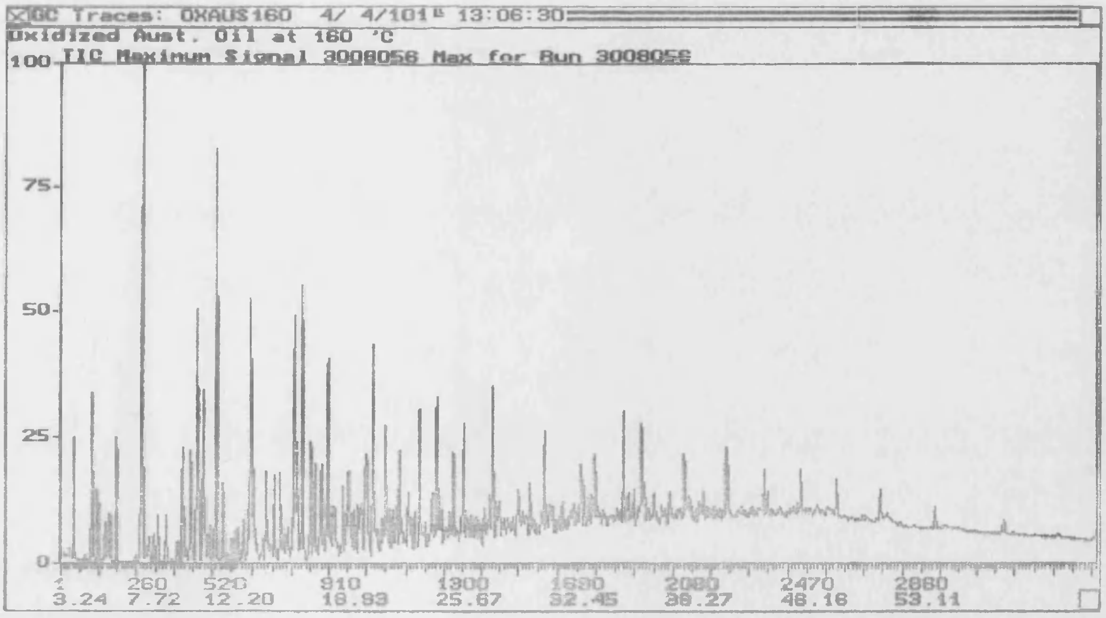

E 1.16: GC-MS spectrum traces for oxidised Australian oil at 160 °C

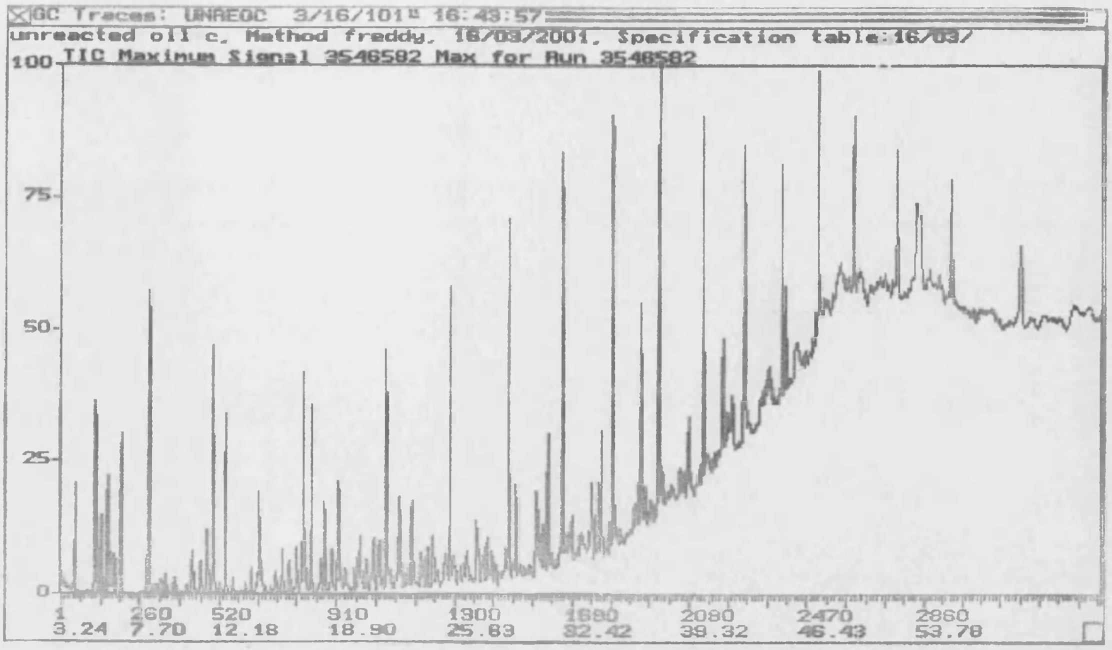

E 1.17: GC-MS spectrum traces for oil C

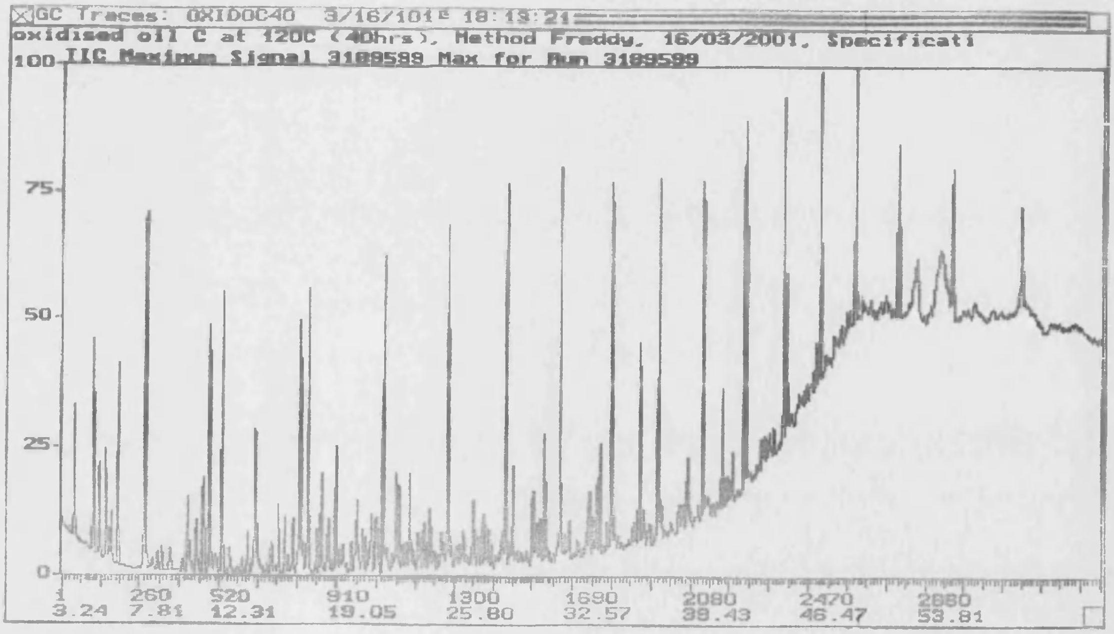

E 1.18: GC-MS spectrum traces for oxidised oil C after 40 hrs at 120 °C

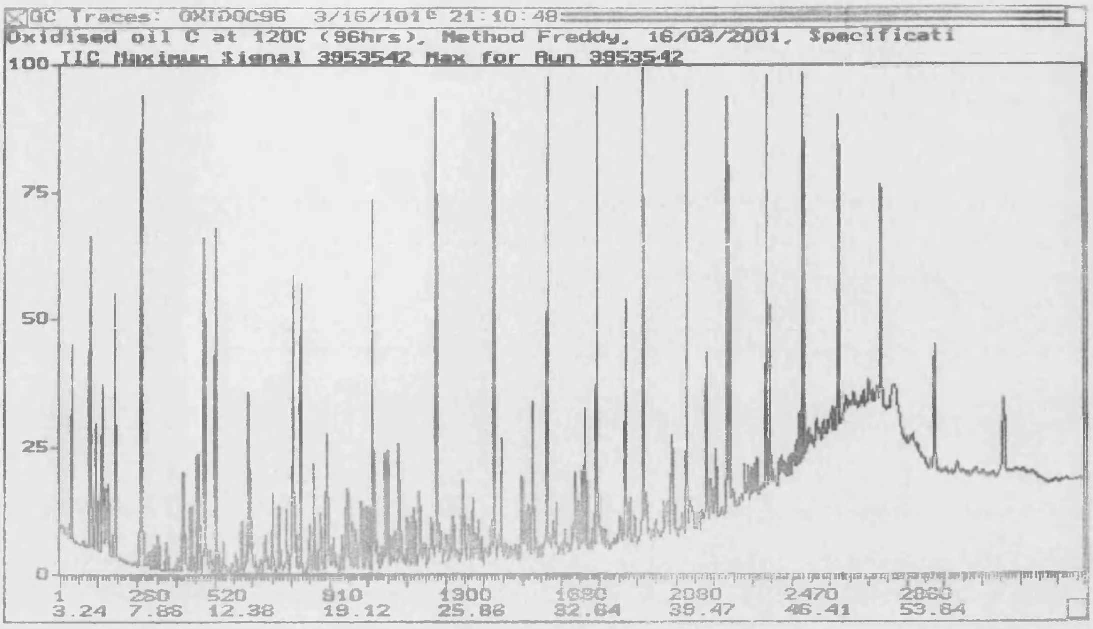

E 1.19: GC-MS spectrum traces for oxidised oil C after 96 hrs at 120 °C

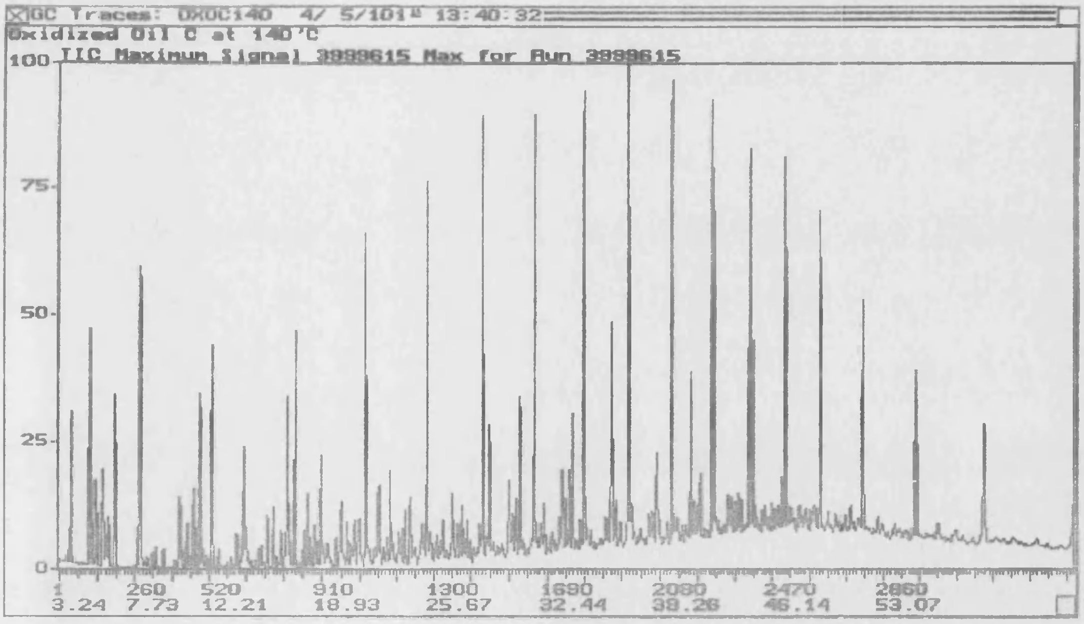

E 1.20: GC-MS spectrum traces for oxidised oil C at 140 °C

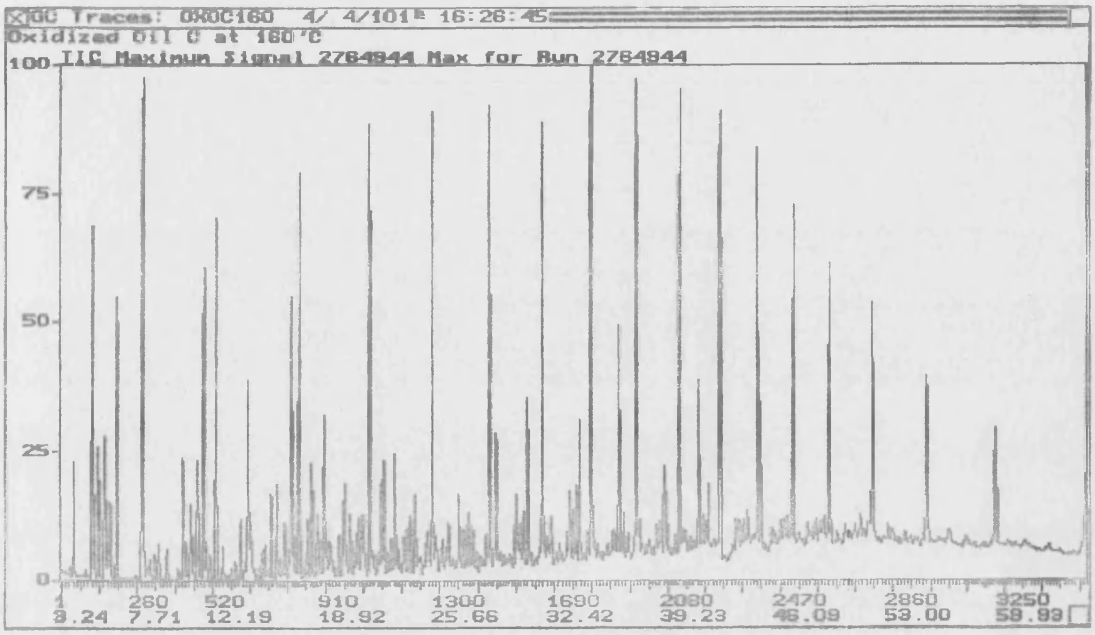

E 1.21: GC-MS spectrum traces for oxidised oil C at 160 °C

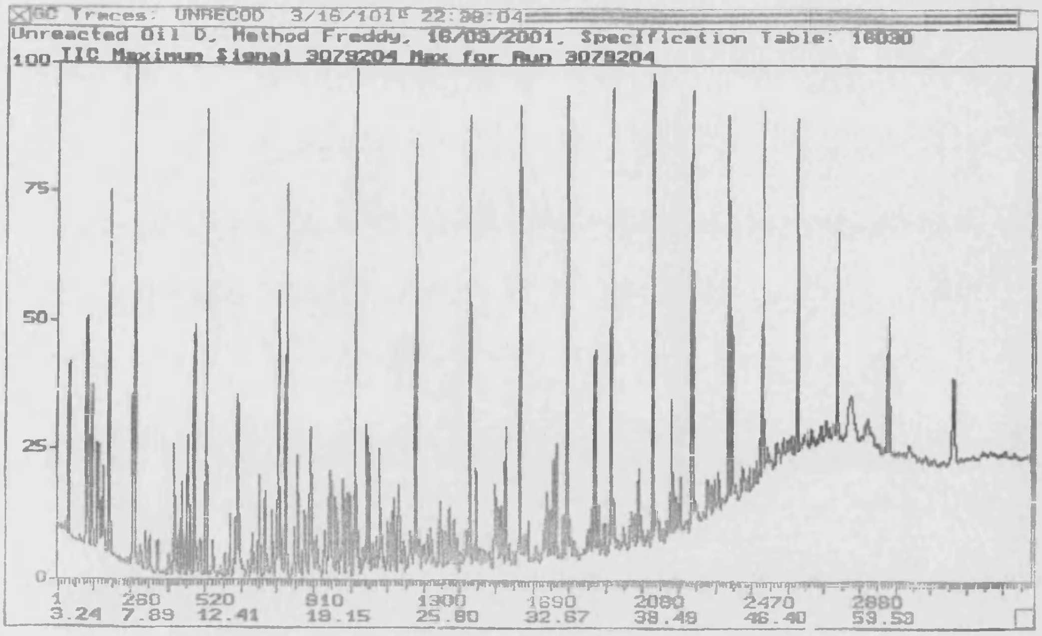

E 1.22: GC-MS spectrum traces for oil D

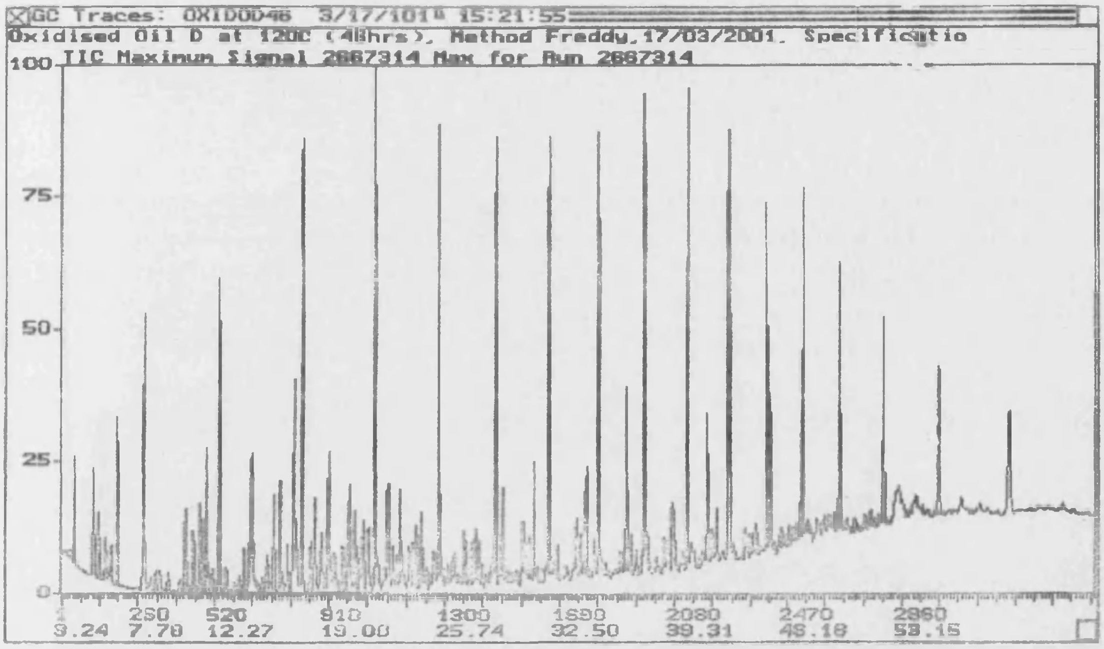

E 1.23: GC-MS spectrum traces for oxidised oil D after 46 hrs at 120 °C

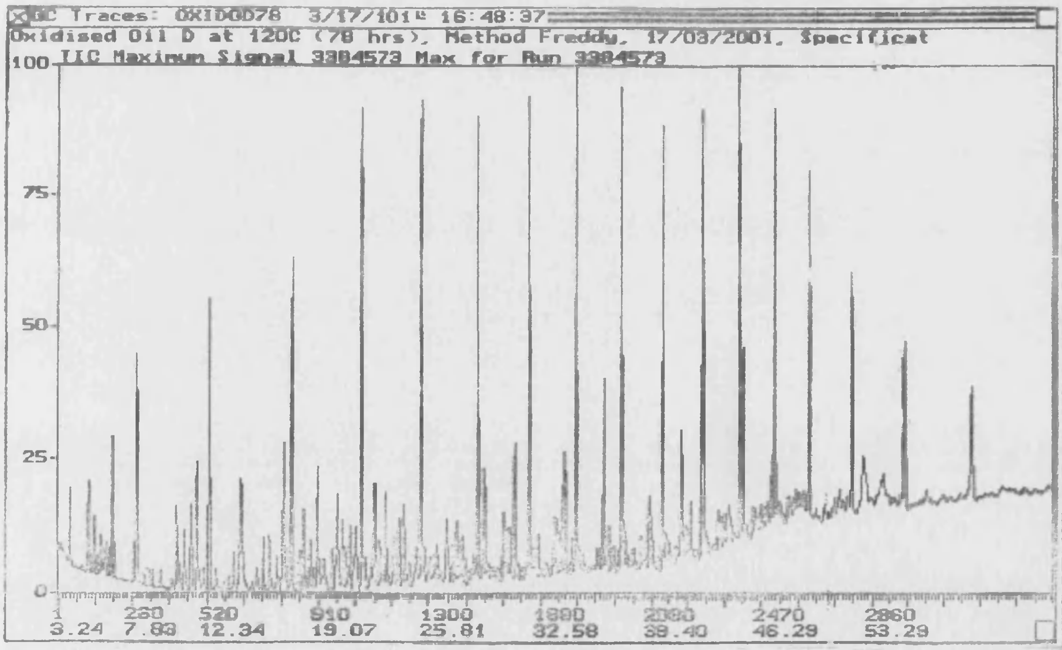

E 1.24: GC-MS spectrum traces for oxidised oil D after 78 hrs at 120 °C

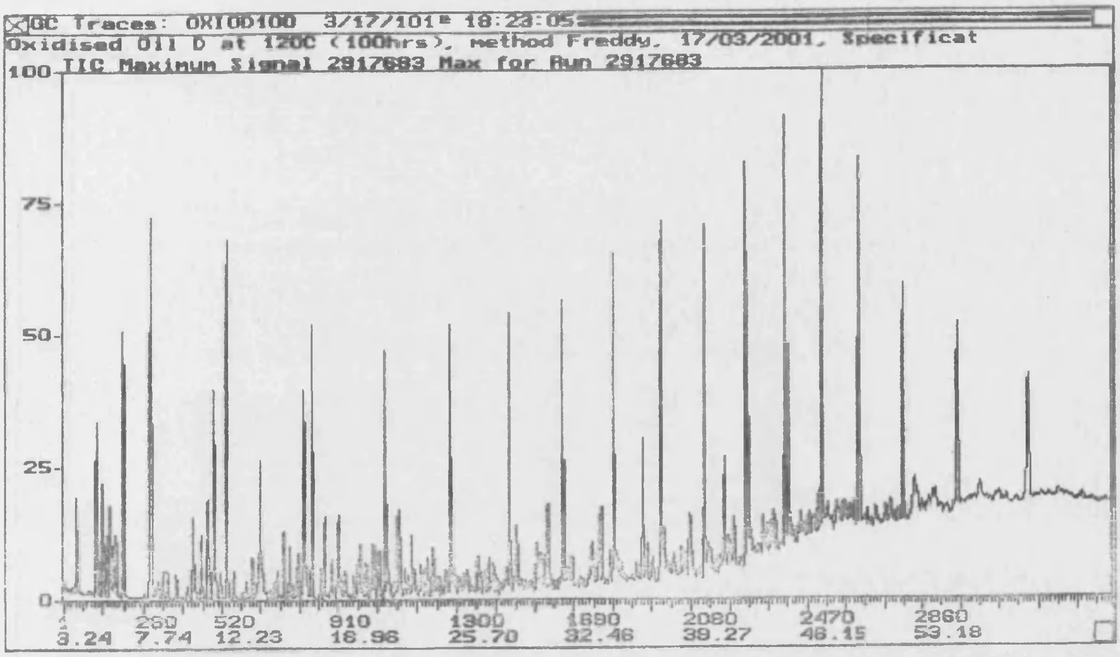

E 1.25: GC-MS spectrum traces for oxidised oil D after 100 hrs at 120 °C

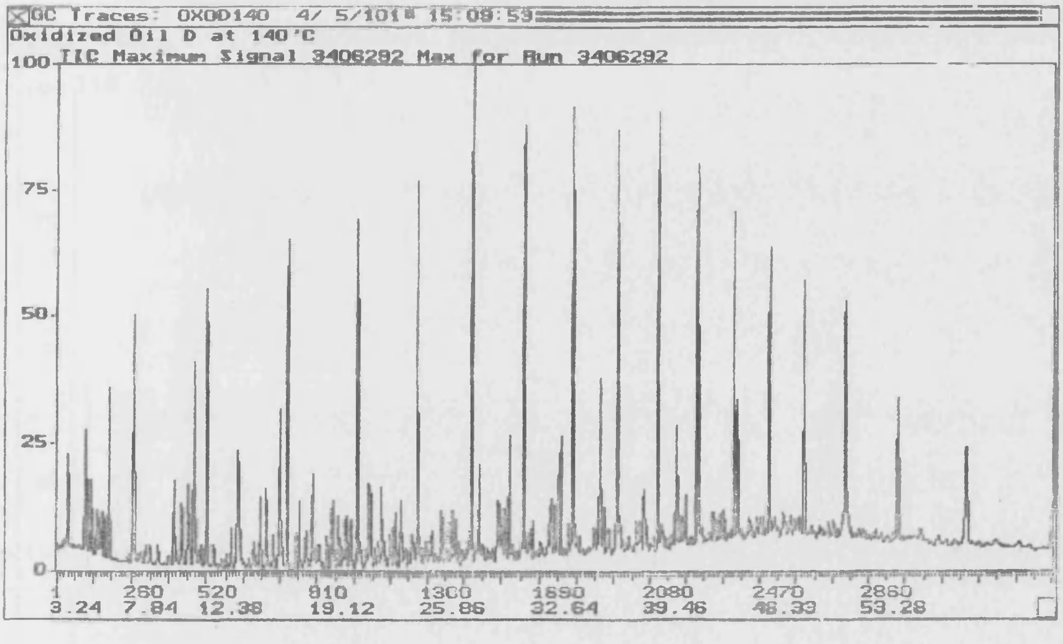

E 1.26 GC-MS spectrum traces for oxidised oil D at 140 °C

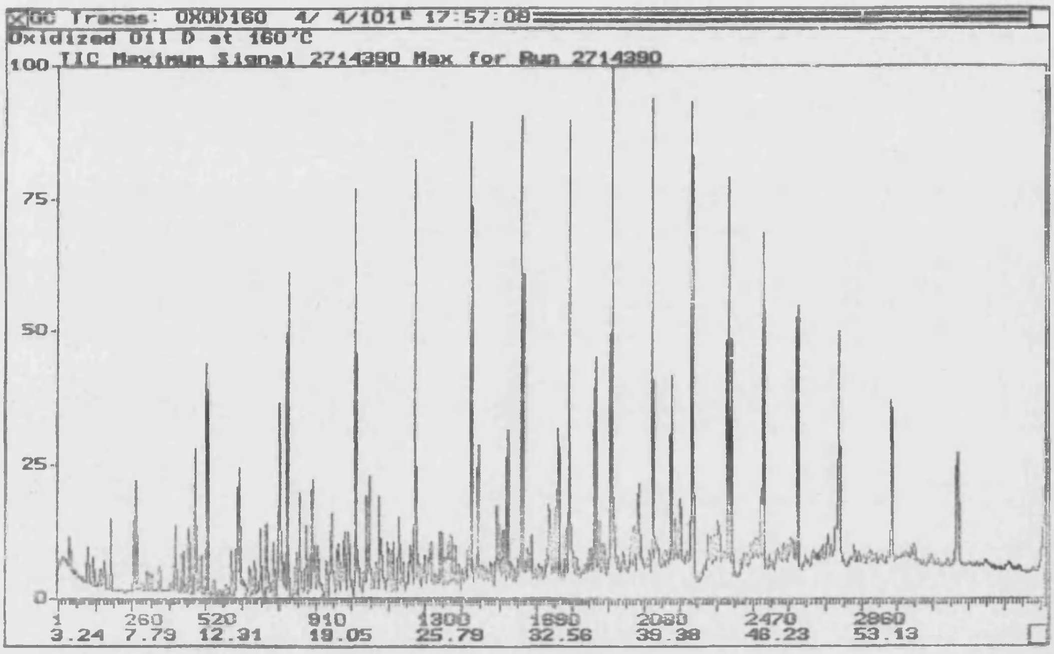

E 1.27: GC-MS spectrum traces for oxidised oil D at 160 °C

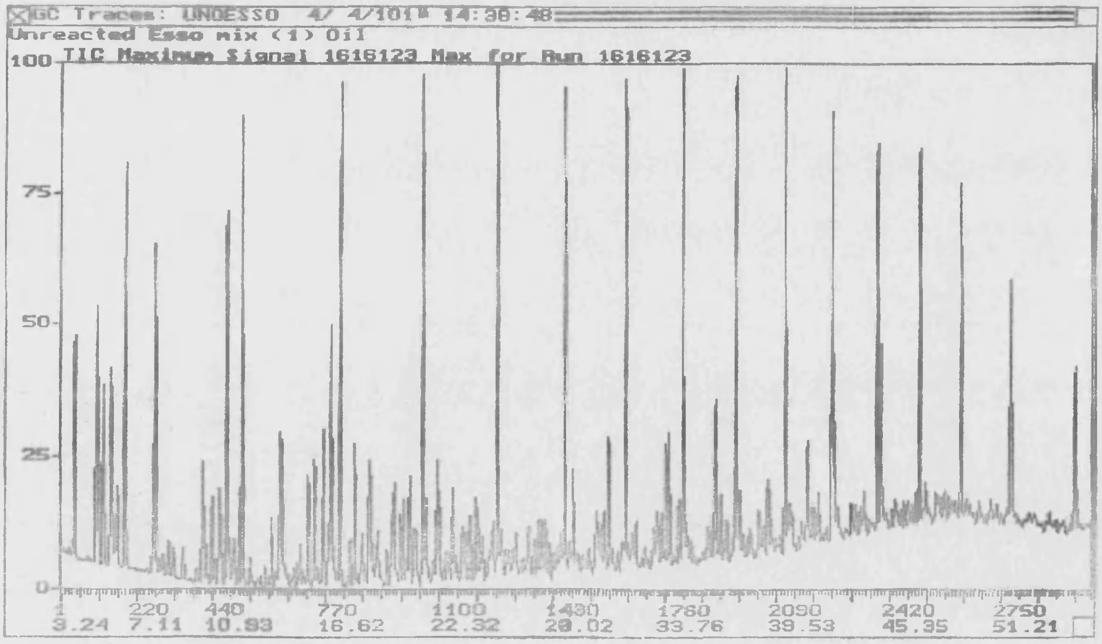

E 1.28: GC-MS spectrum traces for Esso Mix1 oil

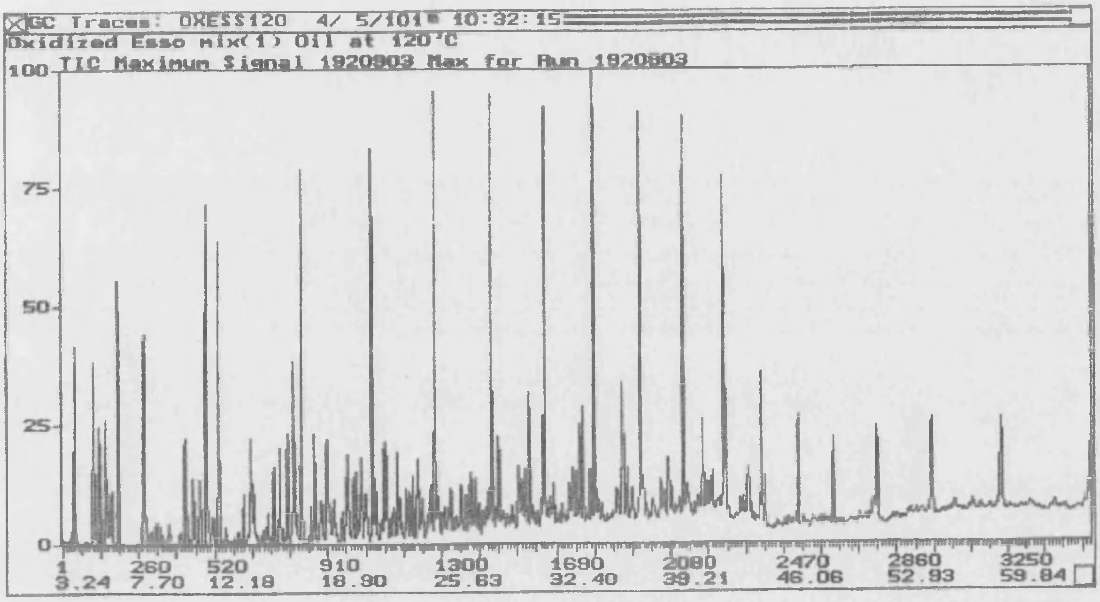

E 1.29: GC-MS spectrum traces for oxidised Esso Mix1 at 120 °C

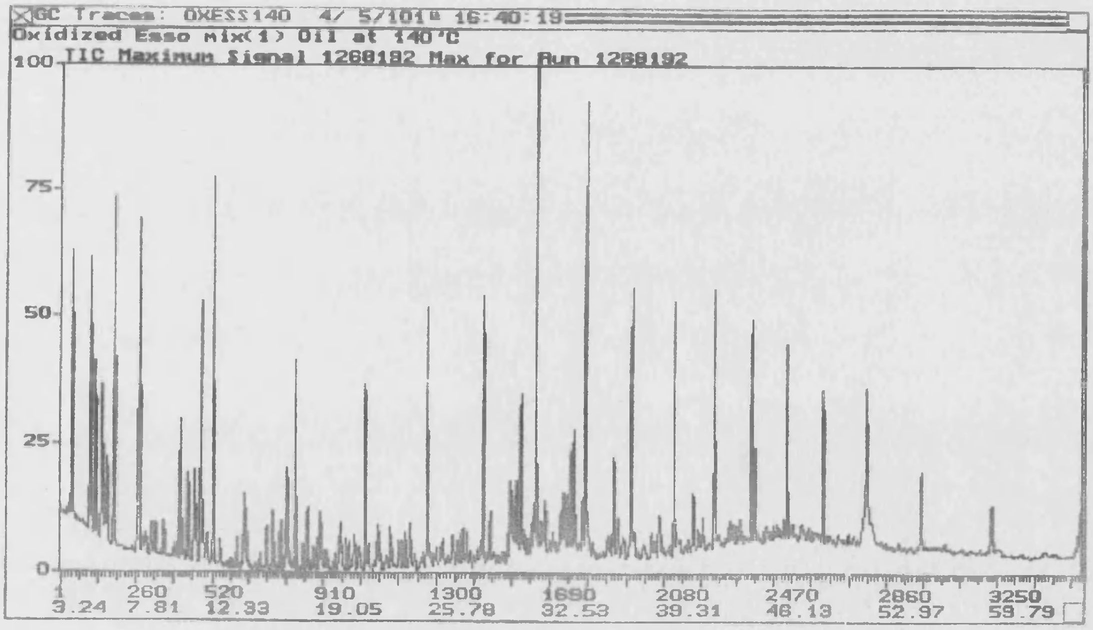

E 1.30: GC-MS spectrum traces for oxidised Esso mix(1) at 140 °C

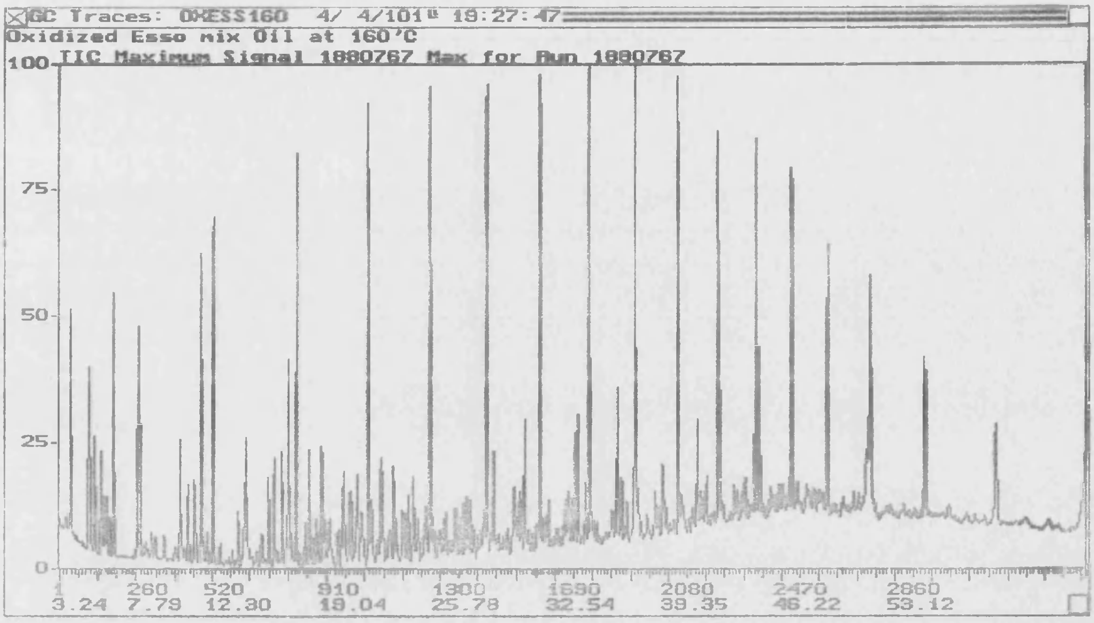

E 1.31: GC-MS spectrum traces for oxidised Esso Mix1 oil at 160 °C

E.2 Identification of GC-MS Spectrum Peaks of Single Organic Compound and Light Crude oil Samples

E 2.1: Gas chromatograph analysis of oxidised pentane at 140 °C

Date of GC-MS run:	21/03/01
Time of GC-MS run:	18.37
Sample:	Pentane
Oxidation temperature:	140 °C
Dilution:	Carbon Disulfide
Injection Size:	1μl
Carrier Gas Split:	40:1
Carrier gas head pressure:	8 p.s.i.
Oven Temperature:	Initial Temperature = 40C for 10 minutes Increasing at 8C per minute Hold at 140C for 30 minutes
Filament Delay:	3 minutes
Filament Total Run Time:	80 minutes
Column:	BP624, 25m, 1.2um

SUMMARY OF PEAKS IDENTIFIED:

Compound Name	Formula	S.I.	Retention Time	Peak Area
Pentanone	$C_5H_{10}O$	83	8.02	4481442
Pentanone	$C_5H_{10}O$	88	8.61	5019936

SI: *Similarity Index*

E 2.2: Gas chromatograph analysis of unreacted and oxidised toluene at 140 °C

Date of GC-MS run:	21/03/01
Time of GC-MS run:	18.37
Sample:	Toluene
Oxidation temperature:	140 °C
Dilution:	Carbon Disulfide
Injection Size:	1μl
Carrier Gas Split:	40:1
Carrier gas head pressure:	8 p.s.i.
Oven Temperature:	Initial Temperature = 40C for 10 minutes Increasing at 8C per minute Hold at 140C for 30 minutes
Filament Delay:	3 minutes
Filament Total Run Time:	80 minutes
Column:	BP624, 25m, 1.2um

SUMMARY OF PEAKS IDENTIFIED:

A. Unreacted Toluene

Compound Name	Formula	S.I.	Retention Time	Peak Area
Toluene	C_7H_8	85	11.99	325708640

B. Oxidised Toluene

Compound Name	Formula	S.I.	Retention Time	Peak Area
Toluene	C_7H_8	88	12.05	147764240
Benzaldehyde	C_7H_6O	91	22.46	956514
Dodecane	$C_{12}H_{26}$	92	28.69	81264256

SI: Similarity Index

E 2.3: Gas chromatograph analysis of unreacted and oxidised xylene at 140 °C

Date of GC-MS run:	21/03/01
Time of GC-MS run:	18.37
Sample:	Xylene
Oxidation temperature:	140 °C
Dilution:	Carbon Disulfide
Injection Size:	1µl
Carrier Gas Split:	40:1
Carrier gas head pressure:	8 p.s.i.
Oven Temperature:	Initial Temperature = 40C for 10 minutes Increasing at 8C per minute Hold at 140C for 30 minutes
Filament Delay:	3 minutes
Filament Total Run Time:	80 minutes
Column:	BP624, 25m, 1.2um

SUMMARY OF PEAKS IDENTIFIED:

A. Unreacted Xylene

Compound Name	Formula	S.I.	Retention Time	Peak Area
P-xylene	C_8H_{10}	90	16.52	32015268
P-xylene	C_8H_{10}	91	16.97	92524640
P-xylene	C_8H_{10}	93	18.12	44353456

B. Oxidised Xylene

Compound Name	Formula	S.I.	Retention Time	Peak Area
P-xylene	C_8H_{10}	90	16.56	55798640
P-xylene	C_8H_{10}	91	17.01	16917960
P-xylene	C_8H_{10}	93	18.18	81264256
Benzaldehyde	C_8H_8O	92	26.83	3974310
Benzaldehyde	C_8H_8O	92	27.40	1682263

SI: Similarity Index

E 2.4: Gas chromatograph of unreacted and oxidised iso-butylbenzene at 140 °C

Date of GC-MS run:	21/03/01
Time of GC-MS run:	18.37
Sample:	Iso-butylbenzene
Oxidation temperature:	140 °C
Dilution:	Carbon Disulfide
Injection Size:	1μl
Carrier Gas Split:	40:1
Carrier gas head pressure:	8 p.s.i.
Oven Temperature:	Initial Temperature = 40C for 10 minutes Increasing at 8C per minute Hold at 140C for 30 minutes
Filament Delay:	3 minutes
Filament Total Run Time:	80 minutes
Column:	BP624, 25m, 1.2um
Filename:	Oxidized iso-butylbenzene

SUMMARY OF PEAKS IDENTIFIED:

A. Unreacted iso-butylbenzene

Compound Name	Formula	S.I.	Retention Time	Peak Area
Iso-butylbenzene	$C_{10}H_{14}$	85	22.93	202562576

B. Oxidised iso-butylbenzene

Compound Name	Formula	S.I.	Retention Time	Peak Area
iso-butylbenzene	$C_{10}H_{14}$	83	23.01	18419286444
Propanone, 2methyl-1-phenyle	$C_{10}H_{12}O$	90	30.95	28405836
Hexylbenzene	$C_{12}H_{18}$	93	31.45	5336767

SI: *Similarity Index*

E 2.5: Gas chromatograph of unreacted and oxidised n-hexylbenzene at 140 °C

Date of GC-MS run:	21/03/01
Time of GC-MS run:	18.37
Sample:	n-hexylbenzene
Oxidation temperature:	140 °C
Dilution:	Carbon Disulfide
Injection Size:	1µl
Carrier Gas Split:	40:1
Carrier gas head pressure:	8 p.s.i.
Oven Temperature:	Initial Temperature = 40C for 10 minutes Increasing at 8C per minute Hold at 140C for 30 minutes
Filament Delay:	3 minutes
Filament Total Run Time:	80 minutes
Column:	BP624, 25m, 1.2um

SUMMARY OF PEAKS IDENTIFIED:

A. Unreacted n-hexylbenzene

Compound Name	Formula	S.I.	Retention Time	Peak Area
n-hexylbenzene	$C_{12}H_{18}$	94	30.28	13453466
n-hexylbenzene	$C_{12}H_{18}$	90	31.72	205869248

B. Oxidised n-hexylbenzene

Compound Name	Formula	S.I.	Retention Time	Peak Area
n-hexylbenzene	$C_{12}H_{18}$	91	31.69	160555856
1-hexanone, 1 phenyle	$C_{12}H_{16}O$	88	38.53	40226800

SI: *Similarity Index*

E 2.6: Gas chromatograph of unreacted and oxidised n-dodecane at 140 °C

Date of GC-MS run:	21/03/01
Time of GC-MS run:	18.37
Sample:	Dodecane
Oxidation temperature:	140 °C
Dilution:	Carbon Disulfide
Injection Size:	1µl
Carrier Gas Split:	40:1
Carrier gas head pressure:	8 p.s.i.
Oven Temperature:	Initial Temperature = 40C for 10 minutes Increasing at 8C per minute Hold at 140C for 30 minutes
Filament Delay:	3 minutes
Filament Total Run Time:	80 minutes
Column:	BP624, 25m, 1.2um

SUMMARY OF PEAKS IDENTIFIED:

A. Unreacted n-dodecane

Compound Name	Formula	S.I.	Retention Time	Peak Area
Dodecane	$C_{12}H_{26}$	91	28.73	95550016

B. Oxidised n-dodecane

Compound Name	Formula	S.I.	Retention Time	Peak Area
Undecane	$C_{11}H_{24}$	91	25.35	2518353
Dodecane	$C_{12}H_{26}$	90	29.02	171985696
Tridecane	$C_{13}H_{28}$	90	31.81	71841680
Dodecanone	$C_{12}H_{24}O$	80	34.85	6870606
Dodecanone	$C_{12}H_{24}O$	92	35.32	3085882
Dodecanone	$C_{12}H_{24}O$	87	35.58	2562810

SI: *Similarity Index*

E 2.7: Gas chromatograph of unreacted and oxidised Australian oil at 120 °C

DETAILS OF ANALYSIS

Sample:	Unreacted Australian oil
Dilution:	Carbon Disulfide
Injection Size:	1µl
Carrier Gas Split:	40:1
Carrier Gas Head Pressure:	8psi
Oven Temperature:	Initial temp = 40C for 10 minutes
	Increase at 8 C per minute
	Hold at 140 C for 30 minutes
Filament Delay:	3 minutes
Filament Total Run Time:	80 minutes
Column:	BP624, 25m, 1.2um

SUMMARY OF PEAKS IDENTIFIED:

Formula	S.I.	R.T	Peak Area
C_6H_{12}	88	3.98	2054104
C_6H_{12}	87	5.12	4669119
C_7H_{16}	94	6.60	1703267
C_7H_{16}	91	8.15	9043127
C_8H_{16}	93	11.37	1127230
C_7H_8	92	11.75	2272115
$C_6H_{12}N_2$	75	12.47	3499220
C_7H_{14}	87	14.40	1327642
C_8H_{10}	88	16.95	2540579
C_9H_{20}	83	17.43	1614435
C_9H_{18}	90	17.93	922944
C_9H_{18}	81	18.95	1618012
$C_{10}H_{22}$	88	21.60	6657
$C_{10}H_{18}$	80	24.31	1238596
$C_{11}H_{24}$	89	25.31	630343
$C_{11}H_{20}$	82	26.30	566996
$C_{10}H_{16}O$	84	26.97	855121
$C_{12}H_{26}$	74	28.67	649168
$C_{13}H_{28}$	77	31.77	434747
$C_{15}H_{28}$	69	36.39	810562
$C_{12}H_{26}$	88	37.02	537830
$C_{16}H_{34}$	77	40.1	432263
$C_{16}H_{34}$	76	42.57	254607

DETAILS OF ANALYSIS

Sample:	Oxidised Australian oil at 120 °C
Dilution:	Carbon Disulfide
Injection Size:	1µl
Carrier Gas Split:	40:1
Carrier Gas Head Pressure:	8psi
Oven Temperature	Initial temp = 40C for 10 minutes
	Increase at 8 C per minute
	Hold at 140 C for 30 minutes
Filament Delay:	3 minutes
Filament Total Run Time:	80 minutes
Column:	BP624, 25m, 1.2um

SUMMARY OF PEAKS IDENTIFIED:

Formula	S.I.	R.T	Peak Area
C_6H_{12}	73	3.92	5638994
C_6H_{12}	81	5.04	10560313
C_7H_{16}	74	6.48	4283398
C_7H_{14}	71	8.03	18085230
$C_6H_{12}O_2$	62	11.29	3177778
C_8H_{18}	67	1241	7377829
$C_6H_8O_2$	62	14.34	1157047
C_7H_8	95	16.89	5746455
C_9H_{18}	67	17.36	4183462
C_9H_{18}	67	18.89	4172177
$C_{10}H_{22}$	74	21.54	3766954
C_8H_{16}	85	22.29	3126322
$C_{10}H_{18}$	79	24.24	2713889
$C_{11}H_{24}$	68	25.24	2897637
$C_{10}H_{16}O$	78	26.86	2266546
$C_{12}H_{26}$	69	28.61	3810288
$C_{13}H_{28}$	67	31.72	1767590
$C_{15}H_{28}$	63	36.33	2226048
$C_{16}H_{34}$	67	39.95	1484965
$C_{16}H_{34}$	71	42.51	775762
$C_{16}H_{34}$	72	46.92	732521

SI: *Similarity Index*

E 2.8: Gas chromatograph of oxidised Australian oil at 140 and 160 °C

DETAILS OF ANALY SIS

Sample:	Oxidised Australian oil at140 °C
Dilution:	Carbon Disulfide
Injection Size:	1µl
Carrier Gas Split:	40:1
Carrier Gas Head Pressure:	8 psi
Oven Temperature: minutes	Initial Temp = 40 °C for 10 increasing at 8 °C per minute to 140 °C for 30 minutes
Filament Delay:	3 minutes
Filament Total Run Time:	80 minutes
Column:	BP 624, 25m, 1.2l

SUMMARY OF PEAKS IDENTIFIED:

Formula	S.I.	RT	Peak Area
C_6H_{12}		3.90	3811152
$C_7H_{12}O_2$		5.03	2068203
C_7H_{16}		5.35	3258568
C_7H_{16}		4.64	4281759
C_7H_{14}		7.99	1746600
C_8H_{18}		10.41	3140542
C_8H_{18}		10.88	2641671
C_8H_{18}		11.26	8371861
$C_{10}H_{13}FO_3$		11.64	1244788
$C_{10}H_{22}O$		12.38	2316852
C_8H_{16}		12.80	1416678
C_8H_{18}		14.32	7043688
C_9H_{18}		15.18	1738763
$C_{11}H_{24}$		15.66	1640563
$C_{10}H_{22}$		16.02	1733670
$C_8H_{14}O$		16.85	1167207
C_9H_{20}		17.33	4635699
C_9H_{18}		17.83	1769422
C_9H_{18}		18.45	2195150
C_9H_{18}		18.87	3915372
$C_{12}H_{24}$		21.51	1887092
$C_{10}H_{18}$		22.25	2750011
$C_{10}H_{16}O$		23.53	1742204
$C_{11}H_{22}$		24.91	933331
$C_{12}H_{24}O$		28.59	3283118
$C_{10}H_{18}O_4$		30.84	1022862
$C_{15}H_{32}$		31.70	1586724
$C_{15}H_{22}O_2$		33.79	2134469
$C_{15}H_{32}$		34.62	873539

DETAILS OF ANALYSIS

Sample:	Oxidised Australian oil at 160 °C
Dilution:	Carbon Disulfide
Injection Size:	1µl
Carrier Gas Split:	40:1
Carrier Gas Head Pressure:	8psi
Oven Temperature:	Initial temp = 40C for 10 minutes Increase at 8 C per minute Hold at 140 C for 30 minutes
Filament Delay:	3 minutes
Filament Total Run Time:	80 minutes
Column:	BP624, 25m, 1.2um

SUMMARY OF PEAKS IDENTIFIED:

Formula	S.I.	R.T	Peak Area
C_6H_{12}	68	3.73	2124586
C8H16O	78	5.08	2159510
C_7H_{16}	80	5.38	2038134
C_7H_{16}	91	6.62	3025070
C_7H_{14}	85	8.06	18476664
C_8H_{16}	84	11.30	11616991
$C_8H_7FO_3$	82	11.68	2585032
C_8H_{16}	91	12.84	1928078
C_8H_{16}	76	14.34	8344226
C_9H_{18}	80	15.20	2579836
C_9H_{20}	83	15.68	2314873
C_9H_{20}	86	16.05	1992012
$C_6H_{14}O$	81	16.87	1065439
C_9H_{20}	72	17.36	6208143
C_9H_{18}	75	17.86	2325906
$C_{12}H_{22}$	76	18.48	3360522
C_9H_{18}	79	18.89	5195846
$C_{10}H_{20}$	71	21.54	5662682
$C_{12}H_{24}$	73	22.26	2321304
$C_{10}H_{16}O$	71	23.54	2522474
$C_{10}H_{18}$	72	24.23	3598046
$C_{11}H_{24}$	85	25.24	2862209
$C_{11}H_{20}$	84	26.23	2080114
$C_{11}H_{22}O$	81	28.60	3954243
$C_{13}H_{28}$	86	31.72	1911345
$C_{13}H_{22}N_2O_2$	88	36.33	1839878
$C_{15}H_{32}$	91	39.96	1081852
$C_{19}H_{40}$	86	42.51	2511951
$C_{15}H_{32}$	84	44.73	874718

$C_{19}H_{40}O_3$		36.32	1758754
$C_{21}H_{44}$		37.37	1683809

$C_{19}H_{40}$	87	46.94	975157
$C_{20}H_{40}O$	88	49.13	134595

E 2.9: Gas chromatograph of unreacted and oxidised oil C at 120 °C

DETAILS OF ANALYSIS

Sample:	Unreacted oil C
Dilution:	Carbon Disulfide
Injection Size:	1µl
Carrier Gas Split:	40:1
Carrier Gas Head Pressure:	8psi
Oven Temperature:	Initial temp = 40C for 10 minutes Increase at 8 C per minute Hold at 140 C for 30 minutes
Filament Delay:	3 minutes
Filament Total Run Time:	80 minutes
Column:	BP624, 25m, 1.2um
Filename:	OILD1

SUMMARY OF PEAKS IDENTIFIED:

Formula	S.I.	R.T	Peak Area
C_6H_{12}	75	3.95	934965
C_6H_{12}	76	5.10	3E+06
C_7H_{16}	76	6.54	2E+06
C_7H_{14}	78	8.08	5E+06
C_7H_8	90	11.73	3E+06
C_8H_{18}	85	12.45	3E+06
C_8H_{16}	75	14.37	922655
C_8H_{10}	88	16.92	2E+06
C_9H_{20}	72	17.38	3E+06
$C_{10}H_{22}$	70	21.57	2E+06
$C_{11}H_{24}$	74	25.26	2E+06
$C_{12}H_{26}$	72	28.64	2E+06
$C_{13}H_{28}$	78	31.74	2E+06
$C_{14}H_{30}$	75	34.67	2E+06
$C_{15}H_{32}$	76	37.41	3E+06
$C_{19}H_{40}$	73	40.15	6E+06
$C_{19}H_{40}$	70	42.43	2E+06
$C_{16}H_{32}$	70	42.54	2E+06
$C_6H_{13}N$	70	44.75	3E+06
$C_{21}H_{44}$	69	46.30	4E+06
$C_{19}H_{40}$	73	46.97	1E+06
$C_{19}H_{40}$	70	48.77	2E+06
$C_{19}H_{40}$	69	49.16	2E+06
$C_{16}H_{32}$	71	51.55	2E+06
$C_{16}H_{32}$	71	51.79	2E+06
$C_{25}H_{52}$	70	55.16	1E+06

DETAILS OF ANALYSIS

Sample:	Oxidised oil C at 120 °C
Dilution:	Carbon Disulfide
Injection Size:	1µl
Carrier Gas Split:	40:1
Carrier Gas Head Pressure:	8psi
Oven Temperature:	Initial temp = 40C for 10 minutes Increase at 8 C per minute Hold at 140 C for 30 minutes
Filament Delay:	3 minutes
Filament Total Run Time:	80 minutes
Column:	BP624, 25m, 1.2um
Filename:	OILD1

SUMMARY OF PEAKS IDENTIFIED:

Formula	S.I.	R.T	Peak Area
C_6H_{12}	73	4.00	1989860
C_6H_{12}	78	5.15	4385072
C_7H_{16}	74	6.61	3469040
C_7H_{14}	75	8.19	9113206
C_7H_8	89	11.81	3951771
C_8H_{18}	85	12.53	4511709
$C_8H_8O_2$	65	14.46	2380992
C_8H_{10}	90	16.99	4064746
C_9H_{20}	69	17.45	3719936
$C_{10}H_{22}$	77	21.64	4212319
$C_{11}H_{24}$	71	25.34	3953281
$C_{12}H_{26}$	68	28.72	5063390
$C_{13}H_{28}$	71	31.83	4986446
$C_{14}H_{30}$	73	34.74	4961122
$C_{20}H_{40}O$	69	36.43	3523171
$C_{15}H_{32}$	72	37.48	5540300
$C_{15}H_{32}$	71	40.07	6015552
$C_{16}H_{34}$	70	42.51	7835878
$C_{19}H_{40}$	70	44.82	8495518
$C_{19}H_{40}$	72	47.04	8787228
$C_{19}H_{40}$	73	48.67	7931310
$C_{21}H_{44}$	72	49.25	6772608
$C_{21}H_{44}$	76	51.91	7607212
$C_{22}H_{46}$	75	55.46	5873716
$C_{23}H_{48}$	77	59.87	5385095

SI: Similarity Index

E 2.10: Gas chromatograph of oxidised oil C at 140 and 160 ℃

DETAILS OF ANALYSIS

Sample:	Oxidised Oil C at140 °C
Dilution:	0.2 ml / 1.4 ml
Injection Size:	1µl
Carrier Gas Split:	40:1
Carrier Gas Head Pressure:	8 psi
Oven Temperature:	Initial Temp = 40 °C for 10 minutes Increasing at 8 °C per minute to 140 °C for 30 minutes
Filament Delay:	3 minutes
Filament Total Run Time:	80 minutes
Column:	BP 624, 25m, 1.2l

SUMMARY OF PEAKS IDENTIFIED:

Formula	S.I.	RT	Peak Area
C_6H_{12}	89	3.94	3572814
C_6H_{12}	75	5.07	9062195
C_7H_{16}	69	5.38	3177168
$C_6H_{14}O_7$	73	5.76	7404979
C_7H_{16}	72	6.51	5830828
C_7H_{14}	71	8.04	14180682
C_8H_{18}	90	10.46	3193300
C_8H_{16}	76	11.3	4146899
C_8H_{18}	71	10.92	1983655
$C_8H_7FO_3$	65	11.68	6881686
C_8H_{18}	85	12.42	7306585
C_9H_{18}	70	14.33	7432784
C_9H_{20}	72	15.69	1830556
C_9H_{20}	69	16.04	1812229
$C_8H_{10}N_2O_2$	73	16.88	7697246
C_9H_{20}	68	17.37	7153412
C_8H_{10}	78	18.09	2271348
C_9H_{18}	72	18.88	5513326
$C_{10}H_{22}O$	73	20.09	4160335
$C_{10}H_{22}O$	71	21.54	10390219
C_9H_{12}	77	22.26	1706592
$C_{11}H_{24}$	70	22.39	1511691
$C_{10}H_{20}$	77	23.04	3647259
$C_{10}H_{16}O$	74	24.2	2626425
$C_{11}H_{24}$	75	25.24	10261289
$C_{12}H_{26}$	73	28.62	1197583
$C_{13}H_{28}$	76	29.03	3279995
$C_{11}H_{24}$	74	30.86	4518958
$C_{13}H_{28}$	78	31.73	11363082
$C_{15}H_{32}$	73	33.96	3843976
$C_{14}H_{30}$	77	34.66	11639216
$C_{15}H_{32}O$	81	36.33	8692460
$C_{15}H_{32}$	82	37.38	13564214
$C_{15}H_{32}$	86	39.98	12595675

DETAILS OF ANALYSIS

Sample:	Oxidised oil C at 160 °C
Dilution:	Carbon Disulfide
Injection Size:	1µl
Carrier Gas Split:	40:1
Carrier Gas Head Pressure:	8psi
Oven Temperature:	Initial temp = 40C for 10 minutes Increase at 8 C per minute Hold at 140 C for 30 minutes
Filament Delay:	3 minutes
Filament Total Run Time:	80 minutes
Column:	BP624, 25m, 1.2um

SUMMARY OF PEAKS IDENTIFIED:

Formula	S.I.	R.T	Peak Area
C_6H_{12}	75	3.93	1785106
C_6H_{12}	76	5.05	9326427
C_7H_{16}	87	5.38	3325578
$C_6H_{14}O_2$	83	5.76	4157177
C_7H_{14}	79	6.11	2417553
C_7H_{16}	81	6.50	6499607
C_7H_{14}	80	8.04	16243378
C_8H_{18}	82	10.43	3683402
C_8H_{18}	84	10.90	2244640
C_8H_{16}	79	11.29	4458358
$C_8H_7FO_3$	80	11.67	8400275
C_8H_{18}	81	12.41	8480383
C_8H_{16}	78	12.81	637756
C_9H_{20}	77	13.88	1212742
C_9H_{18}	74	14.33	6586474
$C_{11}H_{24}$	76	15.67	2121580
C_9H_{20}	78	16.03	1916865
C_8H_{10}	83	16.48	1071994
C_8H_{10}	82	16.86	6899256
C_9H_{20}	87	17.35	8160061
C_9H_{18}	85	17.85	1137812
C_8H_{10}	89	18.07	2593022
$C_{12}H_{22}$	93	18.47	1991958
C_9H_{18}	92	18.86	5397071
$C_{10}H_{22}O$	83	20.07	4048315
$C_{10}H_{20}$	91	21.06	3121901
$C_{12}H_{24}O$	90	21.53	9859305
C_9H_{12}	94	22.25	1479783
$C_{11}H_{24}$	83	22.37	1816982
$C_{11}H_{24}$	81	23.01	2738392
$C_{10}H_{20}O_2S$	67	23.93	1035747
$C_{11}H_{24}$	76	23.79	723419
$C_{11}H_{22}$	74	23.67	1900798
$C_{12}H_{26}$	73	25.22	8128038

$C_{15}H_{32}$	88	41.14	6112784
$C_{15}H_{32}$	90	42.43	21640336
$C_{15}H_{32}$	91	44.74	15607292
$C_{19}H_{40}$	74	46.95	10864349
$C_{21}H_{44}$	73	49.16	10236847
$C_{21}H_{44}$	78	51.81	9657281
$C_{21}H_{44}$	69	55.14	8704470
$C_{21}H_{44}$	80	59.46	7729443

$C_{13}H_{28}$	76	26.75	2160650
$C_{11}H_{22}$	77	28.59	8506114
$C_{13}H_{28}$	74	29.00	2331307
$C_{15}H_{32}$	78	30.84	3089094
$C_{14}H_{30}$	79	31.71	8058573
$C_{19}H_{40}$	82	33.94	2553540
$C_{21}H_{44}$	84	34.62	9291015
$C_{17}H_{36}$	79	36.31	5854482
$C_{17}H_{36}$	75	37.36	9350708
$C_{21}H_{44}$	72	39.07	2670974
$C_{21}H_{44}$	71	39.93	8402734
$C_{19}H_{40}$	69	41.13	4080842
$C_{19}H_{40}$	68	42.39	14330757
$C_{19}H_{40}$	73	44.71	6935224
$C_{21}H_{44}$	76	44.94	6469340
$C_{21}H_{44}$	79	49.11	5705320
$C_{21}H_{44}$	82	51.76	6137108
$C_{21}H_{44}$	79	55.09	5564778
$C_{21}H_{44}$	74	59.39	4884800

E 2.11: Gas chromatograph of unreacted and oxidised oil D at 120 °C (46 hrs)

DETAILS OF ANALYSIS

Sample:	Unreacted oil D
Dilution:	Carbon Disulfide
Injection Size:	1µl
Carrier Gas Split:	40:1
Carrier Gas Head Pressure:	8psi
Oven Temperature:	Initial temp = 40C for 10 minutes Increase at 8 C per minute Hold at 140 C for 30 minutes
Filament Delay:	3 minutes
Filament Total Run Time:	80 minutes
Column:	BP624, 25m, 1.2um

SUMMARY OF PEAKS IDENTIFIED:

Formula	S.I.	RT	Peak area
C_6H_{12}	90	3.96	3137372
C_6H_{12}	87	5.10	7799076
C_7H_{16}	94	6.56	9121593
C_7H_{14}	91	8.10	17885666
C_8H_{18}	88	11.75	7521791
C_8H_{10}	88	12.50	11597093
C_9H_{20}	88	16.96	8132083
$C_{10}H_{22}$	83	17.44	8256940
$C_{11}H_{24}$	93	21.64	9610024
$C_{12}H_{26}$	92	25.34	8625500
$C_{13}H_{28}$	94	28.72	9363839
$C_{14}H_{30}$	92	31.85	8801315
$C_{15}H_{32}$	89	34.76	8672568
$C_{15}H_{32}$	91	36.47	6043815
$C_{16}H_{34}$	86	37.50	8445258
$C_{17}H_{36}$	83	40.09	9941508
$C_{17}H_{36}$	87	41.27	3703657
$C_{19}H_{40}$	85	42.54	6127466
$C_{19}H_{40}$	84	44.87	8471651
$C_{21}H_{44}$	89	47.10	8226599
$C_{21}H_{44}$	92	49.31	7825864
$C_{21}H_{44}$	79	52.01	6335792
$C_{21}H_{44}$	84	55.41	5243528

SI: *Similarity Index*

DETAILS OF ANALYSIS

Sample:	sample: oxidised oil D (120 °C)(46 hrs)
Dilution:	Carbon Disulfide
Injection Size:	1µl
Carrier Gas Split:	40:1
Carrier Gas Head Pressure:	8psi
Oven Temperature:	Initial temp = 40C for 10 minutes Increase at 8 C per minute Hold at 140 C for 30 minutes
Filament Delay:	3 minutes
Filament Total Run Time:	80 minutes
Column:	BP624, 25m, 1.2um

SUMMARY OF PEAKS IDENTIFIED:

Formula	S.I.	RT	Peak area
C_6H_{12}	92	3.96	1171269
$C_6H_{16}O_2$	93	5.09	3672825
C_7H_{16}	91	6.56	4131886
C_7H_{14}	89	8.09	8510618
C_7H_8	86	11.73	3669766
C_8H_{18}	89	12.47	6005030
C_8H_{10}	91	16.93	4258584
C_9H_{20}	93	17.42	4906964
$C_{10}H_{22}$	91	21.61	4872188
$C_{11}H_{24}$	90	25.30	5403136
$C_{12}H_{26}$	88	28.68	6491588
$C_{13}H_{28}$	90	31.80	6449714
$C_{14}H_{30}$	91	34.71	6849678
$C_{15}H_{32}$	93	36.40	46448555
$C_{15}H_{32}$	87	37.46	7945708
$C_{16}H_{34}$	82	40.04	7794288
$C_{17}H_{36}$	85	41.22	3354586
$C_{17}H_{36}$	83	42.48	5785580
$C_{19}H_{40}$	81	44.83	6911306
$C_{19}H_{40}$	86	47.04	6816690
$C_{21}H_{44}$	89	49.24	6606203
$C_{21}H_{44}$	92	51.90	5405704
$C_{21}H_{44}$	86	55.28	4937704
$C_{21}H_{44}$	90	59.28	4710282

E 2.12: Gas chromatograph of oxidised oil D at 120 °C (78 and 100 hrs)

DETAILS OF ANALYSIS

Sample:	sample: oxidised oil D (120 °C)(78 hrs)
Dilution:	Carbon Disulfide
Injection Size:	1µl
Carrier Gas Split:	40:1
Carrier Gas Head Pressure:	8psi
Oven Temperature:	Initial temp = 40C for 10 minutes Increase at 8 C per minute Hold at 140 C for 30 minutes
Filament Delay:	3 minutes
Filament Total Run Time:	80 minutes
Column:	BP624, 25m, 1.2um
Filename:	OREAC025

SUMMARY OF PEAKS IDENTIFIED:

Formula	S.I.	RT	Peak area
C_6H_{12}	89	3.95	1302452
$C_8H_{16}O_2$	92	5.09	3197220
C_7H_{16}	89	6.55	3769448
C_7H_{14}	91	8.09	8714282
C_7H_8	88	11.73	4388429
C_8H_{18}	91	12.48	7739170
C_8H_{10}	91	16.95	4791821
C_9H_{20}	90	17.43	7105462
$C_{10}H_{22}$	93	21.62	12359621
$C_{11}H_{24}$	88	25.34	10486851
$C_{12}H_{26}$	89	28.72	10746564
$C_{13}H_{28}$	91	31.83	9744670
$C_{14}H_{30}$	88	34.76	9876463
$C_{15}H_{32}$	90	36.45	5886502
$C_{15}H_{32}$	85	37.50	13597926
$C_{16}H_{34}$	86	40.08	3885376
$C_{17}H_{36}$	84	41.26	3847291
$C_{17}H_{36}$	86	42.53	4165338
$C_{19}H_{40}$	83	44.87	1002543
$C_{19}H_{40}$	88	47.08	9843592
$C_{21}H_{44}$	91	49.29	9391304
$C_{21}H_{44}$	90	52.00	7628156
$C_{21}H_{44}$	89	55.41	6404536
$C_{21}H_{44}$	88	59.82	5761840

DETAILS OF ANALYSIS

Sample:	sample: oxidised oil D (120 °C)(100 hrs)
Dilution:	Carbon Disulfide
Injection Size:	1µl
Carrier Gas Split:	40:1
Carrier Gas Head Pressure:	8psi
Oven Temperature:	Initial temp = 40C for 10 minutes Increase at 8 C per minute Hold at 140 C for 30 minutes
Filament Delay:	3 minutes
Filament Total Run Time:	80 minutes
Column:	BP624, 25m, 1.2um
Filename:	OREAC025

SUMMARY OF PEAKS IDENTIFIED:

Formula	S.I.	RT	Peak area
C_6H_{12}	85	3.97	1634704
$C_8H_{16}O_2$	89	5.12	5332540
C_7H_{16}	87	6.59	6309538
C_7H_{14}	86	8.15	13027633
$C_7H_{12}O$	90	11.76	5009582
C_8H_{18}	86	12.51	8217637
C_8H_{16}	88	14.42	20172741
C_8H_{10}	78	16.97	5165700
C_9H_{20}	89	17.44	5277339
$C_{10}H_{22}$	88	21.64	4387239
$C_{11}H_{24}$	83	25.34	4667734
$C_{12}H_{26}$	89	28.71	5237225
$C_{13}H_{28}$	79	31.83	5184092
$C_{14}H_{30}$	78	34.76	5640438
$C_{15}H_{32}$	74	36.45	2701089
$C_{16}H_{34}$	78	40.09	6919116
$C_{17}H_{36}$	82	41.27	2857036
$C_{17}H_{36}$	79	42.54	5813222
$C_{19}H_{40}$	81	42.64	3656026
$C_{19}H_{40}$	80	44.85	8128732
$C_{21}H_{44}$	84	45.07	4342153
$C_{21}H_{44}$	89	47.08	8470802
$C_{21}H_{44}$	86	49.29	8370270
$C_{21}H_{44}$	88	51.99	6932584
$C_{21}H_{44}$	86	55.39	6445432
$C_{21}H_{44}$	79	59.77	4863495

SI: Similarity Index

E 2.13: Gas chromatograph of oxidised oil D at 140 and 160 °C

DETAILS OF ANALYSIS

Sample: Oxidised Oil D at140 °C
Dilution: 0.2 ml / 1.4 ml
Injection Size: 1μl
Carrier Gas Split: 40:1
Carrier Gas Head Pressure: 8 psi
Oven Temperature: Initial Temp = 40 oC for 10 minutes increasing at 8 oC per minute to 140 oC for 30 minutes
Filament Delay: 3 minutes
Filament Total Run Time: 80 minutes
Column: BP 624, 25m, 1.2l

SUMMARY OF PEAKS IDENTIFIED:

Formula	S.I.	RT	Peak Area
C_6H_{12}	87	3.91	1914667
C_6H_{12}	84	5.01	4528010
C_7H_{16}	89	5.35	2141054
$C_6H_{14}O_2$	91	5.72	1882795
C_7H_{14}	92	6.06	1017933
C_7H_{18}	85	6.47	4969854
C_7H_{14}	83	7.98	9750380
C_8H_{18}	88	10.40	3221604
C_8H_{18}	91	10.87	2069509
C_8H_{16}	76	11.25	3510168
$C_8H_7FO_3$	90	11.64	6692501
C_8H_{18}	92	12.38	7539586
C_9H_{18}	93	14.31	4661840
$C_{11}H_{24}$	91	15.67	2198679
C_9H_{20}	89	16.02	2047427
C_8H_{10}	87	16.85	5030246
C_9H_{20}	85	17.33	7635044
C_9H_{18}	79	18.87	3531306
$C_{10}H_{22}$	83	21.52	7839437
C_9H_{12}	86	22.23	1757965
$C_{11}H_{24}$	89	22.37	1360304
$C_{10}H_{20}$	91	23.01	1454754
$C_{10}H_{16}O$	78	24.17	236408
$C_{11}H_{24}$	90	25.23	8319533
$C_{12}H_{26}$	86	28.59	1.2E+07
$C_{10}H_{20}O_2S$	83	29.00	2032128
$C_{11}H_{24}$	87	30.85	3052384
$C_{13}H_{28}$	91	31.72	9351104
$C_{16}H_{20}O$	78	33.79	1994393
$C_{15}H_{32}$	89	33.95	2183357
$C_{14}H_{30}$	91	34.63	9134719
$C_{19}H_{40}$	88	36.32	5731138
$C_{15}H_{32}$	84	37.37	9164244
$C_{15}H_{32}$	86	39.95	9152949

DETAILS OF ANALYSIS

Sample: Oxidised Oil D at160 °C
Dilution: 0.2 ml / 1.4 ml
Injection Size: 1μl
Carrier Gas Split: 40:1
Carrier Gas Head Pressure: 8 psi
Oven Temperature: Initial Temp = 40 oC for 10 minutes increasing at 8 oC per minute to 140 oC for 30 minutes
Filament Delay: 3 minutes
Filament Total Run Time: 80 minutes
Column: BP 624, 25m, 1.2l

SUMMARY OF PEAKS IDENTIFIED:

Formula	S.I.	RT	Peak Area
C_6H_{12}	90	3.88	407417
C_6H_{12}	92	5.00	1068406
C_7H_{16}	90	5.33	650746
$C_6H_{14}O_2$	88	5.75	5700198
C_7H_{14}	86	6.05	491172
C_7H_{16}	90	6.43	1526622
C_7H_{14}	86	7.95	3408321
C_8H_{18}	87	10.37	1807216
C_8H_{16}	91	11.22	1978515
C_7H_8	89	11.60	3032954
C_8H_{18}	88	12.35	4896544
C_9H_{18}	84	14.28	4400596
$C_8H_{14}O$	89	16.82	6015776
$C_{13}H_{28}O$	79	17.83	4635953
C_8H_{10}	88	18.05	2155524
$C_{10}H_{22}O$	89	20.03	8485509
$C_{10}H_{22}$	91	21.48	6471458
$C_{10}H_{11}NO$	86	22.34	3695928
$C_{10}H_{20}$	91	22.98	2307405
$C_{11}H_{24}$	89	25.18	6927585
$C_{12}H_{26}$	90	28.56	7401470
$C_{13}H_{28}$	87	28.98	2027475
$C_{11}H_{24}$	88	30.82	2735176
$C_{13}H_{28}$	91	31.67	7476547
$C_{15}H_{32}$	92	33.92	2745480
$C_{15}H_{32}$	89	34.58	9035855
$C_{19}H_{40}$	90	36.29	5450930
$C_{14}H_{30}$	87	37.33	10093987
$C_{15}H_{32}$	90	39.92	8434198
$C_{15}H_{32}$	91	41.10	4094036
$C_{19}H_{40}$	85	42.36	15505374
$C_{21}H_{44}$	87	44.68	11008467
$C_{21}H_{44}$	88	46.90	7573056
$C_{19}H_{40}$	90	49.08	5580310

$C_{15}H_{32}$	89	41.13	3405435
$C_{21}H_{44}$	79	52.40	1.4E+07
$C_{19}H_{40}$	92	44.72	7228915
$C_{15}H_{32}$	87	44.92	3144646
$C_{19}H_{40}$	83	46.94	7144548
$C_{19}H_{40}$	87	49.12	7064111
$C_{21}H_{44}$	84	51.77	9876613
$C_{21}H_{44}$	82	55.11	6046102
$C_{21}H_{44}$	89	59.42	5145392

$C_{21}H_{44}$	91	51.72	8695298
$C_{21}H_{44}$	93	55.05	5198606
$C_{21}H_{44}$	89	59.32	607614

E 2.14: Gas chromatograph of unreacted and oxidised Esso Mix1 at 120 °C

DETAILS OF ANALYSIS

Sample:	Unreacted Esso Mix1 oil
Dilution:	Carbon Disulfide
Injection Size:	1μl
Carrier Gas Split:	40:1
Carrier Gas Head Pressure:	8psi
Oven Temperature:	Initial temp = 40C for 10 min. Increase at 8 C per minute Hold at 140 C for 30 minutes
Filament Delay:	3 minutes
Filament Total Run Time:	80 minutes
Column:	BP624, 25m, 1.2um

SUMMARY OF PEAKS IDENTIFIED:

Formula	S.I.	RT	Peak Area
C_6H_{12}	90	3.92	2093706
$C_8H_{16}O$	87	5.03	2592355
C7H16	94	5.35	2247052
$C_8H_{14}O_2$	91	5.74	1952442
C_7H_{16}	88	6.48	5187666
C_7H_{14}	88	8.00	5790894
C_7H_8	88	11.65	4705906
C_8H_{18}	83	12.4	6031080
C_9H_{20}	93	13.86	763290
C_9H_{18}	92	14.31	3315571
C_9H_{20}	94	15.67	1436251
C_9H_{20}	92	16.02	1318944
C_8H_{10}	89	16.48	1692883
C_8H_{10}	91	16.86	3669594
C_9H_{20}	86	17.33	5133376
C_8H_{10}	83	18.07	1719397
C12H24	87	18.81	2755578
$C_{12}H_{26}O$	79	20.07	1893686
$C_{10}H_{22}$	85	20.37	655485
C_9H_{12}	83	20.52	871303
C_9H_{12}	86	20.87	1613336
C10H20	87	21.52	4810419
$C_{11}H_{24}$	90	25.22	4705812
$C_{12}H_{26}$	91	28.6	4572635
$C_{13}H_{28}$	87	31.7	4640378
$C_{12}H_{25}$	86	34.63	4705892
$C_{11}H_{24}$	89	37.37	6736060
$C_{15}H_{32}$	88	39.95	4863907
$C_{17}H_{36}$	85	42.4	6507267
$C_{19}H_{40}$	87	44.73	4096628
$C_{19}H_{40}$	90	44.92	2317794

DETAILS OF ANALYSIS

Sample:	Oxidised Esso Mix1 oil at 120 °C
Dilution:	Carbon Disulfide
Injection Size:	1μl
Carrier Gas Split:	40:1
Carrier Gas Head Pressure:	8psi
Oven Temperature:	Initial temp = 40C for 10 min. Increase at 8 C per minute Hold at 140 C for 30 minutes
Filament Delay:	3 minutes
Filament Total Run Time:	80 minutes
Column:	BP624, 25m, 1.2um

SUMMARY OF PEAKS IDENTIFIED:

Formula	S.I.	RT	Peak Area
C_6H_{12}	88	3.93	2399446
C_6H_{12}	89	5.07	4271119
C_7H_{16}	92	5.39	2696786
C_7H_{16}	89	6.51	4574058
C_7H_{14}	90	8.04	5205149
C_7H_8	86	11.68	6356220
C_8H_{18}	90	12.42	5004034
C_9H_{20}	86	13.9	796331
C_9H_{18}	90	14.33	3115448
C11H24	89	15.67	1274303
C_8H_{10}	91	16.05	1444100
C_8H_{10}	89	16.5	1639712
$C_8H_{14}O$	90	16.88	4222626
C_9H_{20}	90	17.34	5164626
C_8H_{10}	88	18.09	1836292
$C_{12}H_{26}O$	87	18.83	3075601
$C_{12}H_{26}O$	89	20.09	2261775
$C_{10}H_{22}$	84	20.38	769114
C_9H_{12}	86	20.53	851860
C_9H_{12}	85	20.88	1663487
$C_{10}H_{11}NO$	89	21.54	6889575
$C_{11}H_{24}$	88	25.23	5445280
$C_{12}H_{26}$	88	28.59	5855702
$C_{13}H_{28}$	89	31.7	5499113
$C_{10}H_{20}O_2S$	90	30.85	1927946
$C_{12}H_{25}$	89	34.63	5681624
$C_{11}H_{24}$	91	37.37	7135518
$C_{15}H_{32}$	90	39.96	5368678
$C_{15}H_{32}$	87	42.4	6242646
$C_{15}H_{32}$	89	44.74	3153897
$C_{19}H_{40}$	87	46.96	1613313

$C_{19}H_{40}$	89	46.94	4088286	$C_{19}H_{40}$	88	49.14	1506887
$C_{21}H_{44}$	90	49.13	3933232	$C_{21}H_{44}$	90	51.77	1591237
$C_{15}H_{32}O$	92	51.76	1687295	$C_{43}H_{88}$	89	55.11	2523771
$C_{43}H_{88}$	87	55.09	3126816	$C_{21}H_{44}$	78	59.42	299492

SI: Similarity Index

E 2.15: Gas chromatograph of unreacted and oxidised Esso Mix1 at 140 and 160 °C

DETAILS OF ANALYSIS

Sample:	Oxidised Esso Mix1 oil at 140 °C
Dilution:	0.2 ml / 1.4 ml
Injection Size:	1μl
Carrier Gas Split:	40:1
Carrier Gas Head Pressure:	8 psi
Oven Temperature:	Initial Temp = 40 °C for 10 minutes increasing at 8 °C per minute to 140 °C for 30 minutes
Filament Delay:	3 minutes
Filament Total Run Time:	80 minutes
Column:	BP 624, 25m, 1.2l

SUMMARY OF PEAKS IDENTIFIED:

Formula	S.I.	RT	Peak Area
C_6H_{12}	90	3.92	2002106
C_6H_{12}	89	5.03	3699940
C_7H_{16}	92	5.35	1796199
$C_6H_{14}O_2$	91	5.74	2108613
C_7H_{14}	88	6.09	739582
C_7H_{16}	87	6.48	3796758
C_7H_{14}	86	8.00	5031944
C_9H_{20}	90	10.42	1201836
C_8H_{18}	92	10.89	1160079
C_8H_{16}	85	11.27	1591780
$C_8H_7FO_3$	87	11.65	3087032
C_8H_{18}	89	12.38	3937257
C_8H_{18}	92	14.31	1111765
$C_{11}H_{24}$	88	15.69	445144
$C_{10}H_{22}$	79	16.04	546874
C_8H_{10}	83	16.50	452697
$C_8H_{14}O$	85	16.86	1422945
C_9H_{20}	86	17.33	1941306
C_8H_{10}	89	18.09	637859
$C_{12}H_{24}$	92	18.81	1133295
$C_{12}H_{26}O$	91	20.08	641472
$C_{13}H_{28}$	90	21.51	1447204
C_9H_{12}	92	22.26	317066
$C_{11}H_{24}$	90	22.38	268856
$C_{12}H_{24}$	88	23.03	510663
$C_{10}H_{16}O$	89	24.19	673964
$C_{11}H_{24}$	87	25.22	1984150
$C_{12}H_{26}$	90	28.59	2232494
$C_{13}H_{24}O_4$	86	29.01	411251
$C_{10}H_{20}O_2S$	83	30.85	1448999
$C_{13}H_{28}$	87	31.71	3953193
C13H26O	89	33.80	949729
C21H44	92	33.95	1103724

DETAILS OF ANALYSIS

Sample:	Oxidised Esso Mix1 oil at 160 °C
Dilution:	Carbon Disulfide
Injection Size:	1μl
Carrier Gas Split:	40:1
Carrier Gas Head Pressure:	8psi
Oven Temperature:	Initial temp = 40C for 10 minutes Increase at 8 C per minute Hold at 140 C for 30 minutes
Filament Delay:	3 minutes
Filament Total Run Time:	80 minutes
Column:	BP624, 25m, 1.2um

SUMMARY OF PEAKS IDENTIFIED:

Formula	S.I.	RT	Peak Area
C_6H_{12}	89	3.88	2421278
C_6H_{12}	90	4.99	3916931
C_7H_{16}	92	5.33	1952380
$C_6H_{14}O_2$	89	5.69	2088960
C_7H_{14}	88	6.04	758481
C_7H_{16}	92	6.43	3977298
C_7H_{14}	91	7.95	5230498
C_8H_{18}	87	10.38	2389221
C_8H_{18}	86	10.85	1526909
C_8H_{16}	89	11.23	2115250
$C_8H_7FO_3$	85	11.61	5643158
C_8H_{18}	86	12.36	5453330
C_9H_{20}	87	13.82	850638
C_8H_{16}	89	14.27	2177181
C_9H_{18}	84	14.39	596061
C_9H_{20}	83	15.64	1412552
C_9H_{20}	90	15.98	1542568
C_8H_{10}	84	16.45	1562728
C_8H_{10}	86	16.83	3781453
C_9H_{20}	89	17.29	5347554
C_8H_{10}	87	18.04	1571560
$C_{12}H_{24}$	90	18.78	2442781
C_9H_{12}	91	20.83	1644575
$C_{12}H_{26}O$	89	20.04	2283173
$C_{13}H_{28}$	90	21.49	5305060
C_9H_{12}	88	22.21	1205181
$C_{11}H_{24}$	91	22.35	954375
$C_{12}H_{26}$	90	22.99	978648
$C_{16}H_{26}O_3$	88	24.15	1820625
$C_{11}H_{24}$	90	25.19	5508166
$C_{12}H_{26}$	88	28.57	5902459
$C_{13}H_{24}O_4$	89	28.98	1194855
$C_{10}H_{20}O_2S$	88	30.8	1759557

$C_{15}H_{32}$	91	34.62	3747994
$C_{15}H_{34}$	93	37.36	2660788
$C_{17}H_{36}$	89	39.95	2243225
$C_{17}H_{36}$	92	42.40	3041383
$C_{21}H_{44}$	90	44.72	1910378
$C_{21}H_{44}$	92	44.92	869426
$C_{21}H_{44}$	89	46.93	1728060
$C_{21}H_{44}$	91	49.13	1547742
$C_{15}H_{32}O$	88	51.77	4222548
$C_{43}H_{88}$	92	55.10	1183872
$C_{23}H_{48}$	93	59.41	830659

$C_{13}H_{28}$	90	31.67	5580988
$C_{12}H_{10}O$	80	33.76	1681715
$C_{15}H_{32}$	86	33.92	1514775
$C_{17}H_{36}$	87	34.58	5751251
C15H32O	83	36.29	3216281
$C_{17}H_{36}$	90	37.34	5723727
$C_{17}H_{36}$	89	39.91	5866506
$C_{21}H_{44}$	88	42.35	7527655
$C_{21}H_{44}$	86	44.68	4768660
$C_{21}H_{44}$	88	44.89	2503904
$C_{21}H_{44}$	90	46.89	4509070
$C_{21}H_{44}$	91	49.08	4210992
$C_{15}H_{32}O$	86	51.71	7575627
$C_{43}H_{88}$	89	55.04	3655310
$C_{21}H_{44}$	90	59.32	3117878

SI: Similarity Index

Appendix F

Appendix F

Analysis result of single organic compound and light crude oil samples using Perkin Elmer 8500 Gas Chromatograph

F.1: Analysis result of hexane

Unreacted hexane

RT	Run 1 Peak Area	Run 1 Amount (%)	Run 2 Peak Area	Run 2 Amount (%)	Run 3 Peak Area	Run 3 Amount (%)	Average Defined Area	Average Weight Percent
0.1	1028	25.4306	1106.856	27.34	1084.37	26.7839	1072.919	26.52
0.2	3004	74.1921	2927.728	72.31	2963.38	73.1955	2964.947	73.23

Oxidised hexane at 140 °C

RT	Run 1 Peak Area	Run 1 Amount (%)	Run 2 Peak Area	Run 2 Amount (%)	Run 3 Peak Area	Run 3 Amount (%)	Average Defined Area	Average Weight Percent
0.1	1336	32.9879	1352.729	33.41	1248.88	30.8473	1312.383	32.42
0.2	1021	25.2215	976.5223	24.12	952.972	23.5384	983.5358	24.29
0.4	1272	31.4117	1316.381	32.51	1246.28	30.7832	1278.131	31.57
0.4	1860	9.1117	1968.082	9.644	2160.06	10.5843	1995.891	9.78

F.2: Analysis result of xylene

Unreacted xylene

RT	Run 1 Peak Area	Run 1 Amount (%)	Run 2 Peak Area	Run 2 Amount (%)	Run 3 Peak Area	Run 3 Amount (%)	Average Defined Area	Average Weight Percent
0.8	3067	15.0303	2989.518	14.65	3032.49	14.8592	3029.805	14.85
1.2	17268	84.82	17570.9	86.1	17445.5	85.4829	17428.13	85.47

Oxidised xylene at 140 °C

RT	Run 1 Peak Area	Run 1 Amount (%)	Run 2 Peak Area	Run 2 Amount (%)	Run 3 Peak Area	Run 3 Amount (%)	Average Defined Area	Average Weight Percent
0.8	8688	42.4977	8467.071	41.49	8502.46	41.6621	8552.418	41.88
1.2	9617	47.1226	9809	48.06	9734.85	47.7007	9720.235	47.63
3.4	2786	10.4839	2591.583	9.589	2661.95	9.8492	2679.924	9.97

F.3: Analysis result of iso-butylbenzene

Unreacted iso-butylbenzene

RT	Run 1 Peak Area	Run 1 Amount (%)	Run 2 Peak Area	Run 2 Amount (%)	Run 3 Peak Area	Run 3 Amount (%)	Average Defined Area	Average Weight Percent
2.6	33393	60.4191	33238.39	59.83	33348.4	60.0271	33326.74	60.09
3.1	21394	39.3521	22236.28	40.03	22073.8	39.7328	21901.31	39.70

Oxidised iso-butylbenzene at 140 °C

RT	Run 1 Peak Area	Run 1 Amount (%)	Run 2 Peak Area	Run 2 Amount (%)	Run 3 Peak Area	Run 3 Amount (%)	Average Defined Area	Average Weight Percent
2.7	22156	39.8804	21545.6	38.78	21441.1	38.5938	21714.17	39.09
3.1	15291	27.5239	16159.57	29.09	16096.6	28.9738	15849.07	28.53
5.2	5135	17.4573	5151.549	17.52	5249.76	17.8492	5178.61	17.61
6.4	4234	14.3957	4205.939	14.3	4243.85	14.4291	4227.945	14.38

F.4: Analysis result of n-hexylbenzene

Unreacted n-hexylbenzene

RT	Run 1 Peak Area	Run 1 Amount (%)	Run 2 Peak Area	Run 2 Amount (%)	Run 3 Peak Area	Run 3 Amount (%)	Average Defined Area	Average Weight Percent
5.9	9219	31.3459	8992.882	30.58	9360.21	31.8247	9190.83	31.25
6.3	19948	67.8212	20176.53	68.6	19736.5	67.1042	19953.53	67.84

Oxidised n-hexylbenzene at 140 °C

RT	Run 1 Peak Area	Run 1 Amount (%)	Run 2 Peak Area	Run 2 Amount (%)	Run 3 Peak Area	Run 3 Amount (%)	Average Defined Area	Average Weight Percent
5.9	8161	28.3109	8489.613	28.86	8848.91	30.0863	8499.797	29.09
6.3	10605	36.0583	10896.78	37.05	10214.5	34.7294	10572.24	35.95
7.8	5578	34.6307	5737.08	35.57	5646.84	35.0104	5653.886	35.07

F.5: Analysis result of n-dodecane

Unreacted dodecane

RT	Run 1 Peak Area	Run 1 Amount (%)	Run 2 Peak Area	Run 2 Amount (%)	Run 3 Peak Area	Run 3 Amount (%)	Average Defined Area	Average Weight Percent
5.5	13491	44.8705	13137.42	44.67	14014.6	47.6495	13547.78	45.73
5.9	15671	53.2781	15284.48	51.97	16382.5	55.7005	15779.18	53.65

Oxidised dodecane at 140 °C

RT	Run 1 Peak Area	Run 1 Amount (%)	Run 2 Peak Area	Run 2 Amount (%)	Run 3 Peak Area	Run 3 Amount (%)	Average Defined Area	Average Weight Percent
5.5	6974	23.7116	6645.029	22.59	6783.5	23.0639	6800.839	23.12
5.9	10369	35.2543	10308.29	35.05	10566.3	35.9253	10414.49	35.41
6.6	4013	13.6452	3831.853	13.03	4126	14.0284	3990.386	13.57
7.1	3380	11.4915	3581.824	12.18	3249.5	11.0483	3403.726	11.57
7.3	4654	15.8235	4487.088	15.26	4717.12	16.0382	4619.392	15.71

F.6: Analysis result of unreacted Australian oil

Carbon Number	RT	Run 1 Amount	Run 2 Amount	Run 3 Amount	Average weight %	Defined Percent
C6	0.22	14.6873	14.3292	14.6505	14.55155	19.9283
C7	0.34	9.7657	9.8852	9.7064	9.63695	13.19777
C8	0.68	2.3735	2.4404	2.1771	2.327875	3.188017
C9	1.7	2.671	2.697	2.417	2.587225	3.543196
C10	2.96	2.3562	2.2793	2.3062	2.3139	3.168878
C10	3.34	3.7086	3.8135	4.0376	3.853233	5.27699
C10	4.15	4.0245	4.0131	4.2661	4.101233	5.616625
C11	4.37	2.124	2.3259	2.4272	2.292367	3.139388
C11	5.1	2.6226	2.5825	2.6521	2.619067	3.586803
C11	5.29	2.2536	2.1195	2.3135	2.228867	3.052425
C12	5.57	1.9032	1.8765	1.8628	1.880833	2.575795
C12	6.2	4.652	4.5094	4.7526	4.638	6.351725
C13	6.63	1.8055	1.8524	1.8865	1.848133	2.531012
C13	7.3	3.7172	3.6666	3.7532	3.712333	5.084028
C14	7.48	2.5163	2.4519	2.5716	2.513267	3.44191
C14	7.81	1.6969	1.7034	1.7101	1.703467	2.332892
C14	8.09	2.2867	2.1649	2.3633	2.271633	3.110994
C15	8.39	3.8708	3.7604	3.7103	3.7805	5.177382
C16	9.2	1.9017	1.8643	1.8204	1.862133	2.550185
C17	9.63	2.3053	2.2943	2.2913	2.296967	3.145688

F.7: Analysis result of oxidised Australian oil at 120 °C

Carbon Number	RT	Run 1 Amount	Run 2 Amount	Run 3 Amount	Average weight %	Defined Percent
C7	0.29	5.1411	5.1842	5.2711	5.20	9.61
C8	0.62	2.6851	2.7419	2.9082	2.78	5.14
C8	0.76	1.9148	1.8057	1.8844	1.87	3.45
C10	2.44	3.3339	3.1977	3.3023	3.28	6.06
C10	2.94	2.2901	2.1863	2.1642	2.21	4.09
C10	3.34	3.1476	3.0524	3.1373	3.11	5.75
C11	4.13	3.1052	2.9796	3.051	3.05	5.63
C11	4.34	2.3132	2.2854	2.2164	2.27	4.20
C12	5.08	2.0842	1.9602	2.0378	2.03	3.75
C12	5.27	3.6342	3.5425	3.6079	3.59	6.65
C12	5.55	1.9338	1.9076	1.8943	1.91	3.53
C13	6.27	3.6196	3.5864	3.6342	3.61	6.68
C13	6.57	1.9214	1.8915	1.9836	1.93	3.57
C14	7.29	3.1932	3.1708	3.1869	3.18	5.89
C14	7.45	2.1043	2.118	2.1745	2.13	3.94
C15	8.06	2.7652	2.1858	2.7808	2.58	4.76
C15	8.37	3.2021	3.1531	3.1426	3.17	5.85
C16	9.18	1.907	1.9735	2.0361	1.97	3.65
C16	9.59	1.9549	1.9732	1.9486	1.96	3.62
C17	10.03	2.2	2.281	2.2771	2.25	4.16

F.8: Analysis result of oxidised Australian oil at 140 °C

Carbon Number	RT	Run 1 Amount	Run 2 Amount	Run 3 Amount	Average weight %	Defined Percent
C7	0.29	7.4653	7.5407	7.5844	7.548625	11.93
C8	0.62	3.3375	3.2524	3.1899	3.2797	5.18
C8	0.76	2.2147	2.1441	2.1201	2.183425	3.45
C9	1.77	2.709	2.638	2.5369	2.651075	4.19
C10	2.42	4.1707	4.3333	3.9294	4.144467	6.55
C10	2.95	2.3784	2.5712	2.2901	2.413233	3.81
C10	3.33	3.5296	3.6807	3.7909	3.667067	5.79
C11	4.13	3.4616	3.5853	3.6841	3.577	5.65
C11	4.35	2.4921	2.5366	2.3132	2.4473	3.87
C12	5.08	2.5712	2.6371	2.4438	2.5507	4.03
C12	5.27	1.993	2.1845	2.0427	2.0734	3.28
C12	5.55	2.0375	2.1319	1.9338	2.0344	3.21
C13	6.29	2.6175	2.5899	2.7679	2.658433	4.20
C13	6.58	1.8026	2.0716	1.9214	1.931867	3.05
C14	7.29	3.3404	3.4576	3.5999	3.465967	5.48
C14	7.46	2.4982	2.688	2.5527	2.579633	4.08
C15	8.06	3.0738	3.2733	3.132	3.1597	4.99
C15	8.38	3.7612	3.8556	3.5365	3.717767	5.87
C16	9.18	1.9752	2.0831	1.907	1.988433	3.14
C17	9.6	2.4628	2.5537	2.3456	2.454033	3.88
C17	10.03	2.7537	2.8553	2.6962	2.7684	4.37

F.9: Analysis result of oxidised Australian oil at 160 °C

Carbon Number	RT	Run 1 Amount	Run 2 Amount	Run 3 Amount	Average weight %	Defined Percent
C7	0.3	10.2113	10.0846	10.1104	10.14	10.43
C8	0.62	4.2358	4.1252	4.1693	4.18	4.30
C8	0.76	3.1609	3.0318	2.9958	3.06	3.15
C9	1.78	3.3548	3.4943	3.2317	3.36	3.46
C10	2.41	5.6997	5.8386	5.9814	5.84	6.01
C10	2.94	3.5793	3.5211	3.6223	3.57	3.68
C10	3.34	5.5632	5.4437	5.6005	5.54	5.70
C11	4.09	4.7396	4.8513	4.6215	4.74	4.87
C11	4.34	3.5938	3.5024	3.4671	3.52	3.62
C11	4.63	2.5483	2.6207	2.4764	2.55	2.62
C12	5.06	3.4983	3.4634	3.6951	3.55	3.65
C12	5.26	2.6975	2.9903	2.8835	2.86	2.94
C12	5.54	2.7962	3.0524	2.9527	2.93	3.02
C12	5.77	2.3962	2.4153	2.2593	2.36	2.42
C13	6.09	3.0968	3.2385	2.9167	3.08	3.17
C13	6.3	3.5892	3.6194	3.3191	3.51	3.61
C13	6.57	2.9647	3.1133	2.8747	2.98	3.07
C13	6.86	2.2856	2.3647	2.1751	2.28	2.34
C14	7.27	4.9836	5.0768	5.1308	5.06	5.21
C14	7.45	3.8184	4.0747	3.7758	3.89	4.00
C14	7.8	2.7398	2.9201	2.6164	2.76	2.84
C15	8.05	3.0894	3.3845	3.2202	3.23	3.32
C15	8.36	2.9857	3.0317	3.1376	3.05	3.14
C16	8.81	2.4837	2.615	2.3511	2.48	2.55
C16	9.18	3.1379	3.2208	3.0603	3.14	3.23
C17	9.59	3.5074	3.6535	3.4501	3.54	3.64

F.10: Analysis result of unreacted oil C

Carbon Number	RT	Run 1 Amount	Run 2 Amount	Run 3 Amount	Average weight %	Defined Percent
C7	0.15	6.0174	5.9129	5.9586	5.96	7.59
C8	0.29	4.7499	4.5263	4.6781	4.65	5.92
C9	1.78	2.3176	2.1848	2.2837	2.26	2.88
C10	2.45	3.0873	3.0254	3.1219	3.08	3.92
C10	2.98	2.2405	2.5283	2.6207	2.46	3.14
C11	3.32		2.7439	2.7817	1.84	2.35
C11	4.38	2.1098	2.3567	2.4324	2.30	2.93
C12	5.15		2.8101	2.8764	1.90	2.41
C12	5.56	3.5066	4.1524	4.2459	3.97	5.05
C13	6.31	2.5432	3.0124	3.0823	2.88	3.67
C13	6.58	2.4651	3.7823	3.8634	3.37	4.29
C14	7.3	2.5371	2.9593	3.0634	2.85	3.63
C14	7.5	2.8901	3.3944	3.4759	3.25	4.14
C15	8.07	2.6624	3.1042	3.1946	2.99	3.80
C15	8.38	3.4344	4.055	4.1329	3.87	4.93
C16	8.86	2.6474	3.0977	3.1869	2.98	3.79
C16	9.2	2.7928	3.2746	3.3505	3.14	4.00
C17	9.61	2.7732	3.236	3.3101	3.11	3.96
C17	10.02	3.793	4.4199	4.5082	4.24	5.40
C18	10.75	2.8828	3.3554	3.4243	3.22	4.10
C20	12.13	2.2107	2.5544	2.6208	2.46	3.14
C24	14.58	2.5526	3.2332	3.12	2.97	3.78
C24	15.13	2.8707	3.4188	3.6253	3.30	4.21
C28	16.15		2.9026	2.9566	1.95	2.49
C44	22.84		4.6911	5.8226	3.50	4.46

F.11: Analysis result of oxidised oil C at 120 °C

Carbon Number	RT	Run 1 Amount	Run 2 Amount	Run 3 Amount	Average weight %	Defined Percent
C7	0.3	4.6205	4.5319	4.4829	4.544025	5.26
C8	0.62	1.6983	1.6745	1.7779	1.72425	2.00
C9	1.78	2.2073	2.1149	2.1982	2.169675	2.51
C10	2.43	3.4964	3.429	3.5302	3.4852	4.03
C10	2.97	2.9596	2.9999	3.0502	3.003233	3.48
C10	3.27	2.7572	3.0655	2.9483	2.923667	3.38
C11	4.34	2.6722	2.651	2.6385	2.6539	3.07
C12	5.11	2.3299	2.4716	2.4264	2.4093	2.79
C12	5.54	4.2875	4.4568	4.3827	4.375667	5.07
C13	6.29	3.0457	3.1384	3.0846	3.089567	3.58
C13	6.57	2.9361	3.9142	3.9258	3.592033	4.16
C14	7.3	2.7821	2.8749	2.8274	2.828133	3.27
C14	7.5	3.0968	3.1368	3.1989	3.144167	3.64
C15	8.06	2.6023	2.655	2.7355	2.664267	3.08
C15	8.37	3.3418	3.446	3.5451	3.4443	3.99
C16	8.85	2.4864	2.5656	2.6165	2.556167	2.96
C16	9.2	2.7678	2.8584	2.9329	2.853033	3.30
C17	9.61	2.7956	2.895	2.9731	2.8879	3.34
C17	10.01	4.0843	4.1993	4.3004	4.194667	4.86
C18	10.75	3.2223	3.3323	3.3991	3.3179	3.84
C20	11.9	1.4439	1.4862	1.5601	1.496733	1.73
C20	12.12	2.5003	2.6215	2.6735	2.598433	3.01
C24	14.1	2.3474	2.3498	2.3568	2.351333	2.72
C24	14.58	2.792	2.9324	3.2716	2.998667	3.47
C24	15.12	2.9548	3.0061	2.8993	2.9534	3.42
C28	16.14	2.8071	2.9055	3.0414	2.918	3.38
C32	18.4	2.4792	1.4985	1.5042	1.8273	2.12
C32	18.9	2.1296	2.1048	2.1468	2.127067	2.46
C44	22.83	5.3098	5.2748	5.1617	5.248767	6.08

F.12: Analysis result of oxidised oil C at 140 °C

Carbon Number	RT	Run 1 Amount	Run 2 Amount	Run 3 Amount	Average weight %	Defined Percent
C7	0.3	4.5051	4.6323	4.5592	4.565533	4.69
C8	0.63	2.2761	2.2869	2.182	2.248333	2.31
C9	1.81	3.0066	3.1096	2.9654	3.0272	3.11
C10	2.91	2.9762	3.093	2.8367	2.968633	3.05
C10	3.29	3.1247	3.0288	2.966	3.039833	3.12
C11	3.89	1.6722	1.7329	1.7793	1.728133	1.78
C11	4.36	2.4869	2.5499	2.6416	2.559467	2.63
C12	5.13	2.4068	2.2113	2.337	2.318367	2.38
C12	5.55	3.3178	3.0789	3.2519	3.2162	3.31
C13	6.3	3.2685	3.4317	3.5119	3.404033	3.50
C13	6.58	3.1846	3.2764	3.3942	3.285067	3.38
C14	7.3	3.1832	3.0739	3.0993	3.1188	3.21
C14	7.51	3.3964	3.5785	3.6081	3.527667	3.63
C15	8.07	2.4168	2.7822	2.8458	2.6816	2.76
C15	8.38	2.9836	3.1621	3.0084	3.051367	3.14
C16	8.86	2.60164	2.6592	2.7955	2.685447	2.76
C16	9.21	3.1849	3.3132	3.2286	3.242233	3.33
C17	9.62	3.1573	3.3582	3.2521	3.255867	3.35
C17	10.03	3.0853	3.0135	3.1514	3.0834	3.17
C18	10.39	3.0563	2.9636	2.9989	3.006267	3.09
C18	10.77	3.7629	3.8058	3.906	3.8249	3.93
C18	11.1	2.4638	2.6739	2.5997	2.579133	2.65
C20	11.83	2.1853	2.3754	2.4461	2.3356	2.40
C20	12.14	2.6386	2.7967	2.8778	2.771033	2.85
C24	14.02	3.4638	3.3214	3.546	3.443733	3.54
C24	14.59	3.6948	3.8746	3.9147	3.828033	3.93
C24	15.14	3.2952	3.5471	3.4897	3.444	3.54
C28	17.12	3.5316	3.5574	3.4986	3.5292	3.63
C32	18.43	2.2913	2.4223	2.3649	2.3595	2.42
C32	18.87	2.3055	2.3068	2.3162	2.3095	2.37
C44	22.79	6.9584	6.7645	6.8803	6.867733	7.06

F.13: Analysis result of oxidised oil C at 160 °C

Carbon Number	RT	Run 1 Amount	Run 2 Amount	Run 3 Amount	Average weight %	Defined Percent
C7	0.31	4.2113	4.3868	4.087	4.228367	4.40
C8	0.65	2.8895	2.6399	2.794	2.774467	2.89
C9	1.87	3.8239	3.546	3.6804	3.683433	3.83
C10	2.43	3.0452	3.1341	3.0249	3.068067	3.19
C10	2.96	2.4198	2.5435	2.6876	2.5503	2.65
C10	3.32	2.338	2.4995	2.5989	2.4788	2.58
C11	4.36	3.3297	2.2237	2.3016	2.618333	2.72
C12	5.12	1.9685	1.9057	1.944	1.9394	2.02
C12	5.54	3.6417	3.491	3.519	3.550567	3.70
C13	6.29	2.581	2.4549	2.5422	2.526033	2.63
C13	6.57	2.4587	2.3429	2.4072	2.402933	2.50
C14	7.3	2.2207	2.1005	2.1628	2.161333	2.25
C14	7.5	2.5728	2.4752	2.5602	2.536067	2.64
C15	8.06	2.0802	2.0037	2.0256	2.0365	2.12
C15	8.37	2.7389	2.5968	2.6948	2.676833	2.79
C16	8.85	2.1137	2.0068	2.0477	2.056067	2.14
C16	9.2	2.3647	2.2398	2.3251	2.309867	2.40
C17	9.61	2.3262	2.2071	2.2516	2.261633	2.35
C17	10.02	3.4058	3.2346	3.2947	3.3117	3.45
C18	10.38	3.3296	3.1245	3.2167	3.2236	3.35
C18	10.75	5.4468	5.1535	5.262	5.287433	5.50
C18	11.09	2.8206	2.6909	2.7365	2.749333	2.86
C20	11.82	2.6782	2.5284	2.5855	2.597367	2.70
C20	12.13	3.3225	3.1147	3.1464	3.194533	3.32
C24	14.01	3.8256	3.6147	3.6019	3.680733	3.83
C24	14.58	2.9864	3.0438	3.0563	3.028833	3.15
C24	15.13	3.7146	3.6934	3.6997	3.702567	3.85
C28	17.11	3.8429	3.9602	3.9097	3.904267	4.06
C32	18	3.3833	3.2983	3.3333	3.3383	3.47
C32	18.43	3.0493	2.8468	2.9648	2.953633	3.07
C44	22.82	7.2318	7.1574	7.3847	7.257967	7.55

F.14: Analysis result of unreacted oil D

Carbon Number	RT	Run 1 Amount	Run 2 Amount	Run 3 Amount	Average weight %	Defined Percent
C7	0.33	4.9808	4.8213	4.7019	4.834667	5.74
C8	0.44	2.4672	2.5629	2.4308	2.486967	2.95
C8	0.64	2.2838	2.4214	2.3867	2.363967	2.80
C8	0.81	2.06029	2.21787	1.96291	2.080357	2.47
C9	1.87	2.6266	2.7993	2.4873	2.637733	3.13
C10	2.42	4.1218	3.9386	3.8742	3.9782	4.72
C10	2.95	3.8188	3.9732	3.7962	3.862733	4.58
C10	3.31	3.3426	3.1762	2.9897	3.1695	3.76
C11	3.88	3.0417	2.9393	2.7238	2.9016	3.44
C11	4.36	3.1308	3.3294	3.0895	3.183233	3.78
C12	5.12	2.537	2.498	2.2779	2.437633	2.89
C12	5.54	4.685	4.8001	4.5049	4.663333	5.53
C13	6.24	3.3527	3.5138	3.4341	3.433533	4.07
C13	6.57	3.7645	3.4231	3.5827	3.5901	4.26
C14	7.28	3.1506	3.3303	3.0278	3.169567	3.76
C14	7.5	3.2932	3.5514	3.3927	3.412433	4.05
C15	8.06	3.5715	3.3268	3.2076	3.368633	4.00
C15	8.37	3.6248	3.4181	3.2875	3.443467	4.09
C16	8.84	2.5422	2.4948	2.2626	2.4332	2.89
C16	9.19	2.9097	2.8194	2.6175	2.7822	3.30
C17	9.6	2.8282	2.6414	2.5307	2.666767	3.16
C17	10.01	4.0207	3.8978	3.6277	3.848733	4.57
C18	10.74	3.2836	2.8284	2.9583	3.023433	3.59
C20	12.12	2.5119	2.3853	2.2512	2.3828	2.83
C20	14	2.8524	3.0881	2.9184	2.952967	3.50
C24	14.57	2.6257	2.4483	2.55	2.541333	3.02
C24	15.11	2.7135	2.6437	2.5425	2.633233	3.12

F.15: Analysis result of oxidised oil D at 120 °C

Carbon Number	RT	Run 1 Amount	Run 2 Amount	Run 3 Amount	Average weight %	Defined Percent
C7	0.31	3.3774	3.3715	3.2044	3.317767	3.59
C8	0.42	2.6052	2.53219	2.50943	2.54894	2.76
C8	0.61	2.5544	2.4122	2.3481	2.438233	2.64
C8	0.76	2.095	2.0465	2.0277	2.0564	2.23
C9	1.76	3.3653	3.2998	3.1522	3.272433	3.54
C10	2.95	3.5496	3.6024	3.6806	3.610867	3.91
C10	3.39	4.6194	4.7854	4.5286	4.644467	5.03
C11	3.83	4.258	4.4201	4.2264	4.3015	4.66
C11	4.31	4.4757	4.7156	4.5297	4.573667	4.95
C11	4.61	2.3981	2.0499	2.1894	2.212467	2.40
C12	5.11	2.751	2.65	2.8777	2.759567	2.99
C12	5.51	2.0839	2.146	2.2136	2.147833	2.33
C13	6.24	3.4168	3.5252	3.5451	3.4957	3.79
C13	6.55	3.6311	3.4336	3.4279	3.497533	3.79
C14	7.24	4.0439	3.9529	3.8698	3.955533	4.28
C14	7.51	4.5309	4.4164	4.2387	4.395333	4.76
C14	8.05	3.9374	4.1783	4.047	4.054233	4.39
C15	8.36	2.6199	2.3669	2.402	2.462933	2.67
C16	9.21	2.9343	2.8829	3.0227	2.946633	3.19
C17	9.62	2.9691	2.6462	2.8821	2.832467	3.07
C17	10.02	2.2078	2.3334	2.4786	2.339933	2.53
C18	10.35	1.6217	1.7223	1.6032	1.649067	1.79
C18	10.77	3.5181	3.7324	3.747	3.665833	3.97
C18	11.08	1.1911	1.2194	1.1834	1.197967	1.30
C20	11.84	1.3612	1.2731	1.1831	1.272467	1.38
C20	12.16	1.6935	1.9115	1.8453	1.816767	1.97
C24	14.57	3.5024	3.6008	3.5705	3.5579	3.85
C24	15.15	3.2158	3.4665	3.3436	3.341967	3.62
C28	16.17	2.8688	2.6326	2.6018	2.701067	2.93
C28	16.62	2.8754	2.7778	2.6206	2.757933	2.99
C44	22.53	2.3672	2.5318	2.6429	2.513967	2.72

F.16: Analysis result of oxidised oil D at 140 °C

Carbon Number	RT	Run 1 Amount	Run 2 Amount	Run 3 Amount	Average weight %	Defined Percent
C7	0.32	1.6815	1.5277	1.3149	1.508033	1.58
C7	0.38	1.7908	1.598	1.7242	1.704333	1.79
C8	0.62	3.066	3.1182	3.0725	3.085567	3.24
C9	1.81	4.0515	4.1789	4.232	4.154133	4.36
C10	2.42	3.1785	3.2846	3.3245	3.262533	3.42
C10	2.95	3.3429	3.0492	3.1643	3.185467	3.34
C10	3.33	2.8701	2.893	2.8452	2.869433	3.01
C11	3.88	2.5542	2.5729	2.6658	2.597633	2.73
C11	4.36	2.972	2.9293	2.8403	2.913867	3.06
C11	4.63	1.4275	1.3295	1.4091	1.3887	1.46
C12	5.12	2.3013	2.3886	2.3061	2.332	2.45
C12	5.54	3.1135	3.2791	3.3626	3.251733	3.41
C13	6.23	3.4573	3.3426	3.2312	3.3437	3.51
C13	6.56	3.6927	3.796	3.8141	3.7676	3.95
C14	7.28	3.0821	3.1512	2.9703	3.067867	3.22
C14	7.5	3.2587	3.3689	3.2031	3.2769	3.44
C15	8.06	3.2428	3.3967	3.0873	3.242267	3.40
C15	8.37	3.1603	3.2212	3.0039	3.128467	3.28
C16	8.84	2.1726	2.1357	2.0894	2.132567	2.24
C16	9.19	2.8783	2.8413	2.8142	2.8446	2.99
C17	9.61	2.5956	2.566	2.6981	2.6199	2.75
C17	10.01	2.9594	2.8938	2.8185	2.890567	3.03
C18	10.75	3.0965	3.1856	3.1413	3.141133	3.30
C18	11.08	1.5333	1.4109	1.6491	1.5311	1.61
C20	11.84	1.4129	1.5062	1.6398	1.519633	1.59
C20	12.13	2.1082	2.365	2.2648	2.246	2.36
C20	12.51	1.3434	1.2685	1.3248	1.312233	1.38
C24	14.58	3.3145	3.3694	3.4051	3.363	3.53
C24	15.12	2.3703	2.1527	2.1596	2.227533	2.34
C28	16.14	2.9875	2.9911	2.8756	2.9514	3.10
C28	16.64	2.4742	2.4479	2.5908	2.5043	2.63
C32	18	2.0242	2.9893	2.0267	2.346733	2.46
C32	18.42	2.4922	2.4586	2.2608	2.403867	2.52
C36	19.69	1.4645	1.4954	1.5575	1.5058	1.58
C36	20.09	1.5978	1.6004	1.6488	1.615667	1.70
C44	22.83	3.9582	4.0469	4.14565	4.05025	4.25

F.17: Analysis result of oxidised oil D at 160 °C

Carbon Number	RT	Run 1 Amount	Run 2 Amount	Run 3 Amount	Average weight %	Defined Percent
C8	0.61	2.0584	1.7852	1.9573	1.933633	2.00
C8	0.77	1.90454	1.6853	1.8529	1.814247	1.88
C9	1.79	3.5669	3.2603	3.4839	3.437033	3.56
C10	2.39	3.0168	2.8746	2.9369	2.942767	3.05
C10	2.88	2.7278	2.4368	2.6163	2.593633	2.69
C10	3.3	3.0587	2.7829	2.8091	2.883567	2.99
C11	3.84	1.3857	1.5807	1.4597	1.475367	1.53
C11	4.06	1.1679	1.1012	1.2482	1.172433	1.21
C11	4.34	2.0473	2.1201	2.291	2.1528	2.23
C11	4.62	1.2013	1.326	1.5064	1.344567	1.39
C12	5.11	2.2179	2.3845	2.1518	2.2514	2.33
C12	5.53	4.0436	4.179	3.9618	4.061467	4.21
C13	6.23	3.0576	3.1086	2.9576	3.041267	3.15
C13	6.56	2.9498	2.748	2.7738	2.823867	2.92
C14	7.28	2.8241	2.6086	2.6966	2.709767	2.81
C14	7.49	2.8542	2.5904	2.6991	2.714567	2.81
C14	7.83	1.026	0.9351	0.9146	0.958567	0.99
C15	8.05	2.2105	2.1729	2.3074	2.230267	2.31
C15	8.37	3.0614	3.1974	2.9922	3.083667	3.19
C16	8.84	2.205	2.4704	2.3568	2.344067	2.43
C16	9.19	2.4121	2.3629	2.4971	2.424033	2.51
C17	9.61	2.6336	2.3953	2.5617	2.5302	2.62
C17	10.02	3.8162	3.7142	3.6977	3.7427	3.88
C18	10.37	1.9643	1.773	1.7964	1.844567	1.91
C18	10.76	2.9329	3.0677	3.1328	3.044467	3.15
C18	11.08	1.2969	1.3323	1.4978	1.375667	1.42
C20	11.83	1.6837	1.5418	1.4689	1.5648	1.62
C20	12.12	2.5353	2.3902	2.2343	2.3866	2.47
C20	12.52	1.3564	1.2793	1.2863	1.307333	1.35
C24	14.57	3.2321	3.1479	2.8007	3.060233	3.17
C24	15.12	2.3401	2.4616	2.4781	2.4266	2.51
C28	16.14	2.9548	2.8138	2.6537	2.807433	2.91
C28	16.64	3.5046	3.6546	3.477	3.5454	3.67
C28	17.1	2.6683	2.7005	2.5583	2.642367	2.74
C32	17.9	2.2695	2.0563	2.3255	2.2171	2.30
C32	18.32	2.1401	2.222	2.0288	2.1303	2.21
C36	19.68	2.1733	2.2018	2.0832	2.152767	2.23
C36	20.06	1.7575	1.8543	1.9595	1.8571	1.92
C44	22.82	5.5536	5.4073	5.6191	5.526667	5.72

F.18: Analysis result of unreacted Esso Mix1 oil

Carbon Number	RT	Run 1 Amount	Run 2 Amount	Run 3 Amount	Average weight %	Defined Percent
C7	0.31	3.3863	3.2841	3.4761	3.382167	3.58
C7	0.38	3.7834	3.6927	3.8692	3.781767	4.00
C8	0.61	1.7161	1.6631	1.8749	1.751367	1.85
C8	0.77	1.6742	1.5874	1.4867	1.582767	1.67
C9	1.81	2.1332	2.2893	2.3897	2.270733	2.40
C10	2.43	2.9048	2.8482	2.9673	2.906767	3.07
C10	2.95	2.8713	3.1212	3.0469	3.013133	3.19
C10	3.39	2.904	3.141	3.0592	3.034733	3.21
C11	4.35	2.2721	2.4911	2.3182	2.360467	2.50
C12	5.13	2.1817	2.3853	2.2654	2.277467	2.41
C12	5.54	3.7579	4.0785	3.8367	3.891033	4.11
C13	6.2	3.1487	3.419	3.3966	3.321433	3.51
C13	6.55	3.0067	3.232	3.1793	3.139333	3.32
C14	7.26	3.473	3.7947	3.6416	3.636433	3.85
C14	7.48	2.941	3.1643	3.0337	3.046333	3.22
C15	8.04	3.2531	3.5454	3.4519	3.4168	3.61
C15	8.35	3.3473	3.6528	3.5119	3.504	3.71
C16	8.82	2.5026	2.6896	2.4942	2.562133	2.71
C16	9.18	2.637	2.8873	2.7993	2.774533	2.93
C17	9.59	2.7386	2.9826	2.6081	2.776433	2.94
C17	9.98	3.4624	3.7708	3.6458	3.626333	3.83
C18	10.37	2.0749	2.265	2.1084	2.149433	2.27
C18	10.73	3.1805	3.4561	3.3955	3.344033	3.54
C18	11.07	2.1058	2.1635	2.2286	2.165967	2.29
C20	11.85	2.1486	2.1989	2.2521	2.199867	2.33
C20	12.11	2.4309	2.7101	2.5514	2.564133	2.71
C24	14.56	2.9772	3.4614	3.3989	3.279167	3.47
C24	15.1	2.7466	3.1448	3.2906	3.060667	3.24
C28	16.12	3.3152	3.5708	3.5997	3.495233	3.70
C28	16.62	4.2191	4.6006	4.4461	4.421933	4.68
C44	22.86	5.7328	5.8643	5.8778	5.824967	6.16

F.19: Analysis result of oxidised Esso Mix1 oil at 120 °C

Carbon Number	RT	Run 1 Amount	Run 2 Amount	Run 3 Amount	Average weight %	Defined Percent
C7	0.31	1.8701	1.6248	1.7482	1.7477	1.89
C7	0.37	1.9958	1.4533	1.4684	1.639167	1.77
C8	0.59	1.4356	1.3496	1.3165	1.367233	1.48
C8	0.75	1.6602	1.5807	1.5589	1.599933	1.73
C9	1.74	2.0876	1.9461	1.8539	1.962533	2.13
C10	2.47	3.0833	3.1946	3.1964	3.1581	3.42
C10	2.98	2.7176	2.7359	2.8906	2.781367	3.01
C10	3.47	2.7264	2.6635	2.8233	2.737733	2.96
C11	3.93	3.1947	3.1593	3.2395	3.197833	3.46
C11	4.44	2.5619	2.6425	2.4283	2.544233	2.75
C11	4.77	1.3908	1.2017	1.4678	1.353433	1.47
C12	5.11	2.1103	2.2117	2.1411	2.154367	2.33
C12	5.52	3.7108	3.7945	3.8631	3.789467	4.10
C13	6.34	3.3376	3.1706	3.1373	3.215167	3.48
C13	6.67	2.2347	2.3641	2.2941	2.297633	2.49
C14	7.25	3.4195	3.3727	3.5818	3.458	3.74
C14	7.63	2.2809	2.3573	2.1048	2.247667	2.43
C15	8.03	3.0849	3.1289	3.2859	3.166567	3.43
C15	8.5	3.1056	3.2964	3.3093	3.2371	3.51
C16	8.82	2.5841	2.6664	2.4442	2.5649	2.78
C16	9.26	2.896	2.7766	2.651	2.774533	3.00
C17	9.7	2.6643	2.5244	2.6162	2.601633	2.82
C17	9.98	3.3184	3.2378	3.4918	3.349333	3.63
C18	10.21	2.1616	2.0179	2.0119	2.0638	2.23
C18	10.68	3.8564	3.7778	3.7852	3.806467	4.12
C18	11.06	1.7058	1.794	1.8626	1.787467	1.94
C20	11.79	1.9952	1.8852	1.9234	1.9346	2.09
C20	12.2	1.7639	1.7562	1.7082	1.742767	1.89
C24	14.55	3.2662	3.2842	3.3228	3.291067	3.56
C24	14.73	3.6176	3.6532	3.5021	3.590967	3.89
C28	16.36	3.2118	3.1652	3.1101	3.162367	3.42
C28	16.87	3.6549	3.7694	3.8462	3.756833	4.07
C28	17.35	2.2019	2.3596	2.2397	2.267067	2.45
C44	22.83	5.9864	6.0124	6.0082	6.002333	6.50

F.20: Analysis result of oxidised Esso Mix1 oil at 140 °C

Carbon Number	RT	Run 1 Amount	Run 2 Amount	Run 3 Amount	Average weight %	Defined Percent
C7	0.31	1.8807	1.8956	1.9661	1.914133	2.10
C7	0.37	1.7078	1.7323	1.8602	1.766767	1.94
C8	0.61	1.411	1.5027	1.3974	1.437033	1.58
C8	0.77	1.3113	1.3728	1.3165	1.333533	1.47
C9	1.8	2.0101	2.0858	1.9979	2.031267	2.23
C10	2.38	2.6251	2.6936	2.7934	2.704033	2.97
C10	2.92	2.4766	2.5178	2.6766	2.557	2.81
C10	3.35	2.8658	2.7148	2.6193	2.7333	3.00
C11	3.83	1.4207	1.4603	1.5943	1.491767	1.64
C11	4.34	2.0361	1.9092	2.1718	2.039033	2.24
C11	4.62	1.2931	1.376	1.32	1.3297	1.46
C12	5.11	1.5835	1.4702	1.4279	1.493867	1.64
C12	5.53	3.4776	3.2316	3.462	3.3904	3.73
C13	6.19	2.2329	2.0366	2.1981	2.155867	2.37
C13	6.55	2.4169	2.6504	2.5836	2.5503	2.80
C14	7.26	3.0159	3.1595	3.1997	3.125033	3.44
C14	7.48	2.4828	2.6429	2.5794	2.568367	2.82
C15	8.03	2.5145	2.3271	2.4283	2.4233	2.66
C15	8.35	2.4824	2.2579	2.3211	2.3538	2.59
C16	8.82	2.1258	1.9321	2.1845	2.0808	2.29
C16	9.18	2.4003	2.231	2.3506	2.3273	2.56
C17	9.59	2.417	2.1956	2.3309	2.3145	2.54
C17	9.98	3.1791	3.1491	3.0828	3.137	3.45
C18	10.37	1.3567	1.2026	1.1792	1.246167	1.37
C18	10.73	2.9637	3.0906	2.8281	2.9608	3.25
C18	11.07	1.6079	1.5131	1.6739	1.5983	1.76
C20	11.85	1.6516	1.5426	1.7459	1.6467	1.81
C20	12.11	1.4651	1.5382	1.6482	1.5505	1.70
C24	14.55	3.4867	3.3163	3.5091	3.437367	3.78
C24	15.1	2.5502	2.4147	2.4526	2.4725	2.72
C28	16.13	2.8538	2.9078	2.7266	2.8294	3.11
C28	16.63	3.4701	3.3115	3.5064	3.429333	3.77
C28	17.09	2.2151	2.1161	2.0645	2.1319	2.34
C32	17.88	1.6871	1.8473	1.9928	1.8424	2.03
C32	18.33	1.7188	1.6836	1.8216	1.741333	1.91
C32	18.64	1.8083	1.7592	1.8268	1.7981	1.98
C36	19.67	1.5607	1.4839	1.6948	1.5798	1.74
C36	20.1	1.6906	1.8385	1.9226	1.817233	2.00
C44	22.85	7.5846	7.6027	7.6996	7.628967	8.39

F.21: Analysis result of oxidised Esso Mix1 oil at 160 °C

Carbon Number	RT	Run 1 Amount	Run 2 Amount	Run 3 Amount	Average weight %	Defined Percent
C7	0.33	2.8264	2.8634	2.9231	2.870967	3.01
C7	0.38	1.8133	1.8133	1.8262	1.8176	1.90
C8	0.62	1.121	1.1512	1.136	1.136067	1.19
C8	0.78	1.1478	1.1537	1.1609	1.154133	1.21
C9	1.82	1.4429	1.5429	1.5657	1.517167	1.59
C10	2.39	2.5914	2.6612	2.7006	2.651067	2.78
C10	2.89	2.4534	2.5824	2.5457	2.527167	2.65
C10	3.36	2.4522	2.5981	2.5545	2.534933	2.65
C11	3.83	1.4982	1.4284	1.5713	1.4993	1.57
C11	4.34	2.0381	2.0955	2.1086	2.080733	2.18
C11	4.62	1.2761	1.3618	1.3121	1.316667	1.38
C12	5.12	1.8452	1.7416	1.912	1.832933	1.92
C12	5.53	3.2991	3.3352	3.4084	3.347567	3.51
C13	6.2	2.7011	2.9824	2.768	2.817167	2.95
C13	6.56	2.4891	2.5521	2.5289	2.523367	2.64
C14	7.27	3.0817	3.1073	3.1516	3.113533	3.26
C14	7.49	2.4985	2.5584	2.5324	2.529767	2.65
C15	8.05	2.8393	2.9529	2.8627	2.884967	3.02
C15	8.37	2.8269	2.7144	2.8968	2.8127	2.95
C16	8.84	2.1613	2.0201	2.1222	2.1012	2.20
C16	9.19	2.2881	2.1397	2.2998	2.242533	2.35
C17	9.6	2.2972	2.1631	2.3128	2.2577	2.36
C17	9.99	3.0048	3.248	3.0137	3.088833	3.23
C18	10.38	1.7467	1.7385	1.7658	1.750333	1.83
C18	10.74	2.7738	2.9463	2.7479	2.822667	2.96
C18	11.08	1.6767	1.4513	1.6951	1.6077	1.68
C20	11.85	1.7478	1.5773	1.7651	1.696733	1.78
C20	12.12	2.1357	1.9988	2.166	2.100167	2.20
C20	12.49	1.4075	1.4863	1.3812	1.425	1.49
C24	14.57	3.2779	2.1877	2.2153	2.5603	2.68
C24	15.11	2.4478	2.7368	2.8537	2.679433	2.81
C28	16.14	2.8874	2.9181	2.8433	2.882933	3.02
C28	16.63	3.6815	3.7764	3.7646	3.740833	3.92
C28	17.1	2.2951	2.0245	2.2358	2.185133	2.29
C32	17.87	1.9431	1.8733	1.9851	1.933833	2.03
C32	18.34	1.7005	1.6281	1.7378	1.6888	1.77
C32	18.67	1.6367	1.6494	1.7496	1.678567	1.76
C36	19.69	1.686	1.7672	1.6484	1.700533	1.78
C44	22.81	10.4752	10.3728	10.2777	10.37523	10.87

Specification Table

- 13oct01 Run Date 10/13/99
s Averaged 41 - 81
ntion time 1.64
ification File: FC43.spt

Range	Ref.	Intens.	Ratio	Status
1-2%	69	559	1.18	pass
100-100%	69	47442	100.00	pass
26-50%	69	24675	52.01	high
40-70%	69	31593	66.59	pass
8-18%	69	8224	17.34	pass
0-4%	69	328	0.69	pass
1.5-4%	69	1647	3.47	pass
1.5-4%	69	1750	3.69	pass
0.1-1%	69	360	0.76	pass

ification Table

- 9904-5 Run Date 10/21/99
s Averaged 46 - 74
ntion time 0.99
ification File: FC43.spt

Range	Ref.	Intens.	Ratio	Status
1-2%	69	1581	1.72	pass
100-100%	69	91778	100.00	pass
26-50%	69	30533	33.27	pass
40-70%	69	70600	76.93	high
8-18%	69	16508	17.99	pass
0-4%	69	901	0.98	pass
1.5-4%	69	3056	3.33	pass
1.5-4%	69	2670	2.91	pass
0.1-1%	69	473	0.52	pass

ification Table

- 030401 Run Date 4/ 3/101

s Averaged 43 - 73

ntion time 1.47

ification File: FC43.spt

Range	Ref.	Intens.	Ratio	Status
1-2%	69	611	1.12	pass
100-100%	69	54669	100.00	pass
26-50%	69	25522	46.68	pass
40-70%	69	25932	47.43	pass
8-18%	69	5845	10.69	pass
0-4%	69	433	0.79	pass
1.5-4%	69	1429	2.61	pass
1.5-4%	69	1470	2.69	pass
0.1-1%	69	327	0.60	pass